Università Campus Bio-Medico di Roma

Corso di dottorato di ricerca in

Scienze Biomediche Integrate e Bioetica

XXXV ciclo a.a. 2019-2020

Autoimmunity and Antibody Response in Diabetes: The Role of Hyperglycemia and Antigen Post Translational Modifications

Ghadeer Alhamar

Coordinatore

Prof. Paolo Pozzilli

Tutore

Prof. Rocky Strollo

31/ 01/ 2023

For mama and baba

And for me, definitely for me.

Statement of Originality

This is to state and certify that the following work is the result of original and independent research. All the methods, data and analyses were performed as stated, with all necessary persons and references cited as appropriate.

Acknowledgements

First, I would like to thank my family, to my parents, Emad Alhamar and Tahani Alali, who believed in me and supported me in paving a path for myself, even when they did not fully understand. Thank you for not only allowing me to pursue my dreams, but for teaching me how to dream in the first place. To my little sisters Kokes and Zooz, who brought light, love, and laughter into this journey of mine, reminding me that there are bigger things to worry about. To my brother Hashim, who, although sarcastically, supported and believed in me. To Ali, although not my brother by blood, thank you for the support and all the cups of coffee. To my absolute favorite little human Dana, you may never know how much your little cuddles helped me write this thesis, but they were an essential part of the process. However, I would like to specifically acknowledge my eldest sister Fatima who, even when you used to sit on me when we were kids, was always a beacon of light I aspired to resemble. Thank you for listening to my rants, to my cries, to my stressed-out spirals, and giving advice, guidance, and reminding me of who I am and that there's no heights to what I can achieve. You are, and will always be, my bezza.

I would not have been able to reach these peaks without the help and support of the dear friends I made along the way. In no particular order, Malak, Camilla, Marina, Niccolò, Flavia, Viola, Giulia, Alessandro and Giulia, thank you for all the café breaks, the laughs, the cries, the help, the support, and being the best lab a random girl from Kuwait to ask for. I was not sure what would happen when I moved to Rome, but you all made leaving the eternal city one of the hardest things I have ever done, and for that I am eternally grateful. I would like to thank Luciana Valente, for always knowing where everything is and for answering all of my less than smart questions. Thank you to Prof. Paolo Pozzilli for his continued guidance and support.

To Swathy, Nadine and Merel, my home away from home, words cannot possibly describe how much your mere existences in my life have impacted me. Thank you for always reminding me to eat, listening to me rant, endless movie nights and karaoke, for all the baked goods and dinners, thank you for letting me lay on the floor and talk me out of my anxiety attacks. Most of all, thank you for being yourselves, I have not known honesty, support, kindness, and……sarcasm like what you have shown me. We're due another Twilight rewatch… just FYI.

Last, but certainly in no way least, I would like to thank, my **SUPER**visor, *Prof.* Rocky Strollo. Truly one of the smartest, creative, kind, and *direct* researchers I have ever met. Even though you're a raging workaholic, thank you for reminding me to take breaks when I needed to, to step back when I needed to, and thank you for always reminding me that there are bigger things to worry about than a failed set of experiments.

Study 1. Autoimmunity to Post Translationally Modified Beta Cell Antigens

Abstract

Background

Type 1 Diabetes (T1D) is a heterogenous autoimmune disorder, whereby the immune system specifically targets and destroys the pancreatic beta cells, leading to little to no insulin production and secretion. T1D is characterized by hyperglycemia, juvenile age of onset, and the presence of one or multiple autoantibodies (AABs) directed towards insulin (INS), glutamate decarboxylase 65 (GAD65), zinc transporter 8 (ZnT8), and islet antigen 2 (IA-2). The gold-standard for diagnosing T1D is via a radio-binding assay detecting the key AABs, with the detection of multiple autoantibodies in genetic susceptible individuals conferring a higher risk of developing T1D. Environmental triggers, such as viral infections, dietary changes, and pollutants, have been implicated in inducing the onset of T1D. However, the current AABs differ from various populations and have a tendency to disappear after initial recognition. Hence there is a need to identify, isolate, and develop more specific biomarkers that can more accurately predict, diagnose and monitor the development of T1D. Although the key instigator of autoimmunity has not been fully elucidated, numerous studies have implicated the role of oxidative stress and reactive oxygen species in initiating an autoimmune response. It has been suggested that increased levels of oxidative stress can induce oxidative post translational modifications (oxPTMs) to native beta cell antigens, forming neo-epitopes. These neo-epitopes appear foreign to the immune system, and thus elicit an immune response. Additionally, the sequence similarities between the neo-epitope and the native epitope induces an immune response towards the native epitope through a mechanism known as epitope spreading. Studies have reported the presence of autoantibodies to oxPTM-INS and hydroxyl modified GAD65 in T1D.

Hypothesis

The main hypothesis of the study is that oxPTMs of native pancreatic β-Cells antigens may play a role in the development of autoimmunity associated with T1D.

Aim 1. The first aim of the study is to deduce the level of reactivity to oxPTM β-cell antigens, focusing on GAD65 and ZnT8, in patients with new-onset T1D.

Aim 2. The second aim is to compare the reactivity of AABs to oxPTM antigens to AABs to native antigens in patients with T1D and healthy controls. As well as, to deduce the efficiency of oxPTM β-cell antigens in being potential biomarkers for T1D compared to native antigens.

Aim 3. The final aim of the study is to determine whether there are any correlations with AAB development to oxPTM or native antigens to patient demographic and clinical information. This includes genetic information pertaining to HLA-typing, markers of oxidative stress, HbA1c levels, and C-peptide levels.

Materials and Methods

A total of N= 69 patients with T1D, N= 32 patients with type 2 diabetes (T2D), and N= 39 healthy controls (HC) were recruited from the outpatient clinic of the Endocrinology and Diabetes department of the Policlinico Campus Biomedico Università di Roma. Patient characteristics and demographic data were collected, along with informed consent. In vitro chemical modifications of INS, GAD65, and ZnT8 were performed to generate oxPTMs modification via glycation (GLY-) with 2M D-ribose, the hydroxyl radical (•OH-) via the Fenton reaction using 100 mM hydrogen peroxide and 100 mM copper chloride, and modification with a 1:100 dilution of 1M hypochlorous acid (HOCl-). The induced modifications were monitored and assessed through SDS-PAGE analysis and Western Blotting, with the subsequent gels imaged with the Chemi-Doc imaging system and quantified with ImageJ. A "homemade" ELISA was devised to measure and detect the levels of antibody reactivity to each native (NT-) and oxPTM-beta cell antigen. This was done by coating a 96 well plate with either NT- or modified antigens (10 µg/mL or 2 µg/mL) in 0.05M bicarbonate-carbonate buffer (pH 6), and incubating the plates overnight at 4ºC. The plates were blocked with either 5% BSA in 1x PBS with 0.1% Tween (PBST) or 5% skimmed milk in PBST. A 1:200 dilution of T1D, T2D or HC serum samples were then prepared in blocking buffer and loaded into the plates. This was followed by the addition of a secondary antibody (rabbit anti-human IgG) also diluted in blocking buffer to the plates. The plates were washed 3 times with PBST and then 3 times with PBS between each step. TMB was then added to the plates to yield a colorimetric reaction, the reaction was stopped with sulphuric acid, and the plates were read on the Tecan M200 plate reader at O.D 450 nm. Carboxymethyl-Lysine was measured with an ELISA assay.

Results

When comparing demographic patient characteristics such as age, gender distribution, BMI, and HbA1c, the T1D were typically younger compared to T2D (median age in years [IQR],13 [9-26] vs 62.50 [52- 68.25], p-value <0.0001, respectively), BMI was lower in T1D than in T2D (median kg/m^2 [IQR], 18 .60 [16.20-20.95] vs 30.40 [24.35-33.05], p-value < 0.0001, respectively).

SDS-PAGE analysis showed that when GAD65 is modified *in vitro* with 2 M D-ribose, there appeared to be an upshift in the molecular weight of GAD65 from bands at 116.8, 54.9 and 22.7 KDa to 117.5, 59.5 and 23.3 KDa in the GLY-GAD65 lane. Similarly, when assessing the band intensity, there was a decrease in band intensity between NT-GAD65 and GLY-GAD65. With •OH-GAD65, there appeared to be 2 faint bands at 60.1 KDa and 53.3 KDa. In comparison to the NT-GAD65, the •OH-GAD65 had a decreased band intensity. Finally, the HOCl-GAD65 showed bands at 117.5, 60.1 and 23.5 KDa. Upon glycation of NT-ZnT8 there was an apparent up-shift in GLY-ZnT8 with distinct bands at 93.1 and 43.2 KDa compared to the NT-ZnT8, which showed clear bands at 83.4 and 36.6 KDa. In comparison, modifying NT-ZnT8 with the hydroxyl radical to yield •OH-ZnT8 showed a similar increase in molecular weight to 88.9, 72.9, and 38.9 KDa compared to the NT-ZnT8 bands at 83.4, 36.6 and 31.0 KDa. HOCl-ZnT8 appeared to have bands at a molecular weight of 77.2 and 31.4 KDa compared to 60.2 and 23.5 KDa seen in the NT-ZnT8 lane.

A cut-off for antibody binding positivity was calculated from the mean IgG binding of the healthy controls towards native or oxPTM beta cell antigens (mean O.D+ 2*standard deviations), resulting in an O.D of 0.5 as the cut-off for the homemade ELISAs developed towards NT- and oxPTM- GAD65 and ZnT8. Using this cut-off, the prevalence of antibody binding towards modified or native beta cell antigens was assessed. This study found that 53.2% (36/69) of patients with new-onset T1D were positive for IgG antibodies to NT-GAD65, 43.49% (30/69) were positive for GLY-GAD65, 17.4% (12/69) were positive for •OH-GAD65 and 39.1% (27/69) were positive to HOCl-GAD65. When determining the binding of oxPTM-GAD65-Ab in patients with new-onset T1D, there was a significant difference in the antibody binding towards •OH-GAD65 compared to NT-GAD65 patients with T1D (mean O.D ± S.D, 1.01 ± 0.40 vs 0.80 ± 0.15, p-value = 0.065, respectively).

When comparing the changes in IgG binding towards native or oxPTM-ZnT8 in the 45.3% (24/53) of patients with new-onset patients with T1D positive for ZnT8-Ab, there appeared to be no significant difference between antibody binding to NT- and GLY-ZnT8 (mean O.D ± S.D, 0.7292 ± 0.1873 vs 0.6118 ± 0.2464, p-value= 0.064, respectively) or NT- and HOCl-ZnT8 (mean O.D ± S.D, 0.7292 ± 0.1873 vs 0.6285 ± 0.2505, p-value= 0.1140, respectively). However, there was an apparent significant decrease in IgG binding between NT- and •OH-ZnT8 (mean O.D ± S.D, 0.73 ± 0.19 vs 0.27± 0.14, p <0.0001, respectively). When assessing the antibody response towards NT- or oxPTM-INS, there was a significant decrease with antibody binding towards NT-INS and GLY-INS (mean O.D ± S.D, 0.221 ± 0.108 vs 0.170 ± 0.081, p-value <0.05, respectively). However there was a significant increase in antibody binding seen between NT-INS and HOCl-INS (mean O.D ± S.D, 0.221 ± 0.108 vs 0.363 ± 0.134, p-value <0.0001, respectively), as well as a significant increase between antibody binding towards NT-INS and •OH-INS (mean O.D ± S.D, 0.221 ± 0.108 vs 0.400 ± 0.129, p-value <0.0001, respectively).

The correlation of the induced IgG response towards NT- or oxPTM-GAD65 was assessed by determining the degree of overlap in the patients towards each antigen. Within the total cohort of N=69 patients with new-onset T1D, 17% of patients were positive for an IgG antibody response towards NT-, Gly-. •OH- and HOCl-GAD65. With a total of 41% (29/69) appearing positive for GLY-GAD65 and 39% (27/69) towards •OH-GAD65. However, 45% of T1D were negative for antibodies directed towards all antigens (NT- and oxPTM-GAD65). When assessing antibody responses to NT- and oxPTM-ZnT8, 59% (41/69) of patients were negative for any antibody response, whereas 33% (23/69) were positive for antibodies against NT-GAD65. There were only 4.3% (3/69) patients with T1D who were positive to both NT- and all oxPTM-ZnT8, 25% (17/69) were positive for IgG antibodies to GLY-ZnT8 and HOCl-ZnT8, and only 5.8% (4/69) were positive to •OH-ZnT8.

Discussion

Research has indicated that PTMs may play a role in the progression of autoimmune diseases. PTMs are able to change the secondary and tertiary structure of proteins, impacting self-tolerance and immunogenic mechanisms. Although the majority of PTMs work to better the function of proteins, those that arise spontaneously, as a

result of a breakdown in homeostasis, can be attributed to the development of autoimmune disorders. Multiple sclerosis, rheumatoid arthritis, and juvenile idiopathic arthritis are just a few of the autoimmune disorders with post-translationally modified autoantigens being named as contributors to the progression of these diseases.

This study suggests that oxPTMs to native β-cell antigens alters the subsequent antigenicity of the targeted proteins and contributes to the progression of clinical T1D in people at-risk of developing T1D. When comparing the reactivity between NT-GAD65 and oxPTM-GAD65, this study showed significantly higher antibody reactivity towards GLY-GAD65, HOCl-GAD65 and NT-GAD65 in patients with new- onset T1D compared to healthy controls and people with T2D. However, there was no significant difference between the IgG antibody reaction towards GLY-GAD65, HOCl-GAD65 and NT-GAD65 in patients with T1D, yet certain patients showed an increased reactivity to GLY-GAD65 compared to NT-GAD65. This suggests the possible role of hyperglycemia or dysregulated glucose in modifying GAD65 in the initial stages before the onset of clinical T1D. In comparison, a significant decrease was seen in the antibody response towards oxPTM-ZnT8 compared to NT-ZnT8, indicating that oxidative modifications to ZnT8 may not impact the immunogenicity of the antigen. Controversially, oxPTMs appeared to increase the immunogenicity of insulin. In fact, patients with T1D developed significantly higher antibody responses towards •OH-INS compared to NT-INS. There was also a significant difference in antibody reactivity to •OH-INS in patients with T1D compared to patients with T2D and HC.

These findings may suggest that the oxidative modification of insulin, specifically through the hydroxyl radical, may be an initial target of immunity in patients at-risk of developing T1D. A phenomena known as molecular mimicry has been suggested to play a role in the spread of autoantigenicity. In molecular mimicry, the sequence similarities between the autoantigen instigating the immune response and the native antigen lead to the immune system targeting the native antigen as well. Thus, ensuing epitope spreading and further stimulating the immune system. Upon the initial seroconversion, the immune system may begin to target the remaining beta cell antigens, such as GAD65 and ZnT8, as well as NT-INS due to the sequence similarity between both NT-INS and •OH-INS. However, further studies are required to confirm the findings, with the recruitment of more patients in the initial phases of T1D. Moreover, it is necessary to identify the exact peptides being targeted by the immune system, and those being modified with oxidative radicals in each beta cell antigen. In conclusion, oxPTMs to the beta cell antigens, insulin, GAD65 and ZnT8, alter the immune response in patients with new onset T1D, however further studies are needed in order to determine the role they play in the development of autoimmunity before the onset of clinical T1D.

Study 2: DiabeSARS; A Tale of Two Pandemics

Abstract

Background

The COVID-19 pandemic was the major health concern of the last 3 years. The sudden onset, and widespread of the SARS-CoV-2 virus, necessitated the expedition of research to fully understand the pathogenesis of the virus and to develop effective treatments. Diabetic patients have consistently been associated with severe and potentially fatal disease, more so than their non-diabetic counterparts. Hence, there is a clear need to fully elucidate the underlying pathology that leads to more severe disease in diabetic patients. Studies have previously assessed the role of underlying inflammation and dysregulated glucose in both T1D and T2D in previous viral infections. However, within the COVID-19 pandemic, although diabetic patients only make up a small percentage of the general population, they seem to comprise a similar percentage of critically ill patients, requiring admission to the intensive care unit as their non-diabetic counterparts. Studies have found the dysregulated glucose, regardless of diabetic state, promotes detrimental viral infections. Yet, the role of the endocrine system on immunometabolic outcomes has not been fully elucidated in terms of COVID-19. Increased hyperglycemia in diabetic patients has been associated with increased potential of glycation to native proteins, in fact, glycated hemoglobin (HbA1c) is consistently measured to monitor the development and progress of diabetes. Studies have demonstrated the glycosylation of both the SARS-CoV-2 spike (S) glycoprotein and the angiotensin converting enzyme 2 (ACE2), the main SARS-CoV-2 receptor. The induced glycosylation has been linked to increased virulence of the SARS-CoV-2 virus, as well as increased host-cell infiltration potential. However, the impact of non-enzymatic glycation, a potential outcome due to the elevated levels of glucose in an overly distressed system, has not been fully elucidated. Additionally, the efficacy of the developed SARS-CoV-2 mRNA vaccine (Pfizer, BioNtech) has not been assessed in terms of glucose control in diabetic patients.

Hypothesis

The main hypothesis is that dysregulated glucose levels may induce glycation of the SARS-CoV-2 S protein, altering the virulence of the disease. With one of the main focuses of this study to determine whether glucose regulation plays a role in vaccine efficacy and, in turn, immune protection against COVID-19.

Aim 1. To induce glycation of the S protein and asses ACE2 binding to both native (NT-) and glycated (GLY-) S protein.

Aim 2. To determine the impact of antibody binding to NT- and GLY-S protein in previous COVID-19 patients.

Aim 3. To evaluate the role of glucose levels and monitoring on the protective immune response in patients following the administration of the SARS-CoV-2 mRNA vaccine (Pfizer-BioNTech, BNT162b2).

Aim 4. In order to better understand the role of hyperglycemia and diabetes in the adverse outcomes of COVID-19, the fourth aim of this study is to evaluate the clinical risk of diabetes and glucose levels on mortality in patients with COVID-19.

Methods

Antibody response to NT- or GLY-S protein in patients with COVID-19 and vaccinated patients

COVID-19 patients with and without diabetes were recruited for this study from specifically designated COVID-19 wards. For the vaccine study, patients were screened and recruited from the Endocrinology and Diabetology unit at Policlinico Campus Biomedico di Roma. With n= 26 patients being T1D and n=32 being diagnosed with T2D. The inclusion criteria for the study were patients >18 years old, scheduled to receive the SARs-CoV-2 mRNA vaccine (Pfizer-BioNTech), signing informed consent, having a diagnosis of T1D or T2D for more than 3 months, and using at least two anti-diabetic drugs in the case of T2D according to the vaccine priority criteria. Demographic and clinical data was collected at each time point involved in the study for all the patients recruited. The study covered a total of 6 months with the following timepoints:

T0 (baseline): before the administration of SARs-CoV-2 mRNA vaccine (within 3 days of the first dose)

T1: 21 days after the first dose (day of the second dose)

T2: 35 days from baseline (T0)

T3: 90 days from baseline (T0)

T4: 180 days from baseline (T0).

The SARS-CoV-2 S protein (0.450 mg/mL) was modified via glycation with equal volumes of 0.5 M D-ribose (sigma), this was incubated overnight at 37ºC and stored short term at 4ºC. The induced modifications were monitored by SDS-PAGE analysis, whereby 5 µg of NT- or GLY-S protein were loaded into the gel wells with equal volumes of Laemmli loading buffer with or without β-mercaptoethanol to promote reducing conditions. The gels were imaged with the Chemi-Doc imaging system from Bio-Rad and quantified with Imagej software. Changes in ACE2 binding towards NT- or GLY-S protein was determined via a homemade ELISA, whereby increasing dilutions of ACE2 (2 µg/mL-0.25 µg/mL) were measured against the same concentration of NT- and GLY-S protein (1 µg/mL). Moreover, COVID-19 patients with and without diabetes were assessed via a homemade ELISA for the antibody response towards NT- and GLY-S protein. The antibody responses were then analyzed depending on the fructosamine levels, measured via a kit (ab228558, abcam). The antibody response induced after immunization with the SARS-CoV-2 mRNA vaccine was measured via a homemade ELISA devised to analyze the IgG response towards NT- or GLY-S protein. Serum samples were collected and assessed at each timepoint and compared to the results of controls without diabetes.

The level of neutralization antibodies was measured via a devised neutralization assay using live SARS-CoV-2 (Vero E6 cells).

Devising a Clinical Risk Score to Assess in-hospital Death from COVID-19

Data from patients for devising the clinical risk score was collected retrospectively from 417 COVID-19 patients admitted to Jaber Al-Ahmed Hospital in Kuwait between February 24th and May 3rd, 2020. Due to the emergency state of the COVID-19 pandemic, the need for signed consent was waived by the ethical committee from the Ministry of Health in Kuwait. Setting the primary outcome as in-hospital death, a series of multivariant logistical regression models were performed to identify independent factors that may be prognostic for the primary outcome. The models were created by adding or removing variables individually depending on the results of the previous logistic regressions, with variables showing a p-value<0.1, being retained in the score. The independent predictive variables included in the final model were gender, asthma, glucose categories, and non-Kuwaiti national. Weighted points were assigned to significant risk factors proportional to their beta regression coefficient values. The effectiveness of the risk score to predict mortality in patients with COVID-19 was analyzed via receiver operating characteristic (ROC) curves, with an AUC of 0.5 or less was taken as insignificant Youden's index was applied to set a cut-off for mortality prediction. Significance was set as a two-tailed p-value <0.05. The score was built using SPSS (IBM Corp. IBM SPSS Statistics for Windows, Version 21.0. Released 2012. Armonk, NY: IBM Corp.). The score was internally validated by a Kuwaiti COVID-19 cohort of N=923 patients, and externally validated using the CoViDiab cohort from Italy (N= 178).

Results

Antibody response to NT- or GLY-S protein in COVID-19 patients and vaccinated patients

Upon assessing the binding of NT- and GLY-S protein (1µg/mL) to serial concentrations of the SARS-CoV-2 receptor ACE2 (2.0 µg/mL to 0.25 µg/mL) there was diminished binding of ACE2 to NT-S vs GLY-S, however this was not significant (mean ± S.D, 0.1393 ± 0.1732 vs 0.1943 ± 0.2355, p-value= 0.6026, respective). Fructosamine levels, which are a short-term assessment of glucose control, were measured in the total COVID-19 patient cohort (N=46). Upon stratification of fructosamine levels, patients with <563 µmol/L had no significant difference between IgG levels to NT- or GLY-S, yet patients with fructosamine levels >563 µmol/L had a significant difference between NT- and GLY-S (mean O.D ± S.D= 0.7945 ± 0.2564 vs 0.6155 ± 0.2369, *p-value= 0.0078*, respectively). When correlating fructosamine levels with the total cohort (N=46), there appeared to be an overall negative correlation to both NT- and GLY-S, yet this was not significant (r= -0.1848, p-value= 0.2188 vs r= -0.2203, p-value= 0.1413, respectively). In diabetic patients (n=22) there appeared to be no correlation with fructosamine levels to the IgG response to either NT- or GLY-S protein (r= 0.04029, p-value= 0.8587 vs r= 0.010201, p-value= 0.9640). However, in the case of non-diabetic COVID-19 patients, there was a strong

negative correlation between fructosamine levels and the immune response to NT- and GLY-S (r= -0.3824, p= 0.1462 vs r=-0.4042, p= 0.0501, respectively).

This study attempted to assess the IgG response towards the COVID-19 Pfizer BioNTech mRNA vaccine in terms of continuous glucose monitoring (CGM) data from N=10 patients with T1D with available CGM profiles. The key measurements assessed were Time-in-range (TIR), which is the percentage of time within a 24 hour period that a patient is within the ideal glucose range, Time-above-range (TAR), which is the percentage of time a patient is above the ideal glucose range in a 24 hour period, and Time-below-range (TBR), which is the percentage of time a patient is below their ideal glucose range. When determining the overall area under the curve (AUC) of the IgG response over all study timepoints (T0-T4) and correlating it with the average TIR, there appeared to be a strong correlation with AUC IgG response and TIR to both NT- and GLY-S protein (r= 0.8082, *p-value= 0.0084* vs r= 0.7996, *p-value= 0.0097*, respectively), with a significant difference between the AUC IgG to NT- and GLY-S protein (*p-value= 0.0034)*. When correlating the AUC IgG of both NT- and GLY-S protein to the average TAR over all study timepoints (T0-T4), there was a strong negative correlation (r= -0.7926, p-value= 0.0108 vs r= -0.7430, p-value= 0.0218, respectively) There was no correlation with HbA1c at T0 or average TBR with AUC IgG response towards native or GLY-S protein**.** When dividing patients with T1D with CGM data (N=13) based on their recommended glucose targets, (TIR > 70% and TBR <25%), there appeared to be a stronger neutralizing antibody response to the native SARs-CoV-2 spike protein who in patients with T1D had a TIR>70% than those who did not (p<0.0001). Furthermore, when assessing the neutralizing antibody response against TBR measurements, patients who had a TBR<25% were more likely to have a stronger neutralizing antibody response (p=0.008), this was seen regardless of HbA1c levels.

Devising a Clinical Risk Score to Assess in-hospital Death from COVID-19

The score was built by assessing the significance of several predictive variables against the primary outcome (in-hospital mortality). The final score included asthma, gender (male), nationality (non-Kuwaiti national), and blood glucose levels (either between 7.0-11.1 mmol/L or >11.1 mmol/L) as independent predictors of mortality in COVID-19. A point system was given to each predictive variable based on the beta coefficients allocated to each variable. The cut-off of the score to predict death was 5.5, showing a specificity of 86.3% and sensitivity of 75% (AUC= 0.901). The clinical risk score requires internal and external validation to assess the potential to predict the primary outcome. Two cohorts were used for internal validation, the initial N=417 Kuwaiti COVID-19 group used to build the score and a separate cohort of N=923 Kuwaiti COVID-19 patients admitted from May 4th to August 26th, 2020, both admitted within one COVID-19 center within Kuwait. External validation was performed using an N=178 CoViDiab Italian cohort. The score was calculated for each patient and then tested against the primary outcome (in-hospital mortality from COVID-19); the score was then plotted as a ROC curve with the AUC calculated. The AUC showed 0.901 ± 0.20 fit for the score for the 417 Kuwaiti cohort, 0.826 ± 0.91 fit for the score for the 923 Kuwaiti cohort, and a 0.687 ± 0.06 fit for the score

for the CoViDiab cohort, with respective negative predictive values of 95.4%, 93.9%, and 94.1%.

Conclusions

Diabetic patients are characterized by hyperglycemia and chronic low-grade inflammation. Upon viral infection, these patients present with more exacerbated immune responses, that may lead to severe disease, ICU admission, and potentially death. The findings in this study suggest that dysregulated fructosamine levels are more strongly correlated with a decreased antibody response towards NT- and GLY-S protein of SARS-CoV-2. Additionally, when assessing the IgG and neutralization antibody response in patients with T1D in association with CGM data, there appeared to be a stronger association with more improved TIR and TAR glucose measurements and a stronger antibody response. This again suggests that better controlled glucose measurements aid in improving the protective immune response towards SARS-COV-2. Finally, the development of the clinical risk score demonstrated that elevated glucose was a stronger predictor of negative outcomes and mortality in COVID-19 related infections than diabetes. In fact, the addition of glucose measurements removed diabetic state as an independent predictor of in-hospital death. In conclusion, maintaining key glucose targets may aid in preventing detrimental outcomes towards not only COVID-19 and other viral infections.

Abbreviations

•OH: Hydroxyl radical

4-HNE: 4-hydroxynonenal

AABs: Autoantibodies

ACE2: angiotensin converting enzyme 2.

Acetyl CoA: Acetyl Coenzyme A

ADA: American Diabetes Association

AGEs: advanced glycated end-products

AITD: autoimmune thyroid disease

APCs: antigen presenting cells.

APS: autoimmune polyendocrine syndrome

ATP: adenosine triphosphate

AUC: area under the curve

CML: Carboxymethyl-Lysine

CNS: central nervous system

COVID-19: Coronavirus disease 2019

CTC1: cluster 1 epitope sites

CTC2: the cluster 2 epitope sites

CTLA4: cytotoxic T-lymphocyte associated protein 4.

DAISY: Diabetes and Autoimmunity Study in the Young

DAMPS: danger-associated molecular patterns

Diabetes Mellitus (DM)

DIPP: Type 1 Diabetes Prediction and Prevention study

DKA: diabetic ketoacidosis

E: envelope protein

ER: Endoplasmic reticulum

ETC: mitochondrial electron transport chain

FAD: flavin adenine dinucleotide

FBG: fasting blood glucose

FPG: fasting plasma glucose

GABA: γ-aminobutyric-acid

GAD65: Glutamate Decarboxylase 65

GADA: GAD65 autoantibodies

GLY: Glycated

GSIS: glucose-stimulated insulin secretion

GWAS: Genome wide association studies

H_2O_2: hydrogen peroxide

HbA1c: Glycated Hemoglobin

HLA: Human Leukocyte Antigen

HOCl: Hypochloric acid modified.

IA-2: Islet Antigen 2

IAA: Insulin autoantibodies

IBD: inflammatory bowel disease

ICU: Intensive care unit

IFIH1: interferon-induced with helicase C domain 1

IFN: interferon

IL: interleukin

IMDIAB: Immunotherapy Diabetes group

INS: Insulin

INS-VNTR: insulin variable tandem repeat

IRFs: interferon regulatory factors

LADA: latent autoimmune diabetes in adults

LADY: latent autoimmune diabetes in the youth

M: membrane protein

MAPKs: mitogen-activated protein kinases

MBP: myelin basic protein

MDA: malondialdehyde

MERS: Middle Eastern Respiratory Syndrome

MHC: major histocompatibility complex

MS: Multiple Sclerosis

N: nucleocapsid protein

NADPH: nicotinamide adenine dinucleotide phosphate oxidase

NETs: neutrophil extracellular traps

NF_{KB}: nuclear factor- kappa B

NOD: non-obese diabetic mice

NSPs: non-structural proteins

NT: Native

O.D.: optical density

$O_2^{-\bullet}$: superoxide anion

ORFs: open reading frames

OSEs: oxidation specific epitopes

OSEs: oxidation specific epitopes

oxLDL: oxidized low-density lipoproteins

oxPTM: oxidative post translational modifications

PAD: peptidyl arginine deiminase

PAMPS: pathogen-associated molecular patterns

PICU: pediatric intensive care unit

PLP: pyridoxal-5'-phosphate

PTMs: post translational modifications.

PTPN2: protein tyrosine phosphatase non-receptor 2

PTPN22: protein tyrosine phosphatase non-receptor 22

RA: Rheumatoid Arthritis

RAGE: receptor of advanced glycation end-products

RAS: renin angiotensin system

RBA: radio-binding assay

RBD: Radio-binding domain

ROC: receiver operating characteristic curve

ROS: Reactive oxygen species

S: spike glycoprotein

SARS: severe acute respiratory syndrome

SLE: Systemic Lupus Erythematosus

SNP: Single nucleotide polymorphism

SPLV: synaptic like vesicles

SPS: stiff person's syndrome

T1D: Type 1 Diabetes

T2D: Type 2 Diabetes

TCA: mitochondrial tricarboxylic acid

TGN: Trans-Golgi network

TLRs: toll-like receptors

TMPRSS2: transmembrane protease serine protease 2

T_{reg} cells: T regulatory cells

tTG: tissue transglutaminase

UV: Ultra-radiation

ZnT8: Zinc Transporter 8

ZnT8A: ZnT8 autoantibodies

β-cells: Beta cells

Table of Contents

Chapter 1. Introduction

1.1.0 Study 1 Introduction

1.1.1 Background

Diabetes mellitus (DM) is an endocrine condition, characterized by dysregulated glucose metabolism. The beta cells (β-cells) located in the pancreatic islets of Langerhans are responsible for the production, storage, and secretion of insulin. Insulin is the main hormone responsible for the regulation of glucose metabolism. In DM, there is a dysregulation of glucose metabolism, either due to the impairment of insulin production or insulin resistance. As of 2017, the prevalence of adult diabetes was around 8.8%, with an expected increase to 9.9% in 2045, implying a 45% increase rate. There are several forms of diabetes characterized, yet DM can be divided into two major types, these are type 1 diabetes (T1D) and type 2 diabetes (T2D) [1, 2]. Although both types of diabetes present with hyperglycemia and require constant monitoring and control, their clinical presentations differ. T1D is often diagnosed in younger (below 20 years of age) and normal weight individuals. In comparison, T2D tends to be diagnosed in overweight or obese and older (above 40 years of age) individuals. The progression to T1D is typically due to the development of autoantibodies (AABs) targeting the pancreatic β-cells in genetically predisposed individuals, while the progression to T2D is related to sedentary lifestyle and diet, as well as an underlying genetic predisposition (figure 1) [3].

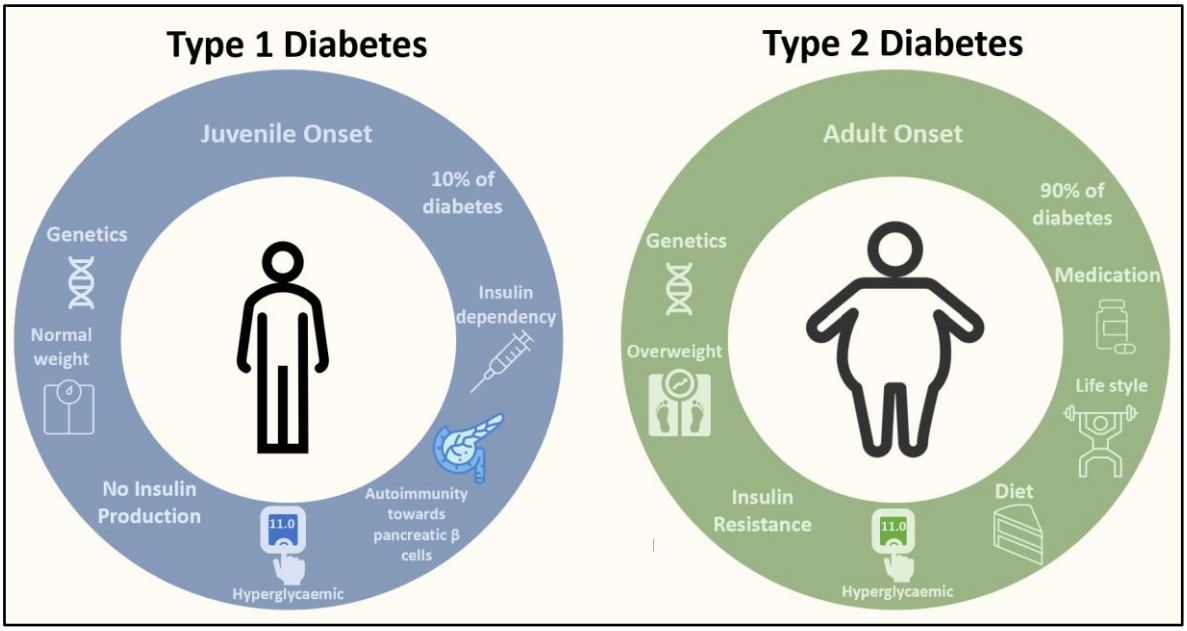

Figure 1. Main differences between type 1 and type 2 diabetes. T1D is characterized by autoimmune destruction of pancreatic β-cells in genetically predisposed individuals. Patients are typical normal weight, juvenile, and are dependent on exogenous insulin. On the other hand, T2D is a result of insulin resistance in older and typically overweight individuals, with a genetic predisposition. Both forms of diabetes present with hyperglycemia and require immediate intervention and treatment to avoid severe complications of diabetes [3].

T1D is an autoimmune disorder characterized by the selective destruction of pancreatic β-cells by the immune system. This leads to depletion of β-cell mass, causing little to no insulin production and secretion. The ensuing insulitis, a hallmark of T1D, is believed to be predominantly mediated by auto reactive T-cells (figure 2)[4]. T1D is typically diagnosed in children or young adults, who tend to present with a fasting blood glucose greater than 7.0 mmol/L, and/or a glycated hemoglobin (HbA1c) greater than 6.5% at least two different time points [5, 6]. Children also tend to present with ketoacidosis, polyuria, polydipsia and weight loss [6]. However, adult onset T1D may occur, with the progression of clinically relevant T1D and overt β-cell destruction being slower and milder than childhood onset T1D [7]. The major diagnostic factor for T1D is the detection of AABs to key β-cell antigens, namely AABs to insulin (INS), islet antigen-2 (IA-2), glutamic acid decarboxylase 65 (GAD65) and zinc transporter 8 (ZnT8) [6].

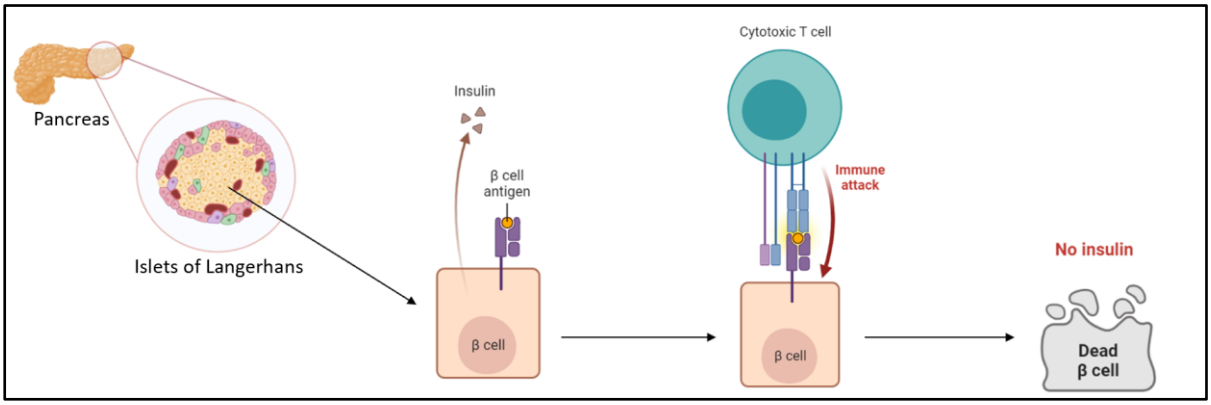

Figure 2. Schematic illustration of the progression of Type 1 Diabetes. Pancreatic β-cells within the Islets of Langerhans are responsible for the production and secretion of insulin. In T1D susceptible individuals, cytotoxic T cells selectively target β-cell specific peptides and antigens, destroying pancreatic β-cells. This leads to a depletion of overall β-cell mass and little to no insulin synthesis or secretion.

It is important to note that environmental factors, such as diet, vitamin D levels or viral infections are suggested to play a role in the development of T1D [8], alongside genetic factors. The genetic polymorphisms associated with increased T1D risk have been defined circa 50 years ago, localized mainly in the class II human leukocyte antigen (HLA) region. More recently, there are around 60 non-HLA loci that have been associated with T1D susceptibility, with research showing that the insulin variable tandem repeat (*INS-VNTR)* gene confers the highest non-HLA risk [9]. Although individuals may have a strong family history of T1D and a genetic susceptibility, they do not always progress to clinically relevant T1D. Hence, there is a need to develop more reliable biomarkers and predictors of T1D in at-risk individuals with higher specificity and sensitivity than the biomarkers currently in use [10].

1.1.2 Reactive Oxygen Species in Health and Disease

Reactive oxygen species (ROS) are a small group of highly reactive molecules that, when kept in physiological levels, play key roles in normal biological development

[11]. Such as, in cellular signaling, the normal mechanism of phagocytes in response to intracellular pathogens, and synthesis of thyroid hormones, to name a few [12]. Although ROS play key roles in normal cellular processes, when there is a major imbalance between the generation and the removal of ROS, this leads to accumulation of ROS and ensuing oxidative stress [13]. Increases in ROS production can be triggered exogenously via ultraviolet (UV) irradiation, hyperthermia, or chemical toxins, or endogenously through senescence pathways, changes in metabolism or inflammation. In fact, when host defenses are triggered, an oxidative burst is seen with high ROS levels to eliminate invading pathogens and forming neutrophil extracellular traps (NETs) [14]. Highly conserved redox reactions produce the major ROS *in vivo*, these are hydrogen peroxide (H_2O_2), the hydroxyl radical (•OH), and the superoxide anion ($O_2^{-\bullet}$) [12].

The oxidants differ greatly in their reactivity and their induced damage. Superoxide is the result of the addition of one electron to oxygen and it can be enzymatically converted by cytosolic or mitochondrial superoxide dismutase to produce H_2O_2. Hydrogen peroxide is relatively stable, making it one of the major ROS involved in redox signally [12]. The hydroxyl radical is produced from the decomposition of H_2O_2 in the presence of a metal ion, in a process known as the Fenton reaction, or from high energy radiation, the hydroxyl radical can oxidize nearly all biological targets [15].

$$H_2O_2 + Fe^{2+} \rightarrow \bullet OH + OH^- + Fe^{3+} \quad [16]$$

Physiological production of ROS stems from two main pathways, the nicotinamide adenine dinucleotide phosphate oxidase (NADPH oxidase, NOX) complex, most notably NOX2, and the mitochondria [17]. The NADPH enzyme complex catalyzes the formation of superoxide by transferring an electron from oxygen to NADPH.

$$NADPH + 2O_2 \leftrightarrow NADP^+ + 2O_2^- + H^+ \text{ [18].}$$

There are 7 enzymes within the NOX enzyme family in mammals, these are NOX 1-5 and DUOX 1-2. NOX enzymes are made up of six transmembrane units, that anchor two heme groups. The heme groups function in mediating the transmembrane transfer from NADPH/$FADH_2$ to molecular O_2. All NOX enzymes also contain an intracellular C-terminal dehydrogenase domain, consisting of FAD (flavin adenine dinucleotide) and NADPH binding sites. These enzymes are widely dispersed throughout the system, they were first identified as major players in phagocytic killing within the oxidative host immune defense system [19]. NOX2 was the first enzyme discovered within the NOX complex and is made up of six different subunits. Namely, the catalytic gp1phox and p22phox subunits, which are localized to the plasma membrane, and the regulatory subunits; p40phox, p47phox, p67phox and small G-protein Rac 1/2, localized to cytosolic components [18].

The mitochondrial electron transport chain (ETC) is another major contributor of ROS production, mainly due to its role in producing oxidative ATP (adenosine triphosphate) [20]. Wong et al., have previously shown in C2C12 myoblasts that around 45% of cellular ROS production comes from the mitochondria and 40% from the NOX complex [21, 22]. Complex I and complex III of the ETC is currently

believed to be the major sources of ROS, such as superoxide anion. Complex I catalyzes the transport of two electrons from NADH to the coenzyme Q (quinone pool), this in turn transfers two protons to the inner mitochondrial membrane, contributing to the proton shift required for ATP production and the final reduction of molecular oxygen [23]. Studies have suggested 11 distinct sites in the mitochondrial ETC involved in ROS production. The main sites are, the flavin site of complex I, the ubiquinone site of complex I, the flavin site of complex II, and the ubiquinone site of complex III [21].

Within β-cells specifically, INS secretion is tightly regulated by mitochondrial function, specifically through ATP production and intracellular calcium regulation. In a normal postprandial state, β-cells detect and transport glucose *via* glucose transporters. The glucose is then phosphorylated to glucose-6-phosphate, which is subsequently glycolyzed to yield pyruvate and then Acetyl Coenzyme A (Acetyl CoA). Acetyl CoA is pushed into the mitochondrial tricarboxylic acid (TCA) cycle to generate ATP by oxidative phosphorylation [24]. Due to an imbalance of antioxidants and ROS, the resultant oxidative stress can induce both cellular and extracellular damage, leading to irreversible DNA and RNA damage and modifications, protein oxidation or lipid peroxidation [14, 17].

1.1.3 Autoimmunity to Post Translationally Modified Antigens

Many studies have attempted to understand the complex mechanism that leads to the breakdown of immune tolerance in autoimmune disorders. The mechanism is believed to incorporate both environmental and genetic factors, as well as dysregulated T and B cells [25]. Within an *normal* system, immune tolerance is the ability of the immune system to remain inactive in response to specific antigens, with self-tolerance being the ability of the immune system to distinguish between self and non-self-antigens. Typically, immune tolerance is achieved through two main processes, central and peripheral tolerance [26]. In central tolerance, autoreactive T and B cells are presented and destroyed within the thymus and bone marrow, respectively. Autoreactive lymphocytes that escape central tolerance are then susceptible to deletion or suppression via peripheral tolerance. The breakdown of immune tolerance has been associated with the pathophysiology of autoimmune disorders.

In recent years, research has been dedicated to the impact of post translational modifications (PTMs) of native antigens and their impact on the loss of immune tolerance [25]. Typically, PTMs are a normal part of biological physiology, with the induction of enzymatic or non-enzymatic modifications being necessary for the final configuration and essential function of a protein. These modified proteins are presented to the immune system during negative and positive selection in the periphery, thus not eliciting an immune response. However, the rise of cell specific PTMs due to abnormal or pathologic processes, may alter protein structure and function. These proteins are typically not presented during negative selection, and in turn go unrecognized by the immune system [27]. In autoimmune disorders, as well as disorders with underlying inflammation as a key feature, increased oxidative stress is believed to induce oxidative PTMs (oxPTMs) to the native antigens,

resulting in neo-epitopes, or “new antigens” that are foreign to the immune system [28].

Oxidized phospholipids can be induced via lipid peroxidation of poly unsaturated fatty acids (PUFA) located in cellular membranes and secretory vesicles. Due to the abundance of PUFA, they are susceptible to enzymatic lipid peroxidation through cyclooxygenases, cytochrome p450 and lipoxygenases, or non-enzymatic processes via ROS and metal ion or hemin catalysts. This oxidation can instigate the formation of oxidized phospholipids and degradation products, which can in turn induce adducts with amino phospholipids or with the amino group of lysine residues creating neo-epitopes. For instance, the oxidation of the PUFA, phosphatidylcholine, causes fragmentation of the phospholipid, in turn generating reactive breakdown products such as 4-hydroxynonenal (4-HNE) and malondialdehyde (MDA) [14].

There are several mechanisms by which neo-epitopes can induce autoimmunity, such as molecular mimicry, epitope spreading and coupling of an autoantigen to an exogenous antigen. In molecular mimicry, the sequence similarities between neo-epitopes or “foreign epitopes” and self-antigens, would induce the activation of autoreactive T and B cells in susceptible individuals [29]. Furthermore, molecular mimicry can be induced upon inflammation in response to a bacterial or viral infection, resulting in autoimmunity due to cross reactive antigens in genetically susceptible individuals [30]. When taking immune tolerance into consideration, an immune response is typically directed towards one or two dominant epitopes in a protein. Epitope spreading occurs when a sub-dominant epitope on that same protein begins to elicit an immune response, usually this occurs in response to tissue damage [31].

Neo-epitopes can behave as danger-associated or pathogen-associated molecular patterns (DAMPS and PAMPS, respectively) [25]. The pattern recognition theory suggests that cells express unique pattern recognition receptors (PRRs) that can identify PAMPs. These receptors include the toll-like receptors (TLRs) found on the surface of antigen presenting cells (APCs), indirectly stimulating the adaptive immune response through the expression and promotion of co-stimulatory molecules and inflammatory cytokines [32]. DAMPs, on the other hand, are believed to be products of dysfunctional metabolism of stressed or necrotic cells and act as alarm signals for the innate immune system [33]. Both PAMPs and DAMPs can stimulate an immune response via the classical PRRs activation, such as nod-like receptors, scavenger receptors, TLR-4, and receptor of advanced glycation end products (RAGE) [25, 32]. The DAMP and PAMP ability to promote cytokine production amplifies the local inflammatory response, instigating a vicious cycle [33, 34].

Furthermore, neo-epitopes have been shown to be targets of natural IgM antibodies [25]. Natural antibodies are predominantly IgM antibodies that are pre-existing without previous exposure to infection or pathogens. They are typically of fetal origin and shown to bind to oxidation specific epitopes (OSEs). Studies have shown the presence of IgM antibodies to OSEs in thromboembolic cardiovascular diseases, specifically to oxidative low-density lipoproteins (oxLDLs) in atherosclerotic plaques [35].

Several autoimmune diseases have shown the breakdown of tolerance and initiation of autoimmunity may be attributed to PTMs and neo-epitopes. Such as in celiac disease, where loss of immune tolerance has been seen due to deamidation of gluten peptides by tissue transglutaminase (tTG) [36]. As well as in rheumatoid arthritis (RA), where autoantigens have been detected towards citrullinated synovial joint proteins [37] and hydroxylated or glycosylated collagen type II [38]. The detection of AABs to citrullinated proteins in RA may occur years before disease onset, leading to detection of these AABs being diagnostic and a marker for disease progression [25]. The study of NETs in systemic lupus erythematosus (SLE) has been an area of concern, with studies showing that the acetylation of histones (H2B) is a target of IgGs within SLE patients [39]. Furthermore, antibodies to oxLDLs have been found in the serum of patients with SLE [40]. Multiple sclerosis (MS) is a neuroinflammatory disorder due to the axonal demyelination of axons mediated by autoreactive B and T cells. However, studies have shown that acetylated myelin basic protein (MBP) peptide (Ac 1-11) can stimulate autoreactive T and B cells in murine models [41]. Table 1 shows a summary of the AABs directed towards post translationally modified antigens in autoimmune disorders.

AUTOIMMUNE DISEASE	PTM	ANTIGEN	REFERENCE
RHEUMATOID ARTHRITIS (RA)	Citrullination Hydroxylation Glycosylation	Collagen Type II	[37, 38]
CELIAC DISEASE (CD)	Deamidation	Gliadin	[36, 42]
SYSTEMIC LUPUS ERYTHEMATOSUS (SLE)	Phosphorylation Acetylation Oxidation	Nucleophosmin Histone H2B oxLDL	[39, 40]
MULTIPLE SCLEROSIS (MS)	Acetylation	MBP	[41]

Table 1. Summary of autoantibodies directed towards post translationally modified antigens in select autoimmune disorders. Adapted from Yang et al [41].

1.1.4 Type 1 Diabetes and Autoantigens

In children, T1D is diagnosed based on the classical symptoms of diabetes, such as polydipsia, polyuria, exhaustion, and drastic weight loss. However, there is typically an average of two-week delay between symptom development and diagnosis, whereby 80% of children develop life threatening diabetic ketoacidosis (DKA) [43]. However, differentiating T1D from T2D is mainly done by detecting specific AABs to native β-cell antigens via a radio-binding assay (RBA) [44].Studies have demonstrated that native pancreatic β-cell antigens are targets of the immune response in T1D, wirh the induced antigen specific immune response appears to be a major factor in β-cell destruction [45].

However, the initiation of autoimmunity and β-cell destruction is not fully known, it is currently speculated that native β-cell antigens are presented by antigen presentation cells (APCs) to naïve T cells, which mature to autoreactive CD4+ T cells and T regulatory cells (T_{reg} cells). Activated autoreactive CD4+ T cells go on to secrete cytokines, in turn activating pancreatic β-cell specific CD8+ T cells, which

secrete further cytokines and recruit more T cells and macrophages. This ensues in a cycle of cytokine production, immune cell recruitment and inflammation, resulting in the destruction and depletion of β-cells [46]. The major targets of the immune system in T1D are INS, GAD65, IA-2, and ZnT8, with AABs to insulin (IAA) and GAD65 (GADA) typically being the first to appear in early childhood T1D [5]. Patients presenting with two or more AABs to native pancreatic β-cell antigens are at an increased risk of progressing to T1D [45].

Endesfelder et al., as part of BABYDIAB, reported that in an initial study of 88 children at-risk of T1D who first seroconvert to IAA positivity and then went on to develop a minimum of two other AABs (n=57), had a 76% increased 10-year risk of developing T1D in those who remained IAA-positive. In comparison, of those 57 children, there was a 23% risk of developing T1D in patients who in the follow-up were IAA-negative [47]. The heterogeneity of T1D increases the difficulty in predicting and monitoring the progression of the disease, leading to studies attempting to identify differential characteristics for predicting T1D. Nieto et al, were able to associate the presence of IAA with younger age, decreased HbA1c levels and higher tTGA titers, IA-2A with older age, and GADA was linked to a lower likelihood of increased tTGA levels and associated with the female sex [48].

Studies of first-degree relatives of T1D and individuals at-risk showed that seroconversion to AAB positivity tends to be months or even years before clinical onset of the disease [44]. This has prompted the development of a widely agreed upon staging for T1D (figure 3), whereby in the first stage individuals at-risk of developing T1D have detectable levels of AABs but remain normoglycemic. In the second stage, β-cell mass begins to deplete, and patients show signs of dysglycemia, but have no other symptoms of diabetes. Finally, in the third stage patients are completely symptomatic with little or no β-cell mass, and, subsequently, little to no insulin production and secretion [49].

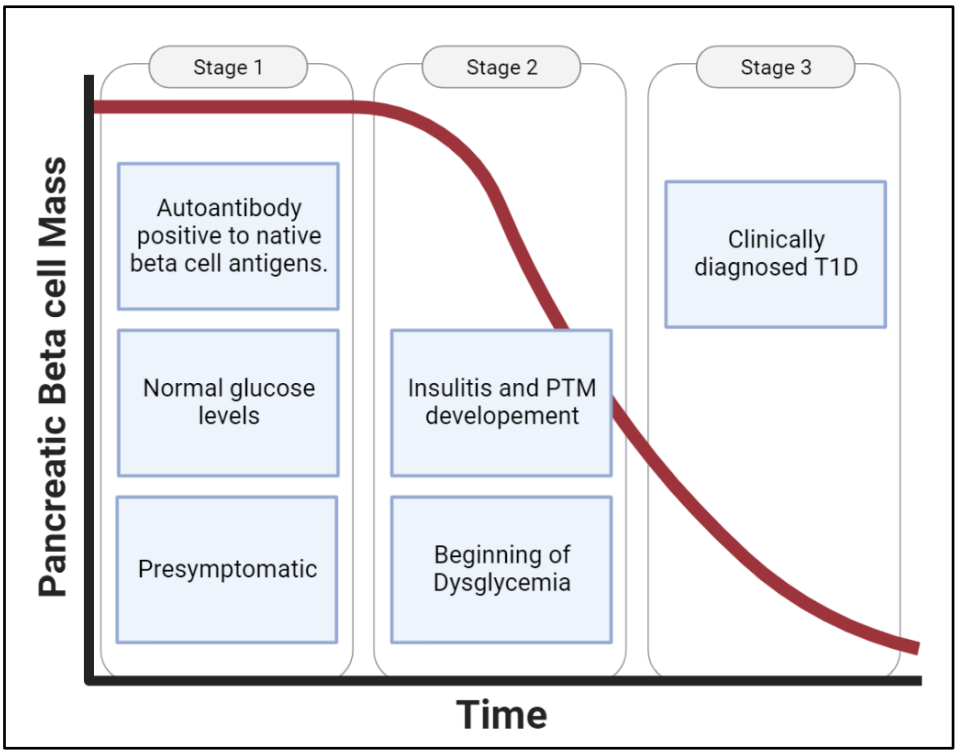

Figure 3. Proposed Staging of Type 1 Diabetes. The figure shows the proposed staging for T1D in genetically susceptible at-risk individuals. In the first stage, at-risk individuals are suggested to be subjected to a triggering event, which leads to the breakdown of immune tolerance and development of an autoantibody response to pancreatic β-cell antigens, namely INS, GAD65, ZnT8 and IA-2. The second stage shows the beginning of β-cell mass depletion, with full-blown insulitis and PTM developments, individuals at this stage remain pre-symptomatic with signs of dysglycemia. In the third and final stage, here individuals show clinical signs and symptoms of T1D, hyperglycemia and little to no insulin production and secretion. Figure adapted from proposed model by Insel et al [49].

Although the staging of T1D has been widely agreed upon (figure 3), the appearance of AABs being current gold-standard for monitoring at-risk individuals and the progression of T1D may need re-evaluation. Studies have shown that the appearance of AABs to one or more of the native β-cell antigens in the sera of at-risk individuals, may not equate to the progression to clinical T1D. Hence, there is a need for developing more specific biomarkers that can more accurately and sensitively predict progression to T1D and aid in the development of treatment targets.

1.1.4.1 Insulin as an Autoantigen

The initial discovery of insulin in 1921 marked the turning point in the treatment of diabetes. Since then, insulin has been subject to years of research to fully elucidate its function in metabolism and diabetes [50]. Insulin is a hormone produced and secreted by the pancreatic β-cells located within the islets of Langerhans. With its main role to regulate the levels of fats and carbohydrates within the system [51]. Insulin is a globular protein with a molecular weight of 5808 Da, it is comprised of 2 chains, the A chain (made of 21 residues) and the B chain (30 residues) bound by 2 disulfide bridges.

In humans, the *INS* gene initially codes for a 110 amino acid polypeptide preproinsulin, the transcription and translation of which is tightly regulated. Preproinsulin consists of a hydrophobic N-terminal signal peptide that mainly functions in interacting with cytosolic ribonucleic signal recognition particles (SRP) [52]. SRP facilitates the translocation of preproinsulin to the endoplasmic reticulum (ER), where it is then cleaved to yield proinsulin. The proinsulin is folded within the ER to its proper conformation with 3 disulfide bonds, this is then transported to the Trans-Golgi network (TGN), with the aid of the cellular endopeptidases' prohormone convertase 1 and 2 (PC1 and PC2) and exoprotease carboxypeptidase E. Proinsulin is cleaved and converted into its active form, yielding insulin (figure 4) and C-peptide (or connector peptide) [53]. Proinsulin is cleaved and converted into insulin and the C-peptide within insulin secretory granules at a 1:1 molar ratio [54].

The resulting insulin and C-peptide are then stored within specified insulin granules in β-cells, facilitating a myriad of processes related to secretory granule maturation. This includes discerning elimination of soluble components, luminal acidification and zinc ion (Zn^{2+}) mediated crystallization of insulin [54].The synthesis, storage, and release of insulin is regulated by multiple factors, with fluctuations in glucose levels being a key modulator of insulin gene transcription and translation [52]. This process has been coined as glucose-stimulated insulin secretion (GSIS), which comprises two key pathways, the triggering, and the amplifying pathway [55].

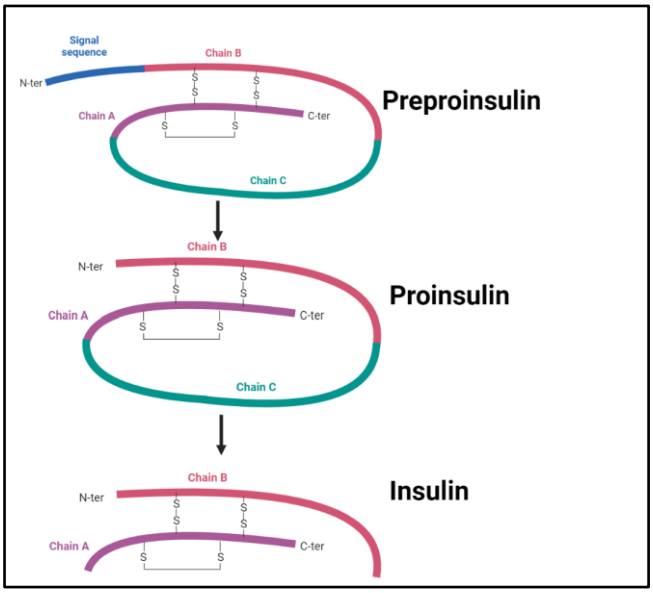

Figure 4. Formation and structure of Insulin from Preproinsulin. Insulin is initially synthesized as preproinsulin in the secretory granules with its transcription and translation tightly regulated. Preproinsulin is cleaved to proinsulin in the endoplasmic reticulum, which is then cleaved to the active form Insulin. Insulin is stored in secretory granules within the β-cells, until it is secreted in response to glucose and other nutrient signals (such as fatty acids and amino acids) [52].

The triggering pathway is induced upon transport and metabolism of glucose, generating ATP, and causing the closure of ATP sensitive potassium (K_{ATP}) channels. Consequently, this activates voltage-gated calcium (Ca^{2+}) ion channels,

the influx of Ca^{2+} ions trigger the exocytosis of readily available insulin secretory granules to the plasma membrane. The secretory granule is then able to fuse to the membrane via tetrameric complexed proteins, facilitating the formation of fusion pores by which insulin is released into the cellular exterior. The triggering pathway culminates in a sharp peak of insulin secretion, that falls within 10-20 minutes of initial glucose stimulation [56, 57]. A secondary group of stimuli activate the amplifying pathway, permitting insulin to be secreted at a constant rate over the course of hours in post-prandial state. This pathway is stimulated even in instances of maximum levels of intracellular Ca^{2+}, independently of K_{ATP} channels. Even though the amplifying pathway continues the release of primed granules, it also recruits an internal pool of secretory granules to the cellular surface [57].

Insulin as a therapy was initially extracted from the pancreas of cattle and pigs in 1980. Barlow and colleagues were able to show that antibodies towards exogenous insulin therapy appeared weeks to months after administration in children with diabetes, impacting insulin function [58]. Moreover, the presence of AABs towards endogenous insulin suggests that immunity is due to defects in self recognition. The initial reporting of insulin as an autoantigen was published in 1983 by Palmer et al., who detected anti-insulin antibodies in the sera of T1D children before treatment with exogenous insulin [50, 59]. However, environmental factors, such as viral infections, have been implicated in instigating autoimmunity [60]. A study on children genetically at-risk for developing T1D, with at least one first-degree relative with T1D, reported that a higher IAA IgG was strongly associated with younger age. IAA was also typically detected as the initial AAB, especially in children with HLA-DR4 [44].

Abiru et al., were able to identify the dominant peptide identified and targeted by T cells was the insulin B chain peptide (B9-23) in animal models [61]. Nakayama and colleagues were able to engineer non-obese diabetic (NOD)- mice by mutating insulin at critical site for autoimmune recognition. These mice had no native insulin, but had functional insulin, interesting they presented with no towards insulin and neither insulitis nor diabetes, suggesting that insulin was a major autoantigen for diabetes in these animal [58, 62]. Furthermore, in NOD-mice, studies have found that AABs towards insulin not only predate clinical disease but are able to also predict T1D [60, 63].

IAAs in humans tend to appear before the AABs directed towards GAD65, ZnT8 and IA-2, further contributing to the belief that insulin plays a key role in T1D [60, 63]. The BABYDIAB study, a German study on infants genetically at-risk for T1D, followed infants from birth at regular intervals until adolescence. They showed that autoimmunity initiates early in life, with the peak period for T1D autoimmunity being between 9 months to 3 years [64]. Patients who presented with higher binding towards IAA, predominantly of IgG1 subclass, were more likely to progress to multiple AAB positivity and T1D than those with lower antibody binding. A higher antibody binding towards IAA was also associated with the younger age of IAA seroconversion and HLA DRB1*04 [65]. Insulin is the only autoantigen within T1D that is solely expressed within β-cells, suggesting that insulin plays an integral role in the pathogenesis of T1D. Moreover, studies not only indicate that IAA are present

within the first 9 months of life, with IAA typically being present within the first positive sample [58].

1.1.4.2 Glutamic Acid Decarboxylase 65 as an Autoantigen

Within the central nervous system (CNS), glutamic acid decarboxylase (GAD) plays an essential role as a neurotransmitter. GAD is a pyridoxal-5'-phosphate (PLP)-dependent enzyme, responsible for catalyzing the α-carboxylation of L-glutamate to yield the essential inhibitory neurotransmitter γ-aminobutyric-acid (GABA). GABA plays a key role in processes such as, tissue development, neurogenesis, and movement [66]. GAD exists as two isoforms that share circa 70% sequence similarity, these are GAD65 and GAD67, even though GAD65 is encoded by a gene on chromosome 10 and GAD67 by a gene on chromosome 2. Both isoforms have been shown to have a highly conserved C-terminal region but show differences in the N-terminal region. Together, these two isoforms supply the body with the entire supply of GABA [67]. They also show differences in their enzyme activity, where GAD67 is constitutively active and localized to the cytoplasm, GAD65, on the other hand, is localized to secretory vesicles and can be activated in its holoenzyme form or inactivated in its apo-enzyme form, depending on the cell's need for the inhibitory neurotransmitter GABA [68].

Although studies have indicated that GABA and GAD65 are present in neurons, it has also been detected in extra neuronal tissue such as the ovaries, testes, and pancreatic β cells. GAD65 has been indicated to be an autoantigen in numerous autoimmune conditions, such as stiff person's syndrome (SPS), autoimmune polyendocrine syndrome (APS) both type 1 and type 2, as well as T1D [69]. GAD65 was identified as an autoantigen in T1D as early as 1982, where GAD65 AABs (GADA) were identified in sera from newly diagnosed T1D in an immunoprecipitation assay [70].

Within the pancreatic islets, GAD65 is localized away from the remaining β-cell autoantigens within synaptic like vesicles (SPLV) (figure 5), where it is postulated to have a paracrine function in the regulation of glucagon [71]. Although both GAD65 and GAD67 show sequence similarity, their role in autoimmunity appears to be epitope specific. With continuous epitopes in the catalytic region of GAD67, along with GAD65, being a target of autoimmunity in SPS, while epitopes located in the middle and C-terminal domain of GAD65 appear to be targeted in T1D [68].

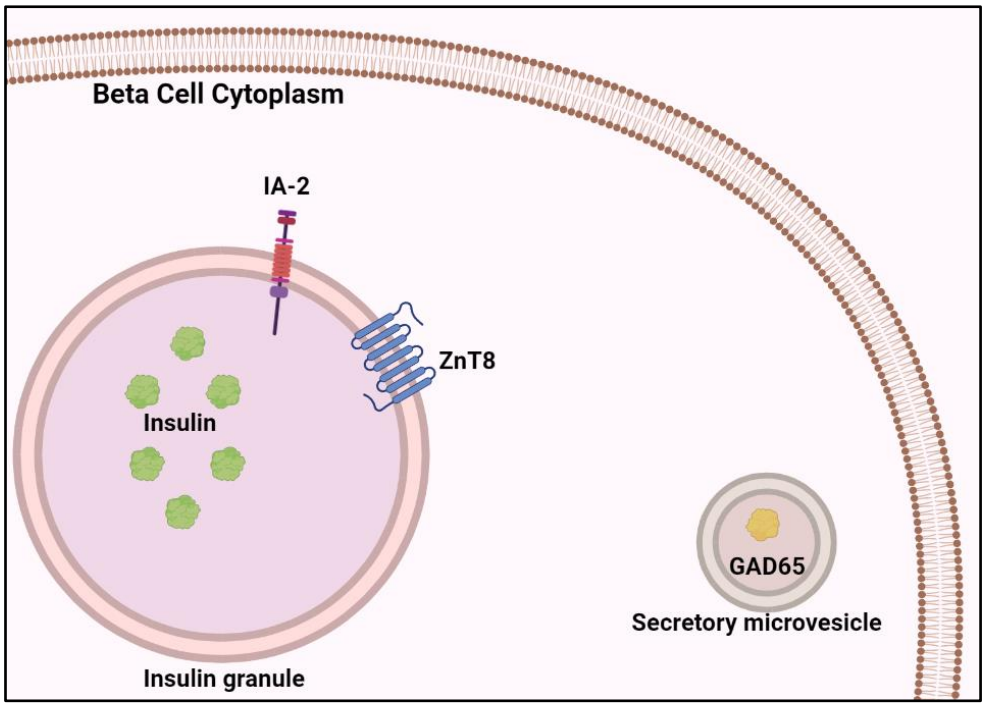

Figure 5. Schematic drawing of the suggested localization of pancreatic β-cell autoantigens. The figure shows stored insulin located in insulin granules within the cytoplasm of the pancreatic β-cell, with the transmembrane IA-2 and ZnT8 proteins anchored to the granule. As well as GAD65 located in secretory microvesicles in the cytoplasm of pancreatic β-cells. Figure adapted from Arvan et al., 2012 [71].

Compared to GAD67, GAD65 is demonstrated to be more flexible and mobile in the C-terminal region, with the distinctive mobility regions overlapping with the regions of high antigenicity [69, 72]. Moreover, GAD65 and GAD67 differ in their electrostatic charge distributions on their cell surfaces. This may indicate why the C-terminal domain is more antigenic in GAD65. In fact, two equally exclusive B-cell clusters, the cluster 1 epitope sites (CTC1) and the cluster 2 epitope sites (CTC2), target two distinct and opposed faces on the C-terminal region of GAD65 [69].

The N-terminal region is not unimportant, it is the site of palmitoylation and determines the localization of GAD65 [72]. In fact, Solimena and colleagues have shown that upon substituting the first 29 amino acid residues of GAD67 with the first 27 amino acid residues of GAD65, displaces the normally cytosolic localized GAD67 to the Golgi. The Golgi is the normal location of GAD65, thus suggesting that the first 27 amino acids within GAD65 have a signal for intracellular signaling [73]. However, with sequence similarities between GAD65 and GAD67, Jayakrishnan et al. reported that in a subset of patients with high titer of anti-GAD65 also presented with anti-GAD67 AABs. This suggests that anti-GAD67 may represent a small sub-group of anti-GAD65 that share an epitope not currently identified [74].

In terms of autoimmunity, although the middle and C-terminal regions have been identified as key targets of the T-cell and B-cell responses. Studies have shown that the immunogenicity can also spread to the N-terminal region [72, 75]. A study on acute and slow progressing T1D in Japan patients reported that the characteristics of

pancreatic autoantigens varied amongst the two groups. Patients with slow progressing T1D were typically older and presented with GAD65 AABs that targeted the N-terminal region, from residues 1-83 [76]. A study by Valdarnini et al., reported, when it comes to GAD65 immunity, a polyclonal antibody was able to recognize two continuous epitopes in the C-terminal region, these are the RTLED and PLGDKVNF amino acid sequences. Whereas a monoclonal antibody was able to identify the FWSFGSE epitope located in the N-terminal region of GAD65. Interestingly, all the targeted epitopes were found in flexible regions of the protein [68].

When comparing T1D and LADA (late-onset autoimmune diabetes in adults), there appeared to be a significantly higher percentage of GADA directed towards the N-terminal in LADA patients. T1D, older T1D, and LADY (latent autoimmune diabetes in the youth) showed higher levels of GADA towards C-terminal domain. Patients with AABs directed to the C-terminal region of GAD65 were also more likely to have lower C-peptide levels and more likely to need treatment with insulin [77].

Pöllänen et al., assessed patients entered into the Type 1 Diabetes Prediction and Prevention study (DIPP), the DIABIMMUNE study, the Finnish Paediatric Diabetes Register, and the Early Dietary Intervention and Later Signs of Beta cell Autoimmunity study for AABs towards either full-length GAD65 (f-GAD65) or N-terminal domain truncated GAD65 (96-585) (t-GAD65). In a cohort of 760 patients, they detected antibodies towards f-GAD65 in 83% of the cohort and 59% to t-GAD65. In those positive for antibodies towards GAD65, patients who were also positive for antibodies towards t-GAD65 were more likely to present with HLA-risk haplotype for T1D than those who were negative (77% vs 53%, p-value<0.001). Furthermore, patients who were also positive for t-GAD65 presented with increased specificity and predictive value for T1D than those positive for f-GAD65 alone (46% vs 15% and 30% vs 21%, respectively) [78].

The presence of GADA has been associated with older age and the HLA-DRB1*03 haplotype. A study on school children from the general population with no previous family history of T1D reported that children with GADA profiles towards the C-terminal domain, were accompanied by higher antibody binding and were more like to present with HLA-DRB1*03. Children with this profile and presenting with antibodies towards insulin or IA-2, were at a higher risk of developing T1D [79]. However, the heterogeneity of GAD65 AABs, and the variation in patient presentation, makes it difficult to rely solely on GADA for prediction and diagnosis of T1D.

1.1.4.3 Zinc Transporter 8 as an Autoantigen

AABs to zinc transporter 8 (ZnT8) in newly diagnosed patients with T1D were discovered in 2007. It is a relatively new autoantigen with few studies discussing its role in T1D pathogenesis [80]. ZnT8, encoded by the *SLC30A8* gene located on chromosome 8q14.11 [81], is the most abundant zinc transporter found in pancreatic β-cells. It is a 369 amino acid transmembrane protein localized to the insulin storage granules, where it supplies zinc ions for the storage and biosynthesis of insulin (figure 6) [81, 82]. Within the insulin secretory granules, insulin is complexed as a

hexamer with 2 Zn^{2+} ions and 1 Ca^{2+} ions, to facilitate efficient insulin storage [83]. Genome wide association studies (GWAS) have inferred an increased in severity and increased risk of developing T1D and T2D based on polymorphisms found in the carboxy terminal of the *SLC30A8* gene. A single nucleotide polymorphism (SNP) at aa325, substituting arginine for tryptophan (R325W) has been attributed to an increased risk for T2D [84]. This SNP has been related to an increase in circulating ratio of proinsulin to insulin, an imbalance of zinc ions in the cytoplasm and secretory vesicles, and a lowered insulin response [84, 85].

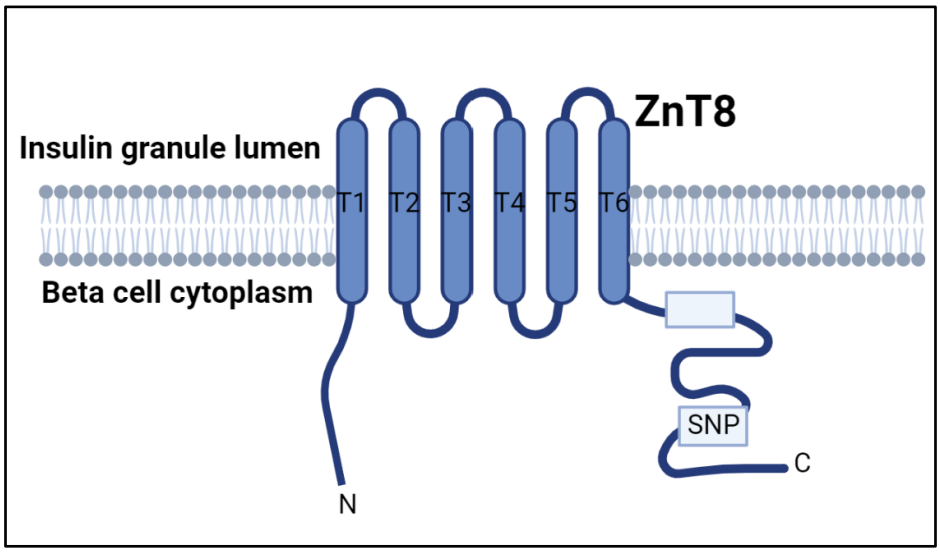

Figure 6. Structural model of Zinc Transporter 8. The figure shows the 6 α helical transmembrane domains of ZnT8 localized to the insulin granule of the β-cell. Polymorphisms in the cytoplasmic C-terminal with a SNP at aa325 (R325) have been suggested to increase risk of T2D. Furthermore, variants at aa325 have been related to AAB specificity in T1D, with AABs being isolated that specifically target R325, Q325 and W325 in ZnT8. Adapted from Daniels et al., 2020 [85].

The importance of ZnT8 in β-cell function and glucose metabolism is further demonstrated in studies involving transgenic mice [85]. A specific ZnT8 β-cell knockout in mice was able to demonstrate abnormal morphology of pancreatic β-cells and impaired regulation of glucose, similar to what is seen in human subjects who carry the ZnT8 risk allele. Further expanding on the importance of ZnT8 in insulin storage and secretion [86]. Moreover, studies have shown AAB specificity to ZnT8 variants in T1D. The AAB response in T1D appears to be focused on 3 variants of ZnT8, these are either arginine (R), glutamine (Q), or tryptophan (W) at amino acid position 325, which can present in combination or alone. Studies in AAB binding show apparent increase in antibody binding towards ZnT8WA than to ZnT8RA [87].

In T1D, the detection of ZNT8A was associated with the acute onset of diabetes, with the overall identification of ZnT8A being linked to younger age. Children were more likely to present with multiple AABs (49.5%) than single autoantibody positivity (7.8%) [88]. In those who were multi-antibody positive, the most common AABs were directed towards ZnT8 and IA-2 than towards GAD65 [88, 89]. Moreover, Wenzlau et

al. were able to report the detection of ZnT8 AABs in 26% of patients diagnosed with T1D who were previously autoantibody negative [81]. Hence, measuring ZnT8A may aid in the prediction and diagnosis of T1D in children. However, the detection of ZnT8A varies amongst different populations. For instance, autoantibodies towards ZnT8 have been detected in 66 to 80% of Caucasian patients at diagnosis of T1D [88] but were only detectable in 28% of Japanese patients with new-onset T1D [90]. This may imply that the key factor leading to the destruction of the β-cells varies amongst differing sub-populations of individuals with T1D.

Moreover, in a Chinese study of in 539 individuals with T1D found that ZnT8A were found in 24.1% of T1D than 1.8% in T2D. When combining the detection of GADA and IA-2A, ZnT8A increased diagnostic sensitivity to 65.5% in patients previously negative for GADA and IA-2A [91]. However, it is important to note that although ZnT8A are highly β-cell specific and are detected in children around 3 years old to adolescence. They have a tendency to gradually decline thereafter [88]. Thus, questions of the diagnostic value and integrity of ZnT8A have risen, with researchers attempting to divulge the pattern of autoimmunity. Studies have demonstrated the strong correlation of ZnT8 autoantibodies with IA-2A, suggesting that the assessment of both these autoantibodies enhances the diagnostic value for T1D (figure 7) [92].

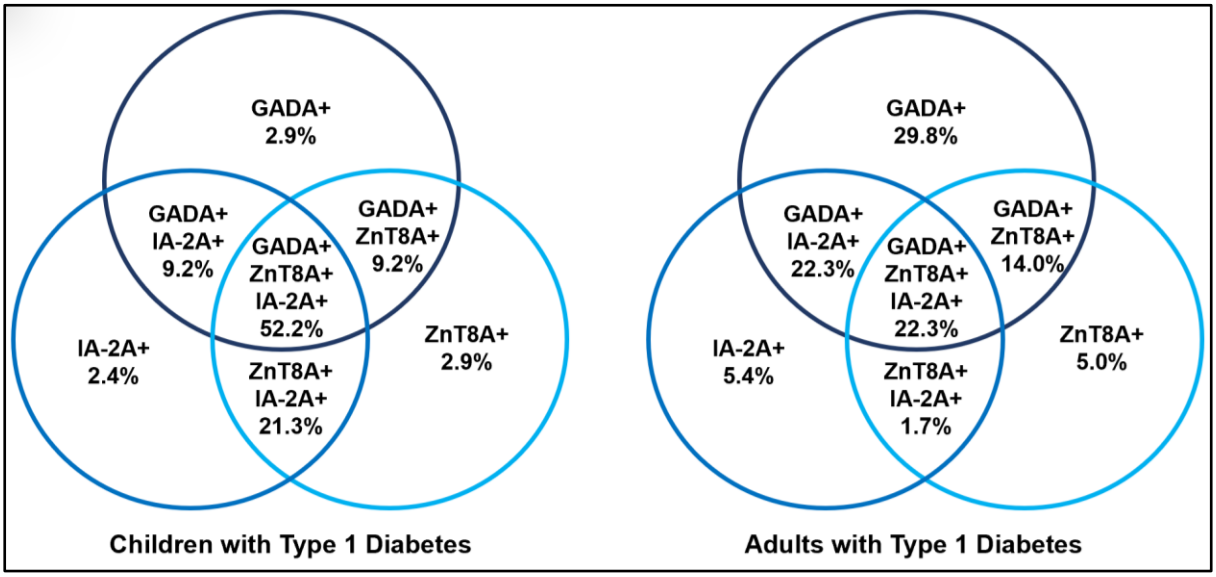

Figure 7. Venn diagram of autoimmunity positivity in children and adults with recent onset Type 1 Diabetes. Adapted from Niechciał et al [88].

1.1.5 Genetic Risks for Type 1 Diabetes

T1D is a highly heterogenous disease that shows a pattern of familial clusters. Around 13% of patients have a first-degree relative with T1D, with this risk changing depending on which family member is afflicted by T1D. If the mother has T1D, individuals have a 3% risk, with fathers there's a 5% risk, and with the siblings of T1D individuals having an 8-10% risk. Monozygotic twins show around a 50 to 70% risk of developing T1D, however if multiple first-degree family members are T1D the risk of inheritance increases [93, 94]. Thus, suggesting that T1D has a genetic

component, with the major genetic risk conferred to the inherited variations of the HLA class II gene located on chromosome 6p21.3. Around 60 other non-HLA genes have also been associated with the risk of T1D, with the majority playing a role in the mediation of immune function [95, 96].

The HLA complex is characterized as part of the major histocompatibility complex (MHC), with its main function in normal physiology being to differentiate self from non-self-antigens [97]. Both MHC class I and class II complexes function by presenting peptides on the surface of cells to T cells for identification and recognition. MHC class I cells are able to induce the activation of CD8+ cytotoxic T cells upon antigen presentation, whereas MHC class II cells instigate the proliferation of CD4+ T cells. Although both MHC class I and class II have similar folds, they differ in the number of chains, MHC class I consists of one α-chain and MHC class II consists of two chains, one α and one β-chain. In both MHC class I and class II, the HLA proteins are the most polymorphic, with each expressed in three gene regions (MHC class I, HLA-A, B and C, vs MHC class II, HLA-DR, -DQ and -DP)(figure 8) [98].

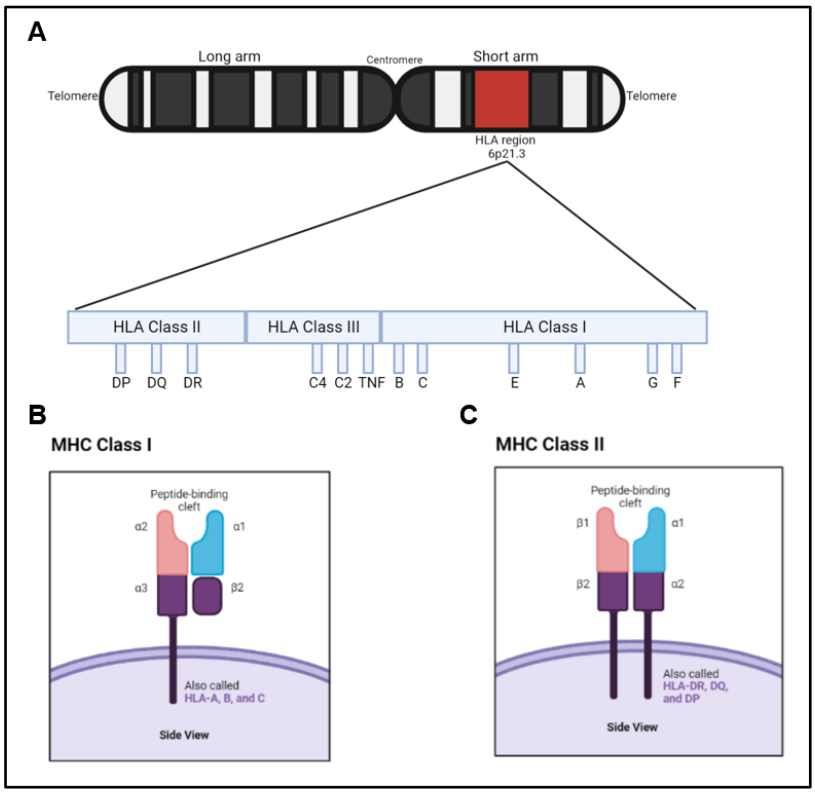

Figure 8. Structure of MHC class peptides. A) Shows the location of the HLA genes on the short arm of chromosome 6. The figure shows the distribution of the HLA class I, II and III, and the main haplotypes. **B)** Depicts the structure of the MHC (HLA) class 1 proteins on the cell surface. The HLA class 1 proteins consist of 3 α chains and one β-chain. **C)** Shows the structure of the HLA class II protein, depicting 2 α chains and 2 β chains [99, 100].

Although the HLA complex plays a major role in the mediation of the immune response, HLA class II antigens have been associated with several autoimmune disorders. Certain heterodimers of HLA class II peptides present antigens to

autoreactive T cells. Celiac disease has been associated with a strong HLA class II link, with the inheritance of HLA haplotypes DQA1*03-DQB1*03 (DR4-DQ8) and DQA1*05-DQB1*02 (DR3-DQ2.5) increasing the risk. An overlap has been seen in children with celiac disease and T1D, which has been associated with the inheritance of overlapping HLA risk genes [101]. In terms of T1D, the most significant HLA loci are the HLA-DR and HLA-DQ, with haplotypes of the HLA alleles HLA-DRB1, HLA-DQA1 and HLA-DQB1 being associated with disease susceptibility. Increased risk susceptibility has been particularly associated with the HLA-DRB1*03-DQA1*05-DQB1*02 (DR3-DQ2) and DRB1*04-DQA1*03-DQB1*03:02 (DR4-DQ8) haplotypes [96]. Furthermore, studies have demonstrated that inheritance of the DQ2.5 and DQ8 molecules present both proinsulin and gluten derived peptides to autoreactive CD4+ T cells. This is especially increased in cases of antigens PTM via enzymatic deamidation of glutamine [101].

The inheritance of varying haplotypes of HLA genes in children with T1D may shed light on the pathogenesis of T1D. The inheritance of HLA class II heterodimers has been associated with both the pathology and instigation of T1D. In fact, the inheritance of heterodimer DQ8 has been associated with autoimmunity triggered towards proinsulin, which is reflected in IAA being the first autoantibody isolated and detected in children who inherit heterodimer DR4-DQ8. Whereas individuals with inherited heterodimer DQ2 typically present with autoimmunity directed towards GAD65, this is represented in patients with DR3-DQ2 presenting with GADA as the first autoantibody detected [94]. However, the appearance of one AAB to β-cell antigens infers a low risk of clinical onset of T1D, around a 1:10 risk. If this is followed by the appearance of a second, third or even fourth AAB, no matter if the target is insulin, GAD65, ZnT8 or IA-2, the risk increases to an 8:10 risk of developing T1D. The second AAB to appear does not appear to have any association with HLA inheritance [44].

Multiple studies have attempted to expand on the association of HLA class II genes on T1D susceptibility, with relatively few assessing the impact of HLA class 1 association. The main role of HLA class I antigens in the immune system is to shape the repertoire of T cells within the thymus and aid in the initiation of T cell mediated antigen specific cytotoxicity. HLA class I consists of around 2893 alleles for 3 loci, making it one of the most polymorphic genes in the genome. A Filipino study of T1D and healthy controls confers a high predisposition based on the inheritance of A*2402, while A*2407 was protective. Another study suggests the allele B*3906 has a strong susceptibility for T1D, whereas B*5701 shows a protective effect [102]. However, the polymorphic nature of the HLA class I genes, and the linkage disequilibrium within the HLA region makes it difficult to identify single alleles that attribute to T1D.

Several non-HLA genes have also been associated with genetic susceptibility for T1D, with the insulin (*INS)* gene appears to have the highest relevance following the HLA genes. The *INS* gene is located on chromosome 11 p15.5 and consists of 3 exons divided by 2 introns. Within the gene, exons 2 and 3 are protein coding, while exon 1 mainly regulates transcription. Exon 2 codes for the B-chain, the signal

peptide, and the N-terminal unit of the connecter peptide of preproinsulin. Finally, exon 3 codes for the remaining of the connecter peptide, as well as the pre-proinsulin A-chain [103]. With the *IDDM2* (insulin dependent diabetes mellitus 2) gene being the second most important gene locus associated withT1D. The IDDM2 locus is the result of variable number tandem repeats (VNTR) and variations in the rs689 SNP on the *INS* gene [104].

Genome wide association studies (GWAS) have identified several T1D associated risk genes, these include *PTPN2* (protein tyrosine phosphatase non-receptor 2), *PTPN22* (protein tyrosine phosphatase non-receptor 22)*, CTLA4* (cytotoxic T-lymphocyte associated protein 4)*, IL-10,* and *IFIH1* (interferon-induced with helicase C domain 1). The majority of the gene associations are due to singular SNPs that cause impairment in the immune system and increase susceptibility to disease [105]. Around 112 genes have been associated with an increased risk of developing T1D. However, circa 65% of these T1D gene associations have been implicated in the other autoimmune diseases. With RA, CD, multiple sclerosis (MS), autoimmune thyroid disease (AITD), and inflammatory bowel disease (IBD) inferring the greatest risk overlap [106].

It is important to note that although HLA and non-HLA risk genotypes have been associated with the development of T1D, not all patients with high-risk phenotypes progress to clinical T1D [49]. The inheritance of T1D is a highly complex process, and the progression to clinical T1D appears to be associated with both genetic and environmental processes. Hence, there is a clear need to identify more specific biomarkers for identifying T1D at-risk individuals.

1.1.6 Mechanism of oxPTMs in β-cell Antigens

Post translational modifications are not a new phenomenon in the pathophysiology of T1D. In fact, the diagnosis and monitoring of the disease tends to depend on assessing the levels of glycated hemoglobin (HbA1c). HbA1c arises from the spontaneous reaction of glucose with the valine residues of the N-terminus of hemoglobin β-chains, resulting in an N-1-deoxy fructosyl [107]. Clinically, glycation is a non-enzymatic, spontaneous reaction between a protein and a reducing sugar, with glucose being a major glycating agent within biological systems. Glucose is able to react with the N-terminal amino group of lysine residues, inducing an initial Schiff's base, which undergoes rearrangement to yield fructosamine (N-(1-deoxy-D-fructos-1-yl) amino acids. In later stages, fructosamine begins to degrade to the more stable advanced glycated end products (AGEs) [108]. Lysine and arginine residues of a protein are typically more susceptible to glycation, especially in cases of coinciding oxidative stress [109].

Studies have begun to indicate ROS modified β-cell antigens may play a role in the pathophysiology of T1D [110]. Normally, APCs, such as dendritic cells and macrophages, function in presenting β-cell antigens to the immune system and release cytotoxic cytokines. The activation of APCs instigates an inflammatory milieu, inducing a state of oxidative stress within the β-cell microenvironment [111]. The β-cells, in both humans and animal models, have been shown to be more

susceptible to increased oxidative damage. This has been attributed to the lowered expression of antioxidant enzymes, namely superoxide dismutase, catalases, and glutathione peroxidases (GPX) [112]. The role of APCs within the pancreas has been extensively studied in multiple low-dose streptozotocin (MLD-STZ) induced T1D animal models, bio-breeding (BB) rats and non-obese diabetic (NOD) mice. Pancreatic islet exposure to cytokines has been seen to cause PTMs of native antigens, as seen in mass spectrometry and BB rats [111].

Type of PTM	Chemical reaction	Amino acid residue modified
Deamidation	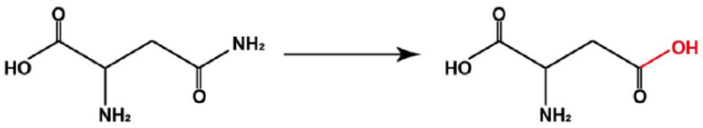	Asparagine Lysine Glutamine
Citrullination	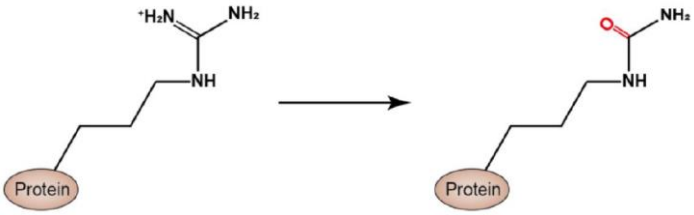	Arginine
Glycosylation	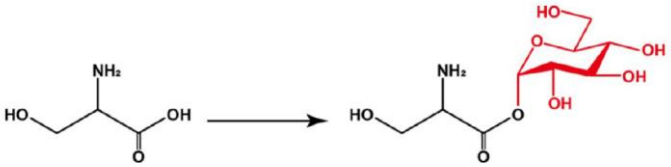	Threonine Serine Lysine
Glycation	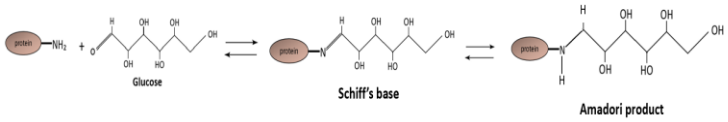	Lysine Arginine Phenylalanine
Disulphide	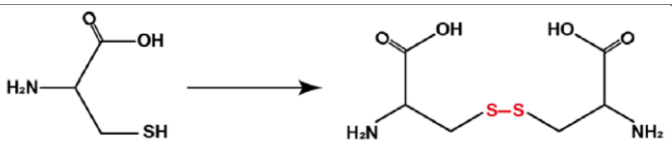	Cysteine
Oxidation	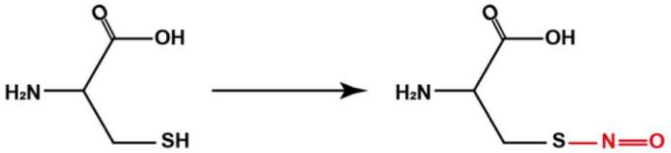	Cysteine Proline Methionine Histidine Tyrosine Phenylalanine
Chlorination	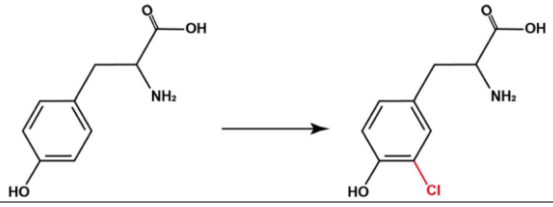	Tyrosine

Table 2. The chemical processes involved in the key post translational modifications discussed, along with the main amino acids targeted. Adapted from Hu et al., 2022 [113].

Increasing evidence and research has come out suggesting the role of PTMs in the pathology and immunogenicity of T1D, table 2 shows the key PTMs discussed. Oxidation and carbonylation are non-enzymatic processes by which ROS, cytokines and oxidative stress are able to induce metal catalyzed PTMs of lysine, arginine, threonine, and proline side chains [113]. In terms of oxidation, Strollo et al. have shown that chain B of insulin is the main target for oxPTMs. Mass spectrometry analysis of the oxPTM insulin was able to show the oxidation of histidine 5 (His5), phenylalanine 24 (Phe24) and cysteine 7 (Cys7), as well as other modifications such as, chlorination of tyrosine 26 and 16 (Tyr26 and Tyr16), and glycation of phenylalanine 1 (Phe1) and lysine 29 (Lys29). A significant increase was seen in antibody binding in the sera of patients with new-onset T1D to oxPTM-INS compared to NT-INS (p-value <0.001) [114]. Furthermore, they have suggested that antibodies to oxPTM-Ins can act as a novel biomarker for prediction and detection of T1D in children [10]. Mannering et al., have also classified a disulfide modified insulin epitope that is recognized by T cells in humans [115].

Van Lummel et al. [116], and McGinty et al. [117], assessed the impact of deamidation of β-cell antigens on their immunogenicity. Deamidation is the process by which asparagine is converted to iso-aspartic or aspartic acid, catalyzed by tTG. Van Lummel et al., were able to deduce 28 deamidated peptides that bind to HLA-DQ8, including IA-2, ZnT8, and proinsulin [116]. Consequently, McGinty et al., demonstrated that antibody binding in T1D with HLA-risk alleles increased upon deamidation of GAD65 [117]. Similarly, Donnelly et al., have stated that deamidated IA-2 and GAD65 increased antigen-antibody binding [118]. Another PTM indicated by several studies in diabetes is citrullination. Citrullination is the enzymatic induced process by which peptidyl arginine is converted to citrulline in the presence of Ca^{2+} ion dependent peptidyl arginine deiminase (PAD) enzymes. Sidney et al., McGinty et al., and Buitinga et al., have demonstrated that citrullination is able to increase and strengthen the recognition between peptides in the insulin B chain and GAD65 and autoreactive T cells via enhancing their affinity towards HLA alleles [117, 119, 120].

Khan et al., have attempted to identify a ROS modified GAD65 as a specific marker in T1D. In their study, Khan et al., induced the *in vitro* hydroxyl (•OH) modification of GAD65 via irradiation with UV light in the presence of hydrogen peroxide. When testing the sera of T1D, there was a significant difference of AABs reactivity to native vs modified GAD65 in T1D (mean O.D ± S.D, 0.37 ± 0.06 vs 0.70 ± 0.08, p-value <0.001, respectively) [121]. Similarly, Moinuddin et al., showed that upon oxidation of GAD65, patients with T1D had higher AAB binding to the ROS-modified GAD65 than the native GAD65 (mean O.D ± S.D, 0.732 ± 0.31 vs 0.376 ± 0.11, respectively). Upon testing sera from STZ-induced diabetic rats to native or ROD-GAD65, there appeared to be an increase in antibody response in ROS-GAD65 than native (mean ± S.D, 0.49 ± 0.08 vs 0.242 ± 0.02, respectively) [122]. Table 3 summarizes the current literature findings of PTMs in T1D.

Beta cell Antigen	Modification	Position	Year	Reference
Insulin A	Disulfide	Cysteine residues A6 and A7	2005	Mannering et al. [115]
Insulin B	Deamidation Citrullination Glycation Oxidation Chlorination	1F, 29L 24F, 7C, 5H 26Y, 16Y	2018 2018 2015 2015 2015	Sidney et al. Strollo et al. [10, 114, 119]
GAD65	Deamidation Citrullination Oxidation		2014, 2020 2014 2009 2015	McGinty et al. Donnelly et al. Khan et al. Moinuddin et al.
IA-2	Deamidation Citrullination	556E, 551E, 548E, 207E, 478E, 533E, 532E, 207E	2018 2014 2020 2018	Marre et al. van Lummel et al. Donnelly et al. Yang et al.
ZnT8	Deamidation Phosphorylation		2014 2012	Van Lummel et al. Scotto et al. Dang et al.

Table 3. Summary of the current research of Post Translational Modifications to native pancreatic β-cell antigens of interest and their impact in immunity and pathogenesis of T1D. Adapted from Hu et al., 2022 [113].

1.2.0 Study 2: DiabeSARS, A Tale of Two Pandemics

1.2.1 SARS-CoV-2 and the COVID-19 Pandemic

Coronaviruses have long been the cause of multiple global pandemics. These viruses are typically of zoonotic origins, and tend to spread to human infection, resulting in severe respiratory distress and viral pneumoniae. Severe acute respiratory syndrome (SARS) in 2002 and Middle Eastern Respiratory Syndrome (MERS) in 2012 are just two examples over the last 20 years of severe pandemics caused by the coronaviruses SARS-CoV and MERS-CoV, respectively [123].

In December 2019, the world was ignited into the throes of a global pandemic due to the spread of the severe acute respiratory coronavirus 2 (SARS-CoV-2) first isolated in Hubei province, China. This showed similar signs to the 2002 SARS-CoV pandemic, with its origins traced back to a live animal market in the Guangdong province, China [124]. On February 11, 2020, the SARS-CoV-2 virus was deemed the COVID-19 global pandemic, which resulted in over 636 million infections worldwide, and over 6 million deaths, naming it one of the most severe pandemics in global history. The rapid transmission and wide spread of the COVID-19 pandemic was attributed to SARS-CoV-2 rapid infectious rate and an increase in global travel [125].

Infection with SARS-CoV-2 typically begins upon inhalation of aerosols containing the virus, binding to the highly abundant ACE2 receptor located on the upper nasal epithelium. At this stage, individuals remain asymptomatic, yet are highly contagious. As the lifecycle of the virus continues and the viral load increases, the SARS-CoV-2 virus moves through the upper respiratory tract via conducting airways [126]. COVID-19 has a wide clinical manifestation, ranging from asymptomatic disease to severe disease characterized by acute respiratory distress syndrome (ARDS). The most common symptoms in mild cases of disease are a dry cough, fever, and fatigue, which may progress to signs of pneumonia in more severe cases [127].

Most patients with COVID-19 present with mild disease, with around 20-40% of patients being characterized as asymptomatic. However, studies have shown that it takes around 1-2 weeks from onset of symptoms for patients to progress to severe disease requiring admission to the intensive care unit (ICU) [128]. Circa 14% and 5% of laboratory confirmed and diagnosed COVID-19 cases were deemed severe or critical, respectively. The major risk factors for progression to severe disease are being male, older age (above 60 years old), having any underlying comorbidities, such as diabetes, hypertension, obesity, cardiovascular disease, and malignancies [129].

Although SARS-CoV-2 is a novel coronavirus, it appears to share circa 79% sequence similarity with SARS-CoV. Human coronaviruses are single-stranded RNA enveloped viruses, with a genome size ranging from 26.4 to 31.7 kilobases, making them one of the largest RNA viruses known. The name *coronavirus* comes from the structure seen on electron microscopy; the virus appears to have protruding spikes resembling a crown [130]. The SARS-CoV-2 genome consists of 14 open reading frames (ORFs) the encodes 29 viral proteins. Around two thirds of the 5’ end of the

genome encodes two polyproteins (PPL-A and PPL-B), which are digested via viral proteases to yield 16 non-structural proteins (NSPs). These NSPs play an integral role in the replication and transcription of the SARS-CoV-2 virus. The structural viral proteins are encoded by four ORFs located on the 3' end of the genome, these are the spike glycoprotein (S), the nucleocapsid protein (N), envelope protein (E) and the membrane protein (M). These structural viral proteins play a role in the infiltration of the host cell, as well as virion assembly and the suppression of the host's immune system [131]. The structure of the SARS-CoV-2 virus is shown in figure 9.

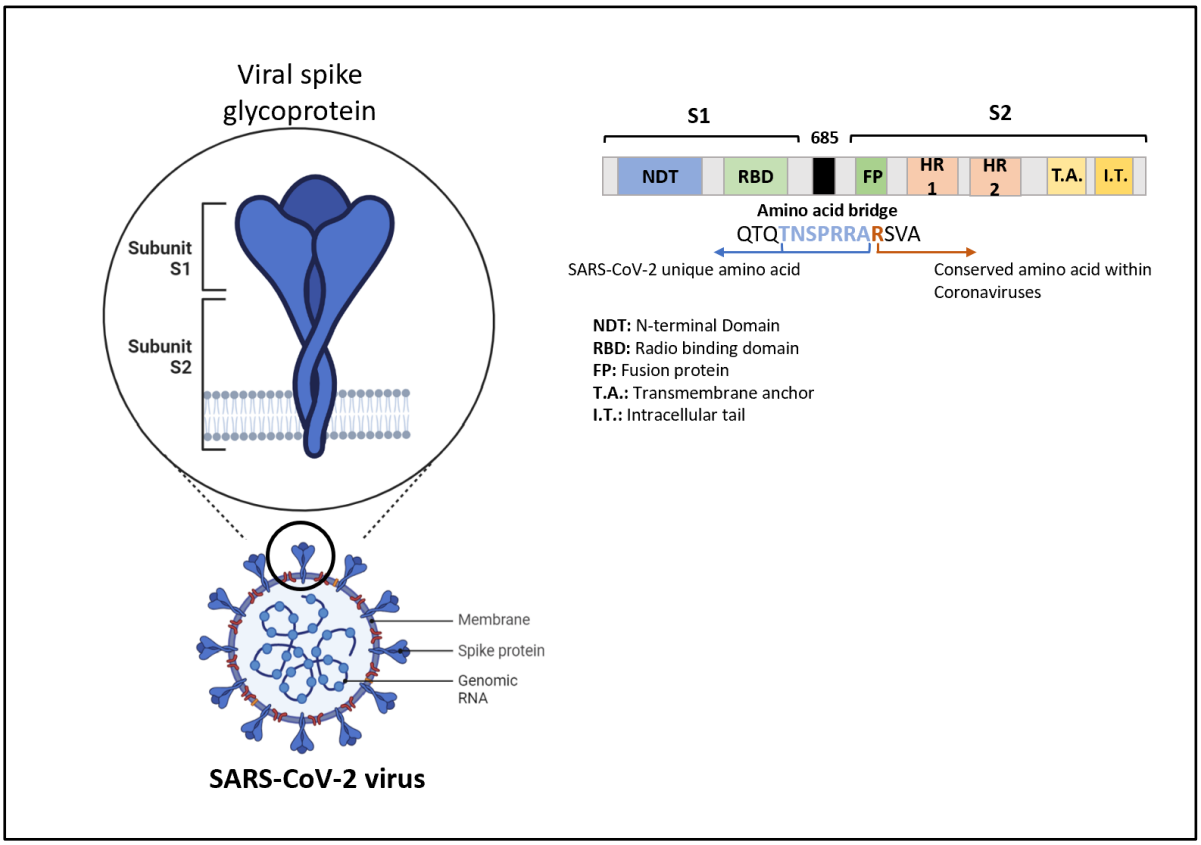

Figure 9. Structure of SARS-CoV-2 virus. The SARS-CoV-2 coronavirus is made up of the viral envelope (E), viral membrane (M), spike protein (S) and genomic RNA. The S protein is made up of two subunits (S1 and S2) [132].

The E protein plays a role in viral assembly and release, and maintaining the activity of the ion channel, involved in viral infection. The M proteins is the amplest transmembrane protein of the viral molecule, functioning in maintaining viral morphology and assembly. Finally, the N protein encapsulates the entirety of the viral RNA and non-structural proteins (NSPs), playing a key role in viral transcriptional processes, genome assembly and replication. The SARS-CoV-2 virus consists of six main open reading frames (ORFs), these are the S protein, the E protein, the N protein, ORF1b, and ORF1a. With several accessory ORFs identified, the main ones are ORF3a/b, ORF7a, ORF6, ORF7b, ORF9b/c, ORF8, and ORF10 [133].

1.2.2 SARS-CoV-2 Binding to ACE2 and Host Cell Infiltration

In order to fully understand the pathogenesis of SARS-CoV-2, many studies have focused on the mechanism by which the virus infiltrates host cells. Similarly, to SARS-CoV, SARS-CoV-2 depends on the angiotensin converting enzyme 2 (ACE2) receptor for entry into the host cell. ACE2, along with ACE, plays a role in mediating the negative impacts of the renin angiotensin system (RAS) in numerous health conditions. RAS is an elaborate system, regulating the normal mechanisms of the cardiovascular, renal and pulmonary system [134].

The main role of RAS is to maintain blood pressure, as well as the homeostasis of electrolytes and fluids, impacting numerous organs, such as the heart, kidneys, and lungs [135]. Within RAS, ACE2 plays a role as a major regulator of the system by facilitating the conversion of angiotensin I and II into Ang 1-9 and Ang 1-7 [136]. Any abnormalities in the signaling cascade can lead to several pathological events. For instance, in cases in which ACE2 is unable to negatively regulated the Ang II/AT_1 receptor, this can instigate end organ damage via the activation of pro-fibrotic and pro-inflammatory cascades [134]. ACE2 exists in two main forms, the full length mACE2 localized to the cell membranes, with a transmembrane anchor and an ectodomain. The mACE2 is the main receptor for SARS-CoV-2 viral entry into host cells. The second form is the soluble sACE2, lacking membrane anchors this form of ACE2 is shed into circulation [137].

The SARS-CoV-2 virus binds via its spike glycoprotein, localized on the viral envelop, to the ACE2 receptor (figure 10), triggering a series of signaling cascades. Upon binding to ACE2, the S protein is cleaved to the S1 and S2 subunits. The S protein is a 1273 aa protein that forms homotrimers that protrude from the viral envelop [138, 139]. The S1 subunit consists of the radio binding domain (RBD) with the radio-binding motif (RBM), which facilitates the binding to the peptidase domain (PD) of ACE2 [140]. This is followed by the proteolytic cleavage of the RBD at the C-terminus, which is mediated by the acid-dependent proteolytic host protease transmembrane protease serine protease 2 (TMPRSS2), is necessary to instigate the interaction with PD. The viral and cellular membranes then fuse following the proteolytic cleavage. Upon S1 and ACE2 binding, ACE2 is cleaved at the extracellular domain via a disintegrin and metallopeptidase domain 17 (ADAM17), and at the intracellular C-domain via TMPRSS2, facilitating viral entry in the host cell [141]. As for the S2 subunit, although it does not directly interact with the ACE2 receptor, it holds essential elements required for virion membrane fusion. The binding of the S1 subunit with ACE2, transits the S2 subunit from the metastable pre-fusion to the stable post-fusion necessary for membrane fusion [141, 142].

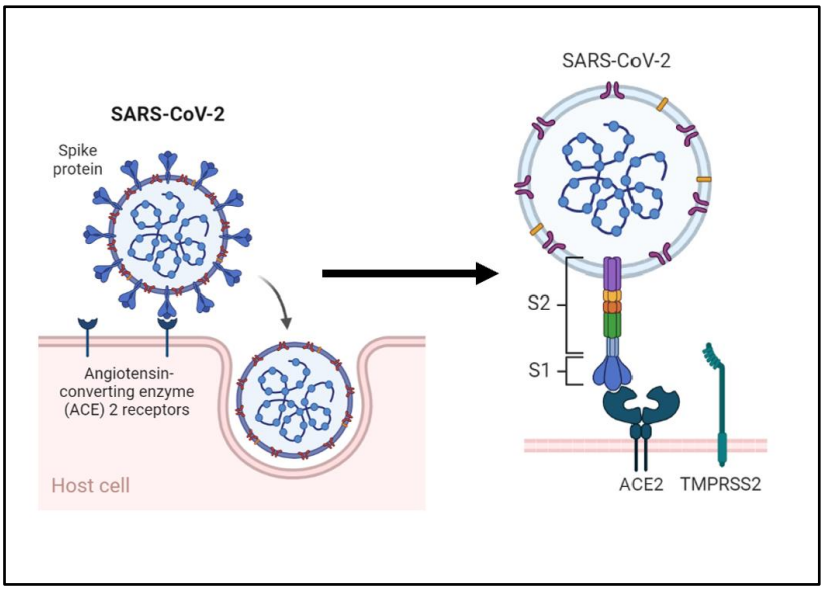

Figure 10. Binding of SARS-CoV-2 to ACE2 receptor facilitating viral entry into the host cell. The SARS-CoV-2 S glycoprotein binds to the ACE2 receptor on host cells dispersed throughout the system. Upon binding, the TMPRSS2 protease helps cleave the S protein, facilitating viral entry. After the virus infiltrates the cell, this triggers inflammatory molecules and cells of the innate immune system (such as macrophages), which recruit T and B cells to the site of the infection.

Upon infiltration of the SARS-CoV-2 virus into susceptible cells, the virus follows the same pathway of previous coronaviruses. It releases its genomic RNA into the cell cytoplasm, where it is translated into polyproteins 1a and 1ab, which encode the NSPs that assist in the formation of the viral replication and transcription complex. These NSPs are capable of reorganizing membranes obtained from the ER and the Golgi complex, forming double membraned vesicles sequestering viral transcription and replication preventing detection by host defenses. Generated viral proteins migrate to the ER and Golgi for packaging and processing where they combine with N proteins and RNA to form newly assembled viral particles. These new SARS-CoV-2 viral particles are able to be transported to the cell membrane via vesicles, undergoing exocytosis into the extracellular matrix. The viral replication cycle exposes it at many instances to being processed and eliminated by the innate immune system [143].

1.2.3 Innate immunity, Cytokine Storm and SARS-CoV-2

The innate immune system is the system's first line defense against COVID-19. There are several points of viral entry and replication where the host defenses can detect viral components and trigger the innate immune response. For instance, the cell surface sensors on the surface of target cells are able to detect the viral S, E, and M proteins on binding to host receptors, and cytoplasmic sensors are able to sense viral nucleic acids and proteins. This is able to trigger and activate the inflammatory pathway, and subsequently cytokine production and cell death.

As stated previously, innate immune cells via PRRs can identify DAMPs or PAMPs, inducing key immune responses and inflammatory signaling [34]. Cells of the innate

immune system include neutrophils, macrophages, dendritic cells, monocytes, and natural killer cells, which are able to produce inflammatory chemokines and cytokines that can clear infected cells and induce cell death [144]. The SARS-CoV-2 virus typically triggers the innate immune response via Toll-like receptors (TLRs), nucleotide-binding oligomerization domain (NOD)-like receptors (NLRs), retinoic acid-inducible gene I (RIG-I)- like receptors (RLRs), and inflammasomes [143].

Upon infiltrating host cells, SARS-CoV-2 triggers the innate immune response via TLRs. TLRs are dispersed widely throughout the system but are abundant within the respiratory tract. They are able to instigate inflammation through two key adaptor molecules, TRIF (Toll/IL-IR domain containing adaptor-inducing interferon- β) [145] and MyD88 (myeloid differentiation primary response 88), which are both able to induce cytokine production. Signaling through MyD88 instigates the downstream activation of nuclear factor- kappa B (NF_{KB}), interferon (IFN) regulatory factors (IRFs), and mitogen-activated protein kinases (MAPKs) (figure 11) [146]. This leads to the transcriptional activation of proinflammatory cytokines, mainly interleukins 6 and 1 (IL-6 and IL-1), and tumor necrosis factor (TNF), as well as inducing the transcription of genes that encode for NLPR3, and IFNs. TRIF signaling instigates and propagates the induction of TLR-3 and TLR-4 transcriptional factors, and IFNs [143].

Zheng et al. demonstrated the expression MyD88 and TLR2 were elevated in patients with increased severity of SARS-CoV-1 and mouse hepatitis virus (MHV) [147, 148], where the induction of MyD88 mediated inflammatory response is critical to produce proinflammatory cytokines and immune defenses in these diseases [149]. Although there have been no studies in the involvement of the remaining TLRs in SARS-CoV-2 infection, TLR3 has been associated with SARS-CoV-1, whereby TLR3 appears to induce a protective role [150]. Furthermore, TLR3 knockout mice were shown to suffer from higher viral load and weakened pulmonary function than healthy mice upon infection with mouse evolved SARS-CoV (MA15). Studies have described that the NLR inflammasome develops in response to SARS-CoV-2. NLRP3 is the most well characterized inflammasomes, with it being triggered in response to SARS-CoV-2 PAMPS/DAMPS, the main PAMPS being the viral E protein, S protein, viral RNA, ORF8b and ORF3a.

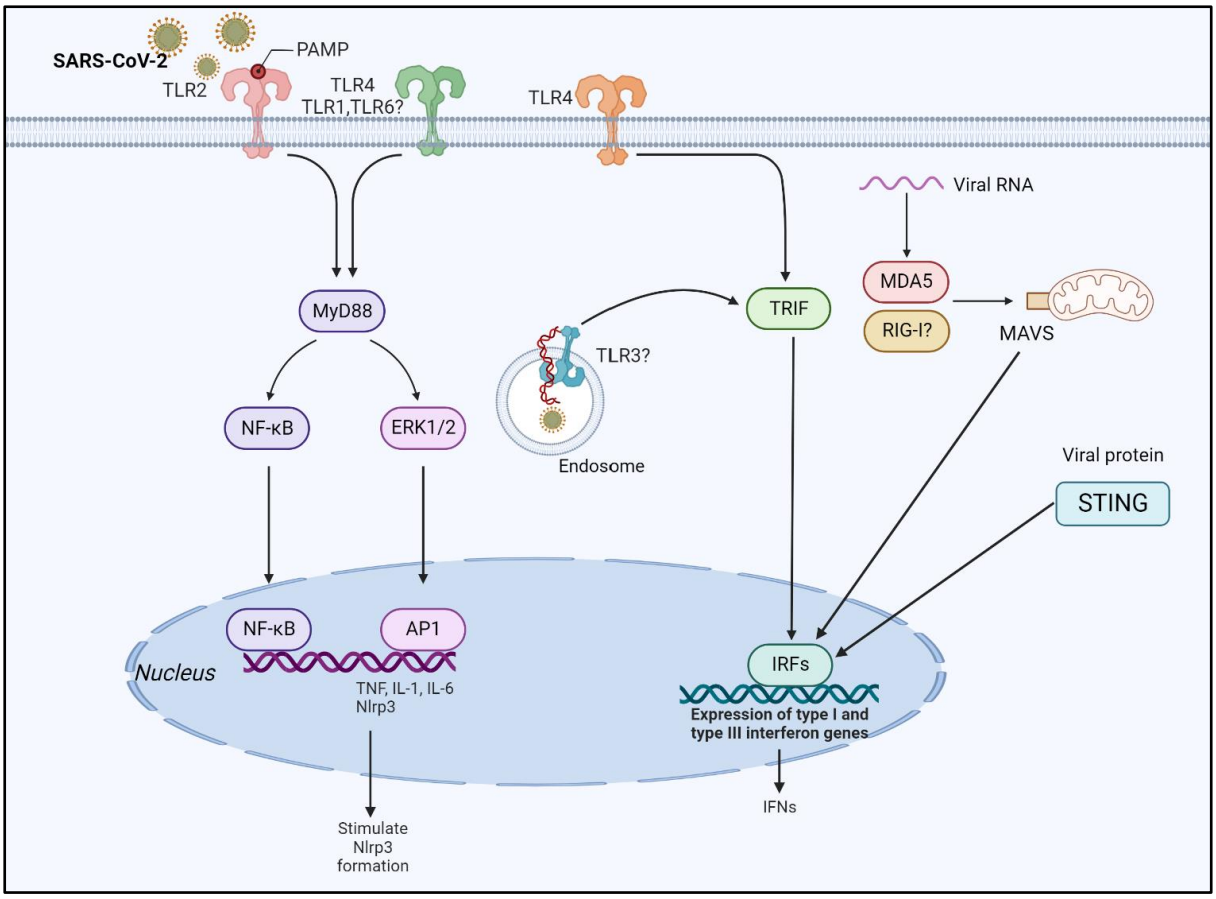

Figure 11. PRR stimulation pathway upon SARS-CoV-2 viral cellular infiltration. The figure depicts the general understanding of PRR pathways stimulate in response to SARS-CoV-2. PRRs localized to the cellular surface and endosomal membranes detect SARS-CoV-2 PAMPs that trigger either MyD88 or TRIF inflammatory pathways. TLR2, TLR1, TLR4, and TLR6 signal through MyD88, activating MAPK and NF_{KB} inflammatory signal pathways. TLR4 and TLR3 can instigate cytokine production via the TRIF pathway, predominantly IFNs. Viral RNA stimulates IFN production via the MDA5 and RIG-1 pathways, that can go on to induce the mitochondrial antiviral signaling pathway (MAVS), and viral proteins potentially induce cytokine production via the STING pathway. Adapted from Diamond et al. [143]. *PRR: Pattern recognition receptor, PAMP: Pathogen-associated patterns recognition, TLR: Toll-like receptor, MyD88: Myeloid differentiation primary response 88, TRIF: Toll/IL-IR domain containing adaptor-inducing interferon-β, NF-$_{kB}$: nuclear factor kappa-light-chain-enhancer of activated B cells, MAPK: Mitogen-activated protein kinase, ERK: Extracellular signal-related kinase, AP1: Activated protein 1, MAVS: Mitochondrial antiviral signaling pathway, MDA5: melanoma differentiation-associated protein 5.*

PRR signaling triggers and influx of IFNs and proinflammatory cytokines, with severe cases of COVID-19 showing elevated levels of IL-6, IL-12, IL-1β, IL-17, IFNβ, IFNγ, TNF, to name a few. The dysregulation and excess production of proinflammatory cytokines in severe COVID-19 have led to have ARDS, multi-organ damage, and cytokine storm. TLR play a key role in innate immunity, and studies have shown that TLR blockers may interrupt IFN production [151].

The main role of the innate immune response is to prevent further viral replication, develop an antiviral environment, and, the major role, initiating the adaptive immune response. Although infection with SARS-CoV-2 is able to instigate a fierce innate

immune response, reports also find the virus is able to evade immunity. This evasion appears to contribute greatly to the virulence seen upon infection. Studies have found that impaired IFN I and III responses have been connected with the development of severe and detrimental COVID-19. With patients showing a downregulated IFN I response, due to viral evasion, being related to increased rates of hospitalization. Consequently, viral evasion of the innate immune response suggests that the SARS-CoV-2 virus is able to continue replicating and avoid the initiation of the adaptive immune response [152].

Hence, due to the delay in initiating adaptive immunity, the innate immune system may attempt to overcompensate and triggers a slightly more aggressive immune response. This has been shown with the high levels of chemokines, cytokines and neutrophils seen in severe COVID-19 patients, and the subsequent organ and lung pathology seen because of this.

1.2.4 COVID-19 and Diabetes

Diabetes and COVID-19 are two concurrent and converging pandemics, with diabetes being characterized as a risk factor for developing severe COVID-19 [153]. Severe and life threatening COVID-19 has been directly correlated with underlying comorbidities, with a study on 72314 COVID-19 cases from the Chinese center for disease control (CDC), showed that individuals with diabetes had the second highest mortality rate (7.3%), following cardiovascular disease (10.5%) [154]. When assessing 136 studies on COVID-19 and individuals with diabetes, there was an increased risk of mortality (OR 1.75, $p< 0.0001$). Although there are few studies comparing T1D and T2D in terms of COVID-19 severity, T2D appeared to have an increased risk of mortality although there was no significant difference, possibly attributed to the small sample size [155].

The direct association with severe COVID-19 and diabetes have not been fully elucidated. However, speculation has been attributed to the underlying microvascular and macrovascular complications of diabetes, including overlapping CVD, hypertension, and obesity. Obesity is a major characteristic of T2D, with adipose tissue being a contributor to proinflammatory cytokines and adhesion molecules [156]. Both T1D and T2D individuals are characterized by underlying low-grade inflammation and dysregulated innate immunity [157], contributing to the severity of COVID-19 and potential ICU admission or death [158].

Studies have indicated that hyperglycemia is a strong predictor of hospitalization from COVID-19. Codo and colleagues have shown that hyperglycemia and elevated glucose positively correlates with SARS-CoV-2 replication via the activation of hypoxia-induced 1α and mitochondrial ROS [159]. Subsequently, T1D and T2D were identified as independent contributing factors to severe disease in SARS-CoV-1 and MERS. In fact, T2D mice infected with MERS presented with a dysregulated immunity, and extensive lung damage and pathology [160].

Furthermore, within diabetes, dysregulated glucose has been extensively studied with processes such as glycation being a routine measure of disease progression. Glycation itself is a non-enzymatic process in which a reducing sugar, such as

glucose, adds a *Schiff's base* to the N-terminal amino group of a protein, forming a fructosamine [108]. Lysine and arginine residues of a protein are typically more susceptible to glycation, especially in cases of coinciding oxidative stress [109]. In diabetes, this phenomenon has been seen in glycated albumin (GA) and HbA1c, both of which are routinely assessed in clinical practice [161, 162]. In SARs-CoV-2, the viral S glycoprotein consists of key lysine and arginine residues that play a role in angiotensin converting ACE2 receptor binding [163]. In fact, one strain of SARs-CoV-2 consists of an N439K substitution in the receptor binding motif (RBM), increasing its affinity for ACE2, in turn increasing its virulence [164]. These sites may be exposed to potential non-enzymatic glycation.

As glycemic control has been linked with an increase in disease severity, it has been postulated that the virulence may be enhanced by non-enzymatic glycation [165]. Glycation can impact the 3-dimensional structure of a protein, changing its final configuration, function, and virulence [166]. Studies have already indicated the glycosylation of the S protein; glycosylation is the enzymatic linkage of a glycan to the O- or N-terminus of a protein. Typically, glycosylation of a protein is a predetermined post translational modification that can produce a mature functional protein, while glycation is an unregulated process that impacts the stability and function of a protein and is highly concentration dependent [167, 168]. In this scenario, glycosylation of the S protein can act as a "sugar-shield", protecting the protein from antibody recognition [163].

Moreover, the risk of severe COVID-19 and ICU admission appeared to be increased upon elevated levels of blood glucose, regardless of diabetic state. This adds to the postulation that hyperglycemia, and dysregulated glucose play a major role in the pathogenesis of COVID-19 [169]. This is similar what was previously seen in the 2003 SARS-CoV-1 outbreak, where survival analysis showed fasting plasma glucose (FPG) was an independent predictor of morbidity and mortality in infected patients [170].

1.2.5 COVID-19, Pancreatitis, and New-Onset Diabetes

As the pandemic progressed, studies have presented data on cases of ketoacidosis overlapping with COVID-19 or appearing weeks after recovery [171]. A multicenter study in the United States (US) reported 64 patients with T1D after a confirmed or suspected COVID-19, with one third presenting with DKA and 50% with hyperglycemia. A study from the national health service (NHS) within the Northwest London pediatric diabetes network reported 30 children between 23 months and 16 years old with new-onset T1D. Of these, 21 (70%) presented with DKA, with 11 (52%) showing signs of severe DKA, 12 patients with clinical shock, and 4 required admissions to the pediatric ICU (PICU) [172].

Furthermore, a Finland study reported an increase in children being admitted to the PICU due to new -onset T1D at Helsinki University Hospital in May 2022. The study assessed 2 cohorts, one pre-pandemic (1 April to 31 October, 2016-2019) and one during the pandemic (1 April to 31 October 2020). The results depicted an increase in PICU admission with severe T1D from 2.89 to 9.35/100,000 persons per year with

an incidence risk ratio (IRR) of 3.25 (95% CI 1.80-5.83, p<0.001) [173]. A retrospective study of 10 post-COVID-19 populations, consisting of roughly 40 million participants, demonstrated a relative risk of 1.62 of developing diabetes in the post-COVID group compared to a non-COVID group [174]. However, it remains unclear whether the occurrence of new-onset diabetes is a direct result of the COVID-19 pandemic, a delay in diagnosis due to lockdowns, or more severe disease presentation following infection with SARS-CoV-2.

As the pancreas has been reported to express the ACE2 receptor within its acinar, ductal and islet cells, there have been implications of pancreatic injury resulting from COVID-19. In fact, studies have been able to isolate SARS-CoV-2 mRNA from pancreatic pseudocysts, potentially suggesting a role of the virus in instigating acute pancreatitis (AP). Other viruses have been implicated in AP, such as the measles, and the coxsackie virus [175]. The COVID-19 pandemic is not the first instance in which viruses have been associated with enhancing autoimmunity. In fact, enteroviruses, such as coxsackievirus B (CVB), mumps virus, cytomegalovirus, and rotavirus, have been previously linked to T1D. CVB4 is the most commonly isolated strain in patients with pre-diabetes or at the onset of T1D [176]. In fact, Stene and colleagues assessed blood samples from the Diabetes and Autoimmunity Study in the Young (DAISY) cohort and found the detection of AABs was significantly increased upon isolation of enterovirus RNA [177].

1.2.6 Viral variants and vaccine efficacy

The severity and wide-spread of COVID-19, along with the lack of specific treatment, made the need for vaccine development priority number one. The previous SARS-CoV-1 and MERS outbreaks, aided in supplying preclinical data available from the vaccine candidates to partly support and accelerate the vaccine development for COVID-19. Vaccines act by inducing an immune response that mimics that of memory and effector subsets, without activating severe and life-threatening inflammation. Studies have shown that the administration of the anti-COVID-19 vaccines instigates the maturation of CD4+ and CD8+ T-lymphocytes, with memory T lymphocytes being found in roughly 70% of vaccinated people [178].

The primary target of the developed vaccines is the SARS-CoV-2 S protein, with the main aim to develop neutralizing antibodies against the RBM to prevent binding of the virus to the ACE2 receptor. However, as the vaccines were developed against the wild-type virus, researchers rushed to determine the efficacy of the vaccine towards mutated forms of the virus [179]. Due to the constant viral mutations, a result of the inherent high error rate of the virus RNA-dependent RNA polymerase (RdRp), SARS-CoV-2 presents with an extremely variable RBM in the S glycoprotein [180]. The WHO has characterized SARS-CoV-2 variants as either variants of interest (VOI) or variants of concern (VOC) (figure 12). The center for disease control (CDC) defined a VOC as a variant associated with the increased virulence and transmission of SARS-CoV-2, as well as an increased ability to evade detection, and resistance to acquired immunity and vaccinations [178].

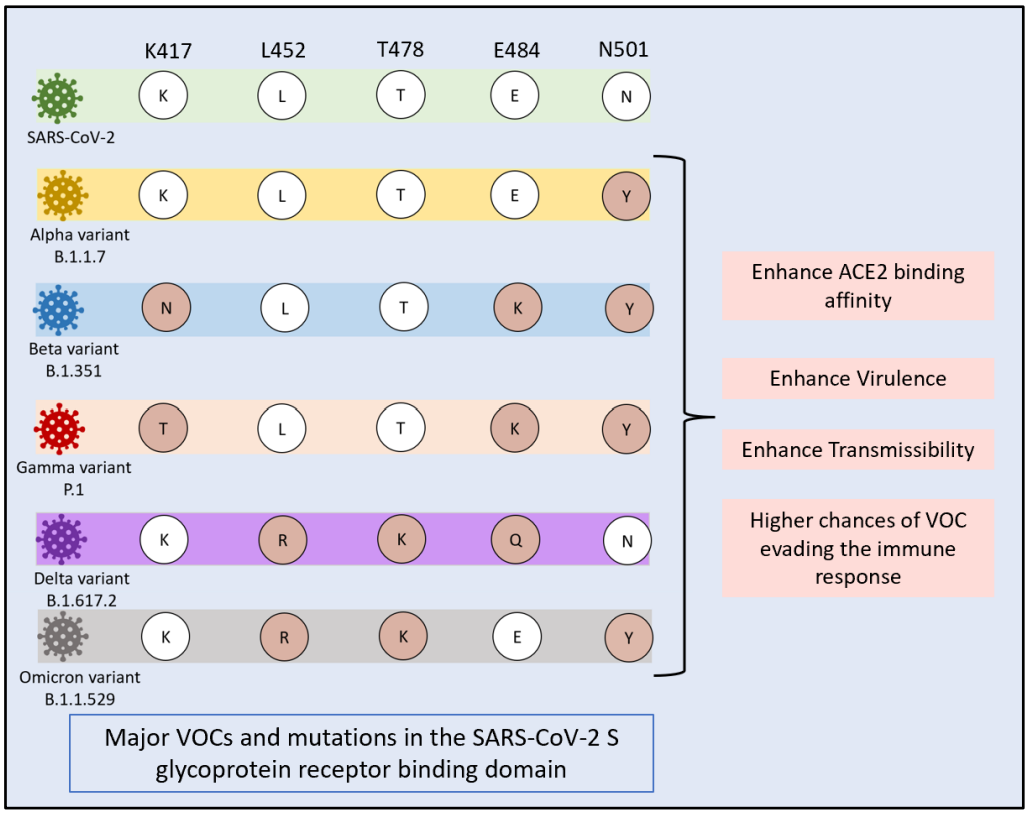

Figure 12. The major variants of concern of the SARS-CoV-2 virus. The figure shows the major VOCs isolated in major resurgences of COVID-19 globally. Alongside mutations within the radio-binding domain of the spike glycoprotein, believed to be a contributor to the increased virulence. Adapted from Khateeb et al [181].

One of the key variants correlated with enhanced pathogenicity of SARS-CoV-2 is the D614G (D: Aspartic acid, G: Glycine) substitution in the S glycoprotein [182]. The Alpha variant (B.1.1.7) was first isolated in December 2020, and responsible for the resurgence of COVID-19 in the United Kingdom (UK). This variant contains 7 missense mutations and deletions within 3 amino acids in the S glycoprotein, including the D614G substitution and the N501Y (N: Asparagine, Y: Tyrosine) substitution within the RBD [183]. Studies have shown that sera from vaccinated individuals shows antibodies with cross neutralization potency to both the wild-type SARS-CoV-2 and the alpha variant, suggesting vaccination or previous infection may offer some protection to the variant [184].

The beta variant (B.1.351) was identified in second wave of COVID-19 in South Africa in October 2020, spreading to more than 111 countries, however it was not as widely predominant as previous strains (less than 10% of COVID-19 cases). This variant consists of multiple non-structural and structural mutations, with three critical mutations being found within the RBD. These are N501Y, E484K, which was found to increase binding to ACE2, and K417N, which is seen to accelerate immune escape while reducing antibody binding efficacy [185].

Furthermore, the gamma variant (P.1), which was initially isolated in Brazil, spread in low rates through 78 countries, yet was highly prevalent in Brazil, French Guiana, and Chile [179]. The three major mutations found within the gamma variant are

similar to those present in the beta variant, which are N501Y, K417T and E484K. This variant is seen to increase transmissibility, ACE2 receptor binding, immune resistance, and risk of re-infection [185]. In comparison, the delta variant (B.1.617.2), which was responsible for the second wave of COVID-19 in India within October 2020, was the most dominant strain in 80% of COVID-19 cases in 52 out of 67 countries the strain was isolated in [179].

The omicron variant (B.1.1.529) was first isolated in November 2021 from an outbreak in South Africa. This lineage consists of more than 50 genetic mutations, with 30 of them within the *S* gene. Several of these gene mutations overlap with previously identified variants, such as N501Y (alpha), E484K (gamma and beta), and P681R (delta). Other mutations, such as S477N and Q498R, were linked to elevated ACE2 binding, virulence, and infectivity. These mutations may be the contributing factor to the increasing epidemiological situation [186].

When looking at vaccine efficacy towards the viral variants compared to the wild types, studies were conducted utilizing pseudoviruses, which may not accurately imitate nature. However, when assessing the efficacy of the mRNA BNT162b2 vaccine developed by Pfizer-BioNTech to the VOC compared to the wild-type SARS-CoV-2, studies showed no change or a mild decrease of nAb against the B.1.1.7 variant pseudovirus. Yet, there was a significant decrease seen in nAb production towards the B.1.351 variant, suggesting that it may be more virulent [179]. A study on the mRNA Pfizer-BioNtech vaccine efficacy in Qatar between February and March 2021, when 50% of COVID-19 cases were due to the B.1.1.7 variant and 44.5% of cases were due to the spread of the B.1.351 variant. The study assessed the protective impact of the vaccine after 14 days from the second dose of the vaccine, the results showed an 89.5% protective nAb effect on the B.1.1.7 variant and a 45% protection against the B.1.351 variant [187].

1.3.0 Hypotheses

This thesis hypothesizes that dysregulated glucose levels may induce oxidative stress, potentially triggering post translational modifications that can produce neoantigens. These neoantigens are then capable of altering the immune response in individuals with T1D.

1.3.1 Study 1: Main Hypothesis and Aims

This study suggests that the induction of oxPTMs to the native beta cell antigens, GAD65, ZnT8 and Insulin, may play a role in the progression of T1D.

Aim 1. The first aim of this study is to investigate the level of reactivity to oxPTM-β-cell antigens, focusing on INS, GAD65 and ZnT8, in patients with new-onset T1D

Aim 2. The second aim is to compare the reactivity of AABs to oxPTM antigens to AABs to native antigens in patients with T1D and healthy controls. As well as, to deduce the efficiency of oxPTM β-cell antigens in being potential biomarkers for T1D.

Aim 3. The final aim of the study is to determine whether there are any correlations with AAB development to oxPTM or native antigens to patient demographic and clinical information. This includes genetic information pertaining to HLA-typing, markers of oxidative stress, HbA1c levels, and fluctuations in C-peptide levels.

1.3.2 Study 2: Main Hypothesis and Aims

The main hypothesis is that dysregulated glucose levels may induce glycation of the SARS-CoV-2 S protein, altering the virulence of the disease. With one of the main focuses of this study to determine whether glucose regulation plays a role in vaccine efficacy and, in turn, immune protection against COVID-19.

Aim 1. The first aim of the study is to induce glycation of the S protein and asses ACE2 binding to both native (NT-) and glycated (GLY-) S protein.

Aim 2. The next aim is to determine the impact of antibody binding to NT- and GLY-S protein in previous COVID-19 patients.

Aim 3. To evaluate the role of glucose levels and monitoring on the protective immune response in patients following the administration of the SARS-CoV-2 mRNA vaccine (Pfizer-BioNTech, BNT162b2).

Aim 4. In order to better understand the role of hyperglycemia and diabetes in the adverse outcomes of COVID-19, the fourth aim of this study is to evaluate the clinical risk of diabetes and glucose levels on mortality in patients with COVID-19.

Chapter 2.0 Materials and Methods

2.1.0 Materials and Methods for Study 1

2.1.1 Patient Recruitment

Participants were recruited from the Immunotherapy Diabetes (IMDIAB) group, and the outpatient clinic of the Endocrinology and Diabetes department of Policlinico Campus Biomedico. Serum samples were retrieved from a total of N=69 patients with T1D introduced to this study, patients were introduced into the study based on a diagnosis of T1D according to the guidelines and criteria set by the American Diabetes Association (ADA), with the age of disease presentation being less than 35 years old, all patients were within the first year of disease onset and insulin therapy. Disease confirmation was typically performed by assessing the presence of GADA, IAA, or tyrosine phosphatase AABs. The patients included in the study lacked the presence of any other chronic disorders. Moreover, sera from N=32 T2D and N=42 healthy participants were included in the study as control groups. Informed consent was signed by patients or parents, and this study received ethical approval from the Ethical Committee from University Campus Bio-medico.

2.1.2 ROS-Modified β-Cell Antigens

Recombinant human GAD65 (Diamyd, rhGAD-65, 3.2 mg/mL, 45-08029-01), was diluted to 1 mg/mL and 0.5 mg/mL in 1x PBS and dialyzed in 1x PBS using the Slide-A-Lyzer G2 dialysis cassette (Thermofisher Scientific, 87723). Following the manufacturer's instructions, the diluted rhGAD65 was dialyzed for 2 hours at room temperature (RT) in 1x PBS (dialysis buffer), the dialysis buffer was then changed, and dialysis continued overnight at 4ºC. The next day, 100 µL of 1 mg/mL dialyzed GAD65 was modified *in vitro* overnight at 37ºC with an equal volume of 4 M ribose (D-ribose, Sigma) to induce glycation, this resulted in a final concentration of 0.5 mg/mL of glycated GAD-65 (GLY-GAD65) in 2 M D-ribose. 100 µL of 1 mg/mL dialyzed GAD65 was also modified overnight at 37ºC via 2 µL of 100 mM hydrogen peroxide (1 M H_2O_2, Sigma) and 100 mM of copper chloride ($CuCl_2$, Sigma) to induce the formation of the hydroxyl radical (•OH) via the Fenton reaction, yielding •OH-GAD65. Finally, 100 µL of 1 mg/mL dialyzed GAD65 was modified overnight at 37ºC via a 1:100 dilution of Hypochlorite acid (1 mmol/L HOCl, *VWR*) giving HOCl-GAD65.

Full length human recombinant ZnT8 (1.2 mg/mL DAG-ZnT8, Creative Diagnostics) was diluted to 0.5 mg/mL in 1x PBS and similarly modified via ROS as GAD65. 100 µL of 0.5 mg/mL Znt8 was modified with equal volumes of 4M D-ribose to yield 0.25 mg/mL glycated Znt8 (GLY-ZnT8), 5 µL of 100 mM H_2O_2 and 5 µL of 100 mM $CuCl_2$ to give hydroxyl modified ZnT8 (•OH-ZnT8), and 2 µL of 1:100 dilution of HOCl to induce HOCl modified ZnT8 (HOCl-ZnT8). All modifications were incubated overnight at 37ºC.

Insulin was modified by incubating 1 mg/mL of native insulin (NT-INS) in PBS with an equal volume of 4M D-ribose (R7500, Sigma) in ddH_2O at 37ºC for at least 3 days to induced glycation, forming glycated insulin (GLY-INS). The protein was modified with

HOCl by adding 9 mM sodium hypochlorite (1 M in 0.1M NaOH stock, BDH 230393L). To prepare 100 µL of HOCl modified insulin (HOCl-INS), a 1:10 dilution of HOCl was prepared in ddH_2O. 10 µL of the dilution was added to 90 µL of NT-INS, and the protein was incubated overnight at 37ºC. Hydroxyl modified insulin (•OH-INS) was prepared by incubating 50 µL of NT-INS (1 mg/mL) with 5 µL of a 1:80 dilution of H_2O_2 in ddH_2O (9 mM, BDH101284N) and 2.5 µL $CuCl_2$ (100 mM), and incubated overnight at 37º. All modifications were stored short-term at 4ºC, and for long term storing the modifications were placed in -20ºC. Bovine serum albumin (BSA, Sigma) was diluted to 0.5 mg/mL in distilled water (dH_2O) and modified similarly to the β-cell antigens to be used as a control antigen.

2.1.3 SDS-PAGE and Western Blot of Modified β-Cell Antigens

A series of SDS-PAGEs were performed to monitor the induced modifications to GAD65 and ZnT8. Initially a 10% SDS-PAGE was performed for GAD65, the resolving gel was composed of 30% *bis*-acrylamide (Sigma), distilled water, 1.5 M Tris (pH 8.8), and 10% ammonium persulphate (APS), with the final buffers added being 10% SDS and TEMED. The resolving gel was mixed and loaded between two 1.5 mm glass plates; a layer of 100% isopropanol was added to the glass plates to prevent the resolving gel from oxidizing until the gel solidified. The volumes of each component are in table 4. A 5% stacking gel was prepared with distilled water, *bis*-acrylamide, 1.0 M Tris (pH 6.8), and 10% APS, the final components added were 10% SDS and TEMED. The buffers were mixed and loaded into the glass plates, a 10 well comb was placed between the glass plates until the gel solidified. The volumes for the stacking gel are in table 5. Roughly 5 to 10 µg of protein was loaded with equal volumes of Laemmli sample loading buffer, with and without β-mercaptoethanol for reducing and non-reducing conditions. The gels were run at 120V for 2 hours and stained for 2 hours with Coomassie brilliant blue. The gels were then washed with ddH_2O and de-stained with methanol/ddH_2O/acetic acid (50/40/10, v/v/v) for 1 hour, changing the de-stain solution every 20 minutes. After de-staining, the gels were then washed with distilled water and imaged using the Chemi-Doc imaging system (Bio-Rad).

Component	Volume (mL)
Distilled water	5.9
30% Acrylamide mix (sigma)	5.0
1.5 M Tris (pH 8.8)	3.8
10% SDS	0.15
10% Ammonium persulphate	0.15
TEMED	0.006

Table 4. Components of 10% SDS-PAGE resolving gel use for GAD65.

Component	Volume (mL)
Distilled water	3.4
30% Acrylamide mix (sigma)	0.83
1.0 M Tris (pH 6.8)	0.63
10% SDS	0.05
10% Ammonium persulphate	0.05
TEMED	0.005

Table 5. Components of 5% SDS-PAGE stacking gel.

A 15% SDS-PAGE gel was prepared for native and modified ZnT8 antigens to monitor any changes in the modifications, the composition can be found in table 6, with a 5% stacking gel (table 5).

Component	Volume (mL)
Distilled water	3.4
30% Acrylamide mix (sigma)	7.5
1.5 M Tris (pH 8.8)	3.8
10% SDS	0.1
10% Ammonium persulphate	0.1
TEMED	0.004

Table 6. Components of 15% SDS-PAGE resolving gel.

Samples were also run on precast 4-20% gradient gels (4-20% Mini-PROTEAN® TGX™, Bio-Rad, #4561093DC). Roughly 5-10 µg of each protein was run loaded to their respective lanes with a 1:1 ratio of either Laemmli buffer with β-mercaptoethanol, to reduce the proteins, or without β-mercaptoethanol. The samples were heated for 5 minutes at 100ºC to denature the proteins and then loaded into the gel and run at 120V for 2 hours with 1x SDS Running buffer (Bio-Rad). Gels were stained with Coomassie blue for 2 hours and then de-stained using 50/40/10 (v/v/v) of methanol, distilled H_2O and acetic acid (sigma) for 1 hour, changing the de-stain solution every 20 minutes. The gels were then left in distilled H_2O overnight to continue processing. Gels were imaged using the Chemi-Doc imaging system (Bio-Rad)

Gels prepared for western blotting were drip dried and blotted using the Trans-Turbo blot transfer system (Bio-Rad). Gels were sandwiched between the Trans-Blot Turbo Mini 0.2 µm Nitrocellulose transfer pack (Bio-Rad, 1704158) in the Turbo blot transfer cassette, and then transferred at 30 mA for 7 minutes at RT. The membranes were briefly stained with Ponceau S red stain (Sigma) to confirm the transfer. Blots were then washed 4 times for 20 minutes with 0.1% PBST, and then blocked with 5% BSA in 0.1% PBST for 2 hours at RT. After blocked, the blots were

washed again 4 times for 20 minutes with 0.1% PBST. Then a 1:200 of patient sera (used as a primary antibody) was prepared in the blocking buffer, and used to stain the blots overnight at 4ºC. The next day the blots were washed 4 times for 20 minutes in 0.1% PBST again, and stained with Goat anti-Human IgG-HRP (sigma) at a 1:5000 dilution for 2 hours at RT. After the incubation, the blots were washed for a final time for 20 minutes 4 times in 0.1% PBST, and then stained with 5 mL of Clarity Western ECL substrate (1:1 ration of substrate 1 and 2) (Bio-Rad, 1705061) for 3-5 minutes. The blots were imaged using the Chemi-Doc imaging system and exposed for 0.05-3 seconds.

2.1.4 Native PAGE Protocol

The Native resolving gel was prepared according to the buffers and volumes present in table 7, with the key exclusion of SDS from all the buffers, including the loading and running buffers. The last buffer added before pouring the gel between the glass plates was TEMED to allow the gel to solidify. A layer of 100% isopropanol was added to the resolving gel, to prevent oxidation. Once solidified, the isopropanol was removed, the gels were then washed with ddH_2O. The stacking gel was prepared according to the buffers and volumes in table 8.

Component	Volume (mL)	
	15%	**20%**
Water (ddH_2O)	4.6	1
30% acrylamide	10.0	10.67
1.5 M Tris pH 8.8	5.0	5
10% APS	0.2	0.160
TEMED	0.008	0.016

Table 7. Native PAGE resolving gel composition and volumes.

Component	Volume (mL)
Water (ddH_2O)	3.4
30% acrylamide	0.83
1.0 M Tris pH 6.8	0.63
10% APS	0.05
TEMED	0.005

Table 8. 5% Stacking gel composition and volumes.

10 µg of Native (NT-INS) insulin and glycated insulin (GLY-INS) were prepared to load in the gel with a 1:1 ration of sample buffer (bromophenol blue), and the samples were heated for 100ºC for 5 minutes. The gels were added to the running chamber, with 1x running buffer with no SDS, and run for 2 hours at 120V. Once the run was finished, the gels were stained with Coomassie brilliant blue for 2 hours. The gels were de-stained with 50/40/10 (v/v/v) methanol, distilled water, and acetic acid

for 2 hours, changing the de-staining solution every 30 minutes. The de-stained solution was washed away with distilled water, and the gels were imaged with the Chemi-Doc system from Bio-Rad.

2.1.5 Native and Modified GAD65 ELISA Protocol

A 96-well Nunc plate (Thermofisher scientific) was coated with 100 µL of 2µg/mL of native or modified GAD65 per well diluted in 0.05M Carbonate/Bicarbonate buffer (pH 9.6) and incubated overnight at 4ºC. The next day, the plates were washed 3 times with 1x PBS and blocked with 5% BSA in 0.1% PBST (1xPBS with Tween 20), and incubated for 2 hours at RT. After the incubation, 100 µL of patient or healthy control (HC) serum diluted 1:200 in blocking buffer was added to the wells and incubated for 2 hours at RT. This was followed by washing the plates 3 times with 0.1% PBST and then 3 times with 1x PBS. 100 µL of a 1:1000 dilution of Rabbit anti-Human IgG-HRP (Sigma) in 0.1% PBST was then added to all the wells and incubated at RT for 2 hours. The plates were washed again 3 times with 0.1% PBST and 3 times with 1x PBS. Finally, 100 µL of 100 µg/mL TMB (3,3', 5,5' -tetramethyl benzidine substrate, Sigma) diluted in 0.1 M sodium acetate (NaOAc, pH 6.0) with 2 µL of 1 M H_2O_2 per 10 mL was added to each well for roughly 3 to 5 minutes. The reaction was then stopped with 50 µL of 20% sulfuric acid (H_2SO_4, Sigma). The plates were read at an optical density (O.D.) of 450 nm with reference wavelength of 610 nm using the Tecan infinite 200pro (Life Sciences). All plates were incubated on a plate shaker.

2.1.6 Native and Modified ZnT8 ELISA Protocol

96 well Nunc plate was coated with 100 µL of 2 µg/mL of native (NT-) or modified ZnT8 per well diluted in 0.05M Carbonate/Bicarbonate buffer (pH 9.6) coating buffer and incubate overnight at 4ºC. The coating buffer was removed, and the plates were washed 3 times with 1x PBS. The plates were then blocked with 200 µL of 5% skim milk (Sigma) in 0.1%PBST (blocking buffer) and incubated for 2 hours at RT. The blocking buffer was removed, and a 100 µL of 1:200 sera sample diluted in blocking buffer for 2 hours at RT. After the incubation, the plates were again washed 3 times with 0.1% PBST and then 3 times with 1x PBS. This was followed by adding 100 µL of a 1:10,000 dilution of secondary antibody (Rabbit anti-human IgG-HRP) in blocking buffer and incubating for 2 hours at RT. The secondary antibody was then removed, and plates were washed again. The plates were padded completely dry and then 100 µL of 100 µg/mL TMB substrate diluted in 0.1 M NaOAc was added to each well for 2-3 minutes. The reaction was stopped with 20% H_2SO_4 and the plates were read on the Tecan at O.D. 450 nm with a reference wavelength of O.D. 610 nm.

2.1.7 Native and Modified Insulin ELISA Protocol

In order to test the activity, a 96-well NUNC plate was coated overnight at 4ºC with 100 µL per well of modified or native insulin in 0.05M Carbonate/Bicarbonate buffer (pH 9.6) at 10µg/mL. The next day, the coating buffer was removed, and the plates were washed 3 times with 1x PBS. The plates were then blocked with 200 µL of 5% BSA in 0.5% PBST per will for 2 hours at RT. After blocking, a 1:200 dilution of

patient or HC sera samples in blocking buffer were added at 100 µL per well, and incubated for 2 hours at RT. The plates were then washed 4 times with 0.1% PBST and 4 times with 1x PBS. After washing, 100 µL of 1:1000 dilution in blocking buffer of rabbit anti-human IgG-HRP (Sigma) was added to each well and incubated for 2 hours and RT. Finally, the plates were washed 4 times with 0.1% PBST and 4 times with 1x PBS. The plates were imaged by adding 100 µL of TMB substrate diluted in 0.1 M NaOAc to each well and left to incubated for 2-3 minutes. The reaction was stopped using 50µL per well of 20% H_2SO_4 and imaged using the Tecan at O.D. 450 nm and reference wavelength of O.D. 610 nm.

2.1.8 Carboxymethyl-Lysine Assay

Human Carboxymethyl-Lysine (CML) was measured using the CML assay kit from Cusabio (CSB-E12798h) following the manufacturer's instructions. Standards were brough to RT and prepared by serially diluting 4000 pg/mL of Standard solution 7 times in the provided sample diluent. Once the kit was brought to RT, 100 µL of Standard or sera samples were added to their designated wells and left to incubate for 2 hours at 37ºC. The liquid was removed, and 100 µL of 1x Biotin Antibody diluted in Biotin antibody diluent to each well and incubated for 1 hour at 37ºC. After the incubation, the wells were aspirated and washed 3 times with 200µL of washing buffer. The plates were patted completely dry and 100 µL of 1x HRP-avidin was added to each well and incubated for 1 hours at 37ºC. The plates were then washed 5 times with 200µL of washing buffer and patted completely dry. 90µL of provided TMB substrate was added to each well and left to incubate for 15-30 minutes at 37ºC. The reaction was stopped with 50µL of stop solution and the plates were read at O.D. 450 nm with a reference wavelength of O.D. 540 nm.

2.1.9 Statistical Analysis

All statistical analyses and graphs were made using GraphPad Prism (GraphPad, San Diego, CA, USA). Continuous data was presented as mean ± standard deviations or median [interquartile range], where appropriate depending on the normal distribution of the data, categorical data was presented as percentages. Differences between antibody groups were assessed via Mann-Whitney test or a parametric unpaired student's t-test, where appropriate. A Pearson's or a Spearman's correlation test were performed where appropriate to determine the association between antibody responses and clinical characteristics. SDS-PAGE gels were assessed using the Chemi-Doc MP imaging system from Bio-Rad, and images were quantified and assessed with Imagej [188].

2.2.0 Study 2 Materials and Methods

2.2.1 Study Design and Patient Recruitment

This was a longitudinal single center study whereby patients included were screened and recruited from the Endocrinology and Diabetology unit at Policlinico Campus Biomedico di Roma. With 26 patients being diagnosed with type 1 diabetes (T1D) and 34 patients with T2D. Inclusion criteria for the study was patients 18 years old or over, scheduled to receive the SARs-CoV-2 mRNA vaccine BNT162b2 (Pfizer-BioNTech), being able to give signed informed consent, having a diagnosis of T1D or T2D for more than 3 months, and using at least two anti-diabetic drugs for the T2D patients, according to the vaccine priority criteria. The exclusion criteria included pregnancy or breastfeeding, younger than 18 years of age, inability or failure to sign informed consent, chronic corticosteroid therapy, end stage renal failure, advanced neoplastic diseases and immunosuppressive therapy for transplantation or autoimmune diseases that require the use of immunosuppressive drugs. The study covered a total of 6 months (5 timepoints, T0-T4) with patient sera from T1D and T2D being collected before first administration of SARs-CoV-2 mRNA vaccine.

T0: baseline, within 3 days of the first dose of the mRNA vaccine.

T1: 21 days after the first dose, and day of the second dose of the vaccine

T2: 34 days from the baseline.

T3: 90 days from the baseline.

T4: 180 days from the baseline.

2.2.2 Peripheral Blood Mononuclear Cells (PBMCs) Extraction Protocol

Patient blood samples were collected and centrifuged down at 300g for 10 minutes with an acceleration a deceleration of 5. The plasma was removed, and the remaining contents of the blood tube were added to a 50mL falcon tube, which was then washed with 1 mL of media (RPMI with PenStrip). The blood contents and media were then slowly added in a 1:1 ratio to Ficoll-Paque (17144003, cytiva), the mixture was then centrifuged at 1200g, RT, for 25 minutes with an acceleration of 7 and deceleration of 2. After the centrifugation, the supernatant was removed, and the buffy coat was collected and added to media in a 1:1 ratio. The samples were again centrifuged at 700 g for 5 minutes, the supernatant was removed, and the pellet was resuspended in media. The cells were counted using trypan blue at a 1:1 ratio and an automated cell counter (Bio-Rad). Then, the samples were centrifuged for a final time and resuspended in freezing mix (90% FBS with 10% DMSO) to have roughly 10 million cells within 1 mL and stored at -80ºC until assayed.

2.2.3 Modification and SDS-PAGE of SARs-CoV-2 Spike (S) Protein

The SARs-CoV-2 S protein (10549-CV-MTO, R&D systems) (0.4 mg/mL) was incubated at 37ºC with equal volumes of 0.5 M D-ribose to induce in vitro glycation. The modifications were confirmed via a 10% SDS-PAGE analysis (table 9). The gels were stained for 2 hours with Coomassie brilliant blue, and de-stained using

50/40/20 (v/v/v) of Methanol, ddH_2O and Acetic acid 1 hour, the gels were then left in ddH_2O overnight at RT. The gels were imaged using Chemi-Doc Imaging system (Bio-Rad).

Component	Volume (mL)
Distilled water	5.9
30% Acrylamide mix (sigma)	5.0
1.5 M Tris (pH 8.8)	3.8
10% SDS	0.15
10% Ammonium persulphate	0.15
TEMED	0.006

Table 9. Components of 10% SDS-PAGE resolving gel.

2.2.4 SARs-CoV-2 Native and modified S protein binding to ACE2

1 ug/mL of NT-S or GLY-S protein were used to coat a Nunc 96 well plate overnight at 4ºC. The plate was washed 4 times with 0.05% Tween 20 in PBS and then blocked with 1x PBS/ 5% Skim milk/ 1% fetal bovine serum/ 0.2% Tween 20 overnight at room temperature. The plate was washed again 4 times, and then incubated with ACE2-IgMu (GTX135683-pro, Genetex) serially diluted from 2ug/mL in blocking buffer for 1 hour at RT. The plates were then washed another 4 times, then incubated with goat anti-mouse HRP at a dilution of 1:20,000 for 1 hour at RT. The plates were washed again, 100 µL of TMB was then added (1:100 in 0.1M sodium acetate) to the plate until a color reaction developed (3 mins). The reaction was stopped with 50 µL of sulfuric acid.

2.2.5 Assessment of antibodies in Diabetic patients after immunization with anti-COVID-19 vaccine

Patient sera from T1D and T2D was collected before first administration (T0) of anti-COVID vaccine, just before the administration of the second dose (T1), 2 weeks after the second dose (T2), 3 months from baseline (T3), and 6 months from baseline (T4). Controls include healthy patients (without T1D and COVID-19). 96 well Nunc ELISA plates were coated with 1 µg/mL of NT- SARs-CoV-2 spike protein (10549-CV-MTO, R&D systems) or 0.5 M ribose modified SARs-CoV-2 spike protein and incubated overnight at 4ºC. The plates were washed four times with 1x PBS/0.05% Tween20 using a plate washer (Stat fax 2600 ELISA washer)**.** The plates were blocked with 200 µL per well of blocking buffer (1x PBS/ 5% skim milk/ 0.1% Tween20) at room temperature for 1 hour. After removing the blocking buffer and washing the plates 3 times, patient or control sera was diluted 3-folds in blocking buffer and incubated at room temperature for 1 hour. Plates were washed, the plate was then incubated with 100 µL per well of 0.4 µg/mL of ACE2-IgMu (GTX135683-pro, Genetex) diluted in blocking buffer for 1 hour at room temperature. After washing the plate was incubated with Goat anti mouse-HRP (A90-116P, Bethyl laboratories) diluted 1:20,000 in blocking buffer and incubated at room temperature

for 1 hour. The plates were washed again and incubated with 100 µL per well of TMB substrate diluted 1:100 in 0.1 M sodium acetate pH 6.0 for 3 minutes. The reaction was stopped with 50 µL of 20% sulfuric acid. The optical density of the plates was read at 450 nm. Protocol adapted from Walker et al [189].

2.2.6 Assessment of antibody response in COVID-19 patients with or without diabetes

96 well Nunc ELISA plates were coated with 2 µg/mL of native SARs-CoV-2 spike protein (10549-CV-MTO, R&D systems) or 0.5 M ribose glycated SARs-CoV-2 spike protein and incubated overnight at 4ºC. The plates were blocked with 200 µL per well of blocking buffer (1x PBS/ 5% skim milk/ 0.1% Tween20) at room temperature for 1 hour. After removing the blocking buffer and washing the plates 3 times, COVID-19 patient or healthy control sera was diluted 1:1280 in 1% skim milk in PBST and incubated at room temperature for 1 hour. The plates were washed again, and incubated with 100uL of rabbit anti-human IgG-HRP at a 1:3000 in 0.1% PBST for 1 hour at RT. After incubation, the plates were washed again and 100 µL per well of TMB substrate diluted 1:100 in 0.1 M sodium acetate pH 6.0 was added for 3 minutes. The reaction was stopped with 50 µL of 20% sulfuric acid. The optical density of the plates was read at 450 nm. Between steps the plates were washed four times with 1x PBS/0.05% Tween20. The ELISA protocol was adapted from Amanat et al [190].

2.2.7 Fructosamine assay

Serum fructosamine levels were assessed via a fructosamine ELISA kit (ab228558, abcam). The supplied fructosamine buffers were pre-warmed to 37ºC. 10 µL of either undiluted serum samples or H_2O were added to a 96-well plate. This was followed by adding 3 µL of fructosamine calibrator was added as a positive control, with the volume adjusted to 10 µL with fructosamine buffer A. Thiol blocking reagent was prepared by adding 2 µL of reconstituted Thiol Blocking reagent and 5 µL of sample cleaning mix to 30 µL of Fructosamine Buffer A to yield a final volume of 37 µL/well. The plate was pre-incubated for 10 minutes at 37ºC, this was followed by adding 3 µL of NBT to each well, with the volume of each well being 50 µL. 200 µL of fructosamine buffer B was added to each well to yield a total final volume of 250 µL. The plate was incubated for 5 minutes at 37ºC. After the 5 minutes incubation (O.D 1), the plates were read at 530 nm, and then read after 15 minutes incubation (O.D 2).

2.2.8 Intracellular cytokine staining and assessment of T-cell immune responses in isolated PBMCs

Cells were thawed in a prewarmed 37ºC water bath until a small piece of ice was left in the cryovial. The cells were resuspended in 1 mL of warmed RPMI with 10% FBS (fetal bovine serum)**.** The cells were centrifuged at 3000 rpm for 5 minutes, the supernatant was removed the cells were resuspended in fresh RPMI with 10% FBS. The cells were counted using Trypan blue (1:1 ratio) and the cells were cultured overnight at 37ºC with 5% CO_2. The next day the cells were centrifuged down at

3000 rpm for 5 minutes and resuspended in RPMI without FBS. For each sample, 3 conditions were set up:

1. Cells with stimulation cocktail (1:800) (manufacturer).

2. Cells with stimulation and inhibition cocktail (1:800) (manufacturer).

3. Cells with stimulation cocktail and SARs-COV-2 Prot_S Complete (130-127-951, miltyenyi Biotech).

The cells were incubated and stimulated at 37ºC for 4 hours. After incubation, the cells were centrifuged at 3000 rpm for 5 minutes and washed with 100µL of 1x running buffer and then centrifuged again. The surface staining cytokines were prepared, these included CD4 and CD8, 1 in 80 at 30 µL per sample in 1x running buffer and incubated in the fridge at 4ºC for 20 minutes. The cells were then centrifuged and washed 2 times in 1x running buffer. The cells were then fixed with 100µL of 10% formalin (or 4% paraformaldehyde) for 12 minutes at RT in the dark. After the incubation, the cells were washed twice with 100 µL of 1x running buffer. The intracellular staining (TNFα, IL-2 and INF) was then prepared in 0.5% Saponine, which was diluted in 1x running buffer, for a total of 40 µL per sample at a 1 in 80 dilution and incubated in the dark for 20 minutes. The cells were then washed twice and resuspended in 1x Running buffer to read on the Cytoflex.

2.2.9 SARS-CoV-2 Microneutralization protocol

A live SARS-CoV-2 assay using the Vero E6 cellular system was used to assess the serum neutralization potency, similar to what was previously described in Capuano et al and Sholukh et al [191, 192]. The collected serum samples were placed and stored at -20 °C, then when needed diluted (1:10; 1:40; 1:160; 1:640) in triplicates and then mixed with 100 TCID50 of SARS-CoV-2 (a clinical isolate, strain VR PV10734, donated very kindly by the Lazzaro Spallanzani Hospital, Rome, Italy). Each mixture of serum and virus was then transferred to 96 well plate, in the company of 5×10^5 /ml Vero E6 (CRL-1586, ATCC, Manassas, Virginia, United States) cells. The monolayers were placed in the incubator at 37 °C until the cytopathic effect (CPE) was viewed via microscopy, this was followed by the cells being stained with crystal violet solution. The serum neutralization titers of each sample was calculated through the highest serum dilution protecting 90% (IC90), 50% (IC50), and 20% (IC20) of the infected wells [190, 193]. This protocol, in its entirety, was performed in a Biosafety Level 3 (BSL-3) laboratory.

2.2.10 Study population for building the Clinical Risk Score for predicting in-hospital death from COVID-19

The clinical risk score was devised from data collected retrospectively from 417 COVID-19 patients admitted to Jaber Al-Ahmed Hospital in Kuwait between February 24th and May 3rd, 2020 [194]. Data collection took place at a time where there was a total hospitalisation rate based off a positive real-time polymerase chain reaction (RT-PCR) of SARS-CoV-2 from a nasopharyngeal swab, without regard of symptoms [195]. Due to this, the patients within the cohort range from those with no symptoms to severe and detrimental cases of COVID-19. Within the study,

asymptomatic COVID-19 was characterised as any individual who has a positive RT-PCR for SARS-CoV-2, but otherwise, did not have any signs or symptoms of viral disease. Consequently, symptomatic patients were defined as COVID-19 patients with mild to moderate symptoms of viral infection, without requiring ICU admission. Finally, severe COVID-19 cases were described as patients who required mechanical ventilation, ICU admission and mortality.

2.2.11 Statistical Analysis used to build the Clinical Risk Score

Continuous variables were presented as measures of central tendency and dispersion, where appropriate, and student's T test was performed to compare differences. While, categorical variables were presented as proportions, with the ranks compared with a X^2 test. Setting the primary outcome as in-hospital death, a series of multivariant logistical regression models were performed in order to identify independent factors that may be prognostic for the primary outcome. The models were created by adding or removing variables individually depending on the results of the previous log regression, retaining only the variables associated with the outcome and a p-value<0.1. Initially, continuous variables, such as age and blood glucose levels, were converted into ordinal figures determined by known cut-offs (age: <50, 51-70, and 70> years of age, blood glucose: <5.5, 5.5.-6.9, 7.0-11.1, and 11.1> mmol/L). Initially, the comorbidities included in the logistic regressions were hypertension, diabetes, malignancy, chronic renal disease, and asthma and tested against the primary outcome (in-hospital death). Similar logistic regression models were performed using demographic data. In the final score, the independent predictive variables included were those with a significant p-value<0.1, with a final regression performed that merged the data.

The independent predictive variables included in the final model were gender, asthma, glucose categories, and non-Kuwaiti national. Weighted points were assigned to significant risk factors proportional to their beta regression coefficient values. The effectiveness of the risk score to predict mortality in patients with COVID-19 was analysed via receiver operating characteristic (ROC) curves. When putting disease prediction into consideration, assessing the area under the curve (AUC) 0.9 or greater, suggest a great fit for the score, meaning that the score is able to predict the primary outcome with high confidence. An AUC between 0.7-0.8 suggests an acceptable fit for the score, which implies that the score may somewhat predict the primary outcome. Finally, an AUC of 0.5 or less was taken as insignificant [196]. Youden's index was applied to set a cut-off for mortality prediction. Significance was set as a two-tailed p-value <0.05. The score was built using SPSS (IBM Corp. IBM SPSS Statistics for Windows, Version 21.0. Released 2012. Armonk, NY: IBM Corp.).

2.2.12 Internal and External validation cohorts for the Clinical Risk Score

In order to determine the efficacy of the devised score, it required both internal and external validation. For the internal validation, a Kuwaiti COVID-19 cohort was recruited between May 4th and August 26th 2020, and the clinical risk score was calculated for each patient. All patient information was collected retrospectively, and

to be included within the validation cohort, the inclusion criteria was based on patients having admission and discharge data. The calculated risk scores for the patients was plotted on a ROC cure, with the AUC calculated in order to assess the “goodness of fit” for the score.

The external validation cohort was comprised of patients from the Italian CoViDiab study cohort. As stated in Maddaloni et al [197], the CoViDiab study was a multi-center retrospective study on patients hospitalized for COVID-19 in four academic hospitals within the Lazio region up until May 15th 2020. Inclusion criteria for the study was patients who were above 18 years of age, with a confirmed positive RT-PCR positive diagnosis of COVID-19 in compliance with the WHO protocols at the time. Furthermore, patients included within the final analysis had both admission and discharge data available.

2.2.13 Ethical Considerations for Clinical Risk Score

In compliance with ethical considerations, ethical approval for the Kuwaiti study was obtained from the committee of health and medical research located at the Ministry of Health (MOC) in Kuwait (IRB 2020/1404). Due to the urgency and the health emergency posed by COVID-19, the need for written informed consent was waived to expedite research.

The ethical requirements for the CoViDiab study followed the principles indicated by the Helsinki Declaration, with ethical approval from the Ethical Committee from Umberto I “Policlinico” General Hospital (reference 5819/2020). Similarly, to the Kuwaiti cohort, due to the emergency situation posed by the COVID-19 pandemic and the retrospective design of the study, the need for written consent was waived in cases of death, impossibility to contact patients and in cases of discharge. However, the anonymity and privacy of the collected data was guaranteed in accordance with the regulations at the time.

Chapter 3.0 Results Study 1: Autoimmunity to β-cell antigens in T1D

3.1 Patient Characteristics

A total of N=69 patients with T1D within the first year of disease onset were recruited into this study, along with N=32 T2D. When comparing demographic patient characteristics such as age, gender distribution, BMI, and HbA1c, the T1D were typically younger compared to T2D (median age in years [IQR],13 [9-26] vs 62.50 [52- 68.25], p-value <0.0001, respectively), BMI was lower in T1D than in T2D (median kg/m^2 [IQR], 18 .60 [16.20-20.95] vs 30.40 [24.35-33.05], p-value <0.0001, respectively), and there was no difference between gender distribution amongst the two cohorts. HbA1c levels were significantly higher in T1D cohort compared to the T2D cohort (HbA1c (%) mean ± S.D, 10.66 ± 2.80 vs 7.61 ± 1.26, p-value <0.001), and although c-peptide data and CML was not available for T2D, T1D showed median c-peptide level of 0.83 ng/mL [0.60-1.24] and a median CML of 50.26 pg/mL [32.91-71.16]. The study cohort demographic data are displayed in table 10.

	Type 1 Diabetes	Type 2 Diabetes	P-value
Total (N)	69	32	
Male (n, %)	31 (47.0%)	15 (47.0%)	
Age (years) (median [IQR])	13 [9-26]	62.50 [52-68.25]	***<0.0001***
BMI (kg/m²) (median [IQR])	18.60 [16.20-20.95]	30.40 [26.35-33.05]	***<0.0001***
HbA1c (%) (mean ± S.D)	10.66 ± 2.80	7.61 ± 1.26	***<0.0001***
C-peptide (ng/mL) (median [IQR])	0.83 [0.60-1.24]	-	
Carboxymethyl Lysine (pg/mL) (median [IQR])	50.26 [32.91-71.16]	-	
HLA haplotype*		N/A	
DR4	18 (46.2%)		
DR3	21 (53.8%)		

Table 10. Demographic information of T1D and T2D patients. The table depicts the major demographic information and differences between the T1D and T2D cohorts included in this study. Normally distributed data was depicted as mean ± standard deviation (S.D), non-normally distributed data was depicted as median [interquartile range], binomial data was shown as percentages. P-values were calculated using student T test's or Fisher's test where appropriate. **Indicates that data was not available for all participants in the study cohort.*

3.2 Monitoring induced ROS modifications of β-cell antigens

3.2.1 Monitoring modifications of GAD65

Upon incubating 0.5-1mg/mL of NT-GAD65 with 2M D-ribose, 10 mM •OH, and a 1:100 dilution of HOCl, the induced modifications were monitored via SDS-PAGE analyses. Roughly 10 µg of each protein was loaded into each lane in a 1:1 ratio with Laemmli buffer and run at 120V for 2 hours. The gel showed that when GAD65 is modified *in vitro* with 2 M ribose, there appeared to be an upshift in the molecular weight of NT-GAD65 from bands at 116.8, 109.4, 54.9, 50.4 and 22.7 KDa to 117.5, 59.5 and 23.3 KDa in the GLY-GAD65 lane. However, the induced modification also caused smearing when run through the gel, suggesting that some of the protein was degraded. Furthermore, bands initially appearing in the NT-GAD65 were lost in the GLY-GAD65 lane. Similarly, when assessing the band intensity, there was a decrease in band intensity between NT-GAD65 and GLY-GAD65. With induction of •OH-GAD65, there appeared to be 2 faint bands at 60.1 KDa and 53.3 KDa, with no other bands appearing in the lane. In comparison, to the NT-GAD65, the •OH-GAD65 had a decreased band intensity. Finally, the HOCl-GAD65 showed bands at 117.5, 60.1, 54.2, 23.5, 23.5 and 11.3 KDa (figure 13). Figure S1 shows the results of a western blot of NT- and oxPTM-GAD65, using a serum pool of 5 patients with T1D as the primary antibody.

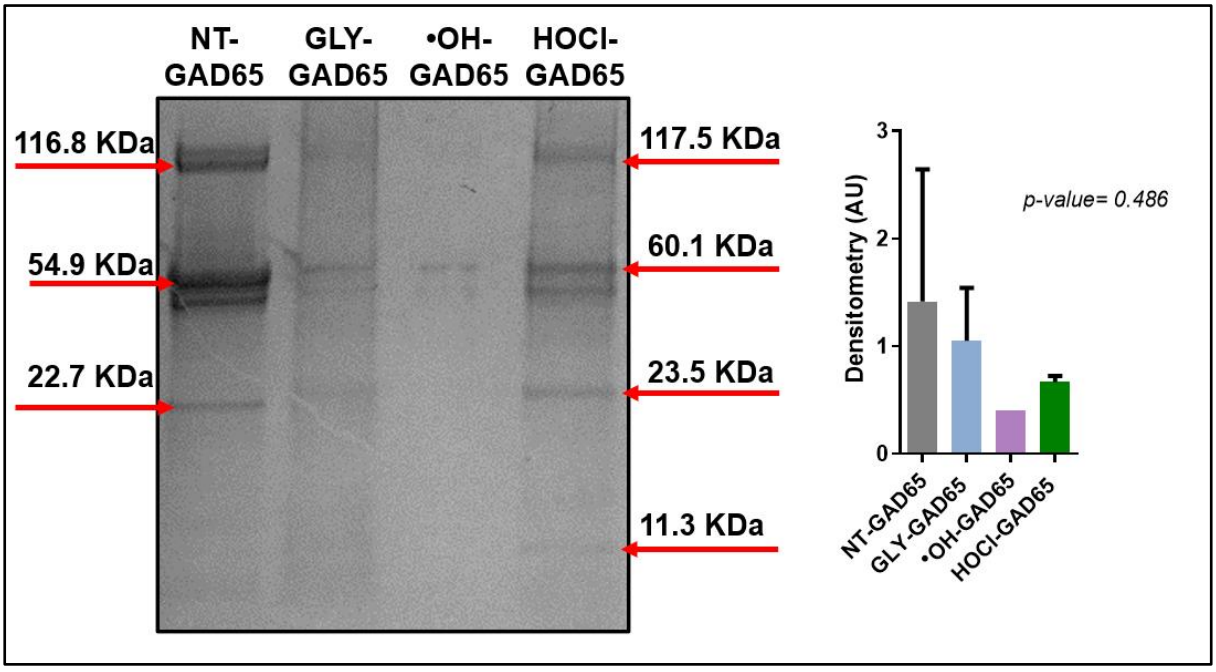

Figure 13. 4-20% gradient SDS-PAGE of NT- and modified-GAD65. Roughly 10µg of protein was loaded in each lane with 1:1 dilution of 2x Laemmli sample buffer with β-mercaptoethanol to allow for the denaturation of the proteins. The gels were run at 120-140V for 2 hours and stained with Coomassie blue for 1 hour. This was followed by the gels being de-stained for 2 hours in 50/40/20 (v/v/v) in methanol/water/acetic acid. The NT-GAD65 lane shows distinct bands at 116.8, 109.4, 54.9, 50.5 and 22.7 KDa. With the GLY-GAD65 lane showing faint bands at 117.5, 59.5 and 23.3 KDa, the •OH-GAD65 lane shows two faint bands at 60.1 and a faint band at 53.3 KDa, and finally HOCl-GAD65 lane shows bands at

117.5, 60.1, 54.2, 23.5 and 11.3 KDa. *The gel was imaged using the Chemi-Doc imaging system from Bio-Rad and quantified using ImageJ software.*

3.2.2 Monitoring modification of ZnT8

Upon modifying 0.5 mg/mL of NT-ZnT8 with 2M D-ribose and running a 12% SDS-PAGE, there was an apparent up-shift in GLY-ZnT8 with distinct bands at 93.1 and 43.2 KDa compared to the NT-ZnT8, which showed clear bands at 83.4 and 36.6 KDa (figure 14A). However, with glycation there was a clear loss of bands previously seen in the NT-ZnT8 lane. In comparison, modifying NT-ZnT8 with the hydroxyl radical to yield •OH-ZnT8 showed a similar increase in molecular weight to 88.9, 72.9, and 38.9 KDa compared to the NT-ZnT8 bands at 83.4, 36.6 and 31.0 KDa as seen in figure 14A. Furthermore, in the •OH-ZnT8 lane, bands appeared more defined further down the lane that were not apparent in the NT-ZnT8 lanes, but these were too faint to be quantified by the Chemi-Doc system. Finally, when running a 4-20% gradient SDS-PAGE, HOCl-ZnT8 appeared to have bands at a molecular weight of 77.2 and 31.4 KDa compared to 60.2, 23.5 and 20.5 KDa seen in the NT-ZnT8 lane, as seen in figure 14B.

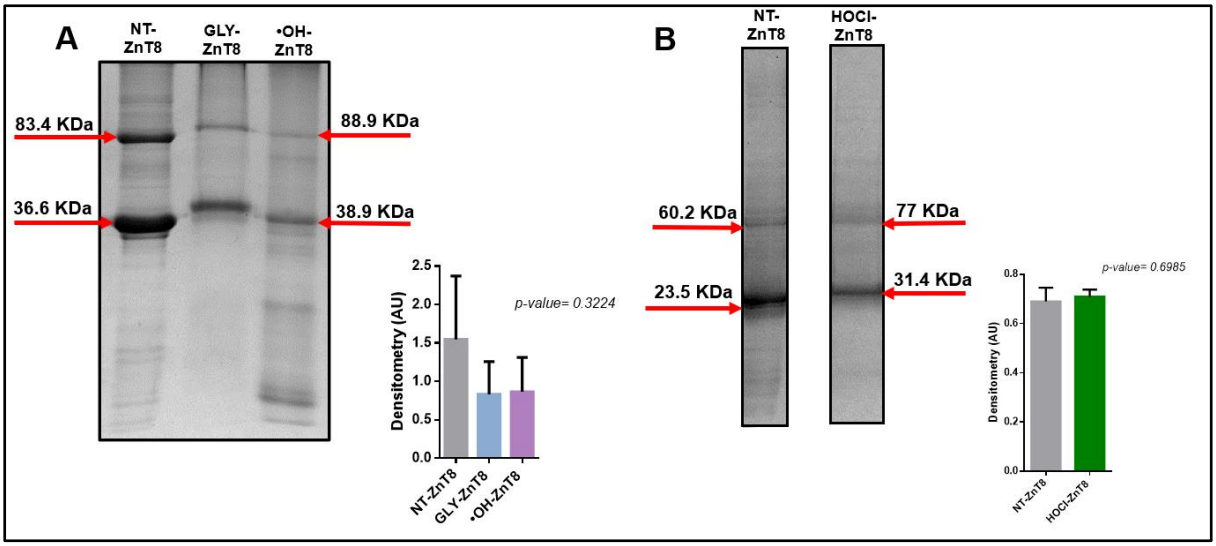

Figure 14. SDS-PAGE analysis of NT- and modified ZnT8. A) 12% SDS-PAGE analysis of NT and modified ZnT8. The NT-ZnT8 lane shows distinct bands at 83.4, 36.6, and 31.0 KDa, GLY-ZnT8 showed bands at 93.1 and 43.2 KDa and a faint band at 39.3 KDa, the •OH-ZnT8 lane shows four distinct bands at 88.9, 72.9, 38.9 and 33.9 KDa, with further bands intensifying throughout the lane compared to the NT-ZnT8. **B) A 4-20% gradient SDS-PAGE of HOCl-ZnT8.** Compared to the NT-ZnT8, HOCl-ZnT8 showed two bands at 77 and 31.4 KDa. *The gels were imaged using the Chemi-Doc imaging system from Bio-Rad and quantified using ImageJ software.*

3.3 Antibody response to native or oxPTM- β-cell antigens

3.3.1 Antibody response to NT- or oxPTM-GAD65

When deducing the antibody response to NT- or oxPTM-GAD65 in patients with T1D (N=69), there was no significant difference between antibody binding towards NT- and GLY-GAD65 in T1D (mean O.D ± S.D, 0.60 ± 0.27 vs 0.53 ± 0.30, p-value= 0.28, respectively). Conversely, there was a significant difference between the IgG response to HOCl-GAD65 and NT-GAD65, similarly there was a significant difference between •OH-GAD65 in comparison to the antibody response towards NT-GAD65 (mean O.D ± S.D, 0.60 ± 0.27 vs 0.48 ± 0.29, p-value= 0.02, and 0.60 ± 0.27 vs 0.48 ± 0.29, p-value < 0.001, respectively). Furthermore, the IgG response to NT- and oxPTM-GAD65 was similar in patients with T2D (N=32) and healthy controls (HC) (N=34), with no significant difference with the IgG response to NT-GAD65 in both groups (mean O.D ± S.D, 0.26 ± 0.13 vs 0.30 ± 0.14, p-value= 0.144, respectively) (figure 15A). Table 11 shows the mean O.D at 450 nm IgG antibody responses to each of the NT- and oxPTM-GAD65 antigens in the T1D, T2D, and HC cohorts.

	Type 1 Diabetes N= 69	**Type 2 Diabetes N=32**	**Healthy Controls N=34**	**P-value**
NT-GAD65	0.60 ± 0.24	0.26 ± 0.13	0.30 ± 0.14	***< 0.0001***
GLY-GAD65	0.52 ± 0.30	0.23 ± 0.15	0.30 ± 0.20	***< 0.0001***
•OH-GAD65	0.37 ± 0.37	0.11 ± 0.11	0.17 ± 0.23	***< 0.0001***
HOCl-GAD65	0.48 ± 0.24	0.17 ± 0.10	0.30 ± 0.30	***< 0.0001***

Table 11. Average IgG antibody response in T1D, T2D, and HC to NT- and oxPTM-GAD65 antigens. *P-values were calculated using a Kruskal-Wallis test**.** Values are depicted as mean O.D ± S.D, with the O.D measured at 450 nm.*

A cut-off for positive antibody responses was calculated from the mean O.D of IgG binding to each antigen of interest (NT-, GLY-, •OH- and HOCl-GAD65), in the serum of HC per 2 standard deviations (formula: mean O.D+ 2*standard deviations). This resulted in an O.D of 0.5 as the cut-off for a positive antibody response (table 12). Using this cut-off, n=36 patients with T1D were positive for IgG antibodies to NT-GAD65 (53.2%), n=30 was positive for GLY-GAD65 (43.49%), n=12 were positive for •OH-GAD65 (17.4%) and n=27 were positive to HOCl-GAD65 (39.1%). Moreover, when utilizing an O.D of 0.5 nm as a cut-off, there was a significant increase in antibody binding towards •OH-GAD65 compared to the NT-GAD65 in T1D (mean O.D ± S.D, 1.01 ± 0.40 vs 0.80 ± 0.15, p-value = 0.065, respectively) T2D (figure 15B).

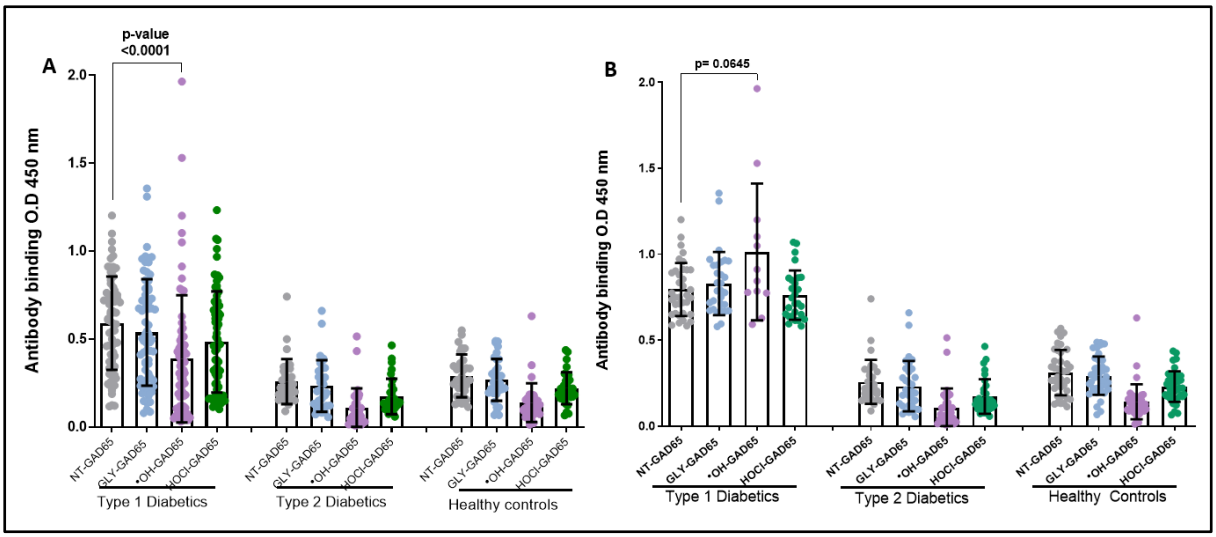

Figure 15. Antibody binding from patient serum to native (NT-) or oxPTM-GAD65. A) ELISA of antibody response in the serum of patients with type 1 diabetes (N=69), patients with type 2 diabetes (N=32) and healthy controls (N=34). **B)** Depicts the antibody binding to NT or modified GAD65 in T1D, T2D and healthy controls after using an O.D 0.5 as the cut-off for positivity. *P-values were calculated using Student's T-test or Mann-Whitney test where appropriate. O.D measured at 450 nm.*

The cut-off for positivity was calculated by utilizing the formula mean O.D at 450 nm for each antigen of interest from the sera of HC + 2*Standard deviations, yielding an O.D 0.5 as the cut-off. Using this cut-off value for antibody positivity, the sensitivity and specificity of the assay was calculated by performing a ROC assessment, and subsequently calculating the positive predictive values (PPV) and the negative predictive values (NPV) for each antigen (table 12).

	NT-GAD65	GLY-GAD65	•OH-GAD65	HOCl-GAD65
%Specificity	87.50%	97.50	95.0%	97.50%
%Sensitivity	60.42%	43.75%	22.92%	37.5%

Table 12. Specificity and sensitivity of "homemade" GAD65 ELISAs, using a cut-off of O.D 0.5 for positivity. A cut-off value for antibody positivity was calculated by assessing the mean O.D at 450 nm of healthy controls + 2* standard deviations. The positive predictive values (PPV) were determined via true positives/ true positives + false positives, and negative predictive values (NPV) was determined via true negatives/ true negatives + false negatives.

Figure 16 depicts the changes of IgG binding towards NT- and oxPTM-GAD65 in 37 patients with T1D who were positive for antibodies against NT-GAD65 after a cut-off of O.D 0.5 (table 12). There was a slight decrease between antibody responses to NT- and GLY-GAD65, however this difference was not significant (mean O.D ± S.D, 0.797 ± 0.025 vs 0.756 ± 0.038, p-value= 0.3686, respectively) (figure 15A). A significant difference was seen in the IgG responses towards NT- and •OH-GAD65 (mean O.D ± S.D, 0.797 ± 0.025 vs 0.58 ± 0.39, p-value= 0.0026, respectively) (figure 15B), as well as a significant difference was seen between NT- and HOCl-GAD65 (mean O.D ± S.D, 0.797 ± 0.025 vs 0.675 ± 0.038, p-value = 0.0272, respectively) (figure 15C).

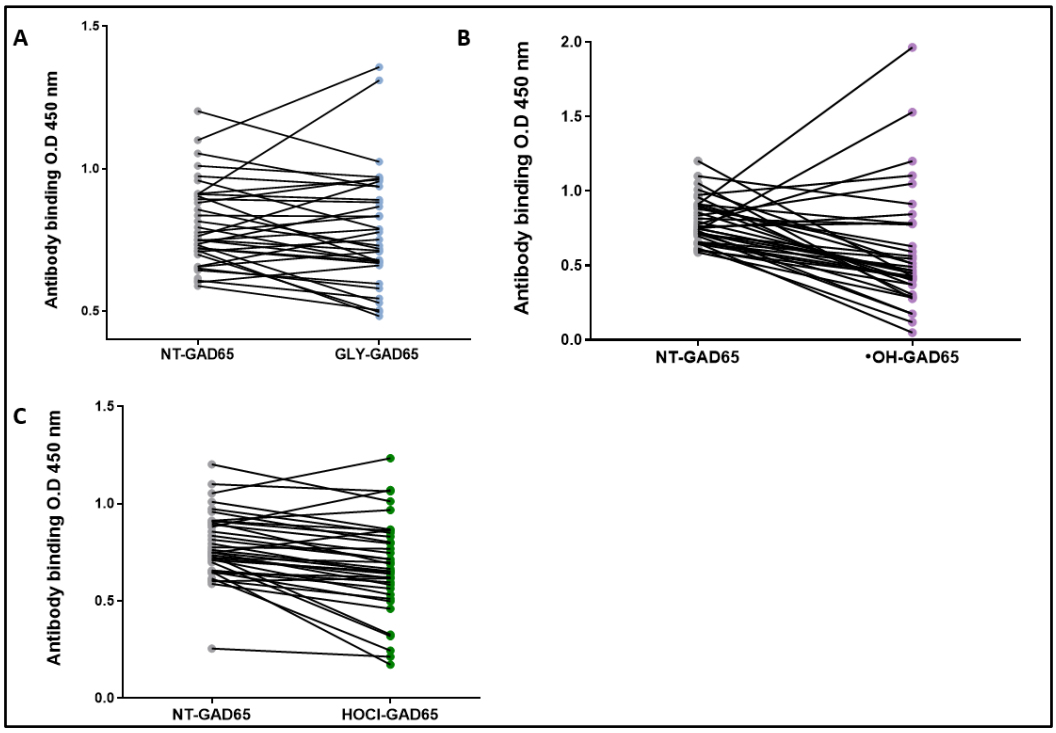

Figure 16. Changes in antibody binding in the sera of patients with new- onset T1D to NT- and modified GAD65. The figure depicts the differences in IgG binding in N=37 T1D who were positive to antibodies to NT-GAD65 after a cut-off of O.D 0.50. **A)** Shows the change between IgG responses to NT- and GLY-GAD65. **B)** Depicts the differences in antibody response to NT- and •OH-GAD65. **C)** Demonstrates the differences in antibody response to NT- and HOCl-GAD65. *P-values were calculated using student T test's and nonparametric Mann-Whitney test where appropriate. O.D was measured at 450 nm.*

3.3.2 Antibody response to NT- and oxPTM-ZnT8

When assessing the IgG response to NT- or oxPTMs- ZnT8 in n=53 patients with new-onset T1D, there appeared to be a significant difference between the antibody response to NT- and GLY-ZnT8 (mean O.D ± S.D, 0.52 ± 0.25 vs 0.43 ± 0.25, p-value= 0.03, respectively), as well a significantly diminished IgG response to •OH-ZnT8 when compared to the antibody response towards NT-ZnT8 (mean O.D ± S.D, 0.21 ± 0.14 vs 0.52 ± 0.25, p-value < 0.0001, respectively). However, there appeared to be no difference between the antibody response to NT-ZnT8 and HOCl-ZnT8 (mean O.D ± S.D, 0.52 ± 0.25 vs 0.45 ± 0.25, p-value= 0.06) (figure 17A). When comparing the IgG response towards NT- and oxPTM-ZnT8 in the sera of patients with T1D, patients with T2D and HC, there was a significant difference between the antibody response towards NT-ZnT8 (p-value= 0.0044) and •OH-ZnT8 (p-value= 0.0013) between all 3 study groups. However, there was no significant difference found between the IgG antibody binding response towards GLY-ZnT8 (p-value= 0.0973) and HOCl-ZnT8 (p-value= 0.0718) between all 3 groups. The average antibody response toward NT- and oxPTM-ZnT8 between patients with T1D, T2D, and HC is shown in table 13.

	Type 1 Diabetes N= 53	Type 2 Diabetes N=20	Healthy Controls N=37	P-value
NT-ZnT8	0.49 ± 0.24	0.36 ± 0.17	0.40 ± 0.22	***0.0044***
GLY-ZnT8	0.40 ± 0.24	0.34 ± 0.16	0.33 ± 0.19	0.0973
•OH-ZnT8	0.21 ± 0.13	0.09 ± 0.05	0.15 ± 0.10	***0.0013***
HOCl-ZnT8	0.45 ± 0.25	0.34 ± 0.18	0.36 ± 0.21	0.0718

Table 13. Average IgG antibody response in T1D, T2D, and HC to NT- and oxPTM-ZnT8 antigens. *P-values were calculated using a Kruskal-Wallis test. Data presented as mean O.D at 450 nm ± S.D.*

The cut-off for antibody positivity for the optimized ELISA for each antigen of interested was calculated by determining the mean O.D of the healthy controls at 450 nm + 2* standard deviations, resulting in an O.D of 0.5 as a cut-off for a positive antibody response towards each antigen of interest. Utilizing an O.D 0.5 as a cut-off, the % sensitivity and % specificity of each developed ELISA was determined. Although the assays showed fair %specificity for NT-, GLY-, •OH-, and HOCl-ZnT8 (75.76%, 78.79%, 100%, and 74.07%, respectively), the % sensitivity varied (41.7%, 25.0%, 8.3%, and 37.5%, respectively) (table 14). When assessing patients with T1D who were IgG positive for antibodies to NT- or oxPTM- ZnT8, using the cut-off of O.D 0.5, 45.3% of patients with T1D were positive for IgG antibodies towards NT-ZnT8. Moreover, 30.2% were positive for GLY-ZnT8, 5.7% were positive for •OH-ZnT8, and 34.0% were positive for IgG antibodies towards HOCl-ZnT8. However, there appeared to be no significant difference in the developed antibody response towards NT-ZnT8 compared to GLY-ZnT8 (mean O.D ± S.D, 0.53 ± 0.58 vs 0.50 ± 0.56, p-value= 0.9414, respectively), the antibody response to NT-ZnT8 compared to •OH-ZnT8 (mean O.D ± S.D, 0.53 ± 0.58 vs 0.52 ± 0.52, p-value= 0.0708, respectively) and HOCl-ZnT8 (mean O.D ± S.D, 0.53 ± 0.58 vs 0.49 ± 0.53, p-value= 0.8695, respectively) (figure 17B).

	NT-ZnT8	GLY-ZnT8	•OH-ZnT8	HOCl-ZnT8
%Specificity	75.76%	78.79%	100%	74.07%
%Sensitivity	41.67%	25.0%	8.3%	37.5%

Table 14. Sensitivity and specificity of homemade ZnT8 ELISA using a cut-off for positivity as O.D 0.50. The cut-off value was calculated by determining the mean O.D of healthy controls + 2*Standard deviations. The positive predictive values (PPV) were determined via true positives/ true positives + false positives, and negative predictive values (NPV) was determined via true negatives/ true negatives + false negatives.

Furthermore, upon analysis of the differences between the IgG binding towards NT-, GLY- and HOCl-ZnT8 in the sera of HC and patients with T2D, there appeared to be no significant differences (mean O.D NT-ZnT8 ± S.D, 0.3719 ± 0.1913 vs 0.3588 ± 0.1701, p-value= 0.8117, mean O.D GLY-ZnT8 ± S.D, 0.3174 ± 0.1836 vs 0.3413 ± 0.1593, p-value= 0.3251, mean O.D HOCl-ZnT8 ± S.D, 0.3448 ± 0.2035 vs 0.3352 ± 0.1796, p-value= 0.8728, respectively). However, there was a significant difference between antibody response towards •OH-ZnT8 in HC and patients with T2D (mean O.D ± S.D, 0.1463 ± 0.09629 vs 0.0939 ± 0.0468, p-value= 0.0345, respectively)

(figure 17B). When comparing the IgG binding in T1D and HC, using a cut-off of O.D 0.5, there appeared to be a significant difference between antibody response towards NT-ZnT8 (mean O.D ± S.D, 0.7425 ± 0.1790 vs 0.3719 ± 0.1913, p-value< 0.0001, respectively), GLY-ZnT8 (mean O.D ± S.D, 0.7469 ± 0.1931 vs 0.3174 ± 0.183, p-value< 0.0001, respectively), •OH-ZnT8, (mean O.D ± S.D, 0.5440 ± 0.0241 vs 0.1463 ± 0.0963, p-value = 0.002, respectively), and HOCl-ZnT8 (mean O.D ± S.D, 0.7324 ± 0.2149 vs 0.3448 ± 0.2035, p-value < 0.0001, respectively) (figure 17B).

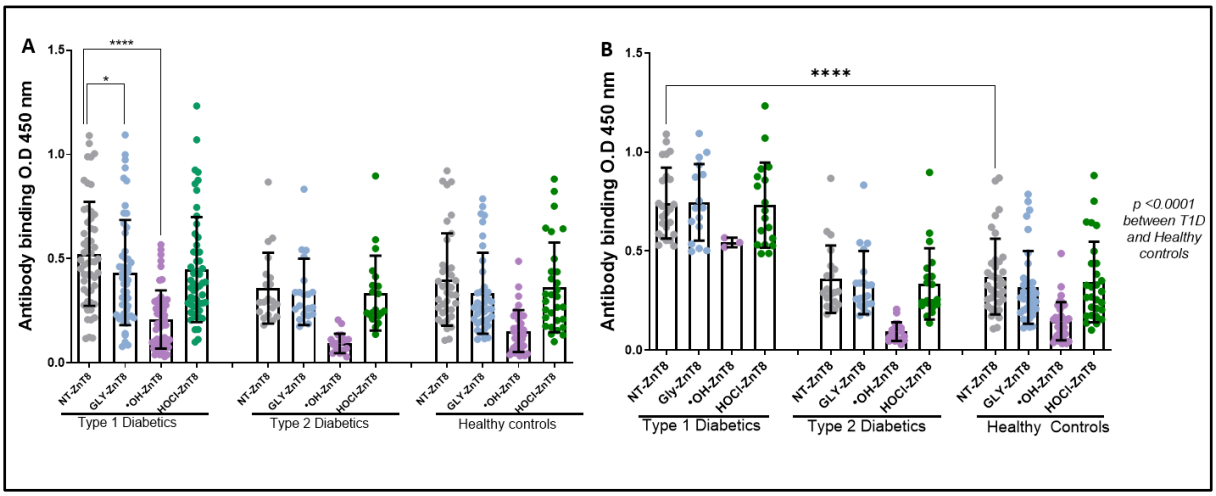

Figure 17. Antibody response in T1D, T2D and healthy controls to NT- or oxPTM-ZnT8. **A)** Depicts the IgG response in N=53 T1D, N=20 T2D and N=37 healthy controls. **B)** Shows the IgG response in T1D, T2D and healthy controls using an O.D. 0.5 ELISA cut-off for positivity. *P-values were calculated using the non-parametric Mann- Whitney Test and ANOVA for comparing ranks, where appropriate. P-values * < 0.05, **** < 0.0001. O.D was measured at 450 nm.*

When comparing the changes in antibody response to NT-ZnT8 and oxPTM-ZnT8 in the 45.3% of patients with new-onset T1D positive for antibodies towards NT-ZnT8, there appeared to be no significant difference between antibody binding to NT- and GLY-ZnT8 (mean O.D ± S.D, 0.7292 ± 0.1873 vs 0.6118 ± 0.2464, p-value= 0.064, respectively) (figure 18A). As well as no significant difference in the antibody response towards NT- and HOCl-ZnT8 (mean O.D ± S.D, 0.7292 ± 0.1873 vs 0.6285 ± 0.2505, p-value= 0.1140, respectively) (figure 18C). However, there was an apparent significant decrease in IgG binding between NT- and •OH-ZnT8 (mean O.D ± S.D, 0.73 ± 0.19 vs 0.27± 0.14, p <0.0001, respectively) (figure 18B).

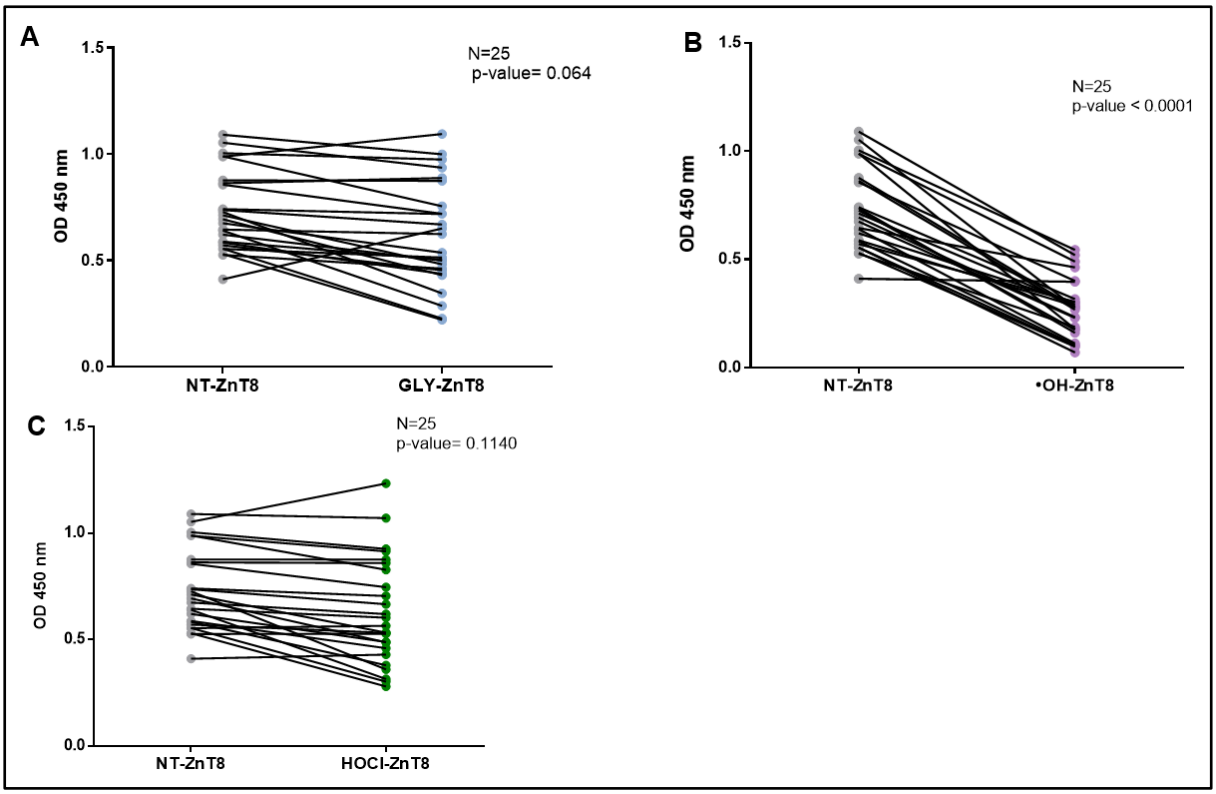

Figure 18. Changes in antibody binding to NT- and oxPTM-ZnT8. A) Comparison in IgG binding to NT- or GLY-ZnT8. **B)** Shows the differences in IgG binding to NT- and •OH-ZnT8. **C)** Depicts the differences in IgG binding to NT- and HOCl-ZnT8 in N=25 patients with T1D after using an ELISA cut-off of O.D. 0.50. *Normal distribution of the data was determined by D'Agostino & Pearson omnibus normality test. P-values calculated using an unpaired parametric Student's T Test. O.D was measured at 450 nm.*

3.3.3 Antibody response to NT- and oxPTM- Insulin

The changes seen between NT- and GLY-INS are sown in the Native-PAGE displayed in figure S2. Interestingly, when assessing the antibody response towards NT- or oxPTM-INS, there appeared to be a significant decrease with antibody binding towards NT-INS and GLY-INS (mean O.D ± S.D, 0.221 ± 0.108 vs 0.170 ± 0.081, p-value <0.05, respectively). However there was a significant increase in antibody binding seen between NT-INS and HOCl-INS (mean O.D ± S.D, 0.221 ± 0.108 vs 0.363 ± 0.134, p-value <0.0001, respectively), as well as a significant increase between antibody binding towards NT-INS and •OH-INS (mean O.D ± S.D, 0.221 ± 0.108 vs 0.400 ± 0.129, p-value <0.0001, respectively) (figure 19).

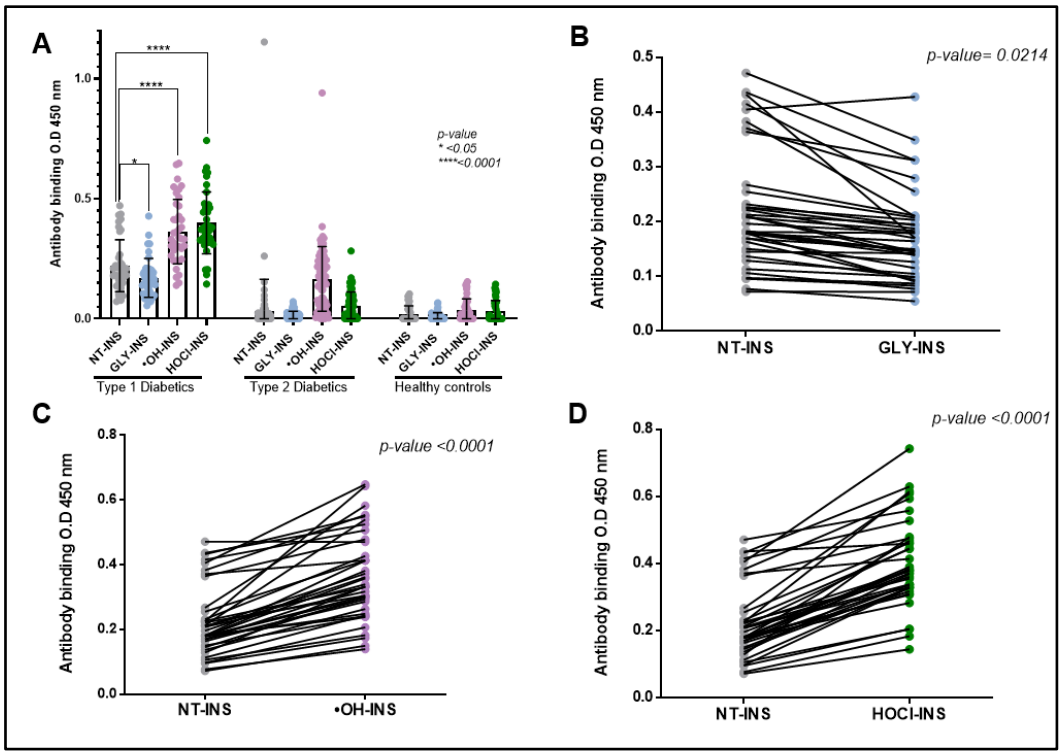

Figure 19. Antibody binding to NT- and oxPTM-INS in patients with new- onset T1D, T2D, and healthy controls (A). Change in antibody binding between native and modified insulin in patients with new-onset T1D. The figures show the differences in antibody binding between native or GLY-INS **(B)**, •OH-INS **(C)**, and HOCl-INS **(D)**. There was an apparent significant difference between NT- and GLY-INS (mean O.D ± S.D, 0.221 ± 0.108 vs 0.170 ± 0.081, p-value= 0.0214, respectively), NT- and •OH-INS (0.221 ± 0.108 vs 0.363 ± 0.134, p-value <0.0001, respectively) and between NT- and HOCl-INS (0.221 ± 0.108 vs 0.399 ± 0.129, p-value <0.0001, respectively). *P-values calculated via Student's T-test or non-parametric Mann-Whitney test where appropriate.*

3.4 Assessment of antibody response to NT- or oxPTM-β-cell antigens based on HLA-risk haplotype

In the study cohort, n=39 patients with new-onset T1D had HLA typing data available. The patients were divided based on their HLA-risk genotype for T1D, whereby n=19 (48.7%) carried the high HLA-risk genotype (HLA-DRB1*04), and n= 20 (51.3%) did not, these patients were characterised as moderate or low HLA-risk types. There was no significant difference between age (9.0 years [7.0-14.0] vs 11.0 years [9.0-13.0], p-value= 0.348), male gender (52.6% vs 40.0%, p-value= 0.527), BMI (17.43 kg/m^2 ± 2.35 vs 18.06 kg/m^2 ± 3.90, p-value= 0.589), HbA1c (10.63% ± 2.07 vs 12.03% ± 3.02, p-value= 0.102), blood glucose (360.80 mg/dL ± 77.33 vs 381.90 mg/dL ± 164.60, p-value=0.643), C-peptide levels (1.17 ng/mL ± 0.57 vs 2.56 ng/mL ± 5.61, p-value=535), and CML (53.68 pg/mL [41.70-86.11] vs 46.46 pg/mL [34.06-71.16], p-value=0.281) among the HLA-DRB1*04 positive and HLA-DRbB1*04 negative groups respectively. Table 15 shows a summary of the patient demographic characteristics.

	Type 1 Diabetes N=39		
	HLA DRB1*04$^+$	**HLA DRB1*04$^-$**	**P-value**
Total, n (%)	18 (48.7%)	20 (51.3%)	
Age, years (median [IQR])	9.0 [7.0-14.0]	11.0 (9.0-13.0)	0.348
Male, n (%)	10 (52.6%)	8 (40.0%)	0.527
BMI, kg/m² (mean ± S.D)	17.43 ± 2.35	18.06 ± 3.90	0.589
Blood glucose, mg/dL (mean ± S.D)	360.8 ± 77.33	381.90 ± 164.60	0.643
HbA1c, %, (mean ± S.D)	10.63 ± 2.07	12.03 ± 3.02	0.102
C-peptide, ng/mL, (mean ± S.D)	1.17 ± 0.57	2.56 ± 5.61	0.535
CML, pg/mL (median [IQR])	53.68 [41.70-86.11]	46.46 [34.06-71.16]	0.281

Table 15. Demographic characteristics of patients with new-onset T1D based inherited HLA-risk haplotype (HLA-DR4). Categorical data is shown as percentages, with continuous data being displayed as mean ± standard deviation or median [interquartile range]. *P-values were calculated via Student's t-test or Mann-Whitney test where appropriate.*

Upon assessing the IgG response to NT- or oxPTM- β-cell antigens (GAD65, ZnT8 and Insulin) in N=39 patients with T1D with available HLA data, the HLA-DR4 positive patients has a significantly lower antibody response to the NT-GAD65 compared to the HLA-DR4 negative group (mean O.D ± S.D, 0.65 ± 0.18 vs 0.79 ± 0.20, p-value= 0.0302). Similarly, there was a decrease in the developed antibody binding response towards GLY-GAD65 in the HLA-DR4 positive group compared to the HLA-DR4 negative group (mean O.D ± S.D, 0.62 ± 0.18 vs 0.82 ± 0.25, p-value= 0.0069, respectively). There was no apparent difference between the antibody response towards •OH-GAD65 and HOCl-GAD65 between the HLA-DR4 positive and HLA-DR4 negative groups. There was a difference in the antibody response towards NT-GAD65 and GLY-GAD65 within the HLA-DR4 negative group, however this was not significant (mean O.D ± S.D, 0.79 ± 0.20 vs 0.82 ± 0.25, p-value= 0.71,

respectively). There was, however, a significant decrease in the antibody response towards •OH-GAD65 when compared to the antibody response to NT-GAD65 within both the HLA-DR4 positive haplotype (mean O.D ± S.D, 0.65 ± 0.18 vs 0.49 ± 0.28, p-value= 0.01) and HLA-DR4 negative haplotype (mean O.D ± S.D, 0.79 ± 0.20 vs 0.67 ± 0.43, p-value= 0.02, respectively) (figure 20A).

Upon assessment of IgG antibody response to NT- or oxPTM-ZnT8 between the HLA-DR4 positive and HLA-DR4 negative T1D groups, there was a significant increase within the IgG binding towards NT-ZnT8 (mean O.D ± S.D, 0.45 ± 0.15 vs 0.65 ± 0.25, p-value= 0.006, respectively), GLY-ZnT8 (mean O.D ± S.D, 0.34 ± 0.13 vs 0.58 ± 0.28, p-value= 0.002, respectively) and HOCl-ZnT8 (mean O.D ± S.D, 0.36 ± 0.10 vs 0.58 ± 0.27, p-value= 0.002, respectively) between the HLA-DR4 positive and HLA-DR4 negative groups, respectively. There was a decrease in the antibody response between the HLA-DR4 positive and negative haplotype groups towards •OH-GAD65, however, this was not significant (mean O.D ± S.D, 0.19 ± 0.13 vs 0.26 ± 0.15, p-value= 0.07, respectively) (figure 20B).

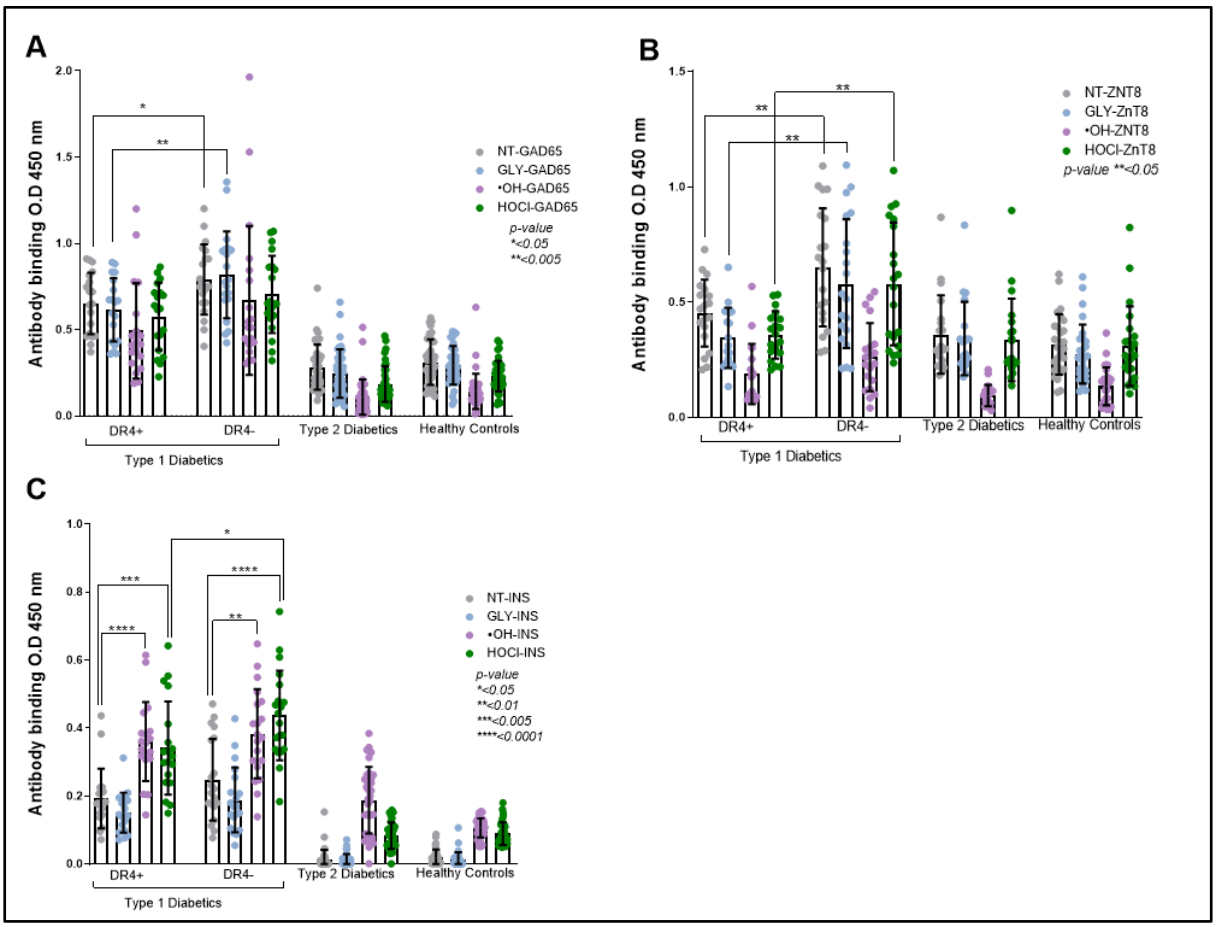

Figure 20. Antibody reactivity to NT- or modified β-cell antigens in n= 39 patients with new onset T1D based on HLA-DR4 risk haplotype, compared with people with T2D and HC. A) The figure shows the IgG response in T1D cohort to NT or oxPTM-GAD6, compared to T2D (n=39) and healthy controls (n=39). **B)** Depicts the difference in IgG binding to NT- or oxPTM-ZnT8 compared to T2D (n=20) and healthy controls (n=28). **C)** Displays the changes in the IgG binding towards NT- or oxPTM-Insulin, compared to T2D

(n=39) and healthy controls (n=39). *Unpaired Student's T-test was performed for normally distributed data sets, and Mann Whitney test for non-normally distributed data*.

These patients also had IgG binding data available towards NT- and oxPTM-Insulin. When comparing the antibody response between groups, there only appeared to be a significant difference between the antibody response towards HOCl-INS within the HLA-DR4 positive and negative groups (mean O.D ± S.D, 0.34 ± 0.14 vs 0.44 ± 0.13, p-value= 0.033, respectively) (figure 20C). However, when assessing the differences in antibody responses within each group, there was a significant difference between antibody response towards NT-INS and •OH-INS within the HLA-DR4 positive group (mean O.D ± S.D, 0.19 ± 0.09 vs 0.36 ± 0.12, p-value < 0.0001, respectively) and HLA-DR4 negative risk groups (mean O.D ± S.D, 0.24 ± 0.12 vs 0.44 ± 0.13, p-value= 0.002, respectively). There was also a significant difference between the antibody response towards NT-INS and HOCl-INS in both the HLA-DR4 positive group (mean O.D ± S.D, 0.19 ± 0.09 vs 0.34 ± 0.14, p-value= 0.0001, respectively) and negative groups (mean O.D ± S.D, 0.24 ± 0.12 vs 0.44 ± 0.13, p-value <0.0001, respectively) (figure 20C).

The differences in IgG binding towards NT- and oxPTM- β-cell antigens based on HLA risk haplotype (DR4 positive and DR4 negative) for T1D are displayed in table 16. When conferring the differences between IgG binding towards patients with T1D who are HLA-DR4 positive or HLA-DR4 negative, patients with T2D and HC, there appeared to be significant differences between the antibody responses towards NT- and oxPTM-β-cell antigens between all groups.

	Type 1 Diabetes				
	HLA-DRB1*04+	**HLA-DRB1*04-**	**Type 2 Diabetes**	**Healthy Controls**	**P-value**
Total (n)	18	21	39	39	
NT-GAD65	0.65 ± 0.18	0.79 ± 0.20	0.28 ± 0.13	0.31 ± 0.13	***< 0.0001***
GLY-GAD65	0.62 ± 0.18	0.82 ± 0.25	0.25 ± 0.14	0.29 ± 0.11	***< 0.0001***
•OH-GAD65	0.50 ± 0.28	0.67 ± 0.43	0.11 ± 0.10	0.14 ± 0.10	***< 0.0001***
HOCl-GAD65	0.58 ± 0.20	0.70 ± 0.22	0.18 ± 0.10	0.23 ± 0.10	***< 0.0001***
NT-ZnT8	0.45 ± 0.15	0.65 ± 0.25	0.36 ± 0.17	0.32 ± 0.13	***< 0.0001***
GLY-ZnT8	0.34 ± 0.13	0.58 ± 0.28	0.34 ± 0.16	0.27 ± 0.13	***0.0003***
•OH-ZnT8	0.19 ± 0.13	0.26 ± 0.15	0.09 ± 0.05	0.13 ± 0.08	***< 0.0001***
HOCl-ZnT8	0.36 ± 0.10	0.58 ± 0.27	0.33 ± 0.18	0.31 ± 0.17	***0.0007***
NT-INS	0.19 ± 0.09	0.24 ± 0.12	0.01 ± 0.3	0.01 ± 0.02	***< 0.0001***
GLY-INS	0.15 ± 0.06	0.19 ± 0.10	0.01 ± 0.02	0.01 ± 0.02	***< 0.0001***
•OH-INS	0.36 ± 0.12	0.38 ± 0.13	0.19 ± 0.10	0.11 ± 0.03	***< 0.0001***
HOCl-INS	0.34 ± 0.14	0.44 ± 0.13	0.08 ± 0.04	0.10 ± 0.03	***< 0.0001***

Table 16. Difference of IgG response to native or modified β-cell antigens in patients with new-onset T1D based on the inheritance of HLA-DR4 haplotype compared with T2D and HC. *Data is displayed as mean O.D at 450 nm ± S.D, p-values were calculated via One-way ANOVA and Kruskal-Wallis test where appropriate.*

3.5 Differences in antibody binding to NT- and oxPTM- β-cell antigens in T1D

The overlapping IgG response induced towards NT- and oxPTM-GAD65 was assessed by determining the degree of overlap in each patient towards each antigen. Within the total cohort of N=69 patients with new-onset T1D, 17% (12/69) of the patients were positive for an IgG antibody response towards NT-GAD65, GLY-GAD65. •OH-GAD65 and HOCl-GAD65. With a total of 41% (29/69) appearing positive for GLY-GAD65 and 39% (27/69) towards •OH-GAD65. However, 45% of T1D were negative for antibodies directed towards all antigens (NT- and oxPTM-GAD65) (figure 21A).

When assessing antibody responses to NT- and oxPTM-ZnT8, 59% (41/69) of patients were negative for any antibody response, whereas 33% (23/69) were positive for antibodies against NT-GAD65. There were only 4.3% (3/69) patients with T1D who were positive to both NT- and all oxPTM-ZnT8, 25% (17/69) were positive for IgG antibodies to GLY-ZnT8 and HOCl-ZnT8, and only 5.8% (4/69) were positive to •OH-ZnT8 (figure 21B).

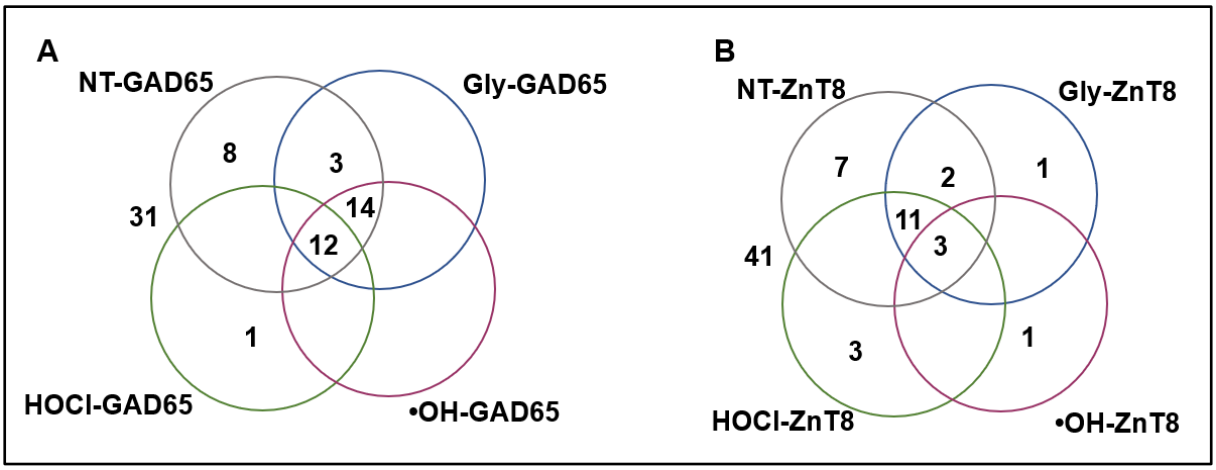

Figure 21. Venn diagram depicting the overlapping IgG response to NT- and oxPTM-β-cell antigens. A) Shows the overlapping IgG response towards NT- and oxPTM-GAD65. When using a cut-off of O.D. 0.5, 17% (12/69) patients with T1D showed IgG binding towards all four antigens. 20.3% (14/69) were positive for 3 antigens, 4.3% were positive for both NT- and GLY-GAD65, and 1.44% (1/69) was positive only for HOCl-GAD65. 44.9% were negative for all four antigens. **B)** Displays the overlapping IgG response towards NT- and oxPTM-ZnT8. Whereby, 59.4% (41/69) of patients with T1D were negative for all four antigens. While 4.3% (3/69) were positive for all four antigens. *A cut-off of O.D 0.5 was used to determine antibody response positivity.*

In order to deduce the heterogeneity of the immune response within n=39 patients with new onset T1D who have complete antibody profiles, the reactivity towards NT- and oxPTM- GAD65, ZnT8 and Insulin were assessed via the heatmap in figure 22. A heterogenous response was clear amongst individuals assessed for autoantibodies towards major autoantigens detected in T1D. Of note, the majority of patients with T1D reacted strongly towards HOCl-Ins and •OH-Ins, compared to NT-Ins, with an evident decrease in IgG binding towards GLY-INS. Furthermore, the

same patients who show a strong reaction towards •OH-Ins, show a diminished response towards •OH-GAD65 and •OH-ZnT8.

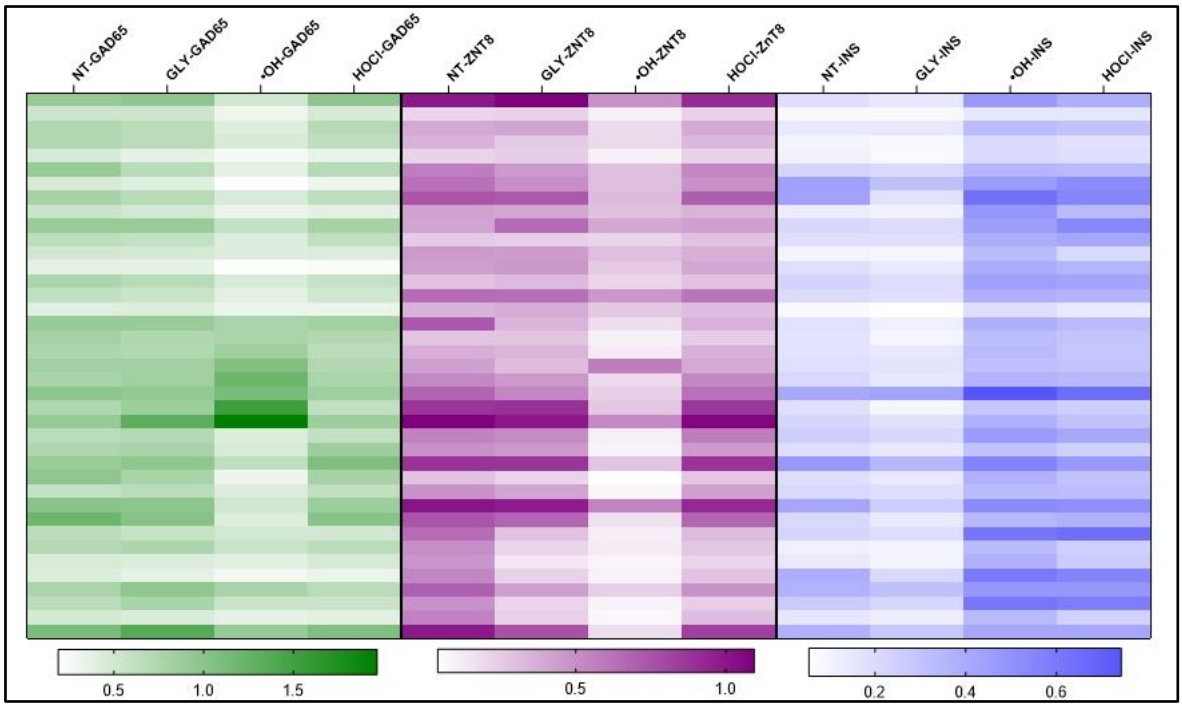

Figure 22. Heat map of antibody responses to NT- and oxPTMs- β-cell antigens (GAD65, ZnT8, and Insulin). The heatmap depicts the heterogeneity of the antibody responses in n=39 patients with new-onset T1D.

3.6 Association of Antibody Responses to NT- or oxPTM- β-cell antigens and Clinical Data in Patients with T1D

When determining the correlations and associations between the clinical data of patients with T1D and the antibody response to NT- and oxPTM- β-cell antigens, there was a positive correlation with CML (pg/mL) and HOCl-GAD65 (r= 0.261, p-value= 0.049). There were no other correlations found within the remaining antigens of interest and CML (table 17) (figure S3). There was a strong negative correlation with age (years) and antibody response to NT- GAD65, GLY-GAD65, •OH-GAD65, or HOCl-GAD65 (r= -0.481 vs r= -0.475 vs r= -0.562 vs r= -0.528, p-value <0.0001, respectively) (figure S4). Interestingly, both HbA1c levels (%) and blood glucose levels (mg/dL) at diagnosis were positively correlated with •OH-GAD65 (r= 3.20, p-value= 0.013, and r= 0.487, p-value= 0.004, respectively) (figure S5 and S6). There were no other significant correlations detected, all correlations with total T1D patient cohort included in this study (N=69) is shown in table 17.

	Age (years)	Carboxymethyl-Lysine (pg/mL)	HbA1c (%)	Blood glucose (mg/dL)	C-peptide (ng/mL)
NT-GAD65	***r=-0.481 p<0.0001***	r=0.120 p=372	r=0.033 p= 0.800	r=0.113 p= 0.530	r=0.102 p= 0.448
GLY-GAD65	***r=-0.475 p<0.0001***	r=0.167 p= 0.215	r= 0.136 p= 0.301	r=0.248 p= 0.148	r=0.108 p= 0.418
•OH-GAD65	***r=-0.562 p<0.0001***	r=0.026 p= 0.850	***r=0.320 p= 0.013***	***r=0.487 p= 0.004***	r=0.070 p= 0.602
HOCl-GAD65	***r=-0.528 p<0.0001***	***r=0.261 p= 0.049***	r=0.091 p= 0.488	r=0.0249 p= 0.901	r=0.117 p= 0.383
NT-ZnT8	r=-0.143 p= 0.262	r=0.128 p= 0.341	r=0.060 p= 0.650	r=0.241 p= 0.177	r=-0.030 p= 0.825
GLY-ZnT8	r=-0.082 p= 0.527	r= 0.206 p= 0.123	r=0.068 p= 0.608	r=0.140 p= 0.436	r=0.111 p= 0.406
•OH-ZnT8	r=0.069 p=0.598	r=0.081 p= 0.549	r=-0.020 p= 0.881	r=0.212 p= 0.236	r=0.120 p= 0.372
HOCl-ZnT8	r=0.040 p= 0.788	r=0.0166 p= 0.241	r=0.066 p= 0.665	r=0.205 p= 0.252	r=0.237 p= 0.118
NT-INS*	r=-0.236 p=0.107	r=0.1600 p= 0.266	r=0.0285 p= 0.851	r=0.195 p= 0.276	r=0.084 p= 0.585
GLY-INS*	r=-0.017 p= 0.908	r=0.098 p= 0.498	r=0.064 p= 0.700	r= 0.244 p= 0.172	r=-0.083 p= 0.626
•OH-INS*	r=-0.117 p= 0.484	r=0.182 p= 0.269	r=0.170 p= 0.260	r=0.182 p= 0.310	r= -0.002 p= 0.988
HOCl-INS*	r=-0.191 p= 0.252	r=0.127 p= 0.442	r=0.091 p= 0.583	r=0.224 p=0.210	r=-0.265 p= 0.112

Table 17. Associations between NT- and oxPTM- β- cell antigens and clinical information at diagnosis in patients with T1D. *Pearson's correlation or Spearman's correlation were performed where appropriate.* *data was not available for all patients.

When analyzing the associations of clinical data in patients who had increased antibody binding to GLY-GAD65 compared to NT-GAD65, there appeared to be a significant positive correlation with GLY-GAD65 and blood glucose levels at onset in

n= 30 patients with T1D with available blood glucose levels (r= 0.202, p-value= 0.312) and no correlation with NT-GAD65 (r= 0.395, p-value= 0.041) (figure 23A). Although, there was no significant difference between the mean O.D of both NT-GAD65 and GLY-GAD65 (mean O.D ± S.D, 0.804 ± 0.154 vs 0.810 ± 0.20, p-value= 0.924, respectively). When assessing the distribution of antibody response to NT-GAD65 or GLY-GAD65 in n=30 T1D based on blood glucose levels (mg/dL) groups (<300, 301-400, >401 mg/dL), there was no significant difference between antibody binding towards NT-GAD65 and GLY-GAD65 within each group. However, there was a significant difference between the antibody binding response to GLY-GAD65 in the >401 mg/dL group and the 301-400 mg/dL group (mean O.D ± S.D, 0.823 ± 0.275 vs 0.619 ± 0.161, p-value <0.05, respectively). There was also a significant difference between antibody responses across all groups and healthy controls (p-value <0.0001) (figure 23B).

When correlating CML (pg/mL) data with antibody binding to NT-GAD65 and HOCl-GAD65 in n=57 patients with T1D with available CML data, a significant correlation was only found in antibody binding towards HOCl-GAD65 and CML (r r= 0.261, p-value= 0.050) (figure 23C). However, when determining the difference of antibody binding to NT-GAD65 or HOCl-GAD65 across three CML groups (<50, 50-70, or >71 pg/mL) there was no significant difference between groups (figure 23D).

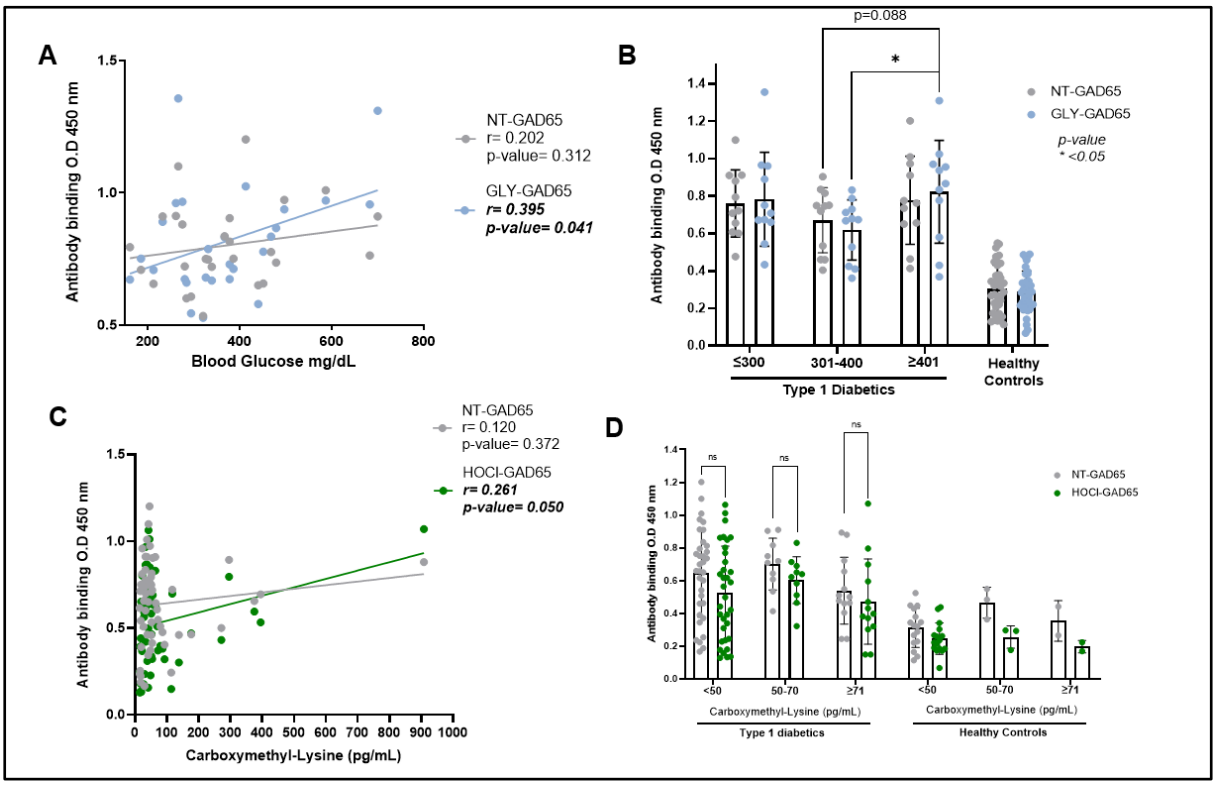

Figure 23. Association of clinical data with NT-GAD65, GLY-GAD65 and HOCl-GAD65 in patients with T1D. A) Depicts the association of blood glucose levels (mg/dL) in NT-GAD65 and GLY-GAD65 in n=30 patients with T1D (r= 0.202, p-value= 0.312 vs r= 0.395, p-value= 0.041, respectively). **B)** The figure shows the distribution of antibody response to NT- or GLY-GAD65 in n=33 T1D based on blood glucose levels (mg/dL) groups <300, 301-400, >401 mg/dL, respectively. Although there was no significant difference between NT- and

GLY-GAD65 in each group, there was a significant difference between antibody bind to GLY-GAD65 in the >401 mg/dL group and the 301-400 mg/dL group (mean O.D ± S.D, 0.823 ± 0.275 vs 0.619 ± 0.161, p-value <0.05, respectively). There was also a significant difference between antibody responses across all groups and healthy controls (p-value <0.0001). **C)** Correlation of NT- and HOCl-GAD65 antibody response in n= 57 T1D, the results show a correlation with HOCl-GAD65 and CML (r= 0.261, p-value= 0.050). **D)** When assessing the difference in antibody binding based on three CML groups (<50, 51-70, >71 pg/mL) there was no significant difference between groups. *Correlation coefficients (r) were calculated via Pearson's or Spearman's correlation where appropriate. P-values were calculated with Student's T test, Man-Whitney test, or One-way ANOVA, where appropriate.*

When determining the association between CML data and antibody binding in NT-INS or •OH-INS in patients with T1D, there appeared to be no significant correlation with either NT-INS and CML (r= 0.160, p-value= 0.266) or •OH-INS and CML (r= 0.135, p-value= 0.350) (figure 24A). However, upon determining the variations in antibody binding to NT-INS or •OH-INS between three CML groups (<50, 52-70, and >71 pg/mL), there was a significant difference between •OH-INS and NT-INS in each group (CML <50 pg/mL: mean O.D ± S.D, 0.240 ± 0.133 vs 0.384 ± 0.174, p-value <0.005)(CML 52-70 pg/mL, mean O.D ± S.D, 0.183 ± 0.088 vs 0.353 ± 0.123, p-value <0.005)(CML >71 pg/mL, mean O.D ± S.D, 0.195 ± 0.131 vs 0.362 ± 0.123, p-value <0.005), respectively. There was a significant difference between antibody response in patients with T1D and the antibody response in healthy controls towards both NT-INS and •OH-INS (p-value<0.0001)(figure 24B).

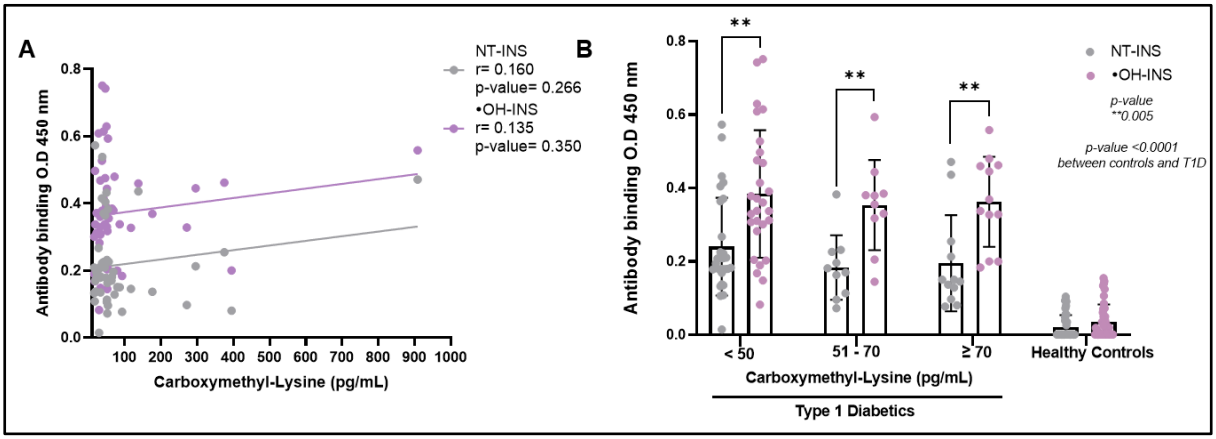

Figure 24. Association of CML data with and antibody binding in response to NT-INS or •OH-INS in patients with T1D. A) Shows the correlation of CML data to antibody binding towards NT- and •OH-INS (r= 0.160, p-value=0.266, vs r=0.135, p-value= 0.350, respectively). **B)** When assessing the antibody binding to NT- and •OH-INS based on three CML groups (<50, 51-70, >71 pg/mL), there appeared to be increased antibody binding to •OH -INS compared to NT-INS in each group (p-value<0.005). *Correlations were calculated with Pearson's r correlation or Spearman's r correlation where appropriate. P-values were calculated using a Student's T-Test, Mann-Whitney Test, and a One-way ANOVA.*

Chapter 4 Results Study 2: Glucose control and the immune response in COVID-19

4.1 ACE2 binding to NT- and Glycated SARS-CoV-2 Spike protein

The SARS-CoV-2 spike protein was modified using 0.5M D-ribose, the modifications were monitored using a 10% SDS-PAGE (figure 25). The SDS-PAGE shows a band of 175 kDa in the NT-S lane, as well as a slightly upshifted band in the GLY-S lane. However, when looking at the peak band area, the GLY-S seems to have a lower peak than the NT-S (mean ± S.D, 4288± 1508 vs 14462 ± 949.1, p-value= 0.04).

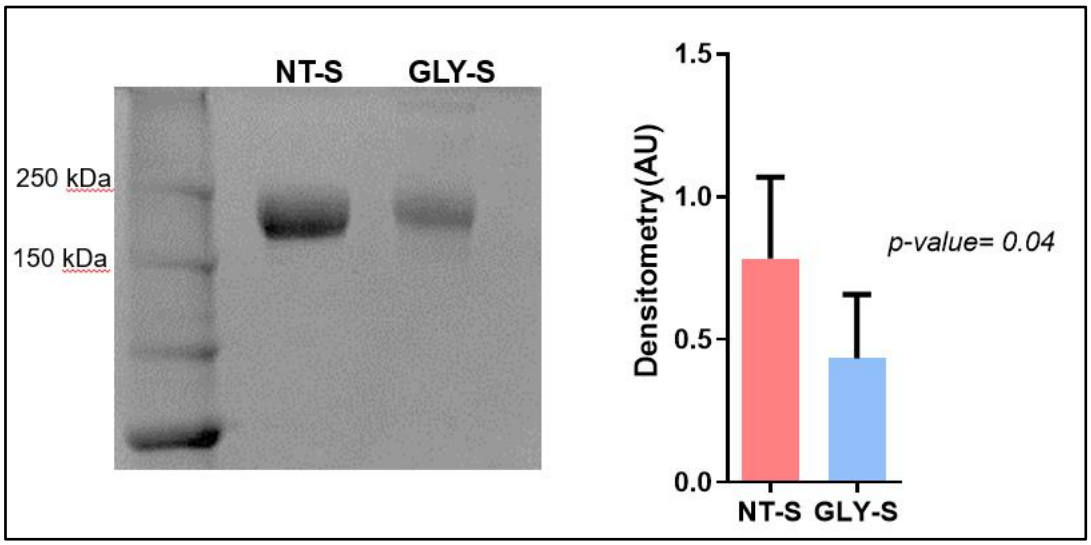

Figure 25. 10% SDS-PAGE analysis of native (NT) and glycated (GLY) SARS-CoV-2 Spike protein. 0.45 mg/mL of NT-S was modified using equal volumes of 0.5 M ribose. Upon glycation, 2 µg of NT- or GLY-S protein was loaded into the gel with a 1:1 ratio of Laemmli sample buffer. *Images were taken using the Chemi-Doc imaging system from Bio-Rad and gels were quantified using ImageJ software.*

Upon assessing the binding of NT- and GLY-S protein (1µg/mL) to serial concentrations of the SARS-CoV-2 receptor ACE2 (2.0 µg/mL to 0.25 µg/mL), the overall ACE2 binding to GLY-S was lower compared to the binding towards NT-S. However, when analyzing this difference, there was no significant difference between the mean O.D between groups (NT-S vs GLY-S) (mean O.D ± S.D, 0.1393 ± 0.1732 vs 0.1943 ± 0.2355, p-value= 0.6026, respectively) (figure 26).

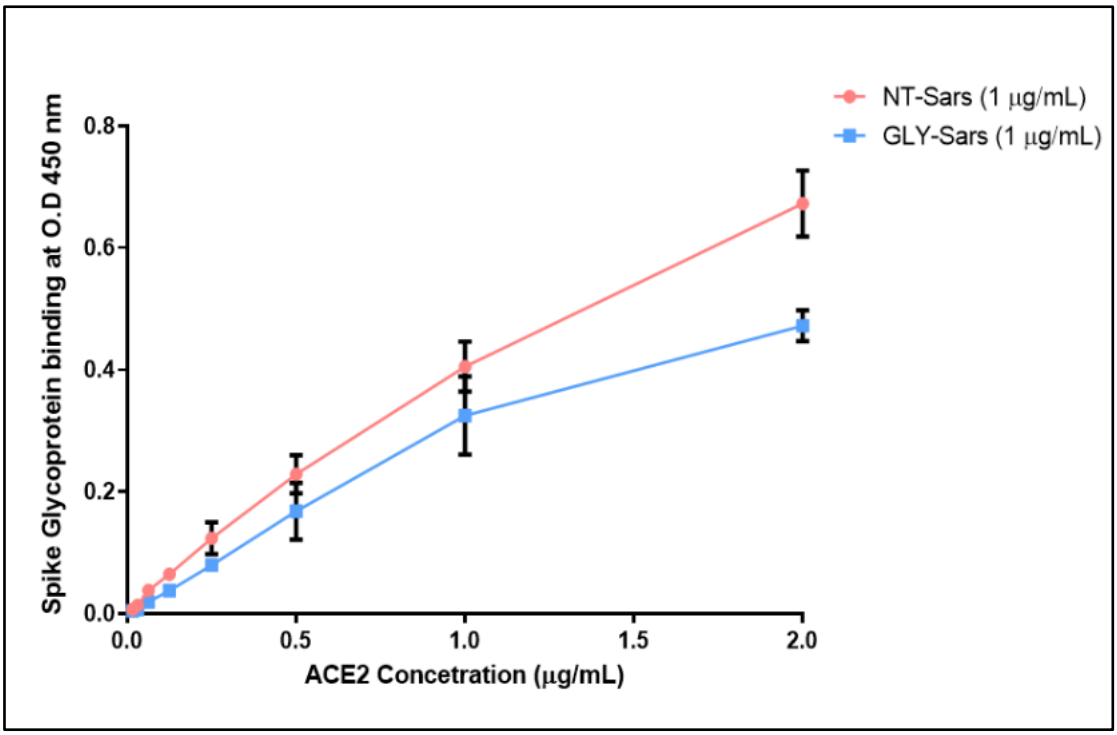

Figure 26. ACE2 binding to NT- or GLY-S protein. The figure Shows the results of 1 µg/mL NT- or GLY-S binding to serially dilutions of ACE2-IgGMu. There appears to be a lower ACE2 binding to GLY-S compared to NT-S, however this difference was not significant (p-value= 0.6026).

4.2 IgG binding to NT or GLY-S protein in patients with previous COVID-19

The IgG response in patients previously infected by COVID-19 (n=46) was tested against both NT- and GLY-S protein (figure 27). Table 18 shows cohort characteristics of the previously infected COVID-19 patients divided based on the presence of diabetes.

	Patients with Diabetes	Patients without Diabetes	P-value
Total (n)	22	24	
Male (%)	19 (86%)	24 (85%)	0.7809
Age (mean ± S.D)	70.45 ± 11.46	69.25 ± 12.40	0.7346
BMI (mean ± S.D)	27.23 ± 4.73	26.94 ± 3.989	0.8196
Fructosamine (µmol/L)	667.9 ± 241.4	580.7 ± 226.0	0.169
Co-morbidities			
Hypertension (%)	16 (72%)	14 (58%)	0.3166
CVD (%)	13 (59%)	5 (20%)	0.0071
ICU admission (%)	16 (72%)	13 (54%)	0.6150
Mortality (%)	3 (13%)	0	0.0635

Table 18. Demographic characteristics of patients previously infected with COVID-19.

There appeared to be a significant difference between the IgG antibody response to NT-S compared to GLY-S in the overall patient cohort (mean O.D ± S.D= 0.7676 ± 0.2670 vs 0.5990 ± 0.2501, p-value= 0.0023, respectively) (figure 27A). Upon stratification with diabetes status, there appeared to be a significant difference between the IgG antibody response to GLY-S compared to NT-S in both patients without diabetes (n=24) (mean O.D ± S.D, 0.7499 ± 0.2695 vs 0.5935 ± 0.2519, p-value= 0.0142, respectively) and diabetic (n=22) groups (mean O.D ± S.D, 0.8200 ± 0.2452 vs 0.6372 ± 0.2284, p-value= 0.0434, respectively) (figure 27B).

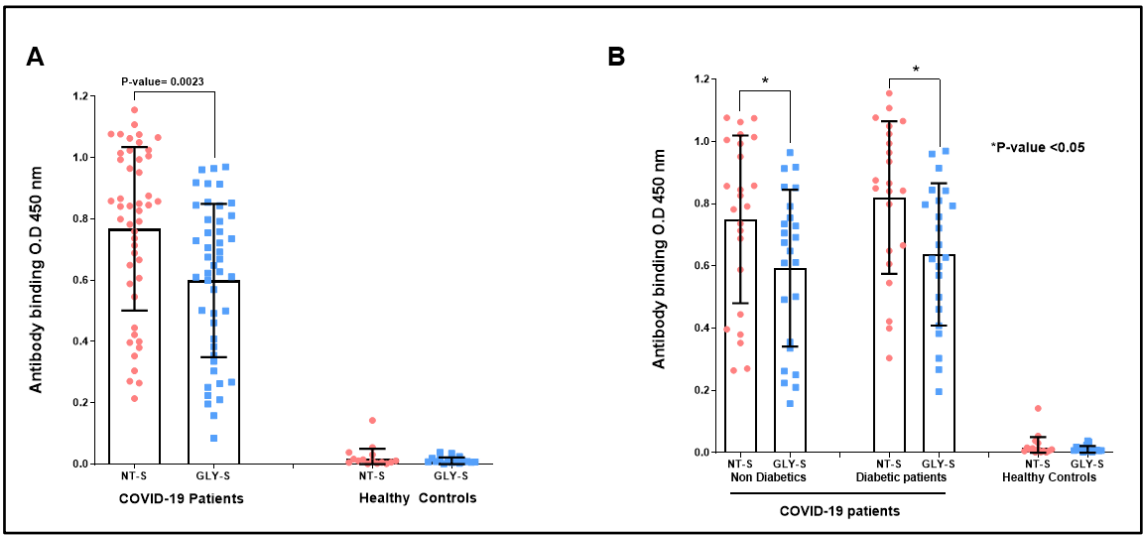

Figure 27. Antibody response to NT- and GLY- SARs-CoV-2 spike protein in Patients with COVID-19. A) The figure shows the results of an ELISA of COVID-19 patients (n=46) to NT- or GLY- Spike protein. There appears to be a statistical difference between the IgG

response in patient sera to the NT- and GLY-S (p-value= 0.0023). **B)** Shows the results of an ELISA of patients with COVID-19 based on their diabetes status. In both groups, the IgG response was higher towards the NT-Spike compared to the GLY-Spike (patients without diabetes; mean O.D= 0.7499 ± 0.2695 vs 0.5935 ± 0.2519, P-value= 0.0142, patients with diabetes; mean O.D= 0.820 ± 0.2452 vs 0.6372 ± 0.2284, P-value= 0.0434). ELISA cut-off value= 0.1425.

4.3 Association of IgG antibody binding in patients with COVID-19 and Fructosamine levels

The induced IgG response was then compared to fructosamine levels (figure 28). Fructosamine levels were measured in the total COVID-19 patient cohort (N=46) because blood glucose was not routinely collected at the time of the patient sampling. This was standard protocol in COVID-19 wards at the peak of the pandemic. Upon stratification of fructosamine levels, patients with <563 µmol/L had no significant difference between IgG levels to NT- or GLY-S, yet patients with fructosamine levels >563 µmol/L had a significant difference between NT- and GLY-S (mean O.D ± S.D= 0.7945 ± 0.2564 vs 0.6155 ± 0.2369, p-value= 0.0078, respectively) (figure 28A).

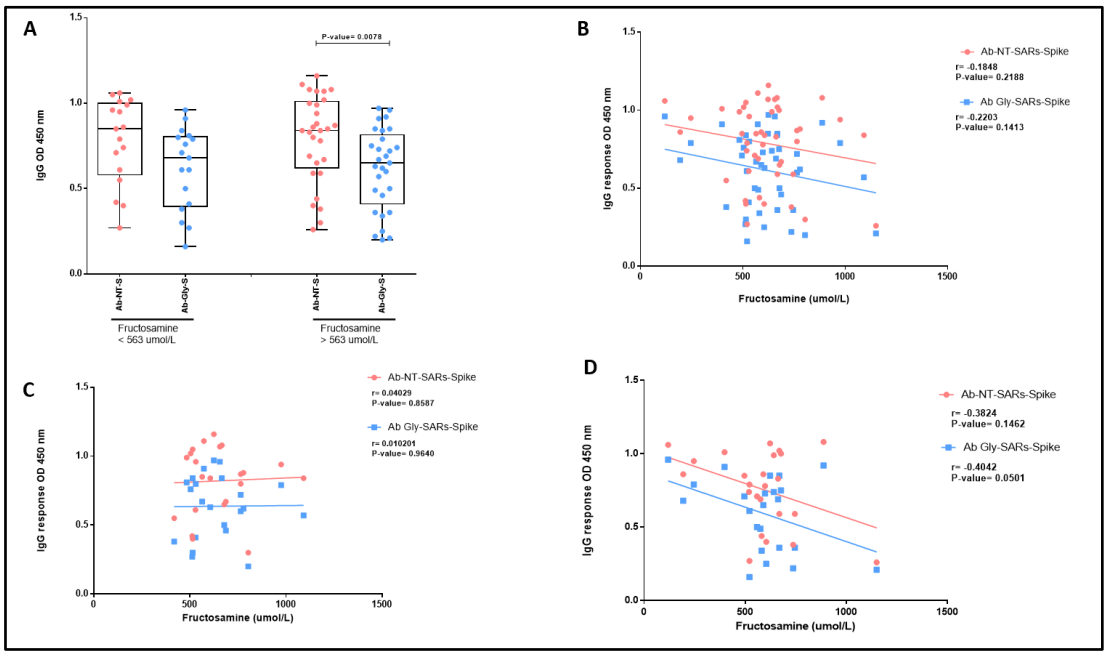

Figure 28. Fructosamine and IgG response to SARs-CoV-2 Spike protein in patients with COVID-19. A) Depicts the IgG response to NT- or GLY-S based on fructosamine levels below or above 563 nmol/L in COVID-19. **B)** Shows the overall IgG response in total COVID-19 patients (n=46) in correlation to fructosamine levels. The figure shows a negative correlation for IgG response to both NT- and GLY-Spike protein, although the results were not significant. **C)** Depicts the correlation of fructosamine levels with IgG response to NT- and GLY-S protein in patients with diabetes (n=22). **D)** The figure shows a correlation analysis between fructosamine levels and IgG response to NT- or GLY-Spike protein in patients without diabetes COVID-19 patient sera (n=24). *Correlation coefficients' (r) were calculated via Pearson's Correlation or Spearman's Correlation where appropriate.*

Furthermore, upon correlation of fructosamine levels with the total cohort (N=46), there appeared to be an overall negative correlation to both NT- and GLY-S, yet this was not significant (r= -0.1848, p-value= 0.2188 and r= -0.2203, p-value= 0.1413, respectively) (fig. 28B). Within patients with diabetes (n=22) there appeared to be no correlation with fructosamine levels to the IgG response to either NT- or GLY-S protein (r= 0.04029, p-value= 0.8587 and r= 0.010201, p-value= 0.9640) (figure 28C). However, in the case of patients without diabetes but with COVID-19, there was a strong negative correlation between fructosamine levels and the immune response to NT-S (r= -0.3824, p= 0.1462) and GLY-S, yet this was only significant in the response towards GLY-S (r=-0.4042, p= 0.0501)(figure 28D).

4.4 Antibody response to NT-S or GLY-S in patients with T1D immunized against COVID-19

The IgG response to the SARS-CoV-2 mRNA vaccine BNT162b2 (Pfizer-BioNTech) in patients with T1D or T2D, but without COVID-19 was assessed over a 6-month period. The study covered 5 timepoints; baseline T0 (within 3 days of the first dose of the vaccine), T1 (21 days from T0 and right before the second dose), T2 (34 day from T0), T3 (90 days from T0), and T4 (180 days from T0). Table 19 shows the demographic characteristics of N=26 patients with T1D, N=34 patients withT2D and N=10 healthy controls included in this study. There was a similar distribution of men and women in both the T1D and T2D cohorts (61% vs 50%, p-value= 0.4383), however the T2D patients were significantly older (mean age (years) ± S.D, 59.94 ± 10.04 vs 38.62 ± 11.16, p-value <0.0001, respectively). Table S1 shows the glucose management methods for each cohort (T1D vs T2D).

	Type 1 Diabetes	Type 2 Diabetes	Healthy controls	P-value
Total (N)	26	34	10	
Male, n (%)	14 (53.8%)	17 (50.0%)		0.4383
Age, years	40 [27-48.75]	62.5 [52-66.75]		***<0.0001***
BMI, kg/m²	24.7 [21.55-27.65]	30.05 [26.5-32.98]		***0.0001***
HbA1c, %	7.263 ± 0.7051	7.569 ± 1.285		0.3064
Pump Users, n (%)	13 (50.0%)	N/A	N/A	
TIR (%)	61.5% [55.5-71.1]			
TAR (%)	28.0% [21.0-41.0]			
TBR (%)	3.0% [2.0-7.5]			
IgG response T0				
NT-S	0.0217 ± 0.0179	0.0103 ± 0.0425	0.0349 ± 0.048	0.6456
GLY-S	0.0251 ±0.0277	0.0036 ± 0.0323	0.0217 ± 0.0248	0.4073
IgG response T1				
NT-S	0.5227 ± 0.2553	0.3701 ± 0.2647	-	***0.0411***
GLY-S	0.5474 ± 0.2479	0.3488 ± 0.2646	-	***0.008***
IgG response T2				
NT-S	1.166 ± 0.1734	0.9753 ± 0.2169	1.266 ± 0.1604	***0.0002***
GLY-S	1.09 ± 0.1655	0.9042 ± 0.2686	1.23 ± 0.1462	***0.0002***
IgG response T3				
NT-S	0.9964 ± 0.2151	0.758 ± 0.2429	0.8622 ± 0.1413	***0.0035***
GLY-S	0.9153 ± 0.1797	0.7143 ± 0.2255	0.837 ± 0.1669	***0.0071***
IgG response T4				
NT-S	0.5802 ± 0.1964	0.6314 ± 0.3078	-	0.5357
GLY-S	0.5613 ± 0.1874	0.5665 ± 0.2913	-	0.9474

Table 19. Demographic characteristics of patients with T1D, T2D and healthy controls. Qualitative data is presented as percentages, while continuous data is presented as mean ± standard deviation or median [interquartile range] depending on normal distribution. *P-values were calculated by Student's T-test, Mann Whitney test, 3-way ANOVA, or Kruskal-Wallis test where appropriate.*

Figure S10 shows the overall antibody response towards NT-S and GLY-S protein in patients with T1D and T2D. In N=26 patients with T1D, there appeared to be a peak

IgG response at T2, with a significant difference between IgG response to NT-S and GLY-S protein (mean O.D ± S.D, 1.166 ± 0.1734 vs 1.090 ± 0.1655, p-value <0.05, respectively) (figure 29A). There was no significant difference between IgG antibody response to NT-S or GLY-S between any other timepoints. In patients with T2D, there was a peak IgG response at T2 towards both NT-S and GLY-S protein, with no significant differences between the antibody responses (mean O.D ± S.D, 0.9753 ± 0.2169 vs 0.9042 ± 0.2686, p-value= 0.2991, respectively)(figure 29B). When comparing the IgG response to NT-S or GLY-S protein in N=10 immunized HC (individuals without diabetes) to immunized T1D and T2D, there was no significant difference at baseline, however at T2, there was a significantly different IgG antibody response to GLY-S in T1D compared to HC (mean O.D ± S.D,1.09 ± 0.1655 vs 1.23 ± 0.1462, p <0.05, respectively). Furthermore, there was a significantly different IgG antibody response in patients with T2D and HC to both NT-S (mean O.D ± S.D, 0.9753 ± 0.217 vs 1.266 ± 0.1604, p-value <0.005, respectively) and GLY-S (mean O.D ± S.D, 0.9042 ± 0.2686 vs 1.23 ± 0.1462, p<0.005, respectively) (figure 29C).

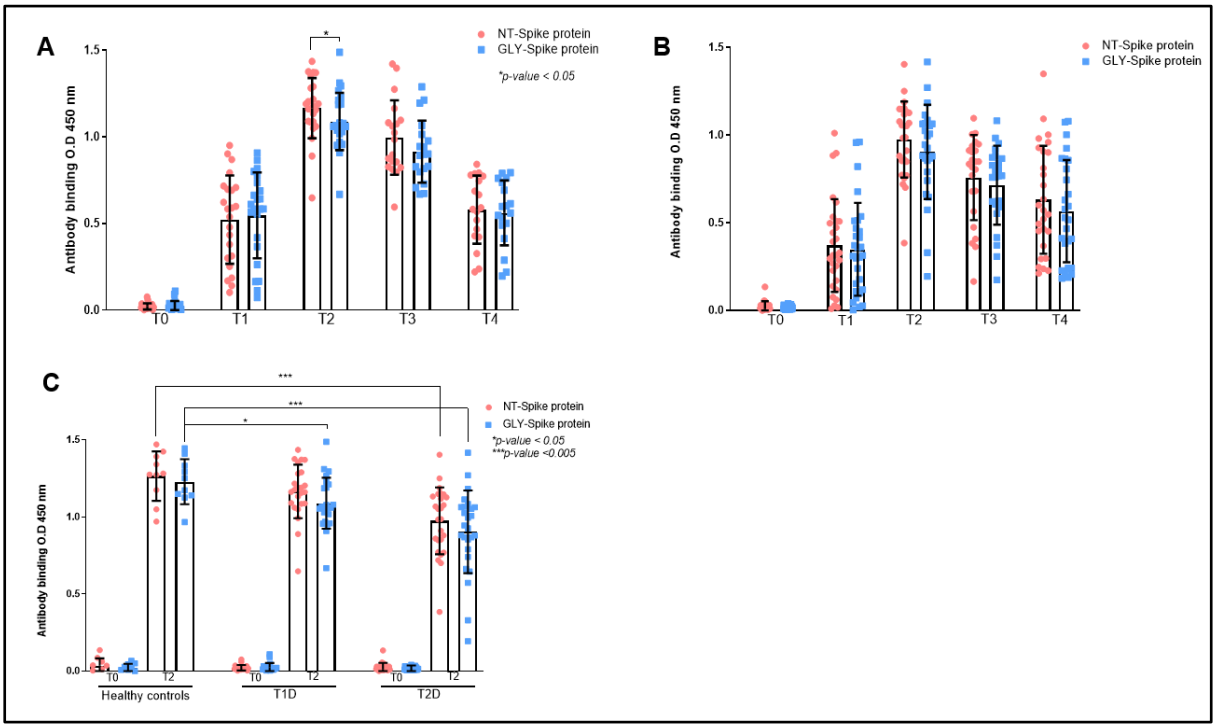

Figure 29. IgG response to NT- or GLY-S protein in patients immunized with the mRNA vaccine BNT162b2 (Pfizer-BioNTech). The figure shows the IgG response over a period of 6 months, starting at the baseline T0, T1 (21 days from T0), T2 (34 days), T3 (90 days), and T4 (180 days from T0) in patients with T1D **(A)** and T2D patients **(B)**. **C)** Shows a comparison of the IgG response in immunized healthy individuals, T1D and T2D patients at T0 (baseline) and T2 (peak IgG response).

4.5 Analysis of continuous glucose monitoring data with IgG response to the SARS-CoV-2 mRNA vaccine in patients with T1D

To understand the efficacy of the vaccine, this study attempted to assess the IgG antibody response in terms of continuous glucose monitoring (CGM) data from N=10 patients with T1D with available CGM profiles. The key measurements assessed were Time-in-range (TIR), which is the percentage of time within a 24 hour period that a patient is within the ideal glucose range, Time-above-range (TAR), which is the percentage of time a patient is above the ideal glucose range in a 24 hour period, and Time-below-range (TBR), which is the percentage of time a patient is below their ideal glucose range. When determining the overall area under the curve (AUC) of the IgG antibody response to NT-S and GLY-S over all study timepoints (T0-T4) and correlating it with the average TIR, there appeared to be a strong correlation with AUC IgG response and TIR to both NT-S (r= 0.8082, p-value= 0.0084) and GLY-S protein (r= 0.7996, p-value= 0.0097) (figure 30A).

When correlating the AUC IgG antibody to of both NT-S and GLY-S protein to the average TAR over all study timepoints (T0-T4), there was a strong negative correlation with TAR and NT-S (r= -0.7926, p-value= 0.0108), as well as a strong negative correlations with TAR and GLY-S(r= -0.7430, p-value= 0.0218) (figure 30B). There was no correlation with average TBR with AUC IgG response towards NT-S or GLY-S protein (figure 30C). Moreover, there was no significant correlation with the antibody response towards NT-S or GLY-S protein in T2D and clinical data, specifically HbA1c (%), BMI (kg/m^2) and visceral fat (cm^3) (figure S14).

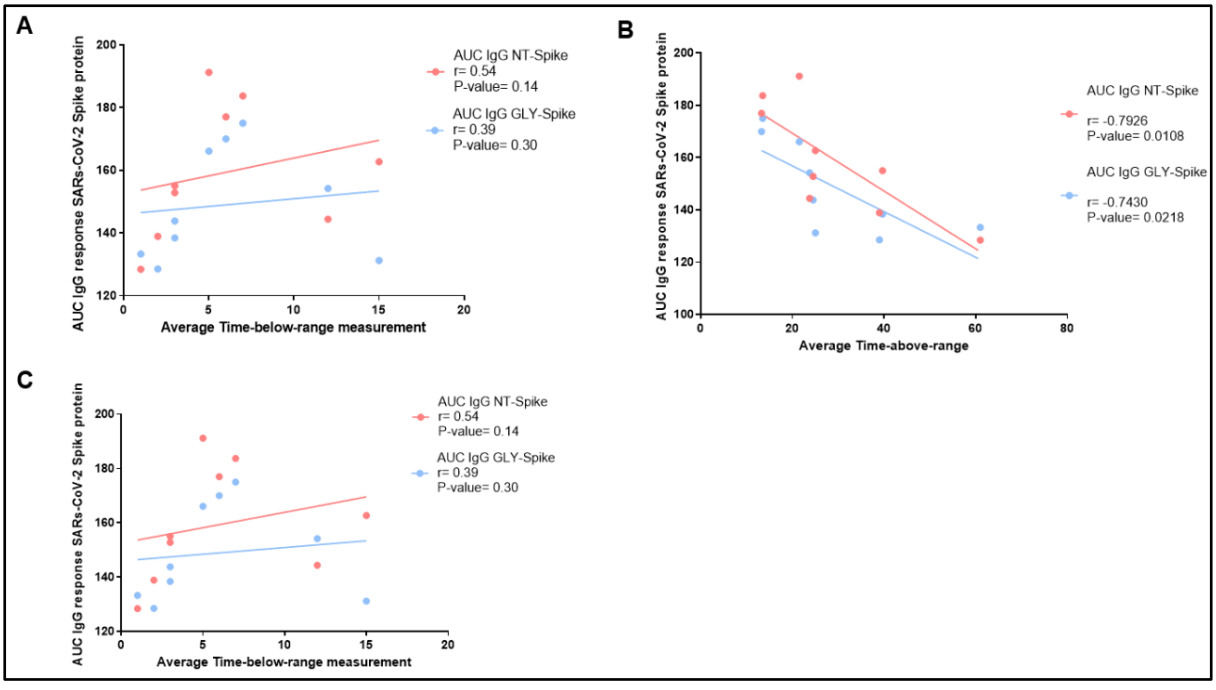

Figure 30. **Correlation of Area Under the Curve (AUC) IgG response to NT- or GLY-S protein with CGM data in N=10 patients with T1D. A)** Shows the AUC IgG response correlated with TIR measurements along all 5 timepoints (T0-T4). There appeared to be a positive correlation in AUC IgG response to NT- and GLY-S protein to TIR (r= 0.8082, p-value= 0.0084 vs r= 0.7996, p-value= 0.0097, respectively). **B)** Depicts the AUC IgG

response correlated with the average TAR measurements over all 5 timepoints (T0-T4). There was a strong negative correlation to both AUC IgG to NT- and GLY-S protein to average TAR measurements (r= -0.7926, p-value= 0.0108 vs r= -0.7430, p-value= 0.0218, respectively). **C)** Shows the AUC IgG response correlated with TBR measurements along all 5 timepoints (T0-T4). There appeared to be no correlation in AUC IgG response to NT- and GLY-S protein to TBR (r= 0.54, p-value= 0.14 vs r= 0.39, p-value= 0.30, respectively). *Correlation coefficients (r) and p-values calculated via a Pearson's correlation or Spearman's correlation where appropriate.*

4.6 Analysis of continuous glucose monitoring data with neutralization antibody response in patients with T1D to the SARS-CoV-2 mRNA (Pfizer-BioNTech).

When dividing patients with T1D with CGM data (N=13) based on their recommended glucose targets, (TIR ≥70% and TAR ≤25%), there appeared to be a stronger neutralizing antibody response to the NT-SARS-CoV-2 spike protein in patients with T1D who had a TIR>70% than those who did not (p<0.0001). Furthermore, when assessing the neutralizing antibody response against TAR measurements, patients who had a TAR≤25% were more likely to have a stronger neutralizing antibody response (p=0.008). Finally, TBR (≤4% or >4%) and HbA1c (≤7% or >7%) levels were not significantly associated with neutralizing antibody response in patients with T1D (figure 31).

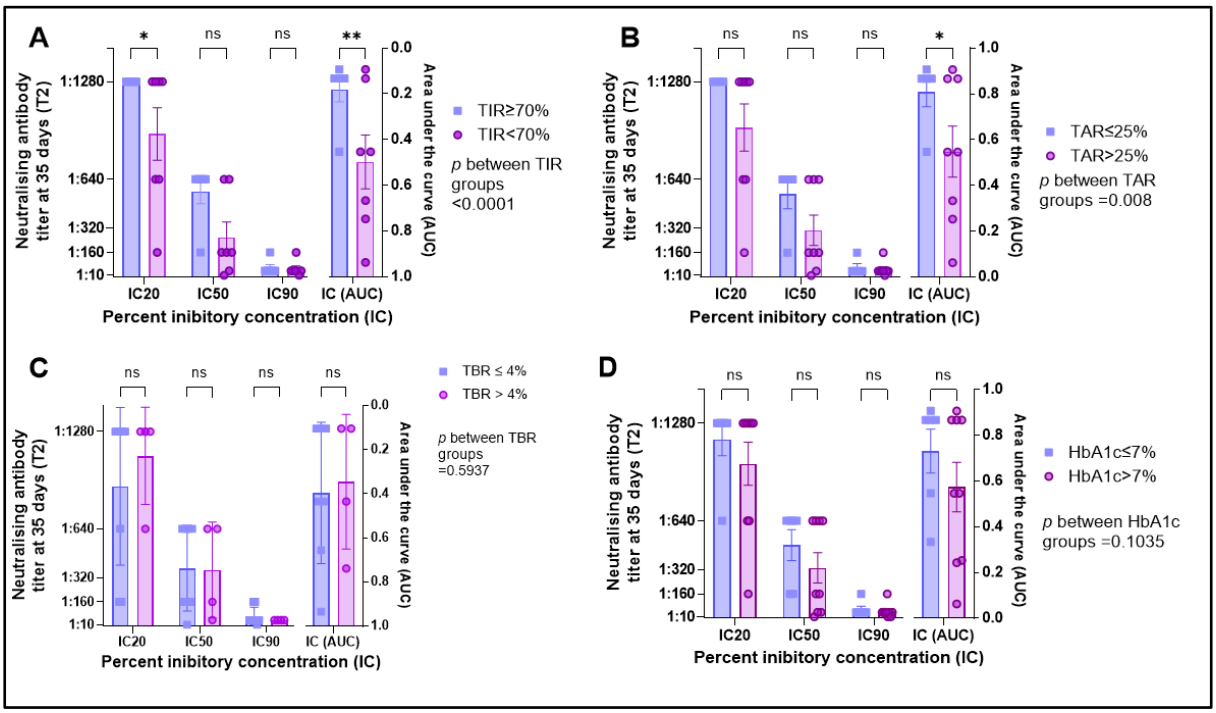

Figure 31. Neutralizing antibody assay in patients with T1D (N=13) based on recommended blood glucose levels. A) When dividing patients with T1D into TIR <70% and TIR≥70% (recommended blood glucose level) groups, patients who had a TIR≥ 70% had a stronger neutralizing antibody response than those who did not ***(p<0.0001).*** **B)** When assessing ideal TAR (≤25%), patients who had an ideal TAR were more likely to have a stronger neutralizing antibody response ***(p=0.008).*** **C)** The figure shows the neutralizing antibody response in T1D based on TBR levels (≤4% or >4%), there was no significant difference seen between groups (p-value= 0.5937). **D)** Shows neutralizing antibody data based on HbA1C levels ≤7% or > 7%. The figure shows no significant association with neutralizing antibody levels and HbA1C data. *P-values calculated based on a 2-way ANOVA, where appropriate.*

4.7 Demographic characteristics of patient cohort used to build the Clinical Risk Score

In order to build a clinical risk score to predict death in patients with COVID-19, an N=417 patient cohort was recruited from Kuwait COVID-19 cohort. The demographic and clinical characteristics of the 417 Kuwaiti patient cohort is displayed in table 20. With the main outcome being set as in-hospital mortality due to COVID-19, the patient cohort was divided into two groups; those who developed the main outcome (n=60), and those who did not (n=357). Patients who developed the primary outcome were more likely to be older (mean age (years) ± S.D, 54.2 ± 12.2 vs 43.9 ± 17.50, p-value <0.0001) and more likely to be male (90.0% vs 58.3%, p-value <0.0001, respectively). In terms of comorbidities, such as hypertension, diabetes, and asthma, were more common in those who succumbed to the primary outcome than those who survived COVID-19 (45.9% vs 26.6% [p=0.0033], 39.3% vs 20.4% [p=0.0016], 19.7% vs 8.1% [p=0.0085], respectively). Moreover, patients who proceeded to the primary outcome were more likely to have glucose levels >11.1 mmol/L than those who survived (44.3% vs 5.0%, p<0.0001, respectively). Furthermore, 100% of the patients who succumbed to in-hospital death were admitted to the ICU compared to 6.2% of those who did not succumb to the primary outcome (p-value <0.0001).

	Primary outcome (in-hospital mortality)		
Variable	**No (n=357)**	**Yes (n=60)**	**P-value**
Age, mean years ± S.D	43.8 ± 17.50	53.6 ± 12.2	***< 0.0001***
Male gender, n (%)	208 (58.3)	54 (90.0)	***< 0.0001***
Kuwaiti, n (%)	228 (63.9)	12 (20.0)	***< 0.0001***
Blood glucose categories (mmol/L)			
<5.5, n (%)	179 (50.1)	5 (8.3)	***< 0.0001***
5.5-6.9, n (%)	113 (31.7)	7 (11.7)	***0.0011***
7.0-11.1, n (%)	47 (13.2)	21 (35.0)	***< 0.0001***
>11.1, n (%)	18 (5.0)	27 (45.0)	***< 0.0001***
Comorbidities			
Diabetes, n (%)	73 (20.4)	24 (40.0)	***0.0016***
Hypertension, n (%)	95 (26.6)	28 (46.7)	***0.0033***
CVD, n (%)	26 (7.3)	13 (21.7)	***0.0013***
Asthma, n (%)	29 (8.1)	12 (20.0)	***0.0085***
ICU admission, n (%)	22 (6.2)	60 (100.0)	***< 0.0001***

Table 20. Clinical and demographic characteristics of a Kuwaiti COVID-19 cohort (N=417) used to build the clinical risk score. *Fisher's exact T test was used to calculate p-values.*

Table 21 shows the clinical and demographic data of the original N=417 Kuwaiti cohort used to build the score, as well as the internal and external validation cohorts. The internal validation cohort consisted of N=923 Kuwaiti COVID-19 patients, while the external validation cohort consisted of N=178 COVID-19 patients from the Italian CoViDiab cohort. Compared to the initial N=417 Kuwaiti cohort, the internal validation group was similar in age, whereas the CoViDiab cohort was older (45.38 ± 17.07 vs 48.34 ± 19.43 vs 63 [54-77], respectively). Moreover, when looking at ICU admission, those progressing to the ICU was similar in the original cohort compared to the internal and external validation groups (19.7% vs 18.0% vs 17.4%, respectively). In terms of the primary outcome, 14.4% of the original Kuwaiti cohort, 13.1% of the internal validation Kuwaiti cohort and 11.8% of the external validation CoViDiab cohort succumbed to the primary outcome.

	Kuwait COVID-19 Cohort (N=417)	**Kuwaiti Internal Validation Cohort (N=923)**	**CoViDiab external validation cohort (Italy) (N=178)**
Age (mean ± S.D), years	45.38 ± 17.07	48.34 ± 19.43	63 [54-77] *
Gender	262 (62.8%)	536 (58%)	106 (59.6%)
Non-Kuwaiti	177 (42.4%)	219 (23.7%)	178 (100%)
Glucose (mmol/L)			
<5.5	184 (44.1%)	272 (29.4%)	64 (36.0%)
5.5–6.9	120 (28.8%)	268 (29.0%)	54 (30.3%)
7.0-11.1	68 (16.3%)	229 (24.7%)	49 (27.5%)
>11.1	45 (10.8%)	141 (15.3%)	11 (6.2%)
BMI (kg/m^2) **			
≤25	-	67 (7.3%)	41 (23.0%)
25-29.9	-	96 (10.4%)	42 (23.6%)
≥30	-	157 (17.0%)	95 (53.4%)
Comorbidities			
- Hypertension	123 (29.5%)	199 (21.5%)	92 (51.7%)
- Diabetes	97 (23.3%)	81 (8.8%)	39 (21.9%)
- CVD	39 (9.4%)	-	23 (12.9%)
-Asthma	41 (9.8%)	42 (4.5%)	-
- Malignancy	12 (2.9%)	24 (2.6%)	8 (4.5%)
ICU admission	82 (19.7%)	166 (18.0%)	24 (17.4%)
Death	60 (14.4%)	121 (13.1%)	21 (11.8%)

Table 21. Demographic characteristics of internal and external validation cohort compared to original Kuwaiti COVID-19 group. **Median age [IQR], this was due to the CoViDiab group not being normally distributed. **BMI data was not available for all patients, and hence was excluded. CVD; cardiovascular disease.*

4.8 Developing the Clinical Risk Score

The score was built by assessing the significance of several predictive variables against the primary outcome (in-hospital mortality). In the final score, presence of asthma, gender (male), nationality (non-Kuwaiti national), and blood glucose levels (either between 7.0-11.1 mmol/L or >11.1 mmol/L) were independently associated with mortality in COVID-19. A score was allocated to each predictive variable based on the beta coefficients allocated to each independent variable (table 22). The cut-off of the score to predict death was ≥5.5, showing a specificity of 86.3% and sensitivity of 75% (AUC= 0.901). The highest risk-score conferred based on the developed clinical risk score was 12.5.

Criteria	Score
Male	2.5
Non-Kuwaiti National	2.5
Asthma	2.5
Blood Glucose 7.0 -11.1 mmol/L	3.5
Blood Glucose >= 11.1 mmol/L	5.0

Table 22. Calculated clinical risk score. Low risk of progression is a total clinical risk score of <5.5, a higher risk of progressing to the main outcome (mortality from COVID-19) is a score of ≥5.5. The cut-off value was calculated based on Youden's index of the score.

4.9 Internal and External Validation of the clinical risk score

The clinical risk score requires internal and external validation to assess the potential to predict the primary outcome (table 23). Two cohorts were used for internal validation, the initial N=417 Kuwaiti COVID-19 group the score was built on and a separate cohort of N=923 Kuwaiti COVID-19 patients admitted from May 4th to August 26th, 2020, both admitted within one COVID-19 center within Kuwait. External validation was performed using an N=178 CoViDiab Italian cohort. The score was evaluated for each patient and then analyzed against the primary outcome (in-hospital mortality from COVID-19); the score was then plotted as a ROC curve with the AUC calculated (figure 32).

Cohort	% Sensitivity	%Specificity	AUC ± SE	Positive Predictive Value (PPV)	Negative Predictive Value (NPV)
Kuwaiti (417)	**75.0**	**86.3**	**0.901 ± 0.20**	**47.8%**	**95.4%**
Kuwaiti (923)	**66.9**	**76.7**	**0.826 ± 0.91**	**30.2%**	**93.9%**
CoViDiab (178)	**66.7**	**70.7**	**0.687± 0.06**	**23.3%**	**94.1%**

Table 23. Comparison of score results within different cohorts. Kuwaiti cohorts were used for internal validation of the score, these are Kuwaiti COVID-19 (417) cohort and Kuwaiti COVID-19 (923). The Italian CoViDiab (178) cohort was used for external validation.

%Sensitivity and %Specificity was derived from the ROC analysis, using the Youden's index (5.5). AUC represents the area under the curve, an AUC of 0.9-1.0 is an excellent fit for the model, 0.8-0.7 is a great fit and 0.6 indicates a good fit. Using a cut off score of 5.5, PPV and NPV were calculated based on the following formula: PPV= True positive/ True Positive + False Positive, NPV= True Negative/ True Negative + False Negative.

When assessing the % sensitivity for the score, there appeared to be 75% for the initial 417 Kuwaiti cohort, 66.9% for the 923 Kuwaiti cohort and 66.7% for the CoViDiab cohort. The %specificity of the score shows 86.3%, 76.7%, and 70.7% in each cohort, respectively. However, the AUC showed 0.901 ± 0.20 fit for the score for the 417 Kuwaiti cohort, 0.826 ± 0.91 fit for the score for the 923 Kuwaiti cohort, and a 0.687 ± 0.06 fit for the score for the CoViDiab cohort, with respective negative predictive values of 95.4%, 93.9%, and 94.1%.

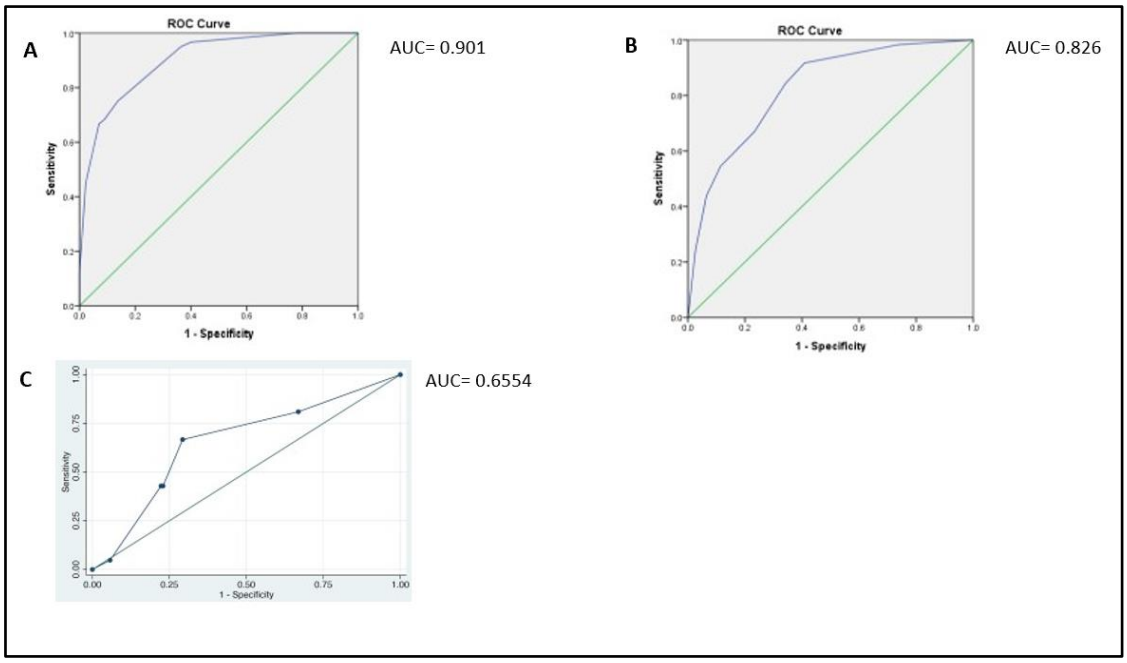

Figure 32. ROC curve for internal and external validation of the clinical risk score. A) Depicts the results of the calculated clinical risk score for mortality within the 417 COVID-19 patient cohort from Kuwait used to build the score. The "goodness of fit" of the score is depicted by the area under the curve (AUC), the AUC for this model is 0.901 indicating a great fit. **B)** Shows a ROC of the score tested on a separate 923 COVID-19 patients hospitalized in Kuwait between May 4th and August 26th, 2020. The AUC for this curve is 0.823, indicating a good fit for the score. **C)** ROC depicting the score tested against the external validation cohort CoViDiab (Italy). The curve has an AUC of 0.655, indicating a fair fit for the score.

Chapter 5.0 Discussion and Future Perspectives

5.1.0 General discussion for study 1

Although T1D only encompasses around 5-10% of total cases of diabetes, the global incidence of T1D has risen from 2.17 per 100,000 people/year to 3.6 per 100,000. In a study of 32 countries in 2017 the total number of registered T1D cases was 234,710. Asian countries, making up 60% of the world's population, showed a T1D prevalence of 32%, closely followed by European countries with a prevalence of 27%. However, the distribution of T1D within individual countries varies, with T1D only encompassing 1% of total diabetic cases in China, and, controversially, making up 17% and 8.6% of total diabetic cases in Finland and the United Kingdom, respectively [198]. Moreover, the general presentation of T1D amongst varying populations present with differing AAB profiles. In fact, evidence has shown that IgG responses, autoantibody levels, as well as antibody binding, vary amongst different study populations. Insinuating that different pockets of patients with T1D may develop autoimmunity in differing ways, however, the key triggering event that results in autoimmunity has yet to be fully elucidated.

The clinical onset of T1D is preceded by a preclinical autoimmune process, whereby AABs to native pancreatic β-cell antigens are found in the serum of at-risk individuals. Currently, the major autoantigens used as biomarkers for T1D include insulin, GAD65, IA-2 and ZnT8. These AABs tend to appear sequentially and before the onset of clinical T1D, with the development of two or more AABs conferring an increased risk to developing T1D. The Environmental Determinants of Diabetes in the Young (TEDDY) study assessed 608 children with high-risk HLA-DR-DQ genetics over 15 years and found the initial AAB in 282 children was IAA, and in 326 was GADA. Following this, the appearance of a second AAB, regardless of type, resulted in around a five-fold increased risk of developing T1D [199].

However, AABs to these antigens appear in multiple autoimmune disorders, thus more specific biomarkers are required. The trigger for autoimmunity in T1D is still widely debated. Studies have demonstrated increase oxidative stress (OS) and ROS in T1D compared to healthy controls [200], leading to the hypothesis that OS and ROS play a role in the development of autoimmunity [201]. More studies are focusing on autoimmunity targeting OS and oxPTM- β-cell antigens and their role in autoimmunity [28].

5.1.1 Autoimmunity to oxPTM- β-cell antigens in Type 1 Diabetes

As previously stated, post translational modifications play a role in normal development. In normal homeostasis, post translational modifications aid proteins in reaching their secondary or tertiary structure. However, post translational modifications of native antigens have been associated with several autoimmune diseases [202].

In this study, we demonstrated that upon oxidative PTMs, the antigenicity, and subsequent antibody response, towards the β-cell antigens, GAD65, ZnT8 and insulin is altered. When assessing immunity to native or modified GAD65 in patients

with new-onset T1D, people with T2D and healthy controls, there appeared to be increased antibody binding to GLY-GAD65, HOCl-GAD65 and NT-GAD65 in patients with T1D compared to healthy controls and T2D as measured in O.D via an ELISA. Although there was no overall significant difference towards IgG reaction to GLY-GAD65, HOCl-GAD65 and NT-GAD65 in patients with T1D, certain individuals showed an increased reactivity to GLY-GAD65 compared to NT-GAD65. This suggests the possible role of hyperglycemia or dysregulated glucose in modifying GAD65 in the early stages before T1D onset. In fact, the TRIGR study (Trial to Reduce IDDM in the Genetically at Risk) attempted to determine whether children at-risk of developing T1D presented with elevated glucose levels, and in turn whether elevated glucose contributed to the developing autoimmune process. They showed that increased glucose levels were able to predict the onset of T1D, but not the development of AABs. In contrast, increased HbA1c was associated with autoantigen production, but not multiple AABs [203]. This further instigates the β- cell stress theory, where it is believed that any element able to cause an increased need for insulin and β-cell stress may impact the progression to T1D [204].

Additionally, studies have reported that markers of oxidative stress are not only elevated in well-established individuals with T1D [205], but are also increased in individuals with normal glucose levels who are characterised as at-risk of developing T1D [206]. Moreover, there have been reports on children at-risk of T1D who presented with constant levels of proteins involved in oxidative stress, this finding was higher before seroconversion than after first autoantibody presentation. Thus, suggesting that patients at-risk of disease present with increased and elevated oxidative stress responses long before the initial clinical onset [207]. Interestingly enough, streptozotocin (STZ) and alloxan (ALX) are vastly used chemicals administered to induce diabetes in mice. They work by binding to glucose transporter- (GLUT-) 2, inducing the development of ROS and specifically targeting and damaging the pancreatic β-cells of these animals [208, 209].

When evaluating modifications via the hydroxyl radical, only 17.4% of patients with T1D showed antibody binding to •OH-GAD65 that was significantly increased when compared to NT-GAD65. In contrast, Khan and colleagues were able to demonstrate that antibody reactivity was increased towards hydroxyl modified GAD65 compared to the native in a majority of their patients with T1D [121]. Moinuddin et al, similarly showed that T1D showed higher antibody binding to ROS-GAD65 than the native unmodified [122]. However, these differences in antibody binding may be attributed to the method by which GAD65 was hydroxyl modified. Both studies by Khan et al. and Moinuddin et al., modified GAD65 via exposure to Ultra-violet (UV) radiation in the presence of H_2O_2, whereas in this study the hydroxyl modification was induced via the Fenton reaction, with H_2O_2 in the presence of $CuCl_2$ as a metal ion catalyst.

Studies that attempted to divulge the structure of GAD proteins have determined that there were several key conserved residues within GAD65 and GAD67. Predominantly, they found 3 conserved histidine residues at positions 167, 241 and 275, and within the active site they found 3 conserved residues were found at alanine 245, lysine 276 and asparagine 243 [210]. These sites, although conserved,

may be susceptible to modifications and become autoimmune targets. Upon elucidating the crystal structure of GAD65, studies were able to divulge key antigenic residues. As previously reported, the C-terminal domain was the target of bulk autoimmunity [211], with mutations, such as the substitution of valine for lysine at position 532 (V532K) and the substitution of histidine for glutamine (H568Q) in the C-terminal domain, and a substitution of lysine to arginine (K358N) in the PLP-domain, enhancing the immunogenicity of GAD65 as an autoantigen [69]. Interestingly, non-enzymatic glycation tends to target lysine, histidine, and arginine residues [212], the possible glycation of immunogenic residues within the C-terminal domain and PLP-domain of GAD65 may enhance antibody binding and T-cell targeting.

When assessing immune response to native and modified insulin in patients with new-onset T1D, antibody reactivity was significantly increased to •OH-INS than to NT-INS, with GLY-INS showing a significant diminished response. Studies from Strollo and colleagues further corroborate our findings, by which they identified that oxPTM derived insulin peptides were targeted by both circulating and T-cell derived AABS [193]. Upon further assessment, they found that most of the autoimmune response was directed to both native A: 12-21, B:11-30, and B:21-30, as well as their oxidatively modified counterparts [193]. Hence, this may further suggest that oxidatively modified insulin may act as a primary autoantigen for T1D, with GAD65 following closely after. In fact, studies have demonstrated that AABs typically present sequentially, with IAA being the first to appear in young children [213], and GADA in adolescents and young adults [214]. Given that our study cohort had a median age of 13 (9-26), it is plausible that immunity targeting GADA was at its peak compared with IAA. However, due to the increased antibody response towards •OH-INS compared to the native form may suggest that autoimmunity towards modified antigens may trigger the immunity seen in T1D.

Although there is published data on oxidatively modified insulin [114, 193] and GAD65 [121], to our knowledge, this is the first reporting of data on oxPTMs-ZnT8. ZnT8 exists as a homodimer of 70 KDa, with a dimeric structure as a ‘V’-shape with two transmembrane domains forming the branches of the ‘V’ and two C-terminal domains at the base of the ‘V’ where most of the dimeric interactions take place. Structurally, the proposed target of autoimmunity in T1D within the ZnT8 homodimer is a short loop located between residues 321-327 of the β2 and α2 of the C-terminal domain. Studies have shown a gap between these two epitopes, which may be an access point for autoantibodies. In fact, an arginine residue at position 325 was highly associated with higher risk for T2D [215].

Modifications in the ZnT8 could potentially be targeting key residues within the ZnT8 dimer that may impact immunogenicity. Hydroxyl modifications have been shown to target amino acids residues such as histidine, asparagine, lysine, and proline [216]. The C-terminal domain consists of Zn^{2+} binding sites that are chelated to histidine at positions 52, 54, 301 and 318, that may be targets of hydroxylation [215]. Furthermore, modification via hypochlorous acid typically targets amino acid residues cysteine, methionine, cystine, histidine, and leucine [217]. The C-terminal domain has been suggested to be the primary target of autoantibodies directed

towards ZnT8 [82]. Hence, the histidine, leucine, and cysteine residues located here may be targets for autoimmunity and susceptible to modification. Studies attempting to map key epitopes involved in autoimmune targeting in ZnT8 were able to identify residues other than R325 that increase the autoantigen role of ZnT8. Wenzlau et al. have shown that alongside R325, the residues R332, E333, K336, and K340 contribute to a major antigenic epitope within ZnT8 [218].

However, this study showed that upon •OH-ZnT8 modification the antibody response in the sera of patients with new-onset T1D was significantly diminished compared to the native antigen, while there was no difference seen with the antibody response towards GLY-ZnT8 and HOCl-ZnT8 in comparison to native ZnT8. Certain T2D and healthy controls also reacted to native and modified ZnT8. This may suggest that developed assay to detect AABs towards modified ZnT8 requires further optimization. However, it may also suggest that antibodies to native and modified ZnT8 are present within T2D. In fact, studies within the Chinese diabetic population have demonstrated that the percentage of ZnT8A antibodies in T1D, latent autoimmune diabetes in adults (LADA), and T2D is 24.1%, 10.7%, and 1.99%, respectively [219]. This study presented with 33.3% of T1D were positive for autoantibodies towards NT-ZnT8 and 30.4% were positive towards oxPTM-ZnT8. However, 20% (4/20) of T2D reacted towards NT- and oxPTM-ZnT8, and 18% of healthy controls reacted to NT- and oxPTM-ZnT8. Although the detection of circulating AABs is common in the general population, it is important to determine whether these AABs detected were specific for ZnT8.

Developed AABs to β-cell antigens have been suggested to appear sequentially in T1D at-risk individuals. The TEDDY study reported that children who developed development a single autoantibody, specifically IAA or GADA, were at an increased risk of developing T1D if they then developed a secondary autoantibody [199]. However, studies have indicated that it is not only the presence of autoimmunity that confers disease, but also the degree of autoantibody binding to its target autoantigen. Interestingly, when assessing the overall antibody profile in 39 patients with recent-onset T1D with antibody data towards NT- and oxidatively modified GAD65, ZnT8 and Insulin, there appeared to be very strong reactivity to •OH-Ins compared to NT-INS, similar reactivity in NT-GAD65 and GLY-GAD65 and had mixed IgG profiles towards ZnT8 and modifications. This may be due to immunity initially targeting a primary autoantigen, such as •OH-INS, and then spreading to the other autoantigens possibly due to a phenomenon known as epitope spreading.

Epitope spreading was first coined in experimental autoimmune encephalomyelitis (EAE), it is characterized by a progressing autoimmune response from its first activation to a chronic condition involving increased levels of antibodies and T cells. There are two forms are epitope spreading, intramolecularly and intermolecularly. Intramolecular epitope spreading occurs within a single antigen, and intermolecular epitope spreading occurs in different antigens [220, 221]. One study on immunization of experimental rabbits with 4-hydroxy-2-nonenal modified and unmodified Ro 60 showed that animals immunized with modified Ro could accelerate epitope spreading in autoimmune diseases, such as SLE [221].

Assessing the T-cell response towards modified antigens is essential in order to confirm whether these antigens are specifically targeted by the immune system. Mannering et al., have confirmed a human T-cell response specific towards a disulfide modified insulin epitope [115]. Strollo et al have demonstrated that the native forms of insulin peptide 4 (LVEALYLVCGERGFFYTPKT, NT-INSP-4) and insulin peptide 6 (ERGFFYTPKT, NT-INSP-6) conferred the highest antibody binding in patients with T1D than the six peptide candidates. However, upon the oxidation of INSP-6 (oxPTM-INSP-6), patients with T1D displayed higher antibody binding to the modified form than the NT-INSP-6 [193]. This may suggest that due to the increase of ROS and oxidative stress in individuals with T1D [222], this may induce the modification of peptides *in vivo*, which the immune system views as foreign and elicits an immune response. Potentially, due to phenomena like epitope spreading and molecular mimicry [223], the sequence similarity between the oxPTM-INSP-6 and NT-INSP-6, may induce a subsequent immune response directed towards NT-INSP-6 in patients.

5.1.2 *HLA*-haplotypes and autoantibodies against post translationally modified β-cell antigens in Type 1 Diabetes

To fully understand the role genetics have in the development of T1D, multiple studies have attempted to assess the link between the HLA genes and development of autoimmunity. The HLA genes have been strongly associated with increased risk of developing T1D. With the aid of genetics, children who are more at-risk of developing T1D are identified as children with high-risk HLA haplotypes were more likely to seroconvert to multiple autoantibody positivity and progress to T1D [224].

The inheritance of certain HLA genotypes has been associated with both the increased risk of T1D, while others have been associated with protective effects. High and severe risk of developing T1D have been associated with the inheritance of DRB1*03:01-DQA1*05:01-DQB1*02:01, also known as the DR3 haplotype, and DRB1*04:01/02/04/05/08-DQA1*03:01-DQB1*03:02/04, or DQB1*02, also called the DR4 haplotype. The risk of developing T1D appears to increase with the inheritance of heterozygous DR3/DR4 haplotype than inheriting the homozygous haplotypes [225]. Moderate risk of developing T1D has been linked to the inheritance of the DR2 haplotype (DRB1*15:01-DQA1*01:02-DQB1*06:02), and in certain cases inheriting DR2 displays a protective effect. Moreover, inheritance of the DR4 haplotype DRB1*0404-DQA1*0301-DQB1*0302 has also been attributed to a moderate risk of T1D [226].

The inheritance of different HLA haplotypes has been associated with differences of AAB development in the progression of T1D. For instance, inheriting the HLA-DRB1*03-DRQB1*02 haplotype has been associated with increased prevalence of GADA, conversely DRB1*04-DQB1*0302, HLA-DRB1*07-DQA1*(0201 or 0301), and HLA-DRB1*09-DQA1*0301 have been linked to a higher levels of IA-2A [227]. When conferring the HLA-risk with responses to PTM β-cell antigens, McGinty et al. demonstrated that 5 peptide modifications of GAD65, specifically deamidation and citrullination, were able to bind to HLA-DRB1*04:01 (DR4). They were able to present that upon *in vitro* enzymatic modification of GAD65, two subsequent

modifications were able to be presented and recognized by T-cell clones from patients with T1D [117].

Of the 69 patients with new onset T1D included in this study, 39 (56.5%) had HLA typing data available as well as full autoantibody profiles. This study reported that the HLA-DR4 haplotype confers a decreased risk in the developing immunogenicity towards NT- and oxPTM-GAD65. With an overall of 48.7% of patients carrying the HLA-DR4 risk haplotype, and 51.3% of patients who did not. Moreover, there appeared to be a significant increase of antibody binding towards NT- and oxPTM-GAD65 in the HLA-DR4 negative group compared to the HLA-DR4 positive group. This is in line with the current literature reports that the HLA-DR4 haplotype may not confer an increased risk of GAD65 immunogenicity in T1D. Studies have demonstrated that 84% of GADA positive patients with T1D presented with DRB1*0301 (DR3) as well as DQB1*0201, suggesting that inheritance of the DR3 haplotype may increase susceptibility to developing autoimmunity to GAD65 and oxidized derivatives.

In terms of immunogenicity towards NT- and oxPTM-ZnT8, patients carrying the HLA-DR4 haplotype had decreased antibody binding towards NT- and oxPTM-ZnT8 compared to those who did not. Moreover, the patients overall showed increased antibody binding towards NT-ZnT8 compared to oxidatively modified ZnT8. Similarly to our findings, Salonen et al. reported that ZnT8A were significantly decreased in patients carrying the HLA-DR3/DR4 heterozygous haplotype [89]. Upon assessment of autoantibody development towards NT- and oxidatively modified insulin, both the HLA-DR4 positive and negative patients with T1D displayed increased antibody binding directed towards •OH- and HOCl-INS compared with NT- and GLY-INS. When analyzing the antibody response between the groups, there was no significant difference between antibody binding towards native or oxPTM-INS. Increasing the number of patients with T1D assessed may aid in deducing a pattern of gene inheritance that increases the risk susceptibly of T1D.

For instance, Triolo and colleagues showed that there was no difference between RBA-IAA in patients with or without HLA-DR4, however, they did show a slight increase in ECL-IAA (electrochemiluminescence assay) in patients with HLA-DR4 compared to those without, however this finding was not significant ($p=0.07$) [228]. HLA genotype association with autoantibodies within the Type 1 Diabetes Prediction and Prevention (DIPP) study reported that the individuals with T1D carrying the DR3-DQ2/x and DR4-DQ2/x genotypes were 36.8% more likely to present with IAA as the first autoantibody at diagnosis [229]. Similarly, a Kuwaiti study also found that patients with T1D presenting with DR3-DRB5 and DQ8 presented with GADA as the major autoantibody, and patients with DR3-4 and DR4 reported IAA as the major autoantibody [230]. Other studies have reported that the DR3-DQ2 haplotype was associated with an initial triggering reaction directed primarily towards GAD65, leading to the GADA being first AAB identified in these patients [94].

The identification of HLA risk haplotypes has been key in identifying and recruiting patients at-risk for developing T1D into clinical trials for the study, prevention, and diagnosis of T1D. However, due to the increased heterogeneity of the disease,

dependence on HLA haplotyping alone is not enough. Moreover, individuals with adult onset T1D present with differing HLA phenotypes than childhood onset T1D. A Chinese study in adult onset T1D reported that patients were more likely to present with less severe disease, lower levels of DKA, and a lower frequency of HLA-DR3, -DR4, and -DR9 haplotypes [231].

5.1.3 Conclusions and Future Perspectives

This study attempted to divulge the key players in the initiation of autoimmunity, with specific focus on the role of oxidative stress and ROS in the development of T1D. Our data suggests that oxidative stress and increased glucose levels may induce non-enzymatic modifications to native pancreatic β-cell antigens, triggering autoimmunity and, in turn, playing a role in the development of T1D. To the best of our knowledge, this study is the first of its kind to assess the role of oxidative modifications towards 3 key autoantigens in T1D. The suggested pathogenesis of autoimmunity induced via increased levels of ROS and oxidative stress are highlighted in figure 33.

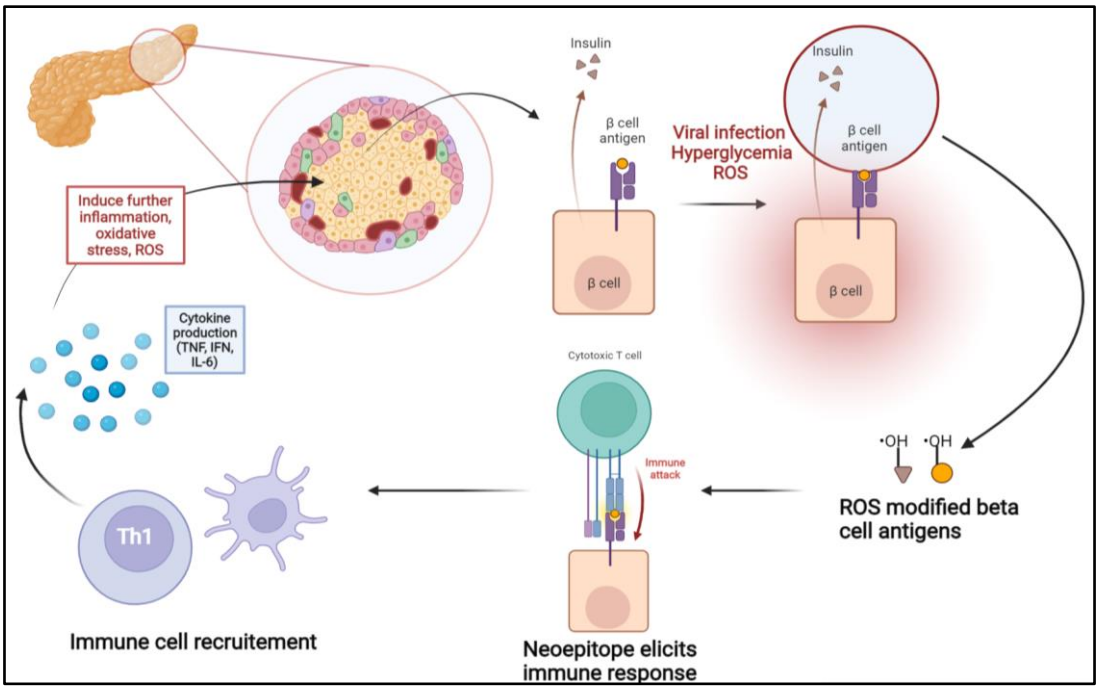

Figure 33. Proposed mechanism of ROS-induced autoimmunity in Type 1 diabetes. The figure depicts a schematic diagram suggesting the potential mechanism of oxidative induced modifications in β-cell antigens following an unknown triggering event. The modified antigens (neo-epitopes) are then target by the immune cells, such as cytotoxic T-cells, which recruit further immune cells to the site of immune reaction expanding the immune response. In turn, recruiting new immune cells to the site of inflammation, triggers further cytokine and ROS production, instigating a cycle of oxidative stress that may further induce oxidative modifications to the β-cell antigens.

Oxidized insulin has been previously associated as a neo-antigenic protein in T1D. With •OH-INS suggested to be a key neo-epitope that is able to elicit an immune response significantly higher than that towards native insulin. Moreover, reports by this group have been able to identify and characterize T cells that specifically target

oxidized insulin peptides in patients with new-onset T1D [193]. The findings in this thesis further supported the hypothesis that oxidized insulin is a major neo-antigen in T1D. Moreover, in comparison, NT- and GLY-GAD65 appear to induce similar reactivity in T1D, with NT-ZnT8 being more predominant than its modified counterparts.

Previous studies have reported that the initial autoantibodies detected in children at-risk of developing T1D are typically IAA or GADA [232]. This in turn suggests that insulin and GAD65 play a role as the primary triggers of autoimmunity within T1D. On the other hand, ZnT8 is hardly ever the primary or sole autoantigen identified in initial seroconversion to autoimmunity seen in T1D. Although ZnT8A can be detected at initial initiation of autoimmunity, it is more often detected at later stages of prediabetes, typically within adolescents [233]. Moreover, studies demonstrate that although ZnT8A may aid in the stratification of T1D diagnosis, these autoantibodies have a tendency to disappear shortly thereafter [234], making them unreliable biomarkers on their own.

To expand upon the findings in this thesis, further optimization of the protocols is required, along with increasing the number of patients assessed. The next requirement would be to elucidate and determine the success of the induced modifications via mass spectrometry in both GAD65 and ZnT8, which has previously been assessed in modified insulin [10]. This is necessary to establish the key residues susceptible to modification by ROS and oxidative stressors. Furthermore, identifying key modified residues able to elicit an immune response is important in understanding the specific T and B-cell responses. This may aid in identifying more specific biomarkers that can more accurately predict, diagnose, and monitor T1D. As well as developing more specific immune modulators and treatments that can postpone the onset of T1D. In conclusion, the findings in this thesis support the hypothesis that oxidative stress and the subsequent development of oxidatively modified neo-epitopes may play a role in the pathogenesis of T1D. However, future studies are necessary to be able to have a concise conclusion.

5.2.0 General Discussion for Study 2

Studies have consistently demonstrated that people with diabetes are at-risk for developing severe, and potentially deadly, cases of COVID-19. Diabetes impacts both the innate and adaptive immune systems, which has been reflected in susceptibility of patients with diabetes for influenza and other viral infections. Reports have further suggested that patients with diabetes are at-risk of recurrent COVID-19 infections, even after vaccination against SARS-CoV-2.

In fact, retrospective studies on antibody response to COVID-19 in people withT2D who did not develop severe disease, with severe disease being defined as requiring ICU admission, showed that patients with diabetes were negative for anti-SARS-CoV-2 antibodies. Thus, supporting the hypothesis that the impaired immune response in diabetes plays a role in the severity of COVID-19 in these individuals [235]. Studies have also shown marked neutrophilia and an increase in T cell subpopulations, specifically Th subsets and natural killer cells, in patients with T2D compared to patients without diabetes and COVID-19 [236].

A whole population study on the impacts of T1D and T2D in patients with COVID-19 in England, found that in over 61 million patients, 0.4% had T1D and 4.7% had T2D. Of the 23,698 in-hospital deaths registered in this study, 31.4% had T2D, 1.5% had T1D, and 0.3% presented with other forms of diabetes. A calculated odds ratio (OR) of developing in hospital death due to COVID-19 in T1D demonstrated an OR of 3.51 (95% C.I. 3.16-3.90) and in T2D OR 2.03 (95% C.I. 1.97-2.09) [237]. These studies have consistently demonstrated the increased severity of COVID-19 in patients with diabetes; however, they do not fully elucidate the root cause of this detrimental immune response. This study attempts to determine whether dysregulated glucose plays a role in the development of immune response towards patients infected with COVID-19, as well as the role glucose plays in the immunogenicity of the SARS-CoV-2 mRNA vaccine (Pfizer, BioNTech).

5.2.1 The role of glycation in immunity towards SARS-CoV-2

Dysregulated glucose levels have been associated with detrimental and life-threatening COVID-19 [169]. A retrospective study of 465 COVID-19 patients in the New York area, showed that dysregulated glucose levels was associated with increased risk of mortality in these patients. Furthermore, instances of increased insulin usage or new insulin needs was also correlated with increased mortality [238]. Moreover, upon infection with SARS-CoV-2, patients with T2D present with a severe and fierce cytokine storm, characterized by increased levels of circulating TNFα and IL-6. Patients with diabetes also more often present with vascular dysfunction, which is consistently linked to the increased inflammatory mechanism [239].

Studies have demonstrated that SARS-CoV-2 is subject to glycosylation, aiding in achieving its virulence. Glycosylation is a well-established PTM, commonly occurring in viruses. It is an enzymatic process, by which glycans are covalently linked to amino acid side chains, increasing viral folding, and promoting interactions with viral receptors [240]. This increased and abnormal glucose levels may be responsible for

glycation of the SARS-CoV-2 S protein, and thus altering its virulence. Glycation is not a rare phenomenon in cases of hyperglycemia and patients with diabetes. Whereby, non-enzymatic glycation occurs via the Maillard reaction, during which the carbonyl group of reducing sugars reacts with the amine groups of amino acids, peptides, or proteins. Research has shown that primary amines are more reactive and susceptible to glycation than secondary or tertiary amines. It has been shown that the primary amines of Lysine side chains are highly exposed to glycation [241]. The SARS-CoV-2 S glycoprotein consists of a myriad of lysine residues on the protein surface, with Lys417 being a key residue that forms a salt-bridge with Asp30 of ACE2 [142].

In this study, we demonstrated that the *in vitro* glycation of the SARS-CoV-2 S protein impacted antibody binding. Patients with and without diabetes (both T1D and T2D), had significantly lower binding to GLY-S compared to NT-S. Furthermore, upon fructosamine assessment, patients with higher levels of fructosamine appeared to have significantly diminished IgG binding to GLY-S compared to NT-S. This may indicate that the glycation of the spike protein is able to evade the immune system more efficiently than the native unmodified spike protein. Interestingly, patients with no previous history of diabetes demonstrated a strong negative correlation with fructosamine levels and antibody response to both NT- and GLY-S protein, whereas patients with diabetes did not. This may suggest that patients with diabetes were closely monitored in terms of glucose levels, whereas patients without diabetes were not. This may also be due to stress-induced hyperglycemia, this occurs when there is a transient elevation in hyperglycemia in response to a metabolic condition. Stress-induced hyperglycemia is a common place phenomenon in patients admitted to the ICU [242]. Hence, they presented with increased levels of dysregulated glucose that may have been able to induce glycation, hyperglycemia, and inflammation in response to COVID-19. Furthermore, hyperglycemia may stimulate antigen glycation, which has previously been demonstrated to reduce antibody recognition [114].

Viral infections are able to induce an increased hyperglycemic state in both patients with and without diabetes. This has been seen in respiratory syncytial viral infection and the previous 2003 SARS-CoV-1 pandemic. Moreover, COVID-19 has been associated with the development of new-onset diabetes, whether this form of diabetes can be characterized as T1D or T2D or another form is yet to be defined. However, this new-onset diabetes is characterized by sudden acute hyperglycemia and DKA [243]. Multiple reports attempted to divulge the canonical and non-canonical cellular infiltration pathways of SARS-CoV-2 by assessing tissues derived from diabetic, non-diabetic and COVID-19 infected patients. A myriad of studies agree that the pancreatic and endothelial tissues house the ACE2 receptor.

When assessing the binding differences between NT- and GLY-S protein to ACE2, there appeared to be diminished binding of the GLY-S to ACE2 compared to the NT. However, this difference was not significant. In fact, an in-silico study based on available x-ray crystallography structure of the ACE2, and SARS-CoV-2 spike glycoprotein RBD system showed that upon glycation of the lysine residues in the S

protein there were 19 non-polar stabilized amino acid pairings. In comparison, the NT-S and native ACE2 binding shows 30 amino acid pairings that show non-polar interactions between these two proteins [244]. This may suggest that upon glycation of the S protein ACE2 binding is diminished, the SARS-CoV-2 virus finds new modes of entry into host cells.

Host cell receptors such as neuropilin 1 (NRP1), CD147, and dipeptidyl peptidase (DPP4) have been brought up as entry points for SARS-CoV-2. NRP1 is highly expressed throughout the system, it is found in the olfactory epithelium, respiratory epithelium, and nasal cavity epithelial cells to name a few. The effects SARS-CoV-2 has on the nervous system have been suggested to be linked to entry via the olfactory NRP1 receptor. Studies have demonstrated that DPP4 has similar expression profiles as ACE2. Furthermore, major respiratory injuries from MERS-CoV have been related to entry via DPP4, hence studies have ventured into determining the role of this receptor in SARS-CoV-2 entry [245].

Studies have also suggested that the increased virulence seen in diabetic patients towards COVID-19 may, in fact, be associated with the modification and alteration of the ACE2 receptor. D'Onofrio et al. studied the impact of *in vitro* glycation on the ACE2 receptor, and whether it enhances viral binding and entry, in turn expediting the risk of myocardial infarction elevated in patients with T2D following infection with COVID-19. Their study found that human ACE2 could be non-enzymatically glycated with 120 mM of glucose at 7 sites (Lys631, Lys659, Lys689, and Lys619) with only Lys353 being found to bind to the RBD of the S protein. However, the impact of this glycation only slightly impacted binding to S protein [246].

5.2.2 SARS-CoV-2 mRNA vaccine immunogenicity in diabetic patients

Diabetic patients have been shown to be highly susceptible to influenza-like viruses, leading to deadly outcomes[247]. Hence, there was a clear need to accelerate the administration of vaccinations to avoid severe and detrimental infections. However, it remains necessary to assess the efficacy of these vaccines in diabetic patients who already show impaired immunity. For instance, although cases of influenza vaccination show no apparent difference between developed immunity in diabetic vs non-diabetic patients. However, patients with high HbA1c levels were shown to have a delayed immune response to the vaccine [248]. Upon the emergence of SARS-CoV-1 at the turn of the 21st century, this aided in expediting the vaccine development towards SARS-CoV-2. Similarly to its predecessor, the dominant immunogen in SARS-CoV-2 was the S glycoprotein, with isolated neutralizing antibodies from COVID-19 patients specifically targeting the RBD [249].

This study attempted to determine the efficacy of the SARS-CoV-2 mRNA vaccine BNT162b2 (Pfizer, BioNTech) in diabetic patients. The mRNA vaccine itself has been seen to be effective against the Alpha (B.1.1.7) variant and Beta (B.1.351) variant of SARS-CoV-2 in a study conducted in Qatar. Abu-Raddad et al. were able to deduce that after 14 days of immunization with the second dose of the BNT162b2 mRNA vaccine, there was an 89.5% effectiveness (95% C.I 85.9-92.3) against B.1.1.7 variant and 75.0% effectiveness (95% C.I 70.5-78.9) effectiveness against

the B.1.351 variant [250]. However, when assessing the effectiveness of the vaccine towards the Omicron and Delta variants in the U.S.A, studies found that the vaccine had an estimated effectiveness of 67.3% (95% C.I 65.0-69.4) against the Omicron variant after 3 doses of the mRNA vaccine compared to unvaccinated controls. As well as the vaccine had a 93.5% (95% C.I 92.9-94.1) estimated effectiveness against the Delta strain after 3 doses of the vaccine compared to unvaccinated controls [251].

When assessing the overall IgG response in T1D and T2D, the induced antibody response following immunization appeared to follow a similar profile in both cohorts. Whereby, the peak IgG response was seen at T2, which is two weeks after administration of the second dose. This finding is similar to that of Papadokostaki et al., who showed that there was a peak IgG response in diabetic patients 7-15 days after the second dose of the BNT162b2 vaccine, comparable to that of non-diabetic patients, which remained up to 2 months after administration of the vaccine [252]. Upon assessing the impacts of glucose control on the vaccine response in T1D, our data showed that pre-vaccination glucose correlates with a higher anti-spike glycoprotein binding and neutralizing antibody response in T1D. These results further imply that well-controlled glucose levels may improve the immune response. Moreover, the increasingly positive correlation between CGM data and the overall IgG response to both NT- and GLY-S proteins than to HbA1c, may suggest that day to day glucose control is more pivotal for the ideal immune response generated by the vaccine. Furthermore, patients with T1D appear to have a more prominent and improved neutralizing antibody response correlating with TIR > 70% compared to those with a TIR <70%. Insinuating that improved glucose control, may also improve the production, secretion, and activity of neutralizing antibodies.

HbA1c gives a measurement of blood glucose levels over two to three months [253], however it does not give any indication of day to day glucose fluctuations. Moreover, studies have shown a significant degree of discordance between CGM data and HbA1c in around 40% of patients with T1D [254]. Recent studies have similarly shown that there was no correlation with HbA1c levels and the antibody response in T1D and T2D following the administration of the SARS-CoV-2 vaccine [252, 255]. However, a study on T2D and post-vaccine glucose control showed that in patients with an HbA1c ≥ 7% had a lower neutralizing antibody and T-cell response than those with an HbA1c < 7%. Furthermore, Marfella and colleagues suggested that poor glycemic control after the administration of the BNT162b2 vaccine was associated with a limited immune response towards SARS-CoV-2, as well as recurrent infections in T2D [256]. This contrasts with our study, where the data showed no association with HbA1c and antibody response in T2D patients, however this may be associated with the limited number of T2D.

Several studies have assessed the impact of the SARS-CoV-2 vaccination on glycemic control. A study by Gouda and colleagues analyzed the impact of the vaccination on CGM data of adolescent T1D. They found a slight decrease in TIR data and a change in glucose levels, however neither of these were significant [257]. Heald et al. also demonstrated short-term changes in blood glucose levels post

administration of the SARS-CoV-2 vaccine, notably in patients with lower HbA1c levels [258]. This differs from our findings, whereby there was no significant difference between CGM data before or after administration of the vaccine. In fact, our findings are comparable to that of D'Onofrio and colleagues, who depicted no comparable difference between TIR three days before administering the vaccine and 14 days following vaccination [259].

Hyperglycemia has long been linked to dysregulated innate immunity. Studies have shown that hyperglycemia induces overproduction of protein kinase C, which may inhibit the migration of neutrophils. In turn, this can prevent phagocytosis by neutrophils and macrophages, superoxide production, and decreases NETs formation [260, 261]. Hyperglycemia has also been linked to impaired pathogen recognition by TLRs in diabetic patients [261]. Moreover, studies have also demonstrated that dysregulated and increased glucose can induce accelerated immunosenescence, reduced vaccine protection, and reduced antibody responses [262].

Furthermore, upon assessing vaccine efficacy in patients with T2D and BMI, there appeared to be no significant association with overall IgG response (figure S14-S15). However, there was a trend seen in both waist circumference and visceral fat and a strong negative correlation with the induced antibody response following SARS-CoV-2 vaccination. Similarly, studies have shown that visceral fat is increasingly associated with increased risk of developing severe or detrimental cases of COVID-19 than BMI or subcutaneous fat [263]. Controversially, Watanabe and colleagues, found that baseline BMI in obese individuals correlated with diminished cell-mediated and humoral immunity. However, weight loss and blood glucose reduction, the immune response was much improved [264].

Based on these findings, it may be suggested that it is not the BMI itself, but the adipose tissue distribution that impacts the severity of disease and the elicited immune response. Obesity has been previously associated with chronic low-grade inflammation, worsening hypertension and cardiovascular disease (CVD). However, within the context of COVID-19, obese patients have survived renal injury, respiratory symptoms and pulmonary embolism, they have also presented with better short- and medium-term prognoses than they're normal weight counterparts. This phenomenon, deemed the obesity paradox, has also been seen in other respiratory diseases and chronic obstructive pulmonary disease (COPD) [265]. Studies on obese patients and COVID-19 have found that these patients were more likely to be admitted to the ICU, however there was no significant difference in mortality rates [266].

Hence, reports have been focusing on the impact of adipose tissue distribution on the impact of disease pathogenesis and severity. In fact, reports on European populations with on COVID-19 were able to assess that visceral fat was a stronger predictor of mortality and severity of disease than both subcutaneous fat and BMI [263].

5.2.3 The role of glucose in mortality in patients with COVID-19

The COVID-19 pandemic varied between different global populations. Certain pockets suffered from severe, detrimental, and deadly disease, while others presented with, relatively, mild to moderate conditions. Due to the overwhelming toll this disease had on global medical resources, an apparent necessity to quickly and easily identify patients who were the most at-risk to develop severe disease, requiring ICU admission, was top priority. Therefore, this study attempted to devise a clinical risk score, which would aid in stratifying and identifying the potential patients likely to suffer from severe, possibly deadly, cases of COVID-19.

The developed clinical risk score in this study presented that the male gender, being a non-Kuwaiti national, the presence of asthma, and blood glucose levels greater than 7.0 mmol/L. Interestingly, the addition of blood glucose between 7.0 and 11.0 mmol/L and greater than 11.1 mmol/L, but not diabetic state, within the clinical risk score, further suggest the importance of glucose management within COVID-19. In fact, studies have demonstrated that even in non-diabetic patients, hyperglycemia was significantly associated with negative outcomes of COVID-19, such as elevated presence of pneumonia and mortality, compared with patients with no signs of hyperglycemia [267]. Lombardi et al. were able to identify that in a study of 1938 hospitalized patients with COVID-19 in New York City were at an increased risk of mortality when presenting with in-hospital uncontrolled hyperglycemia, with a hazard ratio of 1.54 ($p= 0.049$) [268]. Similarly, a Kuwaiti study reported that fasting blood glucose greater than 7.0 mmol/L was an independent predictor of ICU admission and severity of COVID-19 [169].

Retrospective studies have shown that glucose levels are independent predictors of severe and detrimental COVID-19. A study from South Korea assessed 106 inpatients with COVID-19, demonstrating that age, chronic lung disease, diabetes, and fasting plasma glucose (FPG) were elevated in patients who had passed away due to complications from COVID-19. Upon assessing the hazard ratio via a Cox regression model, this study found that age above 68 years and FPG of 168 mg/dL or higher were significant predictors ($p< 0.05$) of mortality. Moreover, elevated FPG was identified as a significant predictor of death even in patients without diabetes ($p< 0.04$) [269]. Zhang and colleagues further demonstrate that during the outbreak of the omicron variant, elevated blood glucose levels were independent predictors of severe cases of COVID-19 and delayed variant clearance. Moreover, there appeared to be a decrease of 16.5-fold of the neutralizing antibody titer in response following three doses of the inactivated vaccine in patients with an elevation of blood glucose levels [270].

COVID-19 is not the first instance of diabetes, hyperglycemia and dysregulated glucose playing a role in severe and detrimental disease. During the 2003 SARS-CoV-1 pandemic, studies were similarly able to demonstrate that fasting plasma glucose was significantly elevated in SARS-CoV-1 patients who passed away compared to those who survived and individuals without SARS-CoV-1 (9.7 ± 5.2 vs 6.5 ± 3.0 vs 5.1 ± 1.0 mmol/L, $p<0.01$, respectively). Moreover, the presence of diabetes and increased hyperglycemia were recognized as independent predictors of severity and death to SARS-CoV-1 [170]. When assessing the impact of community

diseases, patients with T2D were more likely to have severe and deadly cases of community acquired pneumonia, with glycemic control being able to prevent chronic vascular complications [271].

HbA1c has consistently been correlated with increased severity and duration of diseases. A case-control retrospective study on patients with (n> 34000) and without (n> 342000) pneumonia showed a relative risk (RR) of 1.23 (95% C.I 1.19-1.28) in T2D. When assessing this risk based on > 9% or < 7% HbA1c, the results revealed a RR 1.60 (C.I 1.44-1.76) and a RR 1.22 (C.I 1.14-1.30), respectively [272]. A 14-year follow-up study of 12954 controls and 4748 patients with T1D with bacterial infections, divided the patients based on HbA1c groups (<7%, 7-7.9%, 8-8.9%, 9-9.9%, >10%), found that frequency of infection was significantly increased in patients with T1D and positively correlated with HbA1c [273].

As previously stated, hyperglycemia and dysregulated glucose impact the immune system by inducing increased cytokine productions, such as IL-6 levels in response to monocytes, IL-1, TNFα, and decreasing the production of NETs and phagocytosis [260, 274]. Additionally, the immune system has been reported to be able to function at relatively low levels of glucose, for instance CD8+ T cells were found to be able to fully function with as little as 0.5 mM. The immune system is further able to upregulate glucose transporters, which is believed to be an attempt to quench pathogens of glucose [275]. A myriad of pathogens have a tendency to favor a hyperglycemic environment for replication [276]. In fact, studies have shown that SARS-CoV-2 replication is heightened in conditions of high glucose levels [159]. Thus, it can be suggested, that in cases of diabetes, where even in a state of fasting glucose is elevated, this pathway and method of protection subsequently fails [275].

5.2.4 Conclusions and Future Perspectives

Even though the dysregulated immune response in diabetic patients, along with lower cellular function and microvascular complications, were well established to aggravate complications, viral infections were not a major concern. In developed countries, diabetic patients were more likely to suffer from recurrent non-life-threatening infections, such as urinary tract infections [277], and T2D has been associated with increased risk of lower respiratory tract infections O.R 1.3 (95% C.I 1.11-1.52), fungal infections O.R 1.41 (95% C.I 1.24-1.61), and skin and mucosal bacterial infections O.R 1.32 (95% C.I 1.13-1.55) [275].

However, the COVID-19 pandemic has turned the spotlight back on diabetic patients and their increased risk of developing severe, potentially deadly, diseases. Although research has consistently correlated the role of blood glucose and hyperglycemia in mediating the immune response, the question arises, how does the endocrine system impact the immune system? The metabolic regulation of immune cells was predominantly via cytokines, particularly after their activation. However, as a protective mechanism against viral infections, recent reports have suggested that systemic metabolic changes act as part of the defense mechanism [278]. Dysregulation of this system, particularly within T1D and T2D, is believed to be contribute to the severe immune response seen in response to infection.

Hence, the findings in this thesis strongly suggest that proper glucose control is potentially a major factor in disease prognosis in COVID-19, regardless of diabetic state. Additionally, due to the continued reporting of high glucose levels in numerous infections negatively impacting diabetic patients, further supports the notion that glucose plays a chief function in managing the immune system.

This study is not without its limitations, the limited number of COVID-19 patients and patients followed after vaccination may deter the results. Moreover, the retrospective nature of key aspects of this study made it impossible to seek missing information. However, the findings do suggest that further studies on the overlap of the endocrine and immunological systems require more in-depth analysis to fully expand upon the intertwining roles they play in protection against infection. The COVID-19 pandemic should mark as an essential learning curve, whereby the necessity of understanding the dysregulated and over extended immune response in diabetic patients is essential to, in turn, be able to develop strategies to protect against severe and potentially deadly disease in diabetic and non-diabetic patients.

References

1. Standl, E., et al., *The global epidemics of diabetes in the 21st century: Current situation and perspectives.* Eur J Prev Cardiol, 2019. **26**(2_suppl): p. 7-14.
2. Koye, D.N., et al., *The Global Epidemiology of Diabetes and Kidney Disease.* Adv Chronic Kidney Dis, 2018. **25**(2): p. 121-132.
3. Tan, S.Y., et al., *Type 1 and 2 diabetes mellitus: A review on current treatment approach and gene therapy as potential intervention.* Diabetes Metab Syndr, 2019. **13**(1): p. 364-372.
4. Pugliese, A., *Insulitis in the pathogenesis of type 1 diabetes.* Pediatr Diabetes, 2016. **17 Suppl 22**: p. 31-6.
5. Katsarou, A., et al., *Type 1 diabetes mellitus.* Nat Rev Dis Primers, 2017. **3**: p. 17016.
6. DiMeglio, L.A., C. Evans-Molina, and R.A. Oram, *Type 1 diabetes.* Lancet, 2018. **391**(10138): p. 2449-2462.
7. Roep, B.O., et al., *Type 1 diabetes mellitus as a disease of the beta-cell (do not blame the immune system?).* Nat Rev Endocrinol, 2021. **17**(3): p. 150-161.
8. Esposito, S., et al., *Environmental Factors Associated With Type 1 Diabetes.* Front Endocrinol (Lausanne), 2019. **10**: p. 592.
9. Redondo, M.J., A.K. Steck, and A. Pugliese, *Genetics of type 1 diabetes.* Pediatr Diabetes, 2018. **19**(3): p. 346-353.
10. Strollo, R., et al., *Antibodies to post-translationally modified insulin as a novel biomarker for prediction of type 1 diabetes in children.* Diabetologia, 2017. **60**(8): p. 1467-1474.
11. Bardaweel, S.K., et al., *Reactive Oxygen Species: the Dual Role in Physiological and Pathological Conditions of the Human Body.* Eurasian J Med, 2018. **50**(3): p. 193-201.
12. Di Dalmazi, G., et al., *Reactive oxygen species in organ-specific autoimmunity.* Auto Immun Highlights, 2016. **7**(1): p. 11.
13. Chen, Q., et al., *Reactive oxygen species: key regulators in vascular health and diseases.* Br J Pharmacol, 2018. **175**(8): p. 1279-1292.
14. Binder, C.J., N. Papac-Milicevic, and J.L. Witztum, *Innate sensing of oxidation-specific epitopes in health and disease.* Nat Rev Immunol, 2016. **16**(8): p. 485-97.
15. Davies, M.J., *Protein oxidation and peroxidation.* Biochem J, 2016. **473**(7): p. 805-25.
16. Tsuneda, T., *Fenton reaction mechanism generating no OH radicals in Nafion membrane decomposition.* Sci Rep, 2020. **10**(1): p. 18144.
17. Lin, W., et al., *Reactive Oxygen Species in Autoimmune Cells: Function, Differentiation, and Metabolism.* Front Immunol, 2021. **12**: p. 635021.
18. Elumalai, S., et al., *NADPH Oxidase (NOX) Targeting in Diabetes: A Special Emphasis on Pancreatic beta-Cell Dysfunction.* Cells, 2021. **10**(7).
19. Schiffers, C., et al., *Redox Dysregulation in Aging and COPD: Role of NOX Enzymes and Implications for Antioxidant Strategies.* Antioxidants (Basel), 2021. **10**(11).
20. Snezhkina, A.V., et al., *ROS Generation and Antioxidant Defense Systems in Normal and Malignant Cells.* Oxid Med Cell Longev, 2019. **2019**: p. 6175804.
21. Mazat, J.P., A. Devin, and S. Ransac, *Modelling mitochondrial ROS production by the respiratory chain.* Cell Mol Life Sci, 2020. **77**(3): p. 455-465.

22. Wong, H.S., B. Benoit, and M.D. Brand, *Mitochondrial and cytosolic sources of hydrogen peroxide in resting C2C12 myoblasts.* Free Radic Biol Med, 2019. **130**: p. 140-150.
23. Dubouchaud, H., et al., *Mitochondrial NADH redox potential impacts the reactive oxygen species production of reverse Electron transfer through complex I.* J Bioenerg Biomembr, 2018. **50**(5): p. 367-377.
24. Chen, J., et al., *Mitochondrial Reactive Oxygen Species and Type 1 Diabetes.* Antioxid Redox Signal, 2018. **29**(14): p. 1361-1372.
25. Ryan, B.J., A. Nissim, and P.G. Winyard, *Oxidative post-translational modifications and their involvement in the pathogenesis of autoimmune diseases.* Redox Biol, 2014. **2**: p. 715-24.
26. Romagnani, S., *Immunological tolerance and autoimmunity.* Intern Emerg Med, 2006. **1**(3): p. 187-96.
27. James, E.A., M. Pietropaolo, and M.J. Mamula, *Immune Recognition of beta-Cells: Neoepitopes as Key Players in the Loss of Tolerance.* Diabetes, 2018. **67**(6): p. 1035-1042.
28. Dunne, J.L., et al., *Posttranslational modifications of proteins in type 1 diabetes: the next step in finding the cure?* Diabetes, 2012. **61**(8): p. 1907-14.
29. Rojas, M., et al., *Molecular mimicry and autoimmunity.* J Autoimmun, 2018. **95**: p. 100-123.
30. Cusick, M.F., J.E. Libbey, and R.S. Fujinami, *Molecular mimicry as a mechanism of autoimmune disease.* Clin Rev Allergy Immunol, 2012. **42**(1): p. 102-11.
31. Croxford, J.L., J.K. Olson, and S.D. Miller, *Epitope spreading and molecular mimicry as triggers of autoimmunity in the Theiler's virus-induced demyelinating disease model of multiple sclerosis.* Autoimmun Rev, 2002. **1**(5): p. 251-60.
32. Gong, T., et al., *DAMP-sensing receptors in sterile inflammation and inflammatory diseases.* Nat Rev Immunol, 2020. **20**(2): p. 95-112.
33. Patel, S., *Danger-Associated Molecular Patterns (DAMPs): the Derivatives and Triggers of Inflammation.* Curr Allergy Asthma Rep, 2018. **18**(11): p. 63.
34. Rajaee, A., R. Barnett, and W.G. Cheadle, *Pathogen- and Danger-Associated Molecular Patterns and the Cytokine Response in Sepsis.* Surg Infect (Larchmt), 2018. **19**(2): p. 107-116.
35. Eichinger, S., et al., *Natural antibodies to oxidation-specific epitopes: innate immune response and venous thromboembolic disease.* J Thromb Haemost, 2018. **16**(1): p. 31-35.
36. Sollid, L.M. and B. Jabri, *Triggers and drivers of autoimmunity: lessons from coeliac disease.* Nat Rev Immunol, 2013. **13**(4): p. 294-302.
37. Luban, S. and Z.G. Li, *Citrullinated peptide and its relevance to rheumatoid arthritis: an update.* Int J Rheum Dis, 2010. **13**(4): p. 284-7.
38. Myers, L.K., et al., *Relevance of posttranslational modifications for the arthritogenicity of type II collagen.* J Immunol, 2004. **172**(5): p. 2970-5.
39. Liu, C.L., et al., *Specific post-translational histone modifications of neutrophil extracellular traps as immunogens and potential targets of lupus autoantibodies.* Arthritis Res Ther, 2012. **14**(1): p. R25.
40. Hayem, G., et al., *Anti-oxidized low-density-lipoprotein (OxLDL) antibodies in systemic lupus erythematosus with and without antiphospholipid syndrome.* Lupus, 2001. **10**(5): p. 346-51.

41. Yang, M.L., et al., *Oxidative Modifications in Tissue Pathology and Autoimmune Disease.* Antioxid Redox Signal, 2018. **29**(14): p. 1415-1431.
42. Lammi, A., et al., *Antibodies to deamidated gliadin peptide in diagnosis of celiac disease in children.* J Pediatr Gastroenterol Nutr, 2015. **60**(5): p. 626-31.
43. Usher-Smith, J.A., et al., *The pathway to diagnosis of type 1 diabetes in children: a questionnaire study.* BMJ Open, 2015. **5**(3): p. e006470.
44. Ziegler, A.G., et al., *Seroconversion to multiple islet autoantibodies and risk of progression to diabetes in children.* JAMA, 2013. **309**(23): p. 2473-9.
45. Sen, P., et al., *Metabolic alterations in immune cells associate with progression to type 1 diabetes.* Diabetologia, 2020. **63**(5): p. 1017-1031.
46. Han, S., et al., *Novel autoantigens in type 1 diabetes.* Am J Transl Res, 2013. **5**(4): p. 379-92.
47. Endesfelder, D., et al., *A novel approach for the analysis of longitudinal profiles reveals delayed progression to type 1 diabetes in a subgroup of multiple-islet-autoantibody-positive children.* Diabetologia, 2016. **59**(10): p. 2172-80.
48. Nieto, J., et al., *Islet autoantibody types mark differential clinical characteristics at diagnosis of pediatric type 1 diabetes.* Pediatr Diabetes, 2021. **22**(6): p. 882-888.
49. Insel, R.A., et al., *Staging presymptomatic type 1 diabetes: a scientific statement of JDRF, the Endocrine Society, and the American Diabetes Association.* Diabetes Care, 2015. **38**(10): p. 1964-74.
50. Mannering, S.I. and P. Bhattacharjee, *Insulin's other life: an autoantigen in type 1 diabetes.* Immunol Cell Biol, 2021. **99**(5): p. 448-460.
51. Rorsman, P. and F.M. Ashcroft, *Pancreatic beta-Cell Electrical Activity and Insulin Secretion: Of Mice and Men.* Physiol Rev, 2018. **98**(1): p. 117-214.
52. Fu, Z., E.R. Gilbert, and D. Liu, *Regulation of insulin synthesis and secretion and pancreatic Beta-cell dysfunction in diabetes.* Curr Diabetes Rev, 2013. **9**(1): p. 25-53.
53. Baeshen, N.A., et al., *Cell factories for insulin production.* Microb Cell Fact, 2014. **13**: p. 141.
54. Germanos, M., et al., *Inside the Insulin Secretory Granule.* Metabolites, 2021. **11**(8).
55. Meda, P. and F. Schuit, *Glucose-stimulated insulin secretion: the hierarchy of its multiple cellular and subcellular mechanisms.* Diabetologia, 2013. **56**(12): p. 2552-5.
56. Campbell, J.E. and C.B. Newgard, *Mechanisms controlling pancreatic islet cell function in insulin secretion.* Nat Rev Mol Cell Biol, 2021. **22**(2): p. 142-158.
57. Henquin, J.C., *Triggering and amplifying pathways of regulation of insulin secretion by glucose.* Diabetes, 2000. **49**(11): p. 1751-60.
58. Ziegler, A.G., et al., *100 Years of Insulin: Lifesaver, immune target, and potential remedy for prevention.* Med (N Y), 2021. **2**(10): p. 1120-1137.
59. Palmer, J.P., et al., *Insulin antibodies in insulin-dependent diabetics before insulin treatment.* Science, 1983. **222**(4630): p. 1337-9.
60. Harrison, L.C., *The dark side of insulin: A primary autoantigen and instrument of self-destruction in type 1 diabetes.* Mol Metab, 2021. **52**: p. 101288.

61. Abiru, N., et al., *Peptide and major histocompatibility complex-specific breaking of humoral tolerance to native insulin with the B9-23 peptide in diabetes-prone and normal mice.* Diabetes, 2001. **50**(6): p. 1274-81.
62. Nakayama, M., et al., *Prime role for an insulin epitope in the development of type 1 diabetes in NOD mice.* Nature, 2005. **435**(7039): p. 220-3.
63. Zhang, L., M. Nakayama, and G.S. Eisenbarth, *Insulin as an autoantigen in NOD/human diabetes.* Curr Opin Immunol, 2008. **20**(1): p. 111-8.
64. Ziegler, A.G., et al., *On the appearance of islet associated autoimmunity in offspring of diabetic mothers: a prospective study from birth.* Diabetologia, 1993. **36**(5): p. 402-8.
65. Achenbach, P., et al., *Mature high-affinity immune responses to (pro)insulin anticipate the autoimmune cascade that leads to type 1 diabetes.* J Clin Invest, 2004. **114**(4): p. 589-97.
66. Langendorf, C.G., et al., *Structural characterization of the mechanism through which human glutamic acid decarboxylase auto-activates.* Biosci Rep, 2013. **33**(1): p. 137-44.
67. Kakizaki, T., et al., *Rats deficient in the GAD65 isoform exhibit epilepsy and premature lethality.* FASEB J, 2021. **35**(2): p. e21224.
68. Valdarnini, N., et al., *Fine Mapping of Glutamate Decarboxylase 65 Epitopes Reveals Dependency on Hydrophobic Amino Acids for Specific Interactions.* Int J Mol Sci, 2019. **20**(12).
69. Fenalti, G. and A.M. Buckle, *Structural biology of the GAD autoantigen.* Autoimmun Rev, 2010. **9**(3): p. 148-52.
70. Baekkeskov, S., et al., *Autoantibodies in newly diagnosed diabetic children immunoprecipitate human pancreatic islet cell proteins.* Nature, 1982. **298**(5870): p. 167-9.
71. Arvan, P., et al., *Islet autoantigens: structure, function, localization, and regulation.* Cold Spring Harb Perspect Med, 2012. **2**(8).
72. Towns, R. and M. Pietropaolo, *GAD65 autoantibodies and its role as biomarker of Type 1 diabetes and Latent Autoimmune Diabetes in Adults (LADA).* Drugs Future, 2011. **36**(11): p. 847.
73. Solimena, M., *Vesicular autoantigens of type 1 diabetes.* Diabetes Metab Rev, 1998. **14**(3): p. 227-40.
74. Jayakrishnan, B., et al., *An analysis of the cross-reactivity of autoantibodies to GAD65 and GAD67 in diabetes.* PLoS One, 2011. **6**(4): p. e18411.
75. Schlosser, M., et al., *Dynamic changes of GAD65 autoantibody epitope specificities in individuals at risk of developing type 1 diabetes.* Diabetologia, 2005. **48**(5): p. 922-30.
76. Kobayashi, T., et al., *Unique epitopes of glutamic acid decarboxylase autoantibodies in slowly progressive type 1 diabetes.* J Clin Endocrinol Metab, 2003. **88**(10): p. 4768-75.
77. Peng, Y., et al., *GAD65 Antibody Epitopes and Genetic Background in Latent Autoimmune Diabetes in Youth (LADY).* Front Immunol, 2022. **13**: p. 836952.
78. Pollanen, P.M., et al., *Autoantibodies to N-terminally Truncated GAD65(96-585): HLA Associations and Predictive Value for Type 1 Diabetes.* J Clin Endocrinol Metab, 2022. **107**(3): p. e935-e946.
79. Bender, C., et al., *GAD autoantibody affinity in schoolchildren from the general population.* Diabetologia, 2014. **57**(9): p. 1911-8.

80. Wenzlau, J.M., et al., *The cation efflux transporter ZnT8 (Slc30A8) is a major autoantigen in human type 1 diabetes.* Proc Natl Acad Sci U S A, 2007. **104**(43): p. 17040-5.
81. Wenzlau, J.M., et al., *Novel antigens in type 1 diabetes: the importance of ZnT8.* Curr Diab Rep, 2009. **9**(2): p. 105-12.
82. Williams, C.L. and A.E. Long, *What has zinc transporter 8 autoimmunity taught us about type 1 diabetes?* Diabetologia, 2019. **62**(11): p. 1969-1976.
83. Davidson, H.W., J.M. Wenzlau, and R.M. O'Brien, *Zinc transporter 8 (ZnT8) and beta cell function.* Trends Endocrinol Metab, 2014. **25**(8): p. 415-24.
84. Wenzlau, J.M., et al., *A common nonsynonymous single nucleotide polymorphism in the SLC30A8 gene determines ZnT8 autoantibody specificity in type 1 diabetes.* Diabetes, 2008. **57**(10): p. 2693-7.
85. Daniels, M.J., M. Jagielnicki, and M. Yeager, *Structure/Function Analysis of human ZnT8 (SLC30A8): A Diabetes Risk Factor and Zinc Transporter.* Curr Res Struct Biol, 2020. **2**: p. 144-155.
86. Wijesekara, N., et al., *Beta cell-specific Znt8 deletion in mice causes marked defects in insulin processing, crystallisation and secretion.* Diabetologia, 2010. **53**(8): p. 1656-68.
87. Skarstrand, H., et al., *Zinc transporter 8 (ZnT8) autoantibody epitope specificity and affinity examined with recombinant ZnT8 variant proteins in specific ZnT8R and ZnT8W autoantibody-positive type 1 diabetes patients.* Clin Exp Immunol, 2015. **179**(2): p. 220-9.
88. Niechcial, E., et al., *Autoantibodies against zinc transporter 8 are related to age and metabolic state in patients with newly diagnosed autoimmune diabetes.* Acta Diabetol, 2018. **55**(3): p. 287-294.
89. Salonen, K.M., et al., *Autoantibodies against zinc transporter 8 are related to age, metabolic state and HLA DR genotype in children with newly diagnosed type 1 diabetes.* Diabetes Metab Res Rev, 2013. **29**(8): p. 646-54.
90. Kawasaki, E., et al., *Association between anti-ZnT8 autoantibody specificities and SLC30A8 Arg325Trp variant in Japanese patients with type 1 diabetes.* Diabetologia, 2008. **51**(12): p. 2299-302.
91. Yang, L., et al., *The diagnostic value of zinc transporter 8 autoantibody (ZnT8A) for type 1 diabetes in Chinese.* Diabetes Metab Res Rev, 2010. **26**(7): p. 579-84.
92. Lounici Boudiaf, A., et al., *Could ZnT8 antibodies replace ICA, GAD, IA2 and insulin antibodies in the diagnosis of type 1 diabetes?* Curr Res Transl Med, 2018. **66**(1): p. 1-7.
93. Powers, A.C., *Type 1 diabetes mellitus: much progress, many opportunities.* J Clin Invest, 2021. **131**(8).
94. Regnell, S.E. and A. Lernmark, *Early prediction of autoimmune (type 1) diabetes.* Diabetologia, 2017. **60**(8): p. 1370-1381.
95. Sticht, J., M. Alvaro-Benito, and S. Konigorski, *Type 1 Diabetes and the HLA Region: Genetic Association Besides Classical HLA Class II Genes.* Front Genet, 2021. **12**: p. 683946.
96. Ilonen, J., J. Lempainen, and R. Veijola, *The heterogeneous pathogenesis of type 1 diabetes mellitus.* Nat Rev Endocrinol, 2019. **15**(11): p. 635-650.
97. Crux, N.B. and S. Elahi, *Human Leukocyte Antigen (HLA) and Immune Regulation: How Do Classical and Non-Classical HLA Alleles Modulate*

Immune Response to Human Immunodeficiency Virus and Hepatitis C Virus Infections? Front Immunol, 2017. **8**: p. 832.
98. Wieczorek, M., et al., *Major Histocompatibility Complex (MHC) Class I and MHC Class II Proteins: Conformational Plasticity in Antigen Presentation.* Front Immunol, 2017. **8**: p. 292.
99. Undlien, D.E., B.A. Lie, and E. Thorsby, *HLA complex genes in type 1 diabetes and other autoimmune diseases. Which genes are involved?* Trends Genet, 2001. **17**(2): p. 93-100.
100. Muniz-Castrillo, S., A. Vogrig, and J. Honnorat, *Associations between HLA and autoimmune neurological diseases with autoantibodies.* Auto Immun Highlights, 2020. **11**(1): p. 2.
101. Del Pozzo, G., et al., *HLA class II genes in precision-based care of childhood diseases: what we can learn from celiac disease.* Pediatr Res, 2021. **89**(2): p. 307-312.
102. Noble, J.A., et al., *HLA class I and genetic susceptibility to type 1 diabetes: results from the Type 1 Diabetes Genetics Consortium.* Diabetes, 2010. **59**(11): p. 2972-9.
103. Stoy, J., et al., *In celebration of a century with insulin - Update of insulin gene mutations in diabetes.* Mol Metab, 2021. **52**: p. 101280.
104. Carry, P.M., et al., *DNA methylation near the INS gene is associated with INS genetic variation (rs689) and type 1 diabetes in the Diabetes Autoimmunity Study in the Young.* Pediatr Diabetes, 2020. **21**(4): p. 597-605.
105. Sharp, R.C., et al., *Genetic Variations of PTPN2 and PTPN22: Role in the Pathogenesis of Type 1 Diabetes and Crohn's Disease.* Front Cell Infect Microbiol, 2015. **5**: p. 95.
106. Marquez, A. and J. Martin, *Genetic overlap between type 1 diabetes and other autoimmune diseases.* Semin Immunopathol, 2022. **44**(1): p. 81-97.
107. Pohanka, M., *Glycated Hemoglobin and Methods for Its Point of Care Testing.* Biosensors (Basel), 2021. **11**(3).
108. Rabbani, N. and P.J. Thornalley, *Protein glycation - biomarkers of metabolic dysfunction and early-stage decline in health in the era of precision medicine.* Redox Biol, 2021. **42**: p. 101920.
109. Nash, A., et al., *Lysine-arginine advanced glycation end-product cross-links and the effect on collagen structure: A molecular dynamics study.* Proteins, 2021. **89**(5): p. 521-530.
110. Nerup, J., et al., *On the pathogenesis of IDDM.* Diabetologia, 1994. **37 Suppl 2**: p. S82-9.
111. Storling, J., et al., *Do post-translational beta cell protein modifications trigger type 1 diabetes?* Diabetologia, 2013. **56**(11): p. 2347-54.
112. Benakova, S., B. Holendova, and L. Plecita-Hlavata, *Redox Homeostasis in Pancreatic beta-Cells: From Development to Failure.* Antioxidants (Basel), 2021. **10**(4).
113. Hu, A., et al., *Posttranslational modifications in diabetes: Mechanisms and functions.* Rev Endocr Metab Disord, 2022. **23**(5): p. 1011-1033.
114. Strollo, R., et al., *Antibodies to post-translationally modified insulin in type 1 diabetes.* Diabetologia, 2015. **58**(12): p. 2851-60.
115. Mannering, S.I., et al., *The insulin A-chain epitope recognized by human T cells is posttranslationally modified.* J Exp Med, 2005. **202**(9): p. 1191-7.

116. van Lummel, M., et al., *Posttranslational modification of HLA-DQ binding islet autoantigens in type 1 diabetes.* Diabetes, 2014. **63**(1): p. 237-47.
117. McGinty, J.W., et al., *Recognition of posttranslationally modified GAD65 epitopes in subjects with type 1 diabetes.* Diabetes, 2014. **63**(9): p. 3033-40.
118. Donnelly, C. and A. Williams, *Investigating the potential impact of post translational modification of auto-antigens by tissue transglutaminase on humoral islet autoimmunity in type 1 diabetes.* Metabol Open, 2020. **8**: p. 100062.
119. Sidney, J., et al., *Low HLA binding of diabetes-associated CD8+ T-cell epitopes is increased by post translational modifications.* BMC Immunol, 2018. **19**(1): p. 12.
120. Buitinga, M., et al., *Inflammation-Induced Citrullinated Glucose-Regulated Protein 78 Elicits Immune Responses in Human Type 1 Diabetes.* Diabetes, 2018. **67**(11): p. 2337-2348.
121. Khan, M.W., et al., *Characterization of hydroxyl radical modified GAD65: a potential autoantigen in type 1 diabetes.* Autoimmunity, 2009. **42**(2): p. 150-8.
122. Moinuddin, et al., *Immuno-chemistry of hydroxyl radical modified GAD-65: A possible role in experimental and human diabetes mellitus.* IUBMB Life, 2015. **67**(10): p. 746-56.
123. Zhu, N., et al., *A Novel Coronavirus from Patients with Pneumonia in China, 2019.* N Engl J Med, 2020. **382**(8): p. 727-733.
124. Holmes, E.C., et al., *The origins of SARS-CoV-2: A critical review.* Cell, 2021. **184**(19): p. 4848-4856.
125. Hu, B., et al., *Characteristics of SARS-CoV-2 and COVID-19.* Nat Rev Microbiol, 2021. **19**(3): p. 141-154.
126. Parasher, A., *COVID-19: Current understanding of its Pathophysiology, Clinical presentation and Treatment.* Postgrad Med J, 2021. **97**(1147): p. 312-320.
127. Alimohamadi, Y., et al., *Determine the most common clinical symptoms in COVID-19 patients: a systematic review and meta-analysis.* J Prev Med Hyg, 2020. **61**(3): p. E304-E312.
128. Laino, M.E., et al., *Prognostic findings for ICU admission in patients with COVID-19 pneumonia: baseline and follow-up chest CT and the added value of artificial intelligence.* Emerg Radiol, 2022. **29**(2): p. 243-262.
129. Gao, Y.D., et al., *Risk factors for severe and critically ill COVID-19 patients: A review.* Allergy, 2021. **76**(2): p. 428-455.
130. Rossi, G.A., et al., *Differences and similarities between SARS-CoV and SARS-CoV-2: spike receptor-binding domain recognition and host cell infection with support of cellular serine proteases.* Infection, 2020. **48**(5): p. 665-669.
131. Yang, H. and Z. Rao, *Structural biology of SARS-CoV-2 and implications for therapeutic development.* Nat Rev Microbiol, 2021. **19**(11): p. 685-700.
132. Jamison, D.A., Jr., et al., *A comprehensive SARS-CoV-2 and COVID-19 review, Part 1: Intracellular overdrive for SARS-CoV-2 infection.* Eur J Hum Genet, 2022. **30**(8): p. 889-898.
133. Abdel-Moneim, A.S., E.M. Abdelwhab, and Z.A. Memish, *Insights into SARS-CoV-2 evolution, potential antivirals, and vaccines.* Virology, 2021. **558**: p. 1-12.

134. Gul, R., U.H. Kim, and A.A. Alfadda, *Renin-angiotensin system at the interface of COVID-19 infection.* Eur J Pharmacol, 2021. **890**: p. 173656.
135. Ni, W., et al., *Role of angiotensin-converting enzyme 2 (ACE2) in COVID-19.* Crit Care, 2020. **24**(1): p. 422.
136. Gheblawi, M., et al., *Response by Gheblawi et al to Letter Regarding Article, "Angiotensin-Converting Enzyme 2: SARS-CoV-2 Receptor and Regulator of the Renin-Angiotensin System: Celebrating the 20th Anniversary of the Discovery of ACE2".* Circ Res, 2020. **127**(2): p. e46-e47.
137. Scialo, F., et al., *ACE2: The Major Cell Entry Receptor for SARS-CoV-2.* Lung, 2020. **198**(6): p. 867-877.
138. Zhao, X.H., H. Chen, and H.L. Wang, *Glycans of SARS-CoV-2 Spike Protein in Virus Infection and Antibody Production.* Frontiers in Molecular Biosciences, 2021. **8**.
139. Huang, Y., et al., *Structural and functional properties of SARS-CoV-2 spike protein: potential antivirus drug development for COVID-19.* Acta Pharmacol Sin, 2020. **41**(9): p. 1141-1149.
140. Triggle, C.R., et al., *A Comprehensive Review of Viral Characteristics, Transmission, Pathophysiology, Immune Response, and Management of SARS-CoV-2 and COVID-19 as a Basis for Controlling the Pandemic.* Front Immunol, 2021. **12**: p. 631139.
141. Samavati, L. and B.D. Uhal, *ACE2, Much More Than Just a Receptor for SARS-COV-2.* Front Cell Infect Microbiol, 2020. **10**: p. 317.
142. Lan, J., et al., *Structure of the SARS-CoV-2 spike receptor-binding domain bound to the ACE2 receptor.* Nature, 2020. **581**(7807): p. 215-220.
143. Diamond, M.S. and T.D. Kanneganti, *Innate immunity: the first line of defense against SARS-CoV-2.* Nat Immunol, 2022. **23**(2): p. 165-176.
144. Kanneganti, T.D., *Intracellular innate immune receptors: Life inside the cell.* Immunol Rev, 2020. **297**(1): p. 5-12.
145. Ullah, M.O., et al., *TRIF-dependent TLR signaling, its functions in host defense and inflammation, and its potential as a therapeutic target.* J Leukoc Biol, 2016. **100**(1): p. 27-45.
146. Deguine, J. and G.M. Barton, *MyD88: a central player in innate immune signaling.* F1000Prime Rep, 2014. **6**: p. 97.
147. Sariol, A. and S. Perlman, *SARS-CoV-2 takes its Toll.* Nat Immunol, 2021. **22**(7): p. 801-802.
148. Zhao, J., et al., *Intranasal treatment with poly(I*C) protects aged mice from lethal respiratory virus infections.* J Virol, 2012. **86**(21): p. 11416-24.
149. Zheng, M., et al., *TLR2 senses the SARS-CoV-2 envelope protein to produce inflammatory cytokines.* Nat Immunol, 2021. **22**(7): p. 829-838.
150. Totura, A.L., et al., *Toll-Like Receptor 3 Signaling via TRIF Contributes to a Protective Innate Immune Response to Severe Acute Respiratory Syndrome Coronavirus Infection.* mBio, 2015. **6**(3): p. e00638-15.
151. Manik, M. and R.K. Singh, *Role of toll-like receptors in modulation of cytokine storm signaling in SARS-CoV-2-induced COVID-19.* J Med Virol, 2022. **94**(3): p. 869-877.
152. Sette, A. and S. Crotty, *Adaptive immunity to SARS-CoV-2 and COVID-19.* Cell, 2021. **184**(4): p. 861-880.

153. Landstra, C.P. and E.J.P. de Koning, *COVID-19 and Diabetes: Understanding the Interrelationship and Risks for a Severe Course.* Front Endocrinol (Lausanne), 2021. **12**: p. 649525.
154. Wu, Z. and J.M. McGoogan, *Characteristics of and Important Lessons From the Coronavirus Disease 2019 (COVID-19) Outbreak in China: Summary of a Report of 72 314 Cases From the Chinese Center for Disease Control and Prevention.* JAMA, 2020. **323**(13): p. 1239-1242.
155. Kastora, S., et al., *Impact of diabetes on COVID-19 mortality and hospital outcomes from a global perspective: An umbrella systematic review and meta-analysis.* Endocrinol Diabetes Metab, 2022. **5**(3): p. e00338.
156. Kazakou, P., et al., *Diabetes and COVID-19; A Bidirectional Interplay.* Front Endocrinol (Lausanne), 2022. **13**: p. 780663.
157. Abu-Farha, M., S. Hofmann, and H. Ali, *Editorial: Covid-19 and Diabetes.* Front Endocrinol (Lausanne), 2022. **13**: p. 933562.
158. Fleming, N., et al., *An overview of COVID-19 in people with diabetes: Pathophysiology and considerations in the inpatient setting.* Diabet Med, 2021. **38**(3): p. e14509.
159. Codo, A.C., et al., *Elevated Glucose Levels Favor SARS-CoV-2 Infection and Monocyte Response through a HIF-1alpha/Glycolysis-Dependent Axis.* Cell Metab, 2020. **32**(3): p. 498-499.
160. Kulcsar, K.A., et al., *Comorbid diabetes results in immune dysregulation and enhanced disease severity following MERS-CoV infection.* JCI Insight, 2019. **4**(20).
161. Yazdanpanah, S., et al., *Evaluation of glycated albumin (GA) and GA/HbA1c ratio for diagnosis of diabetes and glycemic control: A comprehensive review.* Crit Rev Clin Lab Sci, 2017. **54**(4): p. 219-232.
162. Singh, R., et al., *Advanced glycation end-products: a review.* Diabetologia, 2001. **44**(2): p. 129-46.
163. Harvey, W.T., et al., *SARS-CoV-2 variants, spike mutations and immune escape.* Nat Rev Microbiol, 2021. **19**(7): p. 409-424.
164. Thomson, E.C., et al., *Circulating SARS-CoV-2 spike N439K variants maintain fitness while evading antibody-mediated immunity.* Cell, 2021. **184**(5): p. 1171-1187 e20.
165. Sartore, G., et al., *A role of glycation and methylation for SARS-CoV-2 infection in diabetes?* Med Hypotheses, 2020. **144**: p. 110247.
166. Bansode, S., et al., *Glycation changes molecular organization and charge distribution in type I collagen fibrils.* Sci Rep, 2020. **10**(1): p. 3397.
167. Rabbani, N. and P.J. Thornalley, *Glycation research in amino acids: a place to call home.* Amino Acids, 2012. **42**(4): p. 1087-96.
168. Dozio, E., L. Massaccesi, and M.M. Corsi Romanelli, *Glycation and Glycosylation in Cardiovascular Remodeling: Focus on Advanced Glycation End Products and O-Linked Glycosylations as Glucose-Related Pathogenetic Factors and Disease Markers.* J Clin Med, 2021. **10**(20).
169. Alahmad, B., et al., *Fasting Blood Glucose and COVID-19 Severity: Nonlinearity Matters.* Diabetes Care, 2020. **43**(12): p. 3113-3116.
170. Yang, J.K., et al., *Plasma glucose levels and diabetes are independent predictors for mortality and morbidity in patients with SARS.* Diabet Med, 2006. **23**(6): p. 623-8.

171. Lim, S., et al., *COVID-19 and diabetes mellitus: from pathophysiology to clinical management.* Nat Rev Endocrinol, 2021. **17**(1): p. 11-30.
172. Unsworth, R., et al., *New-Onset Type 1 Diabetes in Children During COVID-19: Multicenter Regional Findings in the U.K.* Diabetes Care, 2020. **43**(11): p. e170-e171.
173. Salmi, H., et al., *New-onset type 1 diabetes in Finnish children during the COVID-19 pandemic.* Arch Dis Child, 2022. **107**(2): p. 180-185.
174. Zhang, T., et al., *Risk for newly diagnosed diabetes after COVID-19: a systematic review and meta-analysis.* BMC Med, 2022. **20**(1): p. 444.
175. Babajide, O.I., et al., *COVID-19 and acute pancreatitis: A systematic review.* JGH Open, 2022. **6**(4): p. 231-235.
176. Filippi, C.M. and M.G. von Herrath, *Viral trigger for type 1 diabetes: pros and cons.* Diabetes, 2008. **57**(11): p. 2863-71.
177. Coppieters, K.T., T. Boettler, and M. von Herrath, *Virus infections in type 1 diabetes.* Cold Spring Harb Perspect Med, 2012. **2**(1): p. a007682.
178. Mistry, P., et al., *SARS-CoV-2 Variants, Vaccines, and Host Immunity.* Front Immunol, 2021. **12**: p. 809244.
179. Hirabara, S.M., et al., *SARS-COV-2 Variants: Differences and Potential of Immune Evasion.* Front Cell Infect Microbiol, 2021. **11**: p. 781429.
180. Li, M., et al., *COVID-19 vaccine development: milestones, lessons and prospects.* Signal Transduct Target Ther, 2022. **7**(1): p. 146.
181. Khateeb, J., Y. Li, and H. Zhang, *Emerging SARS-CoV-2 variants of concern and potential intervention approaches.* Crit Care, 2021. **25**(1): p. 244.
182. Zhou, B., et al., *SARS-CoV-2 spike D614G change enhances replication and transmission.* Nature, 2021. **592**(7852): p. 122-127.
183. Garcia-Beltran, W.F., et al., *Multiple SARS-CoV-2 variants escape neutralization by vaccine-induced humoral immunity.* Cell, 2021. **184**(9): p. 2523.
184. Muik, A., et al., *Neutralization of SARS-CoV-2 lineage B.1.1.7 pseudovirus by BNT162b2 vaccine-elicited human sera.* Science, 2021. **371**(6534): p. 1152-1153.
185. Focosi, D. and F. Maggi, *Neutralising antibody escape of SARS-CoV-2 spike protein: Risk assessment for antibody-based Covid-19 therapeutics and vaccines.* Rev Med Virol, 2021. **31**(6): p. e2231.
186. Callaway, E. and S. Mallapaty, *Novavax offers first evidence that COVID vaccines protect people against variants.* Nature, 2021. **590**(7844): p. 17.
187. Abu-Raddad, L.J., et al., *Effectiveness of the BNT162b2 Covid-19 Vaccine against the B.1.1.7 and B.1.351 Variants.* N Engl J Med, 2021. **385**(2): p. 187-189.
188. Schneider, C.A., W.S. Rasband, and K.W. Eliceiri, *NIH Image to ImageJ: 25 years of image analysis.* Nat Methods, 2012. **9**(7): p. 671-5.
189. Walker, S.N., et al., *SARS-CoV-2 Assays To Detect Functional Antibody Responses That Block ACE2 Recognition in Vaccinated Animals and Infected Patients.* J Clin Microbiol, 2020. **58**(11).
190. Amanat, F., et al., *A serological assay to detect SARS-CoV-2 seroconversion in humans.* Nat Med, 2020. **26**(7): p. 1033-1036.
191. Capuano, R., et al., *Six-month humoral response to mRNA SARS-CoV-2 vaccination in patients with multiple sclerosis treated with ocrelizumab and fingolimod.* Mult Scler Relat Disord, 2022. **60**: p. 103724.

192. Sholukh, A.M., et al., *Evaluation of Cell-Based and Surrogate SARS-CoV-2 Neutralization Assays.* J Clin Microbiol, 2021. **59**(10): p. e0052721.
193. Strollo, R., et al., *Autoantibody and T cell responses to oxidative post-translationally modified insulin neoantigenic peptides in type 1 diabetes.* Diabetologia, 2023. **66**(1): p. 132-146.
194. Alshukry, A., et al., *Clinical characteristics of coronavirus disease 2019 (COVID-19) patients in Kuwait.* PLoS One, 2020. **15**(11): p. e0242768.
195. Alshukry, A., et al., *Clinical characteristics and outcomes of COVID-19 patients with diabetes mellitus in Kuwait.* Heliyon, 2021. **7**(4): p. e06706.
196. Mandrekar, J.N., *Receiver operating characteristic curve in diagnostic test assessment.* J Thorac Oncol, 2010. **5**(9): p. 1315-6.
197. Maddaloni, E., et al., *Clinical features of patients with type 2 diabetes with and without Covid-19: A case control study (CoViDiab I).* Diabetes Res Clin Pract, 2020. **169**: p. 108454.
198. Green, A., et al., *Type 1 diabetes in 2017: global estimates of incident and prevalent cases in children and adults.* Diabetologia, 2021. **64**(12): p. 2741-2750.
199. Vehik, K., et al., *Hierarchical Order of Distinct Autoantibody Spreading and Progression to Type 1 Diabetes in the TEDDY Study.* Diabetes Care, 2020. **43**(9): p. 2066-2073.
200. Morandi, A., et al., *Oxidative stress in youth with type 1 diabetes: Not only a matter of gender, age, and glycemic control.* Diabetes Res Clin Pract, 2021. **179**: p. 109007.
201. Leenders, F., et al., *Oxidative Stress Leads to beta-Cell Dysfunction Through Loss of beta-Cell Identity.* Front Immunol, 2021. **12**: p. 690379.
202. Hester A. Doyle, M.J.M., *Autoantigenesis: The evolution of protein modifications in autoimmune disease.* Current Opinion in Immunology, 2012. **24**(1): p. 112-118.
203. Ludvigsson, J., et al., *Increasing plasma glucose before the development of type 1 diabetes-the TRIGR study.* Pediatr Diabetes, 2021. **22**(7): p. 974-981.
204. Ludvigsson, J., *Why diabetes incidence increases--a unifying theory.* Ann N Y Acad Sci, 2006. **1079**: p. 374-82.
205. Marra, G., et al., *Early increase of oxidative stress and reduced antioxidant defenses in patients with uncomplicated type 1 diabetes: a case for gender difference.* Diabetes Care, 2002. **25**(2): p. 370-5.
206. Matteucci, E. and O. Giampietro, *Oxidative stress in families of type 1 diabetic patients.* Diabetes Care, 2000. **23**(8): p. 1182-6.
207. Liu, C.W., et al., *Temporal expression profiling of plasma proteins reveals oxidative stress in early stages of Type 1 Diabetes progression.* J Proteomics, 2018. **172**: p. 100-110.
208. Lenzen, S., *The mechanisms of alloxan- and streptozotocin-induced diabetes.* Diabetologia, 2008. **51**(2): p. 216-26.
209. Queiroz, L.A.D., et al., *Endangered Lymphocytes: The Effects of Alloxan and Streptozotocin on Immune Cells in Type 1 Induced Diabetes.* Mediators Inflamm, 2021. **2021**: p. 9940009.
210. Capitani, G., et al., *The critical structural role of a highly conserved histidine residue in group II amino acid decarboxylases.* FEBS Lett, 2003. **554**(1-2): p. 41-4.

211. Fenalti, G., et al., *GABA production by glutamic acid decarboxylase is regulated by a dynamic catalytic loop.* Nat Struct Mol Biol, 2007. **14**(4): p. 280-6.
212. Fournet, M., F. Bonte, and A. Desmouliere, *Glycation Damage: A Possible Hub for Major Pathophysiological Disorders and Aging.* Aging Dis, 2018. **9**(5): p. 880-900.
213. Yu, L., Z. Zhao, and A.K. Steck, *T1D Autoantibodies: room for improvement?* Curr Opin Endocrinol Diabetes Obes, 2017. **24**(4): p. 285-291.
214. Grace, S.L., et al., *Islet Autoantibody Level Distribution in Type 1 Diabetes and Their Association With Genetic and Clinical Characteristics.* J Clin Endocrinol Metab, 2022. **107**(12): p. e4341-e4349.
215. Xue, J., et al., *Cryo-EM structures of human ZnT8 in both outward- and inward-facing conformations.* Elife, 2020. **9**.
216. Zurlo, G., et al., *New Insights into Protein Hydroxylation and Its Important Role in Human Diseases.* Biochim Biophys Acta, 2016. **1866**(2): p. 208-220.
217. Hawkins, C.L., D.I. Pattison, and M.J. Davies, *Hypochlorite-induced oxidation of amino acids, peptides and proteins.* Amino Acids, 2003. **25**(3-4): p. 259-74.
218. Wenzlau, J.M., et al., *Mapping of conformational autoantibody epitopes in ZNT8.* Diabetes Metab Res Rev, 2011. **27**(8): p. 883-6.
219. Yi, B., G. Huang, and Z. Zhou, *Different role of zinc transporter 8 between type 1 diabetes mellitus and type 2 diabetes mellitus.* J Diabetes Investig, 2016. **7**(4): p. 459-65.
220. Kurien, B.T., et al., *Oxidatively modified autoantigens in autoimmune diseases.* Free Radic Biol Med, 2006. **41**(4): p. 549-56.
221. Kurien, B.T. and R.H. Scofield, *Autoimmunity and oxidatively modified autoantigens.* Autoimmun Rev, 2008. **7**(7): p. 567-73.
222. Rosa, J.S., et al., *Altered inflammatory, oxidative, and metabolic responses to exercise in pediatric obesity and type 1 diabetes.* Pediatr Diabetes, 2011. **12**(5): p. 464-72.
223. Thaper, D. and V. Prabha, *Molecular mimicry: An explanation for autoimmune diseases and infertility.* Scand J Immunol, 2018: p. e12697.
224. Anand, V., et al., *Islet Autoimmunity and HLA Markers of Presymptomatic and Clinical Type 1 Diabetes: Joint Analyses of Prospective Cohort Studies in Finland, Germany, Sweden, and the U.S.* Diabetes Care, 2021. **44**(10): p. 2269-76.
225. Noble, J.A. and A.M. Valdes, *Genetics of the HLA region in the prediction of type 1 diabetes.* Curr Diab Rep, 2011. **11**(6): p. 533-42.
226. Erlich, H., et al., *HLA DR-DQ haplotypes and genotypes and type 1 diabetes risk: analysis of the type 1 diabetes genetics consortium families.* Diabetes, 2008. **57**(4): p. 1084-92.
227. Howson, J.M., et al., *Evidence that HLA class I and II associations with type 1 diabetes, autoantibodies to GAD and autoantibodies to IA-2, are distinct.* Diabetes, 2011. **60**(10): p. 2635-44.
228. Triolo, T.M., et al., *Association of High-Affinity Autoantibodies With Type 1 Diabetes High-Risk HLA Haplotypes.* J Clin Endocrinol Metab, 2022. **107**(4): p. e1510-e1517.
229. Mikk, M.L., et al., *HLA-DR-DQ haplotypes and specificity of the initial autoantibody in islet specific autoimmunity.* Pediatr Diabetes, 2020. **21**(7): p. 1218-1226.

230. Haider, M.Z., et al., *Association of protein tyrosine phosphatase non-receptor type 22 gene functional variant C1858T, HLA-DQ/DR genotypes and autoantibodies with susceptibility to type-1 diabetes mellitus in Kuwaiti Arabs.* PLoS One, 2018. **13**(6): p. e0198652.
231. Ren, W., et al., *Adult-onset type 1 diabetic patients with less severe clinical manifestation have less risk DR-DQ genotypes than childhood-onset patients.* Diabetes Metab Res Rev, 2021. **37**(1): p. e3357.
232. Jacobsen, L.M., et al., *The risk of progression to type 1 diabetes is highly variable in individuals with multiple autoantibodies following screening.* Diabetologia, 2020. **63**(3): p. 588-596.
233. Achenbach, P., et al., *Autoantibodies to zinc transporter 8 and SLC30A8 genotype stratify type 1 diabetes risk.* Diabetologia, 2009. **52**(9): p. 1881-8.
234. Vaziri-Sani, F., et al., *ZnT8 autoantibody titers in type 1 diabetes patients decline rapidly after clinical onset.* Autoimmunity, 2010. **43**(8): p. 598-606.
235. Pal, R., et al., *Impaired anti-SARS-CoV-2 antibody response in non-severe COVID-19 patients with diabetes mellitus: A preliminary report.* Diabetes Metab Syndr, 2021. **15**(1): p. 193-196.
236. Zhao, R., et al., *Distinguishable Immunologic Characteristics of COVID-19 Patients with Comorbid Type 2 Diabetes Compared with Nondiabetic Individuals.* Mediators Inflamm, 2020. **2020**: p. 6914878.
237. Barron, E., et al., *Associations of type 1 and type 2 diabetes with COVID-19-related mortality in England: a whole-population study.* Lancet Diabetes Endocrinol, 2020. **8**(10): p. 813-822.
238. Mirabella, S., et al., *Glucose dysregulation and its association with COVID-19 mortality and hospital length of stay.* Diabetes Metab Syndr, 2022. **16**(3): p. 102439.
239. Bolla, A.M., et al., *Inflammation and vascular dysfunction: The negative synergistic combination of diabetes and COVID-19.* Diabetes Metab Res Rev, 2022. **38**(7): p. e3565.
240. Gong, Y., et al., *The glycosylation in SARS-CoV-2 and its receptor ACE2.* Signal Transduct Target Ther, 2021. **6**(1): p. 396.
241. Poulsen, M.W., et al., *Advanced glycation endproducts in food and their effects on health.* Food Chem Toxicol, 2013. **60**: p. 10-37.
242. Chavez-Reyes, J., et al., *Susceptibility for Some Infectious Diseases in Patients With Diabetes: The Key Role of Glycemia.* Front Public Health, 2021. **9**: p. 559595.
243. Metwally, A.A., et al., *COVID-19-Induced New-Onset Diabetes: Trends and Technologies.* Diabetes, 2021. **70**(12): p. 2733-2744.
244. Sartore, G., et al., *In silico evaluation of the interaction between ACE2 and SARS-CoV-2 Spike protein in a hyperglycemic environment.* Sci Rep, 2021. **11**(1): p. 22860.
245. Masre, S.F., et al., *Classical and alternative receptors for SARS-CoV-2 therapeutic strategy.* Rev Med Virol, 2021. **31**(5): p. 1-9.
246. D'Onofrio, N., et al., *Glycated ACE2 receptor in diabetes: open door for SARS-COV-2 entry in cardiomyocyte.* Cardiovasc Diabetol, 2021. **20**(1): p. 99.
247. Allard, R., et al., *Diabetes and the severity of pandemic influenza A (H1N1) infection.* Diabetes Care, 2010. **33**(7): p. 1491-3.

248. Goeijenbier, M., et al., *Benefits of flu vaccination for persons with diabetes mellitus: A review.* Vaccine, 2017. **35**(38): p. 5095-5101.
249. Creech, C.B., S.C. Walker, and R.J. Samuels, *SARS-CoV-2 Vaccines.* JAMA, 2021. **325**(13): p. 1318-1320.
250. Abu-Raddad, L.J., et al., *Pfizer-BioNTech mRNA BNT162b2 Covid-19 vaccine protection against variants of concern after one versus two doses.* J Travel Med, 2021. **28**(7).
251. Accorsi, E.K., et al., *Association Between 3 Doses of mRNA COVID-19 Vaccine and Symptomatic Infection Caused by the SARS-CoV-2 Omicron and Delta Variants.* JAMA, 2022. **327**(7): p. 639-651.
252. Papadokostaki, E., et al., *Immunogenicity of SARS-CoV-2 BNT162b2 Vaccine in People with Diabetes: A Prospective Observational Study.* Vaccines (Basel), 2022. **10**(3).
253. Sherwani, S.I., et al., *Significance of HbA1c Test in Diagnosis and Prognosis of Diabetic Patients.* Biomark Insights, 2016. **11**: p. 95-104.
254. Fellinger, P., et al., *HbA1c and Glucose Management Indicator Discordance Associated with Obesity and Type 2 Diabetes in Intermittent Scanning Glucose Monitoring System.* Biosensors (Basel), 2022. **12**(5).
255. Sourij, C., et al., *Humoral immune response to COVID-19 vaccination in diabetes is age-dependent but independent of type of diabetes and glycaemic control: The prospective COVAC-DM cohort study.* Diabetes Obes Metab, 2022. **24**(5): p. 849-858.
256. Marfella, R., et al., *Glycaemic control is associated with SARS-CoV-2 breakthrough infections in vaccinated patients with type 2 diabetes.* Nat Commun, 2022. **13**(1): p. 2318.
257. Gouda, N., et al., *The impact of COVID-19 vaccination on glycaemic control in children and adolescents with type 1 diabetes mellitus on continuous glucose monitoring.* Acta Diabetol, 2022. **59**(12): p. 1609-1614.
258. Heald, A.H., et al., *Analysis of Continuous Blood Glucose Data in People with Type 1 Diabetes (T1DM) After COVID-19 Vaccination Indicates a Possible Link Between the Immune and the Metabolic Response.* J Diabetes Sci Technol, 2021. **15**(5): p. 1204-1205.
259. D'Onofrio, L., et al., *Short-term safety profile of Sars-Cov2 vaccination on glucose control: Continuous glucose monitoring data in people with autoimmune diabetes.* Diabetes Res Clin Pract, 2021. **179**: p. 109022.
260. Jafar, N., H. Edriss, and K. Nugent, *The Effect of Short-Term Hyperglycemia on the Innate Immune System.* Am J Med Sci, 2016. **351**(2): p. 201-11.
261. Berbudi, A., et al., *Type 2 Diabetes and its Impact on the Immune System.* Curr Diabetes Rev, 2020. **16**(5): p. 442-449.
262. Stefan, N., *Metabolic disorders, COVID-19 and vaccine-breakthrough infections.* Nat Rev Endocrinol, 2022. **18**(2): p. 75-76.
263. Favre, G., et al., *Visceral fat is associated to the severity of COVID-19.* Metabolism, 2021. **115**: p. 154440.
264. Watanabe, M., et al., *Rapid Weight Loss, Central Obesity Improvement and Blood Glucose Reduction Are Associated with a Stronger Adaptive Immune Response Following COVID-19 mRNA Vaccine.* Vaccines (Basel), 2022. **10**(1).
265. Lavie, C.J., D.B. Coursin, and M.T. Long, *The Obesity Paradox in Infections and Implications for COVID-19.* Mayo Clin Proc, 2021. **96**(3): p. 518-520.

266. Biscarini, S., et al., *The obesity paradox: Analysis from the SMAtteo COvid-19 REgistry (SMACORE) cohort.* Nutr Metab Cardiovasc Dis, 2020. **30**(11): p. 1920-1925.
267. Long, H., et al., *Plasma glucose levels and diabetes are independent predictors for mortality in patients with COVID-19.* Epidemiol Infect, 2022. **150**: p. e106.
268. Lombardi, A., et al., *In-Hospital Hyperglycemia Is Associated With Worse Outcomes in Patients Admitted With COVID-19.* Diabetes Care, 2022. **45**(11): p. 2683-2688.
269. Chang, M.C., et al., *Fasting Plasma Glucose Level Independently Predicts the Mortality of Patients with Coronavirus Disease 2019 Infection: A Multicenter, Retrospective Cohort Study.* Endocrinol Metab (Seoul), 2020. **35**(3): p. 595-601.
270. Zhang, X., et al., *SARS-CoV-2 omicron variant clearance delayed in breakthrough cases with elevated fasting blood glucose.* Virol J, 2022. **19**(1): p. 148.
271. Peleg, A.Y., et al., *Common infections in diabetes: pathogenesis, management and relationship to glycaemic control.* Diabetes Metab Res Rev, 2007. **23**(1): p. 3-13.
272. Kornum, J.B., et al., *Diabetes, glycemic control, and risk of hospitalization with pneumonia: a population-based case-control study.* Diabetes Care, 2008. **31**(8): p. 1541-5.
273. Simonsen, J.R., et al., *Bacterial infections in patients with type 1 diabetes: a 14-year follow-up study.* BMJ Open Diabetes Res Care, 2015. **3**(1): p. e000067.
274. Vedantam, D., et al., *Stress-Induced Hyperglycemia: Consequences and Management.* Cureus, 2022. **14**(7): p. e26714.
275. Turk Wensveen, T., et al., *Type 2 diabetes and viral infection; cause and effect of disease.* Diabetes Res Clin Pract, 2021. **172**: p. 108637.
276. Landini, M.P., *Early enhanced glucose uptake in human cytomegalovirus-infected cells.* J Gen Virol, 1984. **65 (Pt 7)**: p. 1229-32.
277. Muller, L.M., et al., *Increased risk of common infections in patients with type 1 and type 2 diabetes mellitus.* Clin Infect Dis, 2005. **41**(3): p. 281-8.
278. O'Neill, L.A., R.J. Kishton, and J. Rathmell, *A guide to immunometabolism for immunologists.* Nat Rev Immunol, 2016. **16**(9): p. 553-65.

LIST OF FIGURES

LIST OF TABLES

Supplementary Materials 1

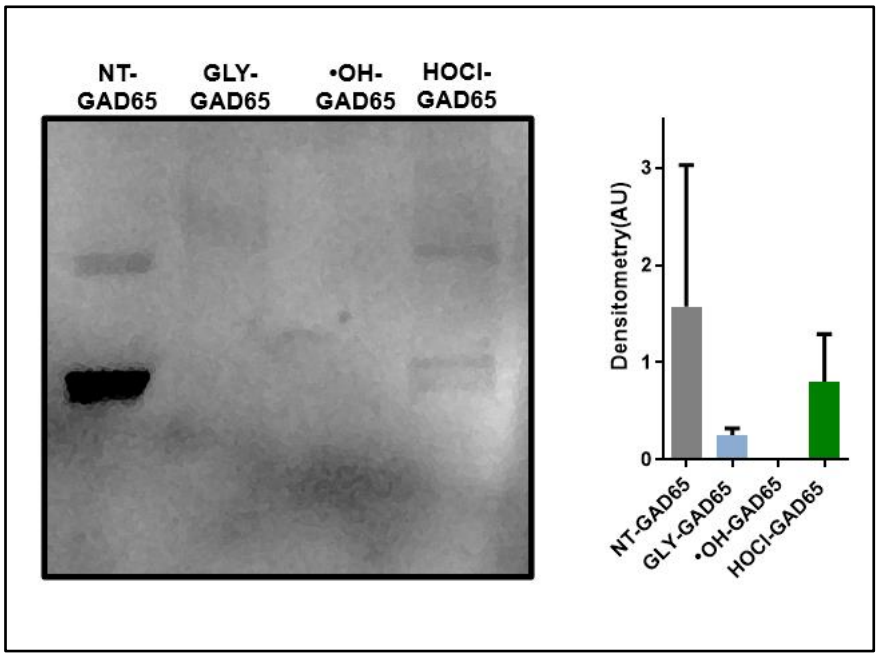

Figure S1. Binding of serum from type 1 diabetic patients to native or oxPTM-GAD65 determined via western blotting. 10µg of native or modified GAD65 was run on a 4-20% gradient SDS-PAGE for 2 hours at 120V. After running the gel, the gel was transferred to a nitrocellulose membrane via the Trans-Blot Turbo transfer system. The membranes were washed with 0.1%PBST and then blocked with 5% BSA in PBST for 2 hours. The membranes were then washed 3 times with 0.1% PBST and stained with the primary antibody overnight at 4ºC. The primary antibody was derived pooling sera from five recent-onset patients with T1D who showed increased reactivity to NT-GAD65. The membranes were washed and stained with secondary antibody for 2 hours. A 1:1 ratio of ECL was added to the membranes and incubated for 5 minutes. The membranes were imaged using the Chemi-Doc imaging system from Bio-Rad and quantified with ImageJ.

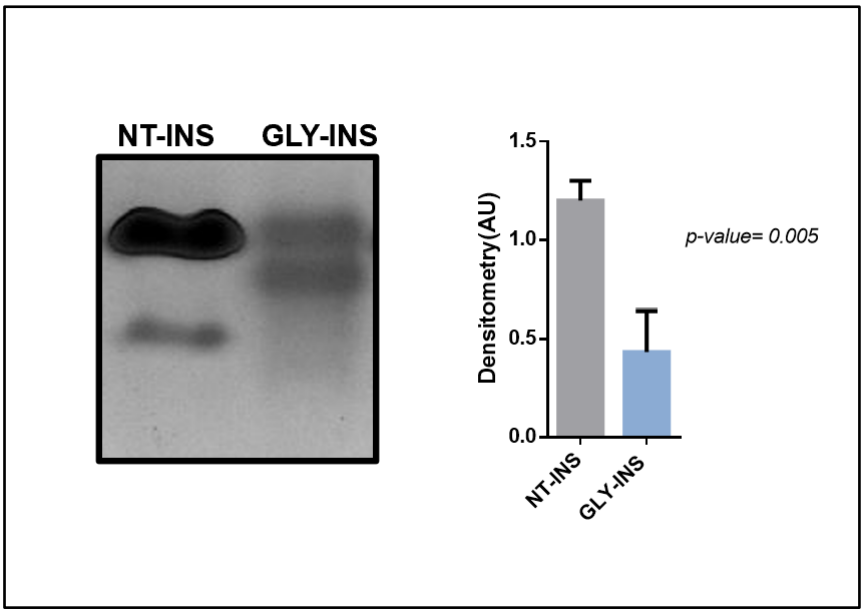

Figure S2. Native PAGE of native or glycated insulin. A 20% native PAGE was prepared, and 5-10 µg of NT- or GLY-INS was loaded with a 1:1 ratio of bromophenol blue loading dye (without SDS). The gel was run for 2 hours at 120V, and then stained for 1 hour with Coomassie blue. The gel was de-stained with 50/40/10 of methanol, distilled water, and acetic acid (v/v/v). The gel shows the A and B chains of insulin in both the NT-INS lane and the GLY-INS lane, with the GLY-INS lane being less defined, as demonstrated by the densitometry graph. The native gel was imaged with the Chemi-Doc system from Bio-Rad, and were analysed with the ImageJ system.

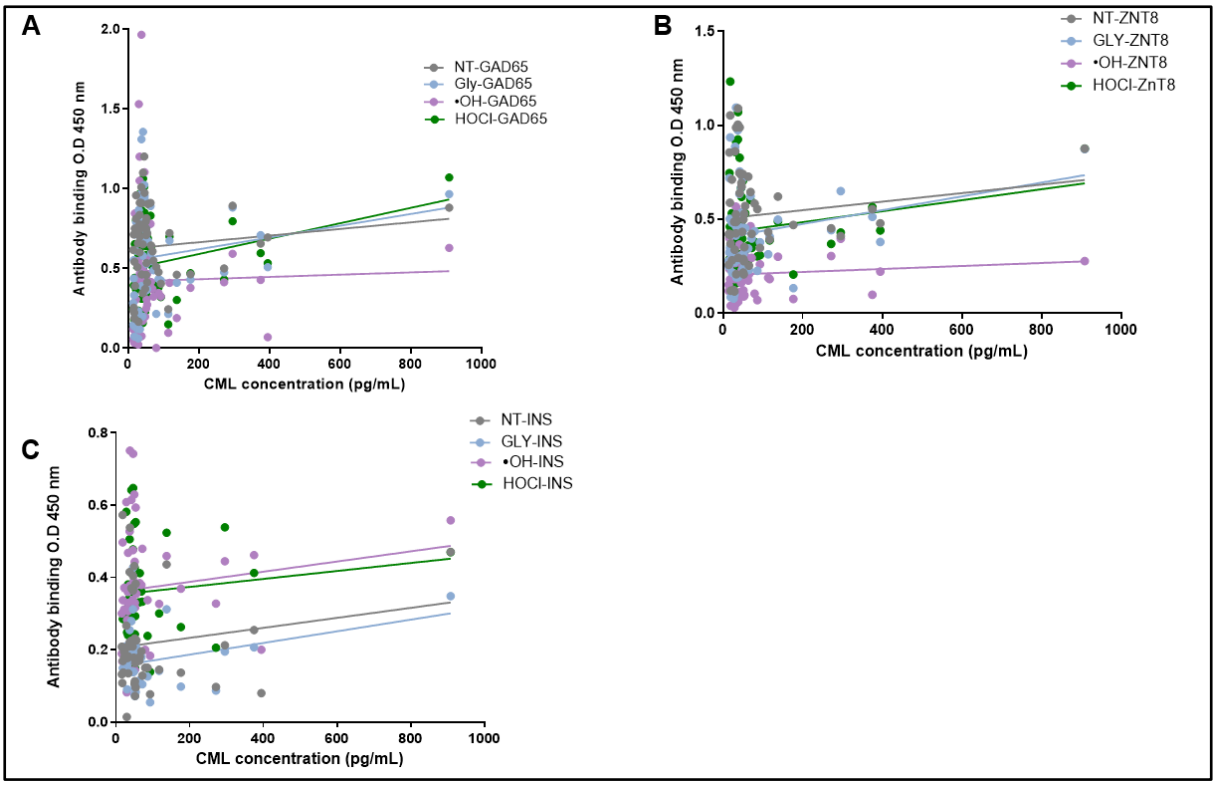

Figure S3. Depicts the correlation between IgG binding towards native and modified β-cell antigens and carboxymethyl-lysine (pg/mL) in patients with T1D. A) Shows the associations between CML and native or modified GAD65 in n=57 patients with T1D. There was no significant correlation with CML and antibody binding towards NT-, GLY- or •OH-GAD65 (r= 0.12, p-value= 0.372, r= 0.167 p-value= 0.215, r= 0.026 p-value= 0.850, respectively). However, there was a significant correlation with antibody response to HOCl-GAD65 and CML data ***(r= 0.261, p-value< 0.05)***. **B)** Displays the antibody associations between NT-, GLY-, •OH- and HOCl-ZnT8 and CML in n=57 patients with T1D. There was no significant correlations between CML and antibody binding towards NT-, GLY-, •OH- and HOCl-ZnT8 (r= 0.128 p-value= 0.341, r= 0.206 p-value= 0.123, r= 0.081 p-value= 0.549, r= 0.166 p-value= 0.241, respectively). **C)** The figure shows the correlation of CML with the antibody response towards NT-, GLY-, •OH- and HOCl-INS in n=50 patients with T1D. There was no significant correlation with NT-, •OH-, and HOCl-INS and CML levels (r= 0.160 p-value= 0.266, r= 0.135 p-value= 0.350, r= 0.127 p-value= 0.442, respectively). However, there was a trend in correlation with CML and GLY-INS ***(r= 0.307, p-value= 0.057).*** *Correlation coefficient (r) and p-values were calculated via Pearson's or Spearman's correlations where appropriate.*

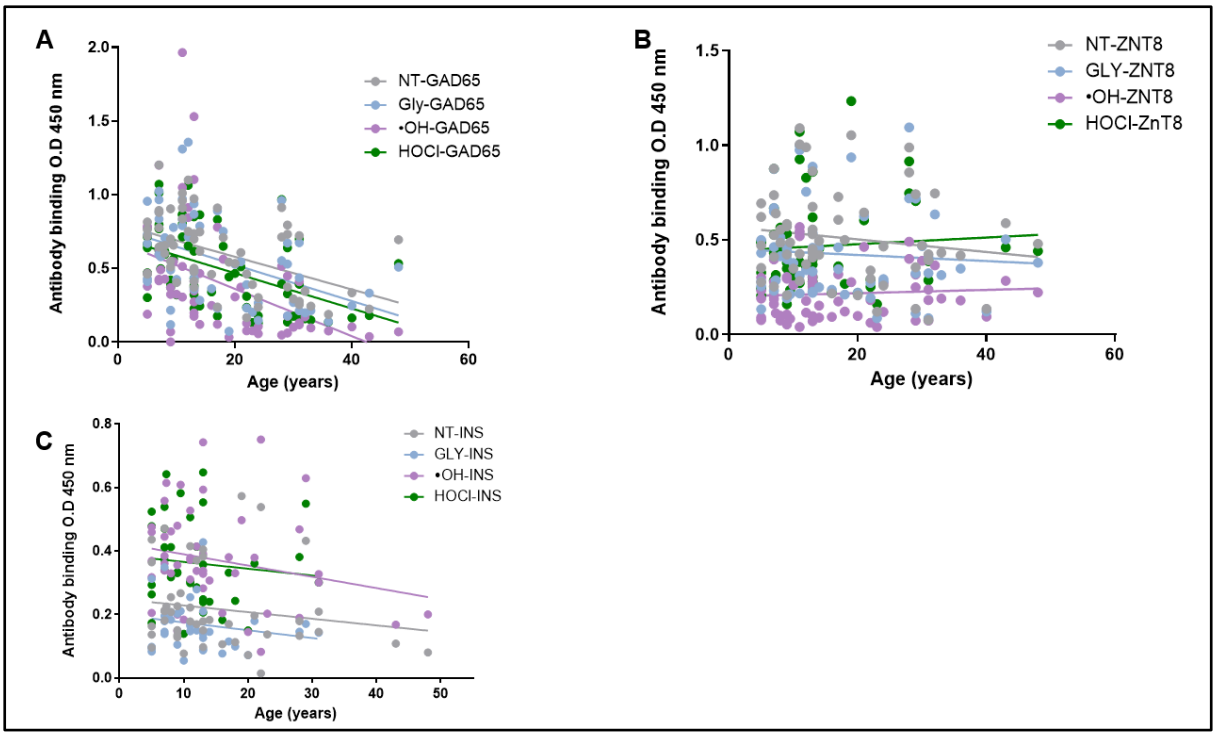

Figure S4. The correlation of age (years) with the antibody response towards native or modified β-cell antigens in type 1 diabetic patients. A) Shows the association between age (years) and the developed IgG response towards NT-, GLY-, •OH- and HOCl-GAD65 in n=68 patients with T1D ***(r= -0.481 p-value< 0.0001, r= -0.475 p-value< 0.0001, r= -0.562 p-value< 0.0001, r= -0.528 p-value< 0.0001, respectively).*** **B)** Depicts the correlation between age and the induced antibody response towards NT-, GLY-, •OH- and HOCl-ZnT8 in n=68 patients with T1D (r= -0.143 p-value= 0.262, r= -0.082 p-value= 0.598, r= 0.040 p-value= 0.589, r= 0.040 p-value= 0.788, respectively). **C)*** The figure shows the associations between age and the antibody response towards NT-, GLY-, •OH- and HOCl-INS (r= -0.236 p-value= 0.107, r= -0.017 p-value= 0.908, r= -0.117 p-value= 0.484, r= -0.191 p-value= 0.252, respectively). *Correlation coefficients (r) were calculated via Pearson's or Spearman's correlation where appropriate. *Antibody data towards NT- or modified INS was not available for all patients, n=39 T1D assessed.*

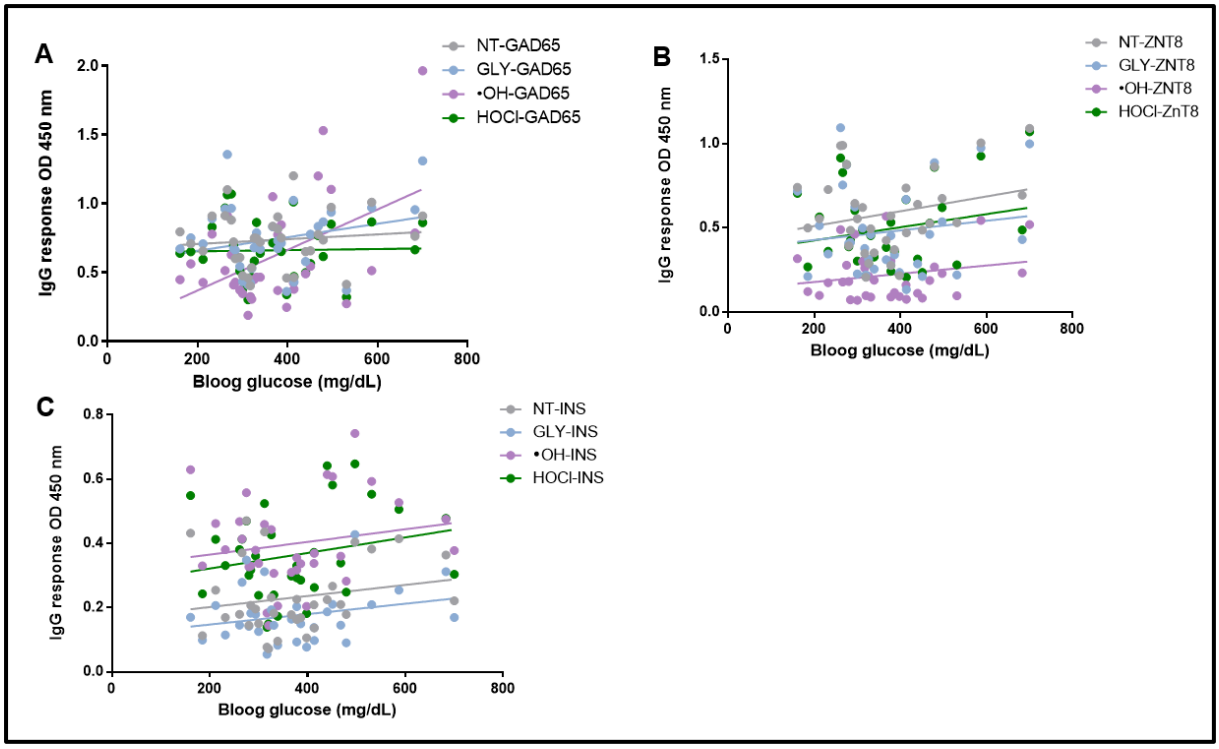

Figure S5. The correlation of blood glucose (mg/dL) with the antibody response towards native or modified β-cell antigens in type 1 diabetic patients. **A)** Shows the association between blood glucose and the developed IgG response towards NT-, GLY-, •OH- and HOCl-GAD65 in n=68 patients with T1D. There was no significant correlation with blood glucose and NT-, GLY- and HOCl-GAD65 (r= 0.113 p-value= 0.53, r= 0.248 p-value= 0.150, r= 0.025 p-value= 0.90, respectively). There was a significant correlation with •OH-GAD65 and blood glucose ***(r= 0.49, p-value= 0.004).*** **B)** Depicts the correlation between blood glucose and the induced antibody response towards NT-, GLY-, •OH- and HOCl-ZnT8 in n=68 patients with T1D (r= 0.241 p-value= 0.18, r= 0.14 p-value= 0.436, r= 0.212 p-value= 0.236, r= 0.205 p-value= 0.252, respectively). **C)** The figure shows the associations between blood glucose and the antibody response towards NT-, GLY-, •OH- and HOCl-INS in n=39 patients with T1D (r= 0.195 p-value= 0.276, r= 0.244 p-value= 0.172, r= 0.182 p-value= 0.310, r= 0.224 p-value= 0.210, respectively). *Correlation coefficients (r) were calculated via Pearson's or Spearman's correlation where appropriate.*

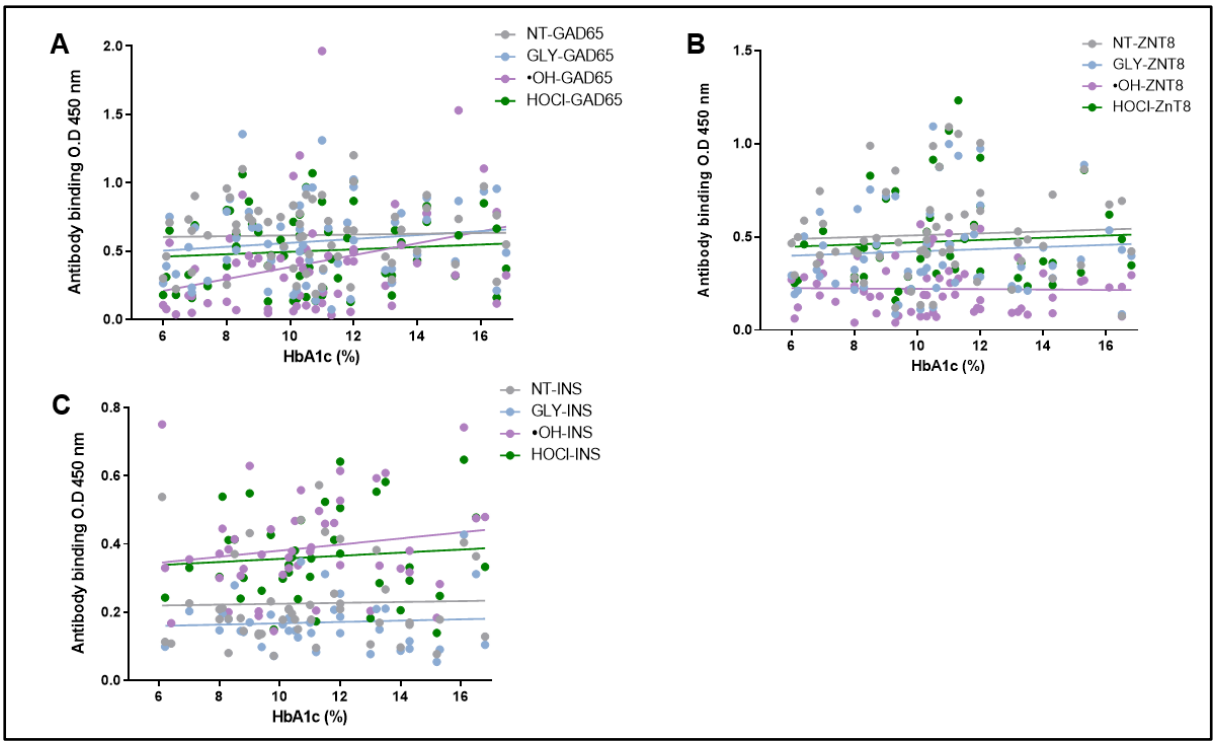

Figure S6. The correlation of HbA1c (%) with the antibody response towards native or modified β-cell antigens in type 1 diabetic patients. A) Shows the association between HbA1c and the developed IgG response towards NT-, GLY-, •OH- and HOCl-GAD65 in n=68 patients with T1D. There was no significant correlation with NT-, GLY-, and HOCl-GAD65 and HbA1c (r= 0.033 p-value= 0.800, r= 0.136 p-value= 0.301, r= 0.091 p-value= 0.488, respectively). However, there was as significant correlation with HbA1c and •OH-GAD65 ***(r= 0.320, p-value= 0.013)***. **B)** Depicts the correlation between HbA1c and the induced antibody response towards NT-, GLY-, •OH- and HOCl-ZnT8 (r= 0.060 p-value= 0.650, r= 0.068 p-value= 0.608, r= -0.020 p-value= 0.881, r= 0.066 p-value= 0.665, respectively). **C)** The figure shows the associations between HbA1c and the antibody response towards NT-, GLY-, •OH- and HOCl-INS (r= 0.029 p-value= 0.851, r= 0.064 p-value= 0.70, r= 0.17 p-value= 0.260, r= 0.091 p-value= 0.583, respectively). *Correlation coefficients (r) were calculated via Pearson's or Spearman's correlation where appropriate.*

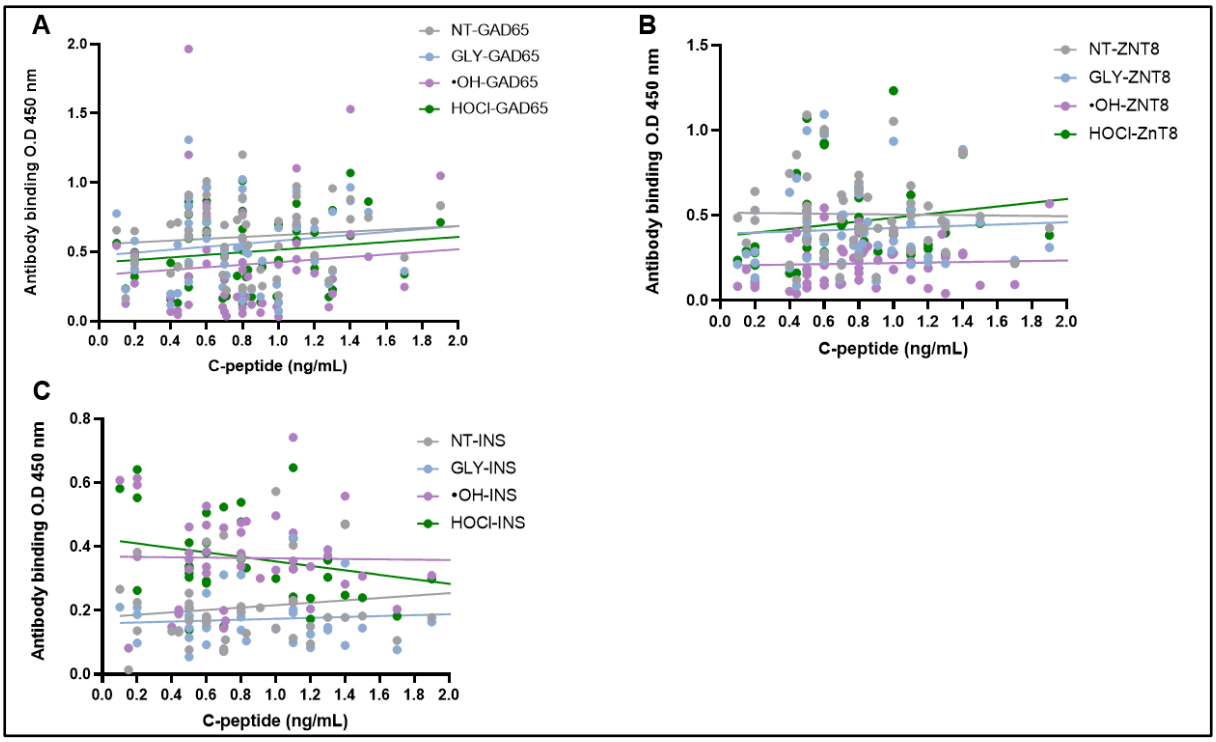

Figure S7. The correlation of C-peptide (ng/mL) with the antibody response towards native or modified β-cell antigens in type 1 diabetic patients. A) Shows the association between C-peptide and the developed IgG response towards NT-, GLY-, •OH- and HOCl-GAD65 in n=68 patients with T1D (r= 0.102 p-value= 0.448, r= 0.108 p-value= 0.418, r= 0.070 p-value= 0.602, r= 0.117 p-value= 0.383, respectively). **B)** Depicts the correlation between C-peptide and the induced antibody response towards NT-, GLY-, •OH- and HOCl-ZnT8 (r= -0.030 p-value= 0.825, r= 0.111 p-value= 0.406, r= 0.120 p-value= 0.372, r= 0.237 p-value= 0.118, respectively). **C)** The figure shows the associations between C-peptide and the antibody response towards NT-, GLY-, •OH- and HOCl-INS in n=39 patients with T1D (r= 0.084 p-value= 0.585, r= -0.083 p-value= 0.626, r= -0.002 p-value= 0.988, r= -0.265 p-value= 0.112, respectively). *Correlation coefficients (r) were calculated via Pearson's or Spearman's correlation where appropriate.*

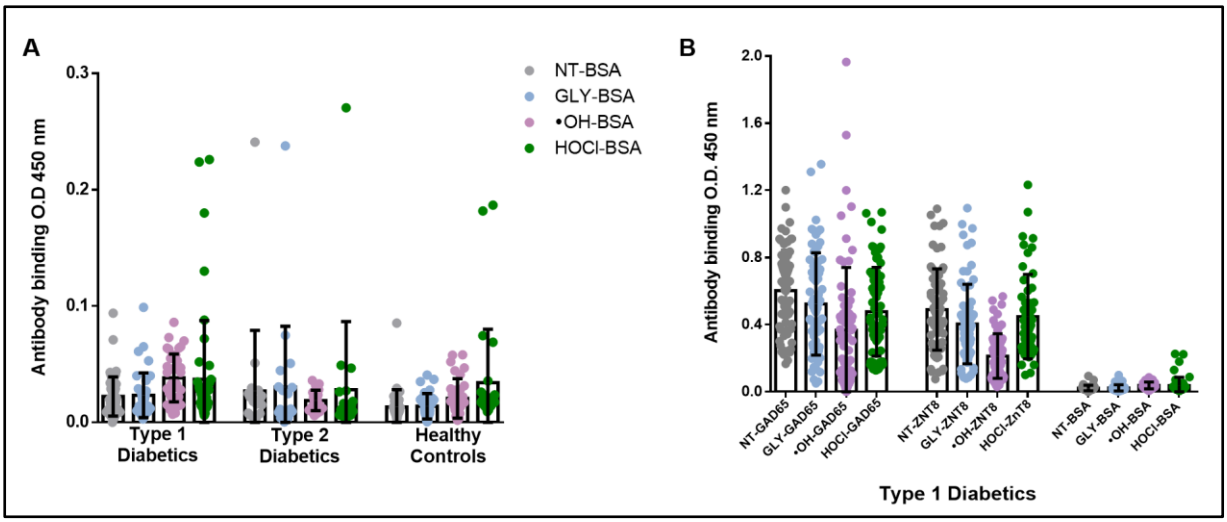

Figure S8. Antibody binding towards native and modified BSA. A) The antibody binding towards native or modified BSA in T1D, T2D and healthy controls. When assessing the antibody binding there was no significant difference between NT- or GLY-BSA binding between T1D and T2D (mean ± S.D, 0.022 ± 0.017 vs 0.027 ± 0.052, p-value= 0.312 and 0.023 ± 0.019 vs 0.0301 ± 0.053, p-value= 0.314, respectively). There was a significant difference between •OH and HOCl-BSA binding between T1D and T2D (0.038 ± 0.021 vs 0.0189 ± 0.009 p-value= 0.002, and 0.0371 ± 0.0504 vs 0.0282 ± 0.0585, p-value= 0.008, respectively). However, when comparing the antibody response between T1D and HC, there appeared to be a difference between antibody binding towards NT- and GLY-BSA (0.022 ± 0.017 vs 0.0132 ± 0.015, p-value= 0.011, and 0.023 ± 0.019 vs 0.0139 ± 0.011, p-value= 0.02, respectively), but there was no difference seen between •OH- and HOCl-BSA between T1D and HC (0.038 ± 0.021 vs 0.0207 ± 0.017, p-value= 0.917, and 0.0371 ± 0.0504 vs 0.0342 ± 0.0459, p-value= 0.850, respectively). **B)** Antibody binding in recent-onset T1D towards NT- and modified GAD65, ZnT8, and BSA.

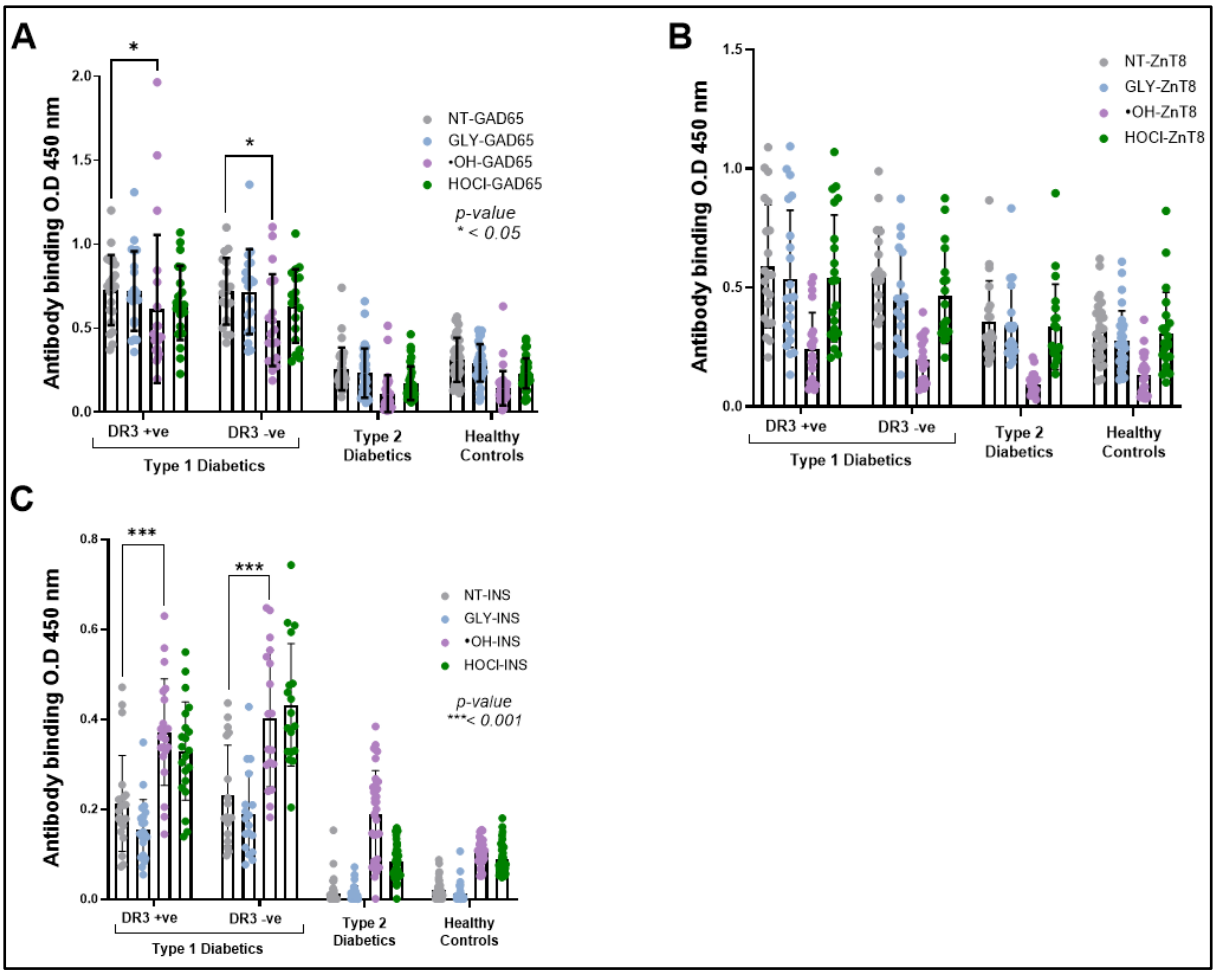

Figure S9. Antibody reactivity to NT- or modified β-cell antigens in n=39 patients with recent onset T1D based on HLA-DR3 risk haplotype, compared with people with T2D and HC. A) Shows no significant difference between the antibody binding to NT- or oxPTM-GAD65 in patients with T1D based HLA-DR3 haplotype. However, there is slight increase in antibody binding towards all antigens of interest in the HLA-DR3 positive group compared to the HLA-DR3 negative group. **B)** Similarly, there was no significant difference between antibody binding between NT- or oxPTM-ZnT8 in HLA-DR3 positive and HLA-DR3 negative haplotypes. **C)** The figure shows no significant difference with antibody binding towards NT- and oxPTM-INS between HLA-DR3 positive and HLA-DR3 negative patients. However, there was a significant difference between that antibody binding towards •OH-INS and NT-INS in the HLA-DR3 positive group (mean O.D ± S.D, 0.3712 ± 0.1183 vs 0.2130 ± 0.1068, p-value= 0.002, respectively), and a significant difference between antibody binding towards •OH-INS and NT-INS in the HLA-DR3 negative group (mean O.D ± S.D, 0.4016 ± 0.1518 vs 0.2301 ± 0.1120, p-value= 0.0005, respectively).

Supplementary Material 2

	Type 1 Diabetes	Type 2 Diabetes
Total (n)	26	34
Microvascular complications, n (%)	6 (23.1%)	8 (23.5%)
Macrovascular complications, n (%)	0 (0.0%)	4 (11.8%)
Additional autoimmune diseases, n (%) *	10 (38.5%)	3 (8.8%)
Metformin, n (%)	0 (0.0%)	29 (85.3%)
DPP4i, n (%)	0 (0.0%)	4 (11.8%)
SGLT2i, n (%)	0 (0.0%)	9 (26.5%)
GLP1-RA, n (%)	0 (0.0%)	18 (52.9%)
Pioglitazone, n (%)	0 (0.0%)	1 (2.9%)
Basal insulin only, n (%)	0(0.0%)	9 (26.5%)
Sulfonylurea, n (%)	0 (0.0%)	7 (20.6%)
MDI, n (%)	13 (50.0%)	4 (11.8%)
Pump users, n (%)	13 (50.0%)	0 (0.0%)
CGM users, n (%)	13 (50.0%)	0 (0.0%)
TIR (%)	61.5% [55.5-71.7]	N/A
TAR (%)	28.0% [21.0-41.0]	N/A
TBR (%)	3.0% [2.0-7.5]	N/A

Table S1. The base clinical characteristics and glucose management and control features of the study populations. *Additional autoimmune diseases comprise vitiligo, coeliac disease and/or autoimmune thyroid disease; MDI, multiple daily insulin injections; CGM, continuous glucose monitoring; TIR, time-in-range; TAR, time-above-range; TBR, time-below-range.*

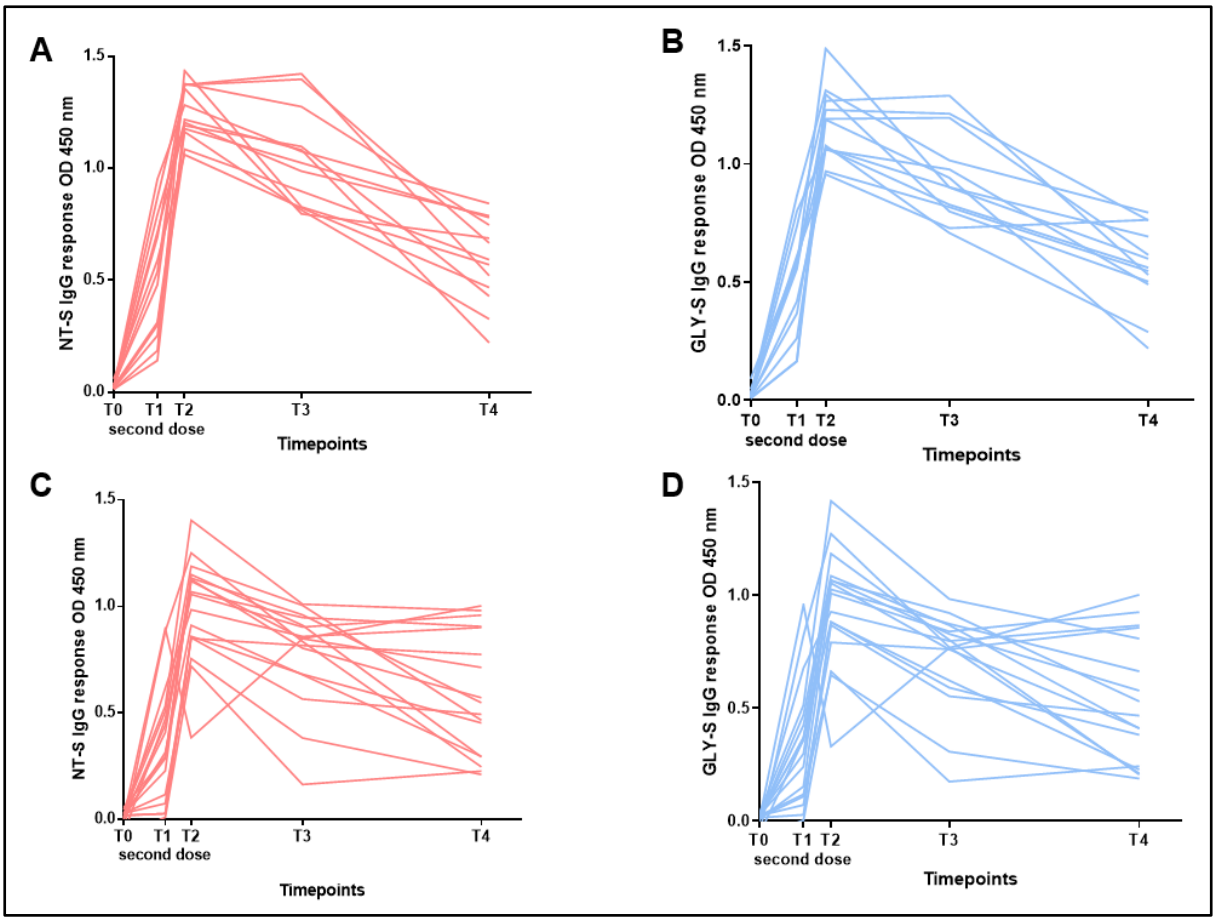

Figure S10. Overall antibody response induced by the mRNA vaccine BNT162b2 (Pfizer, BioNTech) towards native or glycated SARS-CoV-2 spike glycoprotein in T1D (A, B) and T2D (C, D), respectively. The figure shows the IgG response across all the study timepoints in n= 13 T1D with antibody data directed towards all the study timepoints (T0-T4) towards NT-S **(A)** or GLY-S **(B)**. The AUC depicted no significant difference between NT- or GLY-S within patients with T1D (mean AUC ± SD, 154.7 ± 24.26 vs 143.90 ± 21.99, p-value= 0.24, respectively). In terms of T2D (n= 16), there appeared to be no significant difference between mean AUC in T2D towards NT-S **(C)** or GLY-S **(D)** (mean AUC ± SD, 123.8 ± 32.98 vs 115.0 ± 30.74, p-value= 0.43). However, there was a significant difference between the developed antibody response in T1D and T2D towards NT-S and GLY-S (NT-S, 154.7 ± 24.26 vs 123.8 ± 32.98, p-value= 0.009) (143.9 ± 21.99 vs 115.0 ± 30.74, p-value= 0.008), respectively. *T0, 0 days, baseline; T1, 21 days, day of second dose of the vaccine; T2, 35 days from baseline; T3, 90 days from baseline; T4, 180 days from baseline.*

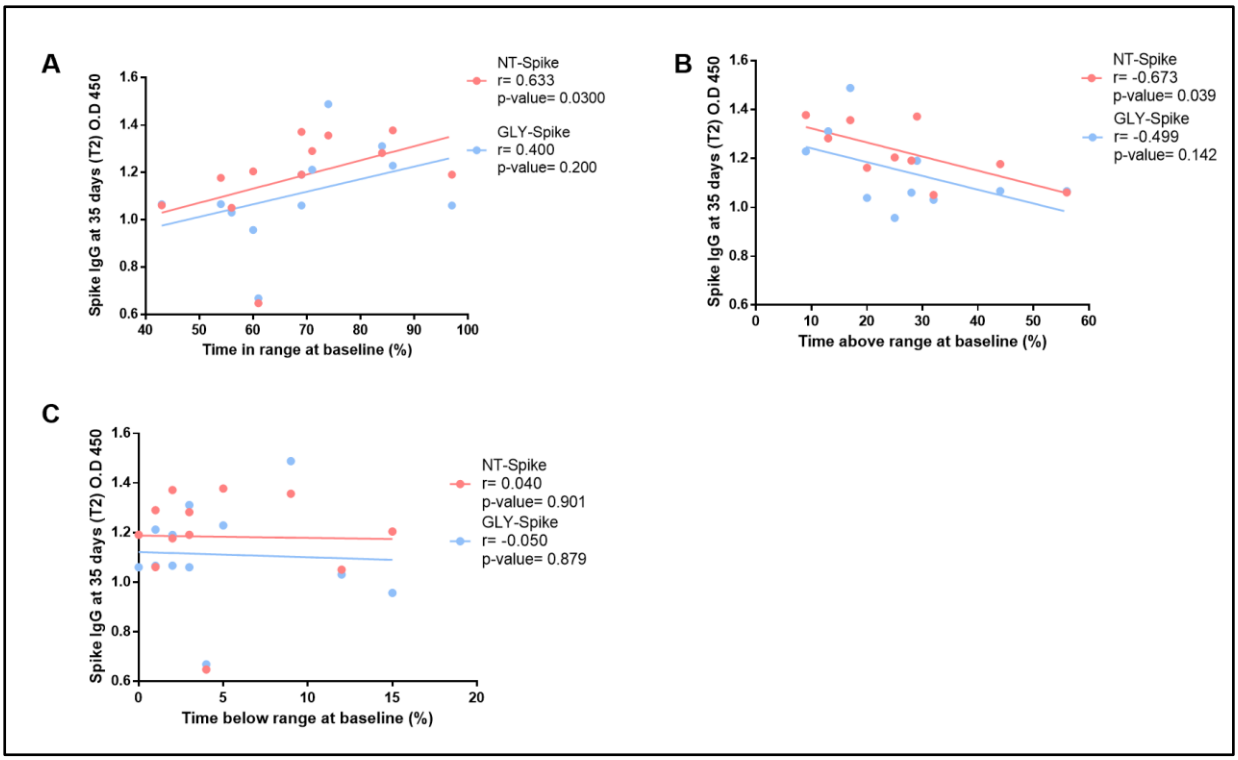

Figure S11. Correlation of baseline CGM data with T2 (35 days) antibody response to native and GLY-Spike glycoprotein in patients with T1D in response to vaccination with the mRNA vaccine BNT162b2 (Pfizer, BioNTech). CGM data was available for n=10 patients with T1D. Upon correlation with TIR **(A)** and TAR **(B)** at baseline (T0) there appeared to be a strong correlation with antibody response to NT-Spike protein (***r= 0.633, p-value= 0.030 and r= -0.673, p-value= 0.039***, respectively), however there was no significant correlation with GLY-Spike protein (r= 0.400, p-value= 0.200 and r= -0.499, p-value= 0.142, respectively). When assessing the correlation with TBR **(C)** at baseline, there was no correlation with the antibody response towards NT- or GLY-Spike glycoprotein (r= 0.40, p-value= 0.901 and r= -0.050, p-value= 0.879, respectively). *CGM, continuous glucose monitoring; TIR, time-in-range; TAR, time-above-range; TBR, time-below-range.*

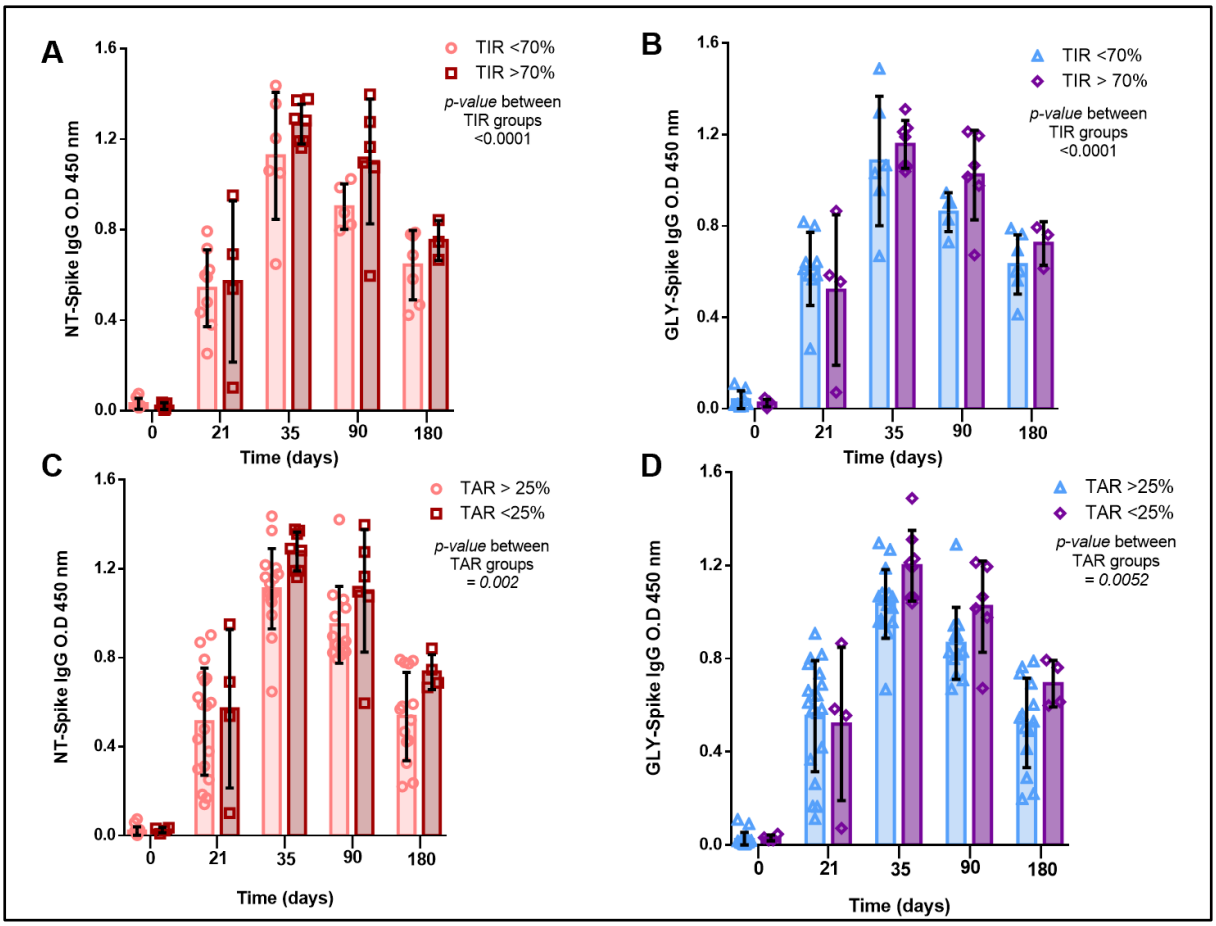

Figure S12. Antibody response induced after vaccination with the mRNA vaccine BNT162b2 (Pfizer, BioNTech) to native or GLY-Spike glycoprotein depending on cut-off values for CGM data. Using a 70% cut-off for TIR, the antibody response towards NT-Spike protein **(A)** and GLY-Spike protein **(B)** was assessed. The results showed a significant difference between the antibody responses (p-value <0.001) amongst groups. When using a 25% cut-off for TAR, the antibody response towards NT-Spike protein **(C)** and GLY-Spike protein **(D)** was assessed, showing a significance of p-value= 0.002 and p-value= 0.0052 between groups.

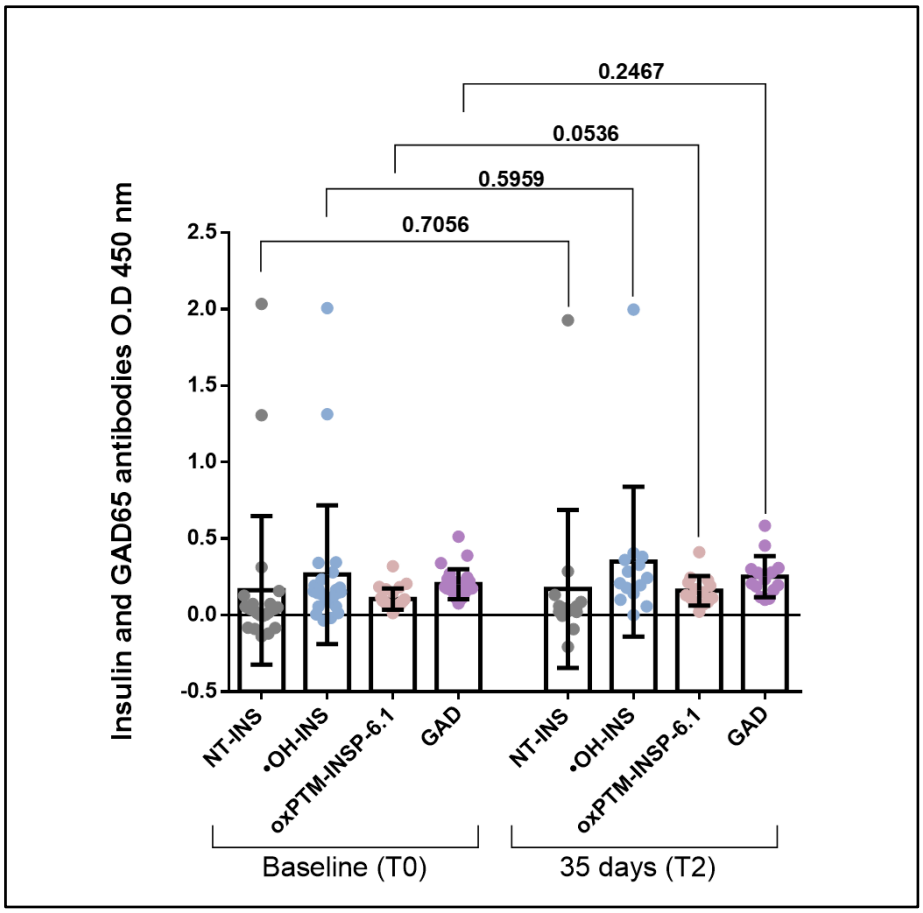

Figure S13. Antibody binding in T1D diabetic patients before and after vaccination towards 4 T1D autoantigens. When testing sera from patients with T1D (n=26) enrolled in the study before vaccination (baseline, T0) and after two doses of the mRNA BNT162b2 vaccine (Pfizer, Bio-techne) (35 days from baseline, T2) to 4 T1D autoantigens there appeared to be no significant difference between antibody responses before or after the vaccine. *NT-INS, native insulin; •OH-INS, hydroxyl-modified insulin, oxPTM-INSP-6.1, oxidatively modified insulin peptide 6; GAD, glutamate decarboxylase 65.*

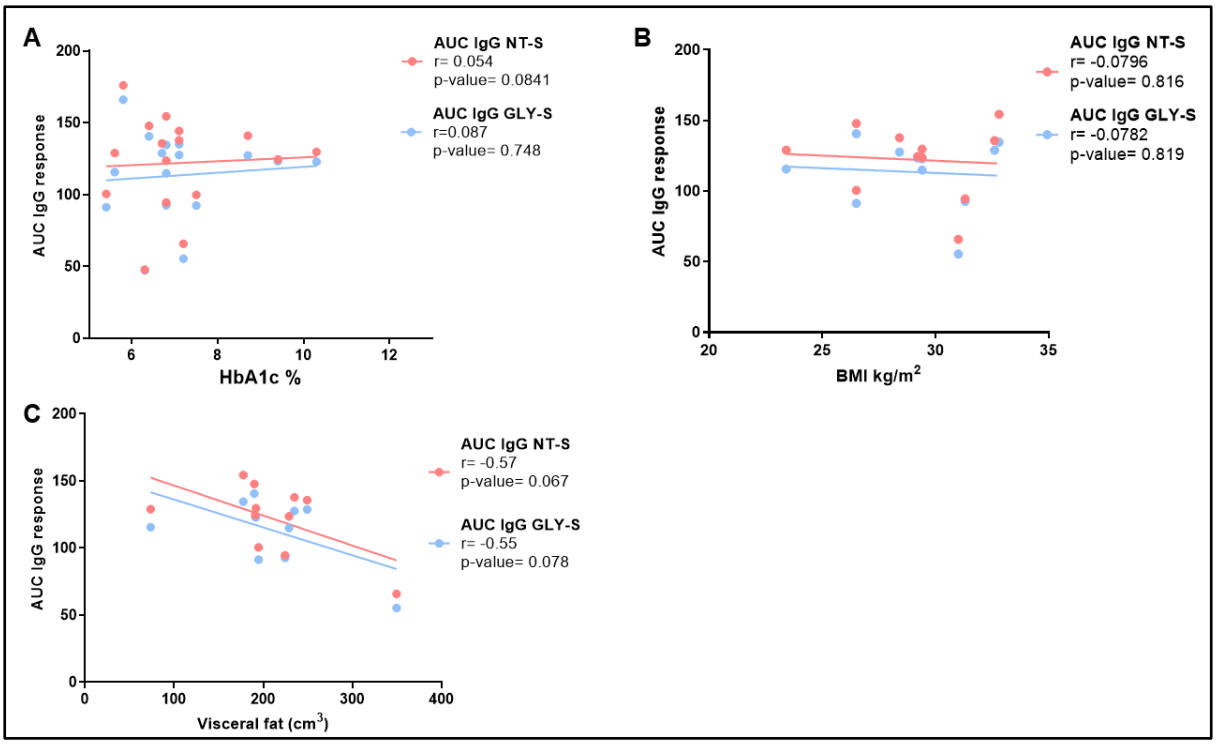

Figure S14. Associations between overall AUC antibody response towards NT- or GLY-Spike protein after vaccination with the mRNA vaccine BNT162b2 (Pfizer, BioNTech) and demographic characteristics in T2D patients (n=16). A) Depicts the association of the antibody response to NT- or GLY-Spike protein and HbA1c (%) (r= 0.054 p-value= 0.084, and r= 0.087, p-value= 0.748, respectively). **B)** There were no correlations when assessing the AUC antibody response towards NT- or GLY-Spike protein with BMI (kg/m^2) (r= -0.0796, p-value= 0.816 and r= -0.0782, p-value= 0.819, respectively). **C)** The figure shows the associations with Visceral fat (cm^3) and AUC antibody response towards NT- or GLY-Spike in T2D (r= -0.57, p-value= 0.067 and r= -0.55, p-value= 0.078, respectively).

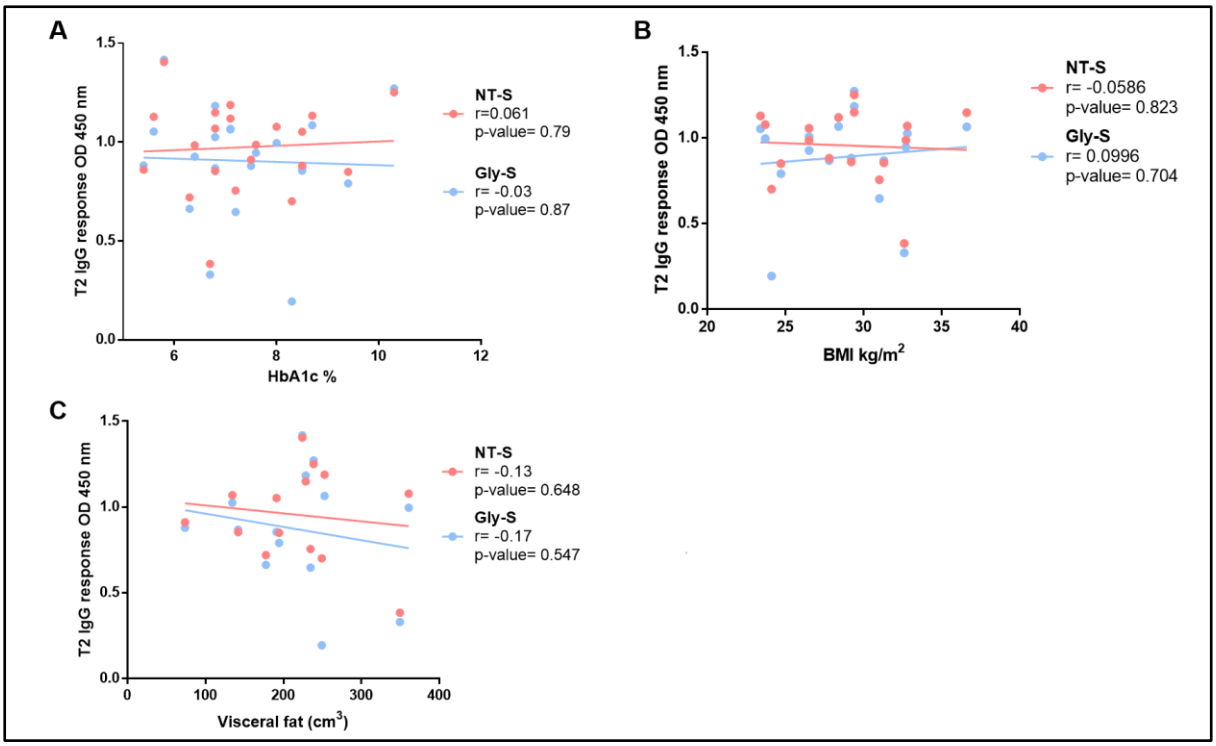

Figure S15. Associations with the IgG response at T2 (35 days from baseline) induced after administration of the mRNA vaccine BNT162b2 (Pfizer, BioNTech) and demographic characteristics in T2D patients (n=16). A) Depicts the association of the antibody response at T2 to NT- or GLY-Spike protein and HbA1c (%) (r= 0.061, p-value= 0.790 and r= -0.03, p-value= 0.87, respectively). **B)** There were no correlations when assessing the peak antibody response at T2 towards NT- or GLY-Spike protein with BMI (kg/m^2) (r= -0.0586, p-value= 0.823 and r= 0.0996, p-value= 0.704, respectively). **C)** The figure shows the associations with Visceral fat (cm^3) and the peak antibody response at T2 towards NT- or GLY-Spike in T2D (r= -0.13, p-value= 0.648 and r= -0.17, p-value= 0.547, respectively).

Results of Logistic regression to build the clinical risk score

Primary outcome (death)	Coef.	Std. Error	z	P-value	95% Confidence Interval
Gender (male =1, female=0)	**1.78**	**0.57**	**3.13**	**0.002**	**0.67, 2.89**
Age					
> 71 years old	**1.30**	**0.78**	**1.67**	**0.10**	**-0.23, 2.82**
Nationality (Kuwaiti=1, non-Kuwaiti=0)	**-1.71**	**0.47**	**-3.68**	**0.000**	**-2.62, -0.80**
Asthma	**1.65**	**0.57**	**2.91**	**0.004**	**0.54, 2.76**
Glucose (mg/dL)					
100-126	**0.51**	**0.63**	**0.80**	**0.42**	**-0.73, 1.74**
126-200	**2.36**	**0.58**	**4.11**	**0.00**	**1.23, 3.50**
> 200	**3.26**	**0.61**	**5.39**	**0.00**	**2.08, 4.45**

Table S2. Logistic regression analysis of the Kuwaiti COVID-19 cohort (N=417 patients) used to build the clinical risk score to predict in-hospital death due to COVID-19. When tested against the primary outcome (death), gender, nationality, asthma and glucose levels appeared to be the most significant variables to predict the outcome. Here age categories were 50-70, and >71 years old, and glucose categories were set as 100-126 vs 126-200 vs > 200 mg/dL.

Publications and Awards Arising from this Work

1. Comment on So et al. Autoantibody Reversion: Changing Risk Categories in Multiple-Autoantibody–Positive Individuals. Diabetes Care 2020; 43:913–917." → *Published Diabetes Care, 2020*.

   Author list: **Alhamar G**, Strollo R, Pozzilli P.

2. Clinical characteristics and outcomes of COVID-19 patients with diabetes mellitus in Kuwait → *Published Heliyon, 2021.* doi:10.1016/j.heliyon.2021.e06706.

   Alshukry A, Bu Abbas M, Ali Y, Alahmad B, Al-Shammari A, **Alhamar G**, Abu-Farha M, AbuBaker J, Devarajan S, Dashti A, Al-Mulla F and Ali H.

3. Development of a clinical risk score to predict death in patients with COVID-19 → *Published Diabetes Metabolism Research and Reviews, 2022.* https://doi.org/10.1002/dmrr.3526

   Author list: **Alhamar G**, Maddaloni, E, Al Shukry A, Al-Sabah S, Al-Haddad M, Al-Youha S, Jamal M, Almazeedi S, Al-Shammari A, Abu-Farha M, Abubaker J, Alattar A, AlOzairi E, Alessandr F, D'Onofrio L, Leto G, Mastroianni C, Mignogna C, Pascarella G, Pugliese F, Ali H, Al Mulla F, Buzzetti R, Pozzilli P.

4. Autoantibody and T cell responses to oxidative post-translationally modified insulin neoantigenic peptides in type 1 diabetes → *Published Diabetologia, 2023.* doi: 10.1007/s00125-022-05812-4.

   Author list: Strollo R, Vinci C, Man YKS, Bruzzaniti S, Piemonte E, **Alhamar G**, Briganti SI, Malandrucco I, Tramontana F, Fanali C, Garnett J, Buccafusca R, Guyer P, Mamula M, James EA, Pozzilli P, Ludvigsson J, Winyard PG, Galgani M, Nissim A.

5. Pre-vaccination glucose time in range positively correlated with antibody response after SARS-COV2 mRNA vaccine BNT162b2 in patients with type 1 diabetes → *Published, JCEM, 2023.*

   Author list: **Alhamar G**, Briganti S, Maggi D, Viola V, Faraj M, Zannella C, Galdiero M, Franci G, Fusco C, Isgrò C, Leanza G, Malandrucco I, Spinelli A, Tramontana F, Iaria D, Tortoriello R, Pieralice S, Rosati M, Napoli N, Matarese G, Pozzilli P, Galgani M, Strollo R.

6. Pre-vaccination glucose time in range positively correlated with antibody response after SARS-COV2 mRNA vaccine BNT162b2 in patients with type 1 diabetes → *Accepted for short oral presentation EASD 2022, Stockholm, Sweden.*
   Presented by **Alhamar G** on behalf of co-authors.